UNIVERSITY OF CALGARY

Lipid Rafts and Signalling in Hematopoietic Cells

by

Laura Darlene Zajchowski

A THESIS

SUBMITTED TO THE FACULTY OF GRADUATE STUDIES

IN PARTIAL FULFILMENT OF THE REQUIREMENTS FOR THE

DEGREE OF DOCTOR OF PHILOSOPHY

DEPARTMENT OF BIOCHEMISTRY AND MOLECULAR BIOLOGY

CALGARY, ALBERTA

NOVEMBER, 2006

Abstract

Lipid rafts are liquid-ordered membrane microdomains with a specific protein and lipid composition in eukaryotic cells. Lipid rafts have functional roles in membrane transport processes, protein sorting, cholesterol homeostasis, and signal transduction. Current evidence suggests that a large number of signalling pathways are compartmentalized within rafts. The highly organized yet dynamic nature of lipid rafts regulates cell signalling by providing a signalling microenvironment that is tailored to produce the appropriate biological response. Alterations in the structure or organization of lipid rafts have been associated with a number of human diseases. Despite intensive investigation, many questions remain regarding the precise properties of rafts in living cells and how these properties correlate with proposed lipid raft functions.

The overall hypothesis of this thesis is that the specific properties of a given lipid raft, including its protein and lipid composition, size, morphology, abundance, and localization, define its function in signal transduction. In order to further characterize the properties of lipid rafts in mammalian cells, a novel proteomic approach was used to investigate the protein composition of lipid raft fractions isolated from hematopoietic cells. This led to the successful identification of a large number of raft proteins, including both novel proteins and known raft markers. The identified proteins provide insight into lipid raft biology in several areas, including the presence and functional significance of rafts in the membranes of the endoplasmic reticulum and mitochondria, the association of rafts with the cytoskeleton, and the apparent existence of a common lipid raft proteome. Current challenges in lipid raft proteomics with respect to the

identification and analysis of signalling proteins and differential proteomics are also discussed.

Proteins anchored to the extracellular leaflet of the plasma membrane by glycosylphosphatidylinositol (GPI) anchors are enriched in rafts and their expression is lost in the human disease paroxysmal nocturnal hemoglobinuria. To further characterize the hypothesized link between raft structure and function, the effect of GPI deficiency on raft-dependent signalling in B lymphocytes was examined. This study demonstrated that a pathologically important alteration in raft structure affects lipid raft function in signal transduction, leading to changes in the associated cellular response.

Acknowledgements

I would like to express my sincere gratitude to my supervisor, Dr. Stephen Robbins, for the privilege of working in his lab and for his continued support and infectious enthusiasm about science. Many thanks as well to the past and present members of the Robbins' lab for making the lab a great place to work. Extra-special thanks to Elizabeth and Alex, who are great friends as well as colleagues. I would also like to express my gratitude to my committee members, Dr. Susan Lees-Miller, Dr. Kamala Patel, and Dr. Don Fujita, for volunteering their time, energy, and helpful feedback over the years. I was extremely fortunate to receive exceptionally generous advice and support from Dr. Julie Deans and members of her lab, especially Tammy Unruh and Maria Polyak, who taught me a lot about B cells. Support and expert advice from Laurie Robertson, Laurie Kennedy, and Fusun Turesin at the University of Calgary Flow Cytometry Facility were also invaluable to me during the course of my studies. The proteomics work could not have been accomplished without the assistance and expertise of Jing Zheng and Dr. Liang Li at the University of Alberta, as well as Ella Ng and Dr. David Schriemer at the University of Calgary. Dr. Taroh Kinoshita of Osaka University kindly provided me with reagents and cell lines. Last, but certainly not least, I am grateful for the patience and unfailing love and support of my husband Eric and my family and friends throughout my PhD journey.

Dedication

To my parents.

Table of Contents

List of Tables

List of Figures and Illustrations

List of Symbols, Abbreviations and Nomenclature

Symbol	Definition
1D	one-dimensional
2D	two-dimensional
AKAP	A kinase anchoring protein
ANOVA	analysis of variance
APC	antigen presenting cell
BAM32	B-lymphocyte adaptor molecule of 32 kDa
BCR	B cell receptor
BLNK	B-cell linker
Btk	Bruton's tyrosine kinase
Cbp/PAG	Csk binding protein/phosphoprotein associated with glycosphingolipid-enriched microdomains
CEA	carcinoembryonic antigen
CKI	casein kinase I
CNTF	ciliary neurotrophic factor
Csk	carboxyl-terminal Src kinase
DAF	decay accelerating factor
DIGs	detergent-insoluble glycolipid-rich membranes
DRMs	detergent-resistant membranes
eNOS	endothelial nitric oxide synthase
EGFR	epidermal growth factor receptor
EM	electron microscopy
ER	endoplasmic reticulum
ERK	extracellular signal-regulated kinase
ESI	electrospray ionization
FcεRI	Fc epsilon receptor I; IgE receptor
FcγR	Fc gamma receptor; IgG receptor
FGFR	fibroblast growth factor receptor

GDNF	glial cell line-derived neurotrophic factor
GEMs	glycolipid-enriched membranes
GFRα	GDNF family receptor α
GLU	glucose
GPI	glycosylphosphatidylinositol
GSK3	glycogen synthase kinase 3
Hck	hematopoietic cell kinase
HRP	horseradish peroxidase
HS1	hematopoietic lineage cell-specific protein 1
hsp70	heat shock protein 70
hsp90	heat shock protein 90
IEF	isoelectric □ocusing
IL-2R	interleukin-2 receptor
iNOS	inducible nitric oxide synthase
IPG	inositolphoshoglycan
IPG gels; IPG strips	immobilized pH gradient gels/strips
ITAM	immunoreceptor tyrosine-based activation motif
ITIM	immunoreceptor tyrosine-based inhibition motif
JNK	c-JUN NH_2-terminal kinase
LAB	linker for activation of B cells
LAT	linker for activation of T cells
mAb	monoclonal antibody
MALDI	matrix-assisted laser desorption ionization
MAN	mannose
MAPK	mitogen-activated protein kinase
MBS	Mes-buffered saline
MβCD	methyl-beta-cyclodextrin
MES	morpholineethanesulfonic acid
MS	mass spectrometry

NCAM	neural cell adhesion molecule
NFAT	nuclear factor of activated T cells
NFκB	nuclear factor-κB
pAb	polyclonal antibody
PBS	phosphate-buffered saline
PDGFR	platelet-derived growth factor receptor
PFMF	peptide fragment mass fingerprint
PI	propidium iodide
PIP_2	phosphatidylinositol-4,5-bisphosphate
PIP_3	phosphatidylinositol-3,4,5-trisphosphate
PI-PLC	phosphatidylinositol-specific phospholipase C
PI-PLD	phosphatidylinositol-specific phospholipase D
PI3K	phosphatidylinositol-3-kinase
PKA	protein kinase A
PKCα	protein kinase C α
PKCθ	protein kinase C θ
PLAP	placental alkaline phosphatase
PLCγ	phospholipase C γ
PMF	peptide mass fingerprinting
PMSF	phenylmethylsulfonyl fluoride
PNH	paroxysmal nocturnal hemoglobinuria
PrP	prion protein
PUFAs	polyunsaturated fatty acids
RT	room temperature
SDS-PAGE	sodium dodecyl sulfate-polyacrylamide gel electrophoresis
SMAC	supramolecular activation cluster
SHIP	Src homology 2 domain-containing inositol phosphatase
SILAC	stable isotope labeling with amino acids in cell culture

TAG-1	transiently expressed axonal surface glycoprotein-1
TCR	T cell receptor
TPA	12-*O*-tetradecanoylphorbol-13-acetate
uPAR	urokinase-type plasminogen activator receptor
UV	ultraviolet
WASP	Wiskott-Aldrich syndrome protein

Chapter One: Lipid Rafts and Little Caves--Compartmentalized Signalling in Membrane Microdomains

1.1 Introduction

As with most other cellular organelles, the plasma membrane is highly organized. Investigations of plasma membrane structure by electron microscopy in the 1950's revealed the presence of multiple small flask-shaped invaginations in the plasma membrane of epithelial and endothelial cells (Palade, 1953; Yamada, 1955). These structures were named caveolae or "little caves" by Yamada based on their characteristic morphology (Yamada, 1955). The cytoplasmic surfaces of caveolae are covered with a membrane coat, of which a principal component is a family of 21-25 kDa integral membrane proteins called caveolins (Glenney Jr., 1992; Rothberg et al., 1992; Scherer et al., 1995; Tang et al., 1996). There are three known caveolin genes—caveolin-1 (also called VIP21) (Glenney Jr., 1992), caveolin-2 (Scherer et al., 1996), and caveolin-3 (Tang et al., 1996). Initiation of translation of the caveolin-1 mRNA occurs at two different sites to generate two isoforms of caveolin-1: caveolin-1α containing residues 1 to 178, and caveolin-1β containing residues 32-178 (Scherer et al., 1995). Both caveolin-1 and caveolin-2 are expressed in a wide range of tissues (Scherer et al., 1997; Smart et al., 1999), while caveolin-3 expression is muscle-specific (Tang et al., 1996).

The availability of caveolin-1 as a marker protein allowed the development of biochemical techniques for the isolation of specialized membrane domains, which co-purified with caveolin-1. The caveolin-associated membrane fraction was characterized by a low buoyant density in sucrose density gradients (Smart et al., 1995) and by insolubility in non-ionic detergents such as Triton X-100 (Sargiacomo et al., 1993). The

detergent-resistant membrane fractions were enriched in cholesterol, sphingomyelin, glycosphingolipids, and proteins that are anchored to the exoplasmic leaflet of the plasma membrane by glycosylphosphatidylinositol (GPI) anchors (Smart et al., 1999). Two additional proteins, flotillin-1 and flotillin-2, also associate with caveolar membranes in certain cell types (Smart et al., 1999). Flotillin-1 (reggie-2) was first identified in caveolin-rich membrane domains isolated from lung tissue and is a close homologue of flotillin-2 (also known as reggie-1 (Bickel et al., 1997)). Flotillin-1 and flotillin-2 have distinct tissue-specific expression patterns and can form stable hetero-oligomeric complexes with caveolins when co-expressed in the same cell (Volonte et al., 1999). Membrane fractions enriched in glycosphingolipids, sphingomyelin, cholesterol, and GPI-anchored proteins can also be isolated from cells lacking both caveolin expression and morphologically identifiable caveolae (Mirre et al., 1996; Wu et al., 1997). This data suggests similar membrane microdomains exist even in cells lacking caveolae. Studies of the composition of low density detergent-resistant membrane fractions also indicate that caveolae-like microdomains are likely to be present in certain intracellular membranes such as the Golgi (Brown and Rose, 1992; Gkantiragas et al., 2001; Kurzchalia et al., 1992; Nichols et al., 2001), endosomes (Helms and Zurzolo, 2004; Parton and Richards, 2003; Vetrivel et al., 2004), phagosomes (Dermine et al., 2001), and lysosomes (Taute et al., 2002).

Detergent insolubility of these membrane microdomains is thought to arise from the formation of a detergent-resistant liquid-ordered phase by cholesterol and sphingolipids containing saturated fatty acid chains (Ahmed et al., 1997). Although the inner leaflet of the membrane in these microdomains has not been extensively

characterized, it seems to be enriched in phospholipids with saturated fatty acids and cholesterol (Fridriksson et al., 1999). The high concentration of saturated hydrocarbon chains results in a tightly packed membrane structure characteristic of a liquid-ordered state, with cholesterol intercalated between the saturated fatty acid chains. In contrast, the surrounding membrane, which has higher concentrations of phospholipids with unsaturated, kinked fatty acid chains, is in a more fluid, liquid-disordered phase. Simons and Ikonen (Simons and Ikonen, 1997) coined the term "lipid rafts" to describe these liquid-ordered microdomains moving within the fluid lipid bilayer.

The nomenclature for these microdomains is highly variable and unstandardized. Caveolae are generally defined by both morphological and biochemical criteria (particularly their invaginated flask-like shape and enrichment in caveolin). Microdomains which are enriched in caveolin as well as those which lack caveolin and caveolar morphology have also been called detergent-insoluble glycolipid-rich membranes (DIGs), glycolipid-enriched membranes (GEMs), detergent-resistant membranes (DRMs), low-density Triton-insoluble domains, or caveola-like domains by various authors, based on biochemical standards alone. Consistent with the terminology proposed by Simons and Toomre (Simons and Toomre, 2000), in this discussion all liquid-ordered membrane microdomains will be referred to as lipid rafts. Thus, the term "lipid raft" will be used in a global sense to include caveolae and all other related microdomains. Some commonly used markers of lipid rafts are summarized in Table 1.1.

1.2 Lipid Rafts: Real or Artifact?

There has been considerable debate over the biological significance of purified detergent-resistant membrane fractions and their relationship to proposed lipid raft

Table 1.1. Lipid Raft Markers

Raft Marker	References
caveolin-1	(Rothberg et al., 1992)
caveolin-2	(Scherer et al., 1996)
caveolin-3	(Tang et al., 1996)
flotillin-1	(Bickel et al., 1997)
flotillin-2	(Bickel et al., 1997)
GPI-anchored proteins	(Harder and Simons, 1999)
Ganglioside GM1	(Harder et al., 1998)
Ganglioside GM3	(Iwabuchi et al., 1998)

domains *in vivo*, as some have argued that biochemically purified raft fractions themselves or the association of specific proteins with these fractions are detergent-induced artifacts (Brown and London, 1997; Lichtenberg et al., 2005; Mayor and Maxfield, 1995; Mayor et al., 1994; Munro, 2003; Nichols, 2005). In addition, several conventional immunofluorescence studies reported that GPI-linked proteins, glycosphingolipids, and/or sphingomyelin were clustered in membrane microdomains only after cross-linking by antibodies (Fujimoto, 1996; Mayor and Maxfield, 1995; Mayor et al., 1994). However, a substantial body of evidence exists supporting the hypothesis that lipid rafts are physiologically significant membrane compartments that exist in living cells even in the absence of cross-linking antibodies.

Examination of model membranes with physiologically relevant lipid compositions indicates that liquid-ordered and liquid-disordered phases coexist, and that liquid-ordered membrane microdomains are probably present in intact cells prior to detergent extraction (Ahmed et al., 1997; Dietrich et al., 2001; Hancock, 2006). Treatment of living cells with chemical cross-linkers results in the formation of oligomers of a GPI-linked form of growth hormone (Friedrichson and Kurzchalia, 1998). Oligomer formation was specific to the GPI-anchored protein, as a transmembrane form of growth hormone was not cross-linked in the equivalent experiment. Cholesterol depletion of cells, which is known to cause loss of morphologically evident caveolae as well as loss of various raft proteins (Pralle et al., 2000; Smart et al., 1999), was found to disrupt the clustering of GPI-anchored proteins and prevent oligomer formation (Friedrichson and Kurzchalia, 1998). This is consistent with the existence of multiple GPI-anchored proteins in lipid rafts on the surface of living cells. Harder *et al.,* (Harder et al., 1998)

cross-linked several GPI-anchored proteins and the raft ganglioside GM1, using antibodies and cholera toxin respectively, and examined the localization of these raft components by immunofluorescence. The raft markers were found in patches, which overlapped extensively with other raft markers, but were sharply separated from a non-raft marker. High resolution imaging studies in live cells using fluorescence resonance energy transfer-based approaches (Rao and Mayor, 2005; Sharma et al., 2004; Varma and Mayor, 1998; Zacharias et al., 2002), laser trap single particle tracking to measure the local diffusion of raft-associated proteins versus non-raft proteins (Kusumi et al., 2004; Pralle et al., 2000), and single molecule microscopy with a saturated lipid probe (Schutz et al., 2000) also support the existence of lipid rafts *in vivo,* although they are often too small (< 250-300 nm) to observe using conventional immunofluorescence in the absence of antibody cross-linking. The classic raft hypothesis proposes that rafts exist as stable lipid-based microdomains of approximately 50-100 nm in diameter, diffusing in the larger "sea" of liquid-disordered membrane, and that membrane proteins dynamically partition into and out of rafts (Edidin, 2003b; Simons and Ikonen, 1997). The size estimates of *in vivo* rafts obtained using microscopic approaches have varied depending on the particular techniques and probes used, however most of the high resolution imaging studies referenced above appear to be more consistent with a model in which much smaller relatively unstable raft domains (less than 10 to 30 nm) are present within the plasma membrane of resting cells. These unstable rafts are thought to be captured and stabilized by interactions with lipid-anchored and transmembrane proteins, resulting in the formation of larger raft assemblies in response to different physiological stimuli,

such as the activation of signalling receptors (for review see (Edidin, 2003b; Hancock, 2006; Kusumi et al., 2004)).

Given that much current knowledge of raft composition and function is based on the analysis of low density detergent-resistant membrane fractions, it is important to consider the relationship of these preparations to what is known regarding the physical properties of rafts *in vivo*. It is clear that there are properties of detergent-resistant membrane fractions that do not correlate with what is known of raft structure and organization *in vivo*. Notably, the size, stability and dynamic behaviour of lipid rafts in living cells cannot be accurately measured by analysis of detergent-insoluble material. For example, when detergent-resistant membrane preparations are examined by electron microscopy (EM), they are observed to be a heterogeneous collection of vesicles, ranging in size from 0.1 to 1 μM in diameter, and sometimes sheets of membrane are also seen (Brown and Rose, 1992; Gafencu et al., 1998; Mirre et al., 1996; Petrie and Deans, 2002; Westermann et al., 1999). However, it is unlikely that these vesicles and sheets existed in the same manner in intact cells. Examination of caveolae in intact adipocyte membranes by EM showed flask-like invaginations about 80 nm in diameter, smaller than many of the purified caveolin-rich detergent-resistant vesicles that had an average size between 100 and 200 nm (Westermann et al., 1999). Furthermore, examination of coverslip-grown cells by light microscopy following detergent extraction revealed what appeared to be a continuous plasma membrane sheet, interrupted by round holes (Mayor and Maxfield, 1995). Both of these observations are consistent with a model in which much smaller rafts coalesce during detergent solubilization of neighbouring non-raft membrane (Shogomori and Brown, 2003). Some studies have shown that detergent insolubility can

underestimate domain associations of certain proteins that are selectively solubilized (Arni et al., 1998; Schroeder et al., 1998; Shogomori and Brown, 2003) and the amount of cellular lipid isolated in these fractions may be increased by lysis at low temperatures (Shogomori and Brown, 2003). However, artifactual creation of domains from previously homogenous bilayers and the recruitment of unassociated proteins into raft fractions during lysis does not seem to occur (Ostermeyer et al., 1999). In addition, there is often a strong correlation between the presence of proteins in rafts assayed by detergent-independent methods, and their enrichment in detergent-resistant membrane fractions (Gupta and DeFranco, 2003; Janes et al., 1999; Shogomori and Brown, 2003; Shu et al., 2000; Viola et al., 1999; Wu et al., 1997). Taken together, all of the above data indicate that, while detergent-resistant raft fractions are not identical in composition or structure to the rafts present *in vivo* prior to detergent lysis, the proteins and lipids present in these fractions are nevertheless largely derived from *bona fide* raft domains present in living cells. Furthermore, an observed enrichment in detergent-resistant membrane fractions strongly suggests that a given protein can associate with rafts *in vivo*.

1.3 Lipid Rafts in Signal Transduction

There is evidence of a role for lipid rafts in a wide array of cellular processes including: 1) transcytosis (Nyasae et al., 2003; Simionescu, 1983), 2) potocytosis (Anderson et al., 1992), 3) an alternative route of endocytosis (Helms and Zurzolo, 2004; Ikonen, 2001; Smart et al., 1999), 3) internalization of toxins, bacteria and viruses (Fivaz et al., 1999; Manes et al., 2003; Parton et al., 1994; Shin et al., 2000), 4) cholesterol transport (Oram and Yokoyama, 1996; Parton, 2003; Smart et al., 1996), 5) calcium homeostasis (Isshiki and Anderson, 1999; Lohn et al., 2000), 6) protein sorting (Ikonen,

2001; Simons and Ikonen, 1997), and 7) signal transduction. The remainder of this discussion will focus on the role of lipid rafts as cellular signalling centres.

Biochemical analysis of the protein composition of purified lipid rafts in a large number of different cell types shows a striking concentration of signalling molecules within lipid rafts (Chang et al., 1994a; Hope and Pike, 1996; Lisanti et al., 1994b; Wu et al., 1997) (Table1.2). On the basis of these observations, a role for lipid rafts in mediating signal transduction has been proposed (Anderson, 1993; Okamoto et al., 1998; Simons and Ikonen, 1997; Simons and Toomre, 2000). In principle, lipid rafts can modulate signalling events in a variety of ways (Figures 1.1 and 1.2). By localizing all of the components of specific signalling pathways within a membrane compartment, lipid rafts could enable efficient and specific signalling in response to stimuli (Figure1.1a). Translocation of signalling molecules in and out of lipid rafts could then control the ability of cells to respond to various stimuli (Figure 1.1b and 1.1c). Differential localization of signalling molecules to lipid rafts versus the bulk plasma membrane could control the access of signalling molecules to each other. For example, a protein activated by phosphorylation might be sequestered within a lipid raft and prevented from interacting with an inactivating phosphatase. The unique raft microenvironment is also capable of altering the behaviour of signalling proteins (Martens et al., 2000). Cross-talk between different signalling pathways could be facilitated if the molecules involved were localized to the same lipid raft. Distinct subpopulations of rafts present on the surface of the same cell might be specialized to perform unique functions (Figure 1.2a). Movement or clustering of lipid rafts could be an efficient means of transporting pre-assembled signalling complexes to specific membrane areas upon stimulation, for example, in

Table 2.2. Protein and Lipid Signalling Molecules Identified in Lipid Rafts

Protein/Lipid	Reference
Transmembrane receptors	
EGF receptor	(Furuchi and Anderson, 1998)
Bradykinin B2 receptor	(Haasemann et al., 1998)
Eph family receptors	(Wu et al., 1997)
TCR	(Xavier et al., 1998)
BCR	(Cheng et al., 1999)
FcεRI	(Holowka et al., 2000)
β1 integrin	(Yebra et al., 1999)
GPI-anchored proteins	
CD59	(Murray and Robbins, 1998)
uPAR	(Stahl and Mueller, 1995)
Ephrin A5	(Davy et al., 1999)
Signalling Effectors	
$G_{\alpha i1}$, $G_{\alpha i2}$, $G_{\alpha i3}$	(Stan et al., 1997)
Src family kinases	(Davy et al., 2000; Furuchi and Anderson, 1998; Liu et al., 1997a; Robbins et al., 1995)
Ras	(Furuchi and Anderson, 1998; Iwabuchi et al., 1998)
PKCα	(Liu et al., 1997a; Stan et al., 1997)
Shc	(Teixeira et al., 1999)
Adenylate cyclase	(Schwencke et al., 1999)
eNOS	(Oh and Schnitzer, 1999)
PLCγ	(Liu et al., 1997a)
PI3K	(Liu et al., 1997a)
SHIP	(Petrie et al., 2000)
Cbp/PAG	(Brdicka et al., 2000; Kawabuchi et al., 2000)
Lipid signalling molecules	
sphinogomyelin	(Fujimoto, 1996)
ceramide	(Liu and Anderson, 1995)
phosphoinositides	(Hope and Pike, 1996)
diacylglycerol	(Liu and Anderson, 1995)

Figure 1.1. Proposed roles of lipid rafts in signal transduction.

Compartmentalized signalling in lipid rafts may occur through a variety of different mechanisms. (A) The receptor (GPI and green rectangle) may be a constitutive resident of the lipid raft, initiating signalling within this site. (B) A cell surface receptor (blue) might reside outside of the raft but be translocated there on ligand binding. (C) Binding of ligand to a receptor (purple) located in lipid rafts may initiate a compartmentalized signal within the rafts (1) that is subsequently downregulated when the receptor complex translocates out of the raft (2). Alternatively, upon ligand binding, the receptor might translocate out of the raft, enabling its association with and activation of signalling molecules present in nonraft membrane (3). Segregation of signalling molecules in this manner could effectively inhibit signalling in the absence of ligand. As in the case of receptors, signals could also be dynamically modulated by translocation of downstream effectors in or out of lipid rafts. (D) The receptor system itself may not be localized within the lipid raft, but on its activation may communicate a signal to the raft that initiates a compartmentalized signal. Note: blue lipids—non-raft membrane; red lipids—raft membrane; yellow circle—receptor ligand; GPI—GPI-anchored protein; Src-f—Src family kinase; blue, green and pink ovals—cytoplasmic signalling proteins associated with raft or non-raft membrane as indicated.

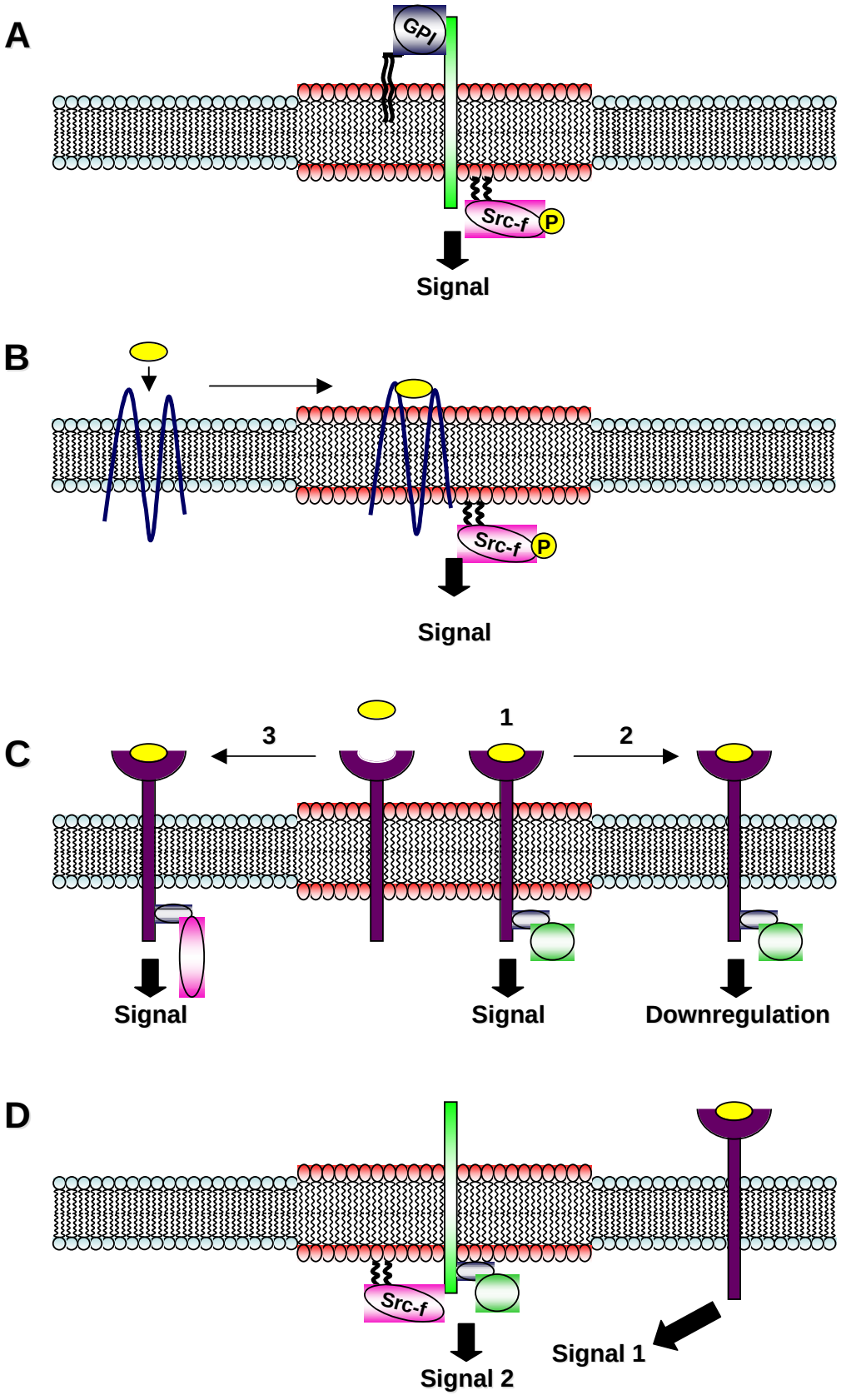
A
GPI
Src-f
P
Signal
B
Src-f
P
Signal
C
3
1
2
Signal
Signal
Downregulation
D
Src-f
Signal 2
Signal 1

Figure 1.2. Lipid rafts allow signalling specificity and formation of higher-order signalling complexes.

(A) Distinct subpopulations of lipid rafts (A and B) with unique protein and lipid compositions and correspondingly specialized functions may be present on the surface of the same cell. In this way, distinct lipid rafts could be involved in the compartmentalization of different signalling pathways. **(B)** Clustering of lipid rafts in response to certain stimuli could rapidly create higher-order signalling complexes that may amplify signals or enhance cross-talk between related signalling pathways (for example, costimulatory signals). Signalling events and interactions with the cell's cytoskeleton are likely to be involved in regulating the clustering of lipid rafts as well as the association of individual proteins with lipid rafts. Clustered rafts might be homogeneous in composition (as indicated by clustering of multiple rafts of the same colour), or they might form spatially organized arrays of different raft subsets (rafts of distinct lipid and protein composition are symbolically represented by different colours in this drawing). Controlled localization of raft clusters to specific areas of the cell membrane would permit spatial regulation of signal transduction, a mechanism that may be important in polarized or migrating cells.

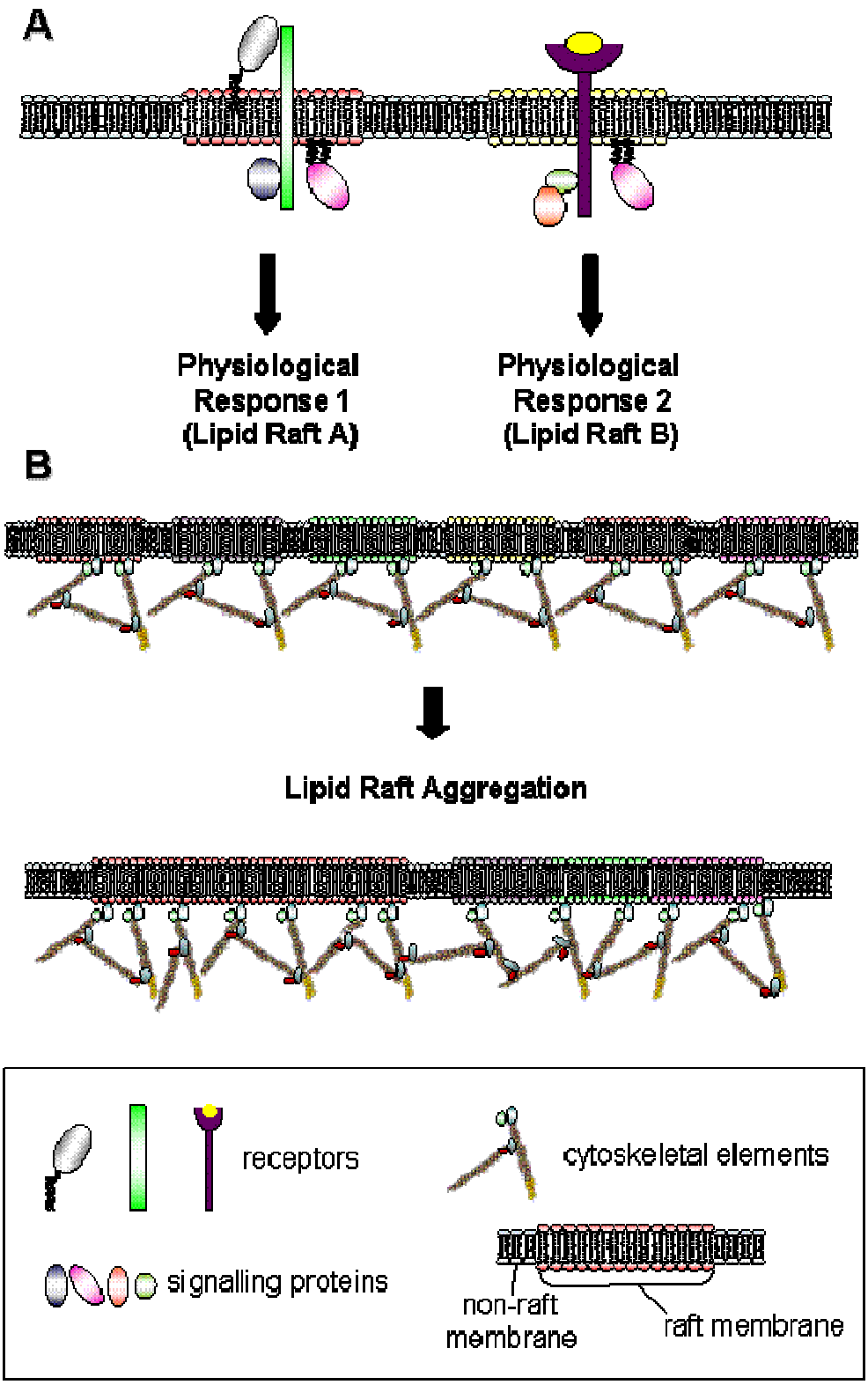
A
Physiological Response 1 (Lipid Raft A)
Physiological Response 2 (Lipid Raft B)
B
Lipid Raft Aggregation
receptors
cytoskeletal elements
signalling proteins
non-raft membrane
raft membrane

polarized or migrating cells (Figure 1.2b). Formation of higher-order signalling complexes by clustering of one or more types of lipid rafts could allow amplification or modulation of signals in a spatially regulated manner. All of the above mechanisms imply that lipid rafts would play an active role in facilitating efficient and specific signalling. However, lipid rafts might also be involved in negatively regulating signals by sequestering signalling molecules in an inactive state.

To date, a large body of evidence has accumulated which confirms the presence of multiple signal transduction pathways with diverse biological effects within lipid raft compartments. This includes signalling mediated by G protein coupled receptors (Becher and McIlhinney, 2005; Haasemann et al., 1998), the epidermal growth factor receptor (EGFR) (Waugh et al., 1999), the platelet-derived growth factor receptor (PDGFR) (Liu et al., 1996), and various GPI-linked proteins (Chapman, 1997; Murray and Robbins, 1998). Compartmentalized signalling in response to insulin (Stralfors, 1997) and fibroblast growth factor-2 (FGF-2) (Davy et al., 2000) has been observed and lipid rafts are also sites of calcium signalling (Isshiki and Anderson, 1999; Lohn et al., 2000). Even our preliminary understanding of the regulation of these compartmentalized signalling pathways clearly indicates that many of the proposed mechanisms by which lipid rafts might control signal transduction are physiologically important, and that lipid rafts may be capable of modulating signal transduction in novel and unanticipated ways.

1.3.1 Growth Factor Receptor Signalling

Downstream components of several growth factor-stimulated signalling pathways including EGF (Anderson, 1998; Smart et al., 1995), PDGF (Liu et al., 1997b; Liu et al., 1996), FGF-2 (Davy et al., 2000; Ridyard and Robbins, 2003), and insulin (Corley

Mastick et al., 1995; Gustavsson et al., 1999; Inokuchi, 2006), are concentrated within lipid rafts. The EGFR and the PDGFR are enriched within lipid rafts in unstimulated cells and activation of tyrosine phosphorylation cascades is observed in rafts upon treatment with EGF or PDGF (Anderson, 1998; Liu et al., 1996; Smart et al., 1995). Early signalling events induced by EGF or PDGF, including activation of tyrosine kinase activity, protein phosphorylation, and, in the case of EGF, recruitment of adaptor proteins and MAPK activation, all appear to occur within lipid rafts (Anderson, 1998; Liu et al., 1996; Stehr et al., 2003). This suggests that signalling via EGF or PDGF is initiated within lipid rafts, and that significant portions of these signalling pathways are organized and co-localized in lipid rafts. Downregulation of the EGF- and PDGF-mediated signals correlated with the loss of the EGF and PDGF receptors from lipid rafts, suggesting a model in which migration of receptors out of lipid rafts following growth factor stimulation is required for their subsequent internalization (and downregulation) by clathrin-dependent endocytosis (Liu et al., 1996; Mineo et al., 1999) (Figure 1.1c). Alternatively, a more recent study suggests that endocytic proteins may be recruited to rafts after EGFR activation, enabling receptor internalization through crosstalk between raft domains and clathrin-coated pits (Puri et al., 2005).

Although the above evidence suggests that both EGFR and PDGFR signals are activated within lipid rafts, other evidence is somewhat contradictory, as it implies that EGFR and PDGFR signalling may be inhibited by sequestration in rafts. Depletion of plasma membrane cholesterol (and disruption of rafts) causes loss of EGFR from detergent-insoluble raft fractions, increased binding of EGF, increased dimerization of the EGFR, and hyperphosphorylation of the EGFR (Pike and Casey, 2002; Ringerike et

al., 2002; Roepstorff et al., 2002). Similarly, PDGF receptors were found to interact specifically with caveolin-1 and caveolin-3, and this interaction inhibited PDGFR kinase activity *in vitro* (Yamamoto et al., 1999). Interestingly, addition of PDGF to cells stimulated sterol efflux and tyrosine phosphorylation of caveolin-1 and led to a transient loss of caveolin-1 associated sterol (Fielding et al., 2004; Fielding et al., 2002). The loss of caveolin-associated sterols was accompanied by an increase in PDGF-dependent protein kinase activity, but sterol loss was only transient, as caveolin was soon relipidated. Based on these observations, it is possible that coordination of cholesterol homeostasis and signalling in rafts is one mechanism that regulates the relative levels of PDGF receptor activation (or inhibition) in both basal and stimulated cells.

Crosstalk between the PDGFR and EGFR pathways appears to occur within lipid raft domains, although again, the details vary depending on the particular experimental context. PDGF stimulation of PDGFR in raft fractions was shown to cause tyrosine phosphorylation of EGFRs present in the same membrane fraction, resulting in a marked decline in the ability of the EGFR to bind EGF (Liu and Anderson, 1999). In contrast, EGF treatment of cells did not cause a reciprocal tyrosine phosphorylation of raft-associated PDGFR (Liu and Anderson, 1999). In this case, specific and unidirectional cross-talk between the PDGFR and the EGFR is apparently facilitated by the co-localization of both signalling pathways within lipid rafts. In a separate study, pre-treatment of cells with EGF prevented subsequent activation of the PDGFR via a mechanism that is thought to involve sequestration of the PDGFR in caveolae in a manner which prevented PDGFR binding to ligand (Matveev and Smart, 2002). Thus, though the detailed mechanisms involved must still be clarified, it appears that regulation

of EGF and PDGF-mediated signals are closely coordinated within rafts. Transactivation of the EGFR by several GPCRs is also thought to occur within rafts, providing additional examples of how crosstalk between different extracellular signals is integrated within these domains (Hua et al., 2003; Hur et al., 2004).

Treatment of LAN-1 human neuroblastoma cells with FGF-2 also results in tyrosine phosphorylation of a number of proteins within lipid rafts, a response which requires the activation of Fyn and Lyn, two Src family kinases localized in lipid rafts (Davy et al., 2000; Ridyard and Robbins, 2003). Although LAN-1 cells express FGFR-2, neither this receptor nor any of the other three FGFRs was found in purified raft fractions. It is possible that the compartmentalized signal is initiated by binding of FGF-2 to an alternative receptor that translocates to or is constitutively present in lipid rafts, such as a heparan sulphate proteoglycan (Gleizes et al., 1996; Quarto and Amalric, 1994). Alternatively, binding of FGF-2 to a receptor outside of lipid rafts, which then communicates a signal to the rafts (Figure 1.1d), could initiate the compartmentalized signal.

Both insulin and EGF have been shown to induce tyrosine phosphorylation of caveolin-1 (Corley Mastick et al., 1995; Kim et al., 2000). Caveolin-1 has been shown to bind raft signalling components including Gα subunits, Ha-Ras, c-Src, PDGFR, and endothelial nitric oxide synthase (eNOS) and seems to inhibit their function, consistent with the idea that lipid rafts might negatively regulate signalling by sequestering molecules in an inactive state (Okamoto et al., 1998). The functional consequences of caveolin-1 phosphorylation are unclear, although it is interesting to speculate that it could affect the ability of caveolin-1 to bind to signalling molecules or cholesterol and/or affect

caveolar structure. In support of this model, phosphorylation of caveolin is correlated with loss of caveolin-bound sterols following activation of the PDGFR (Fielding et al., 2004). Insulin also induces the generation of second messengers within lipid rafts that are responsible for many of insulin's biological effects. A glycolipid found in rafts, similar in structure to the GPI anchors of proteins, is hydrolysed in an insulin-dependent manner to produce an inositolphosphoglycan and diacylglycerol (Stralfors, 1997). The inositolphosphoglycan appears to mediate metabolic effects of insulin by controlling the phosphorylation state of key regulatory enzymes (Stralfors, 1997). The diacylglycerol produced appears to regulate the translocation of the GLUT4 glucose transporter from intracellular membranes to lipid rafts in the plasma membrane where glucose uptake occurs (Gustavsson et al., 1996; Stralfors, 1997). It is not clear whether the insulin receptor itself is localized to lipid rafts, as some investigators have been able to detect it in these compartments but others have not (Corley Mastick et al., 1995; Gustavsson et al., 1999; Inokuchi, 2006). Thus it is unclear whether the insulin receptor initiates its signalling cascade within the lipid rafts, or whether a signal generated by the receptor outside of the lipid rafts is communicated to raft components to initiate the compartmentalized signalling.

1.3.2 Signalling by GPI-anchored Proteins

Compartmentalized signalling has also been observed when a number of GPI-anchored proteins present in lipid rafts are cross-linked by antibodies or by physiologically relevant ligands (Table 1.3). Signalling by GPI-anchored proteins is intriguing, because these proteins have no transmembrane or cytoplasmic domains (Figure 1.3). Therefore, it is unclear how these proteins can effectively communicate a

Table 1.3. GPI-anchored proteins capable of signalling.

Protein	Function	Reference
uPAR	Cell adhesion and migration, localized proteolysis	(Ossowski and Aguirre-Ghiso, 2000)
Thy-1	Activation of T cell, mast cells and basophils	(Draberova et al., 1996; Thomas and Samelson, 1992)
CD59	Inhibition of complement-mediated lysis	(Murray and Robbins, 1998)
CD14	Lipopolysaccharide coreceptor, cytokine expression	(Lund-Johansen et al., 1993)
GFRα	Differentiation	(Saarma, 2000)
CD16	FcγRIIIB; cytokine expression and oxidative burst	(Lund-Johansen et al., 1993)
CD55	Inhibition of complement-mediated lysis; cytokine expression, monocyte activation	(Lund-Johansen et al., 1993)
CD48	Cell adhesion	(Garnett et al., 1993)
CD67	Granulocyte activation	(Lund-Johansen et al., 1993)
CD24	Ligand for P-selectin, activation of cell aggregation	(Sammar et al., 1997)
Ly-6	Cell adhesion; activation of hematopoietic cells	(Gumley et al., 1995)
Ephrin A5	Neuronal guidance; cell adhesion and morphology	(Davy et al., 1999; Davy and Robbins, 2000)
TAG-1	Cell adhesion molecule	(Kasahara et al., 2000)

Protein	Function	Reference
Nogo-66	Inhibits axon regeneration	(Fournier et al., 2001)
PrPC	Cellular isoform of prion protein; lymphocyte activation	(Cashman et al., 1990)
CNTFR α	Cell survival	(Davis et al., 1993)
Gas1	p53-dependent growth suppression	(Ruaro et al., 2000)
CD157	Regulation of myeloid and B cell growth and differentiation	(Itoh et al., 1998; Okuyama et al., 1996)
CD73	purine salvage enzyme; costimulatory molecule in activated T cells	(Resta and Thompson, 1997)
mono (ADP-ribosyl) transferase	neutrophil chemotaxis	(Allport et al., 1996)

Figure 1.3. The structure of the GPI anchor.

All characterized GPI anchors share the common core structure shown here. Phosphatidylinositol is linked through carbon 6 of the inositol ring to a glycan core structure. The terminal mannose residue of the glycan core is linked to phosphoethanolamine by a phosphodiester linkage. The GPI anchor is attached to the protein's C-terminal carboxyl group by an amide linkage to the amino group of phosphoethanolamine. GPI anchors exhibit considerable structural diversity in both the lipid and glycan cores due to substitutions in or additions to the core structure. The fatty acid chains of the phosphatidylinositol lipid core can vary in chain length or saturation and the inositol ring is sometimes acylated (generally by palmitate) at positions 2 or 3. In addition, the glycan core may be differentially modified with the addition of additional sugar residues and/or phosphoethanolamine residues to the sugars in the glycan core. The biological significance of these structural variations is unknown, but it is thought that they may be important for controlling the lateral associations of GPI-anchored proteins with other proteins and lipids in the plasma membrane (Varki et al., 1999). Note: INOS, inositol; GLU, glucose; MAN, mannose.

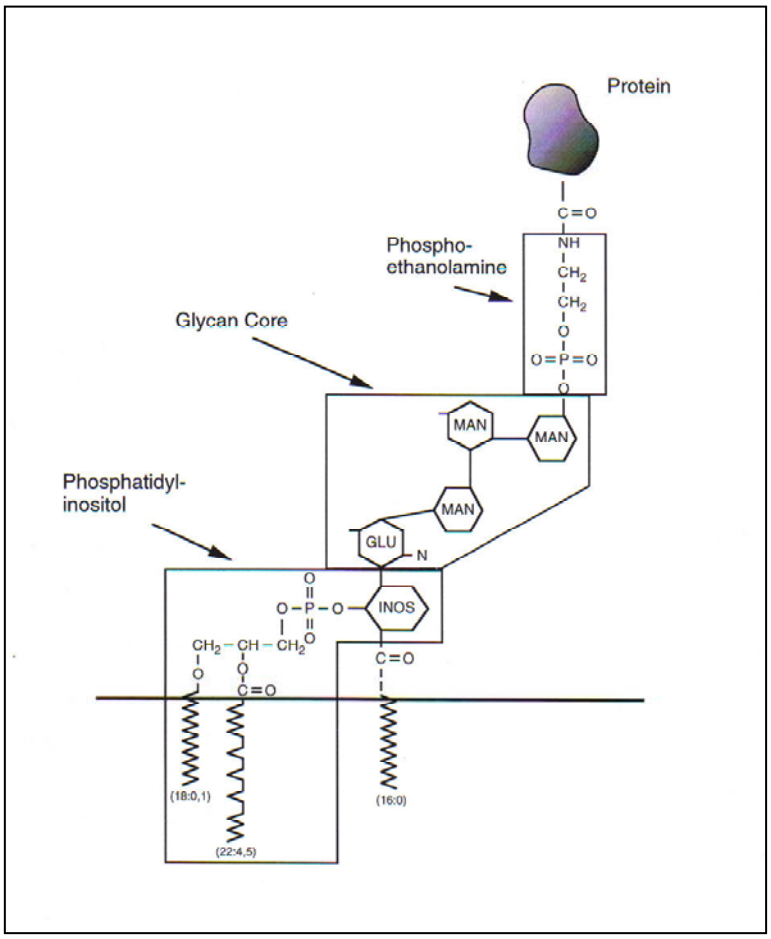
Protein
C=O
NH
CH2
CH2
O
O=P=O
O
Phospho-
ethanolamine
Glycan Core
MAN
MAN
MAN
GLU
N
Phosphatidyl-
inositol
INOS
O
O-P-O
O
CH2-CH-CH2
O
O
C=O
C=O
(18:0,1)
(22:4,5)
(16:0)

signal to intracellular signalling effectors. This is particularly relevant as downstream signalling events induced by GPI-linked proteins often involve cytoplasmic non-receptor tyrosine kinases, particularly the Src family kinases, which also lack transmembrane domains (Davy et al., 1999; Garnett et al., 1993; Murray and Robbins, 1998; Shenoy-Scaria et al., 1993; Stefanova et al., 1993). The Src family kinases are localized to the plasma membrane as a result of acylation modifications (Robbins et al., 1995), and are often found enriched within lipid rafts (see Table 1.2). It is thought that interaction of the GPI-anchored proteins with transmembrane adaptor proteins is required (Figure 1.1a), although in many cases identification of these adaptor proteins remains elusive. Alternatively, a "second messenger" mechanism, in which enzymatic cleavage of a GPI-anchored protein by a specific phospholipase releases signalling mediators, has been proposed as a mechanism of GPI-linked protein signalling (Chan et al., 1989; Movahedi and Hooper, 1997).

An example of a GPI-anchored protein which signals using a transmembrane adaptor protein is GFRα1, which transduces a signal in lipid rafts after binding to its ligand, GDNF, a growth factor important in nervous system and kidney development (Saarma, 2000; Sariola and Saarma, 2003). GDNF binding to the lipid raft-localized GFRα1 results in the recruitment of the transmembrane receptor tyrosine kinase Ret to lipid rafts and association with Src, which is required for effective downstream signalling (Tansey et al., 2000). GFRα1 and Ret are not co-localized prior to GDNF stimulation, but their co-localization in lipid rafts following GDNF treatment appears to be required for at least part of the induced signalling, as disruption of rafts by cholesterol depletion of cells decreases GDNF signalling. Surprisingly, soluble GFRα1 released from cells is

also capable of recruiting Ret to lipid rafts and mediating the prolonged effects of GDNF on target cells (Paratcha et al., 2001). The situation becomes even more complex, as there is evidence that GDNF can also signal through GFRα1 via a Ret-independent mechanism that involves Src family kinase activity (Poteryaev et al., 1999; Sariola and Saarma, 2003; Trupp et al., 1999). Heparan sulphate proteoglycans and the transmembrane p140 isoform of neural cell adhesion molecule (NCAM) may act as transmembrane adaptors in the absence of Ret (Sariola and Saarma, 2003). Ret can also trigger different signalling pathways depending on whether it is located inside or outside of lipid rafts (Sariola and Saarma, 2003; Simons and Toomre, 2000). Overall, these findings suggest that lipid rafts play specific and specialized roles in both GFRα and Ret signalling pathways.

The Eph receptor tyrosine kinases and their surface-bound ligands, the ephrins, have key roles in developmental processes such as angiogenesis and axonal guidance (Drescher et al., 1997; Yancopoulos et al., 1998). Binding of GPI-anchored ephrin-A5 to its cognate receptor (EphA5) initiates two signals—one signal propagated by the transmembrane EphA5 receptor, and a second signal that is transduced through the GPI-anchored ephrin-A5 in lipid rafts. The ephrin-A5 induced signalling results in increased tyrosine phosphorylation of several raft proteins and recruitment of the Src family kinase Fyn to lipid rafts (Davy et al., 1999). Changes in cellular architecture and adhesion that occur in response to the ephrin-A5 mediated signal are dependent on the activity of Fyn (Davy et al., 1999). Ephrin-A5 appears to modulate cell adhesion and morphology by regulating the activation of β1 integrin through "inside-out" signalling (Davy and Robbins, 2000). It is possible that β1 integrin functions as a transmembrane adaptor

protein by interacting directly with ephrin-A5. This has been shown for uPAR, another GPI-anchored protein that regulates cellular adhesion and migration via a signalling cascade involving Src family kinases (Ossowski and Aguirre-Ghiso, 2000). The uPAR-integrin interaction is dependent on the presence of caveolin, which can also modulate integrin function (Wary et al., 1998; Wei et al., 1999), although it is not clear whether caveolin is involved in ephrin-A5 signalling (Davy and Robbins, 2000). Alternatively, ephrin-A5 may modulate β1 integrin function indirectly.

1.3.3 Multicomponent Immune Receptor Signalling

The dynamic nature of lipid rafts is also revealed by studies of a number of different receptor systems in hematopoietic cells, which usually do not express caveolin or have caveolae (Fra et al., 1994; Fra et al., 1995; Parolini et al., 1996). Lipid rafts have been implicated in signalling via the T-cell receptor (TCR) (Janes et al., 2000; Kabouridis, 2006; Langlet et al., 2000), the B-cell receptor (BCR) (Cheng et al., 2001; Cheng et al., 1999; Matsuuchi and Gold, 2001), the IgE receptor (FcεRI) (Holowka et al., 2000) as well as the IL-2 receptor (Marmor and Julius, 2001).

Engagement of TCR complexes by peptide-MHC complexes on the surface of antigen-presenting cells (APCs) leads to the formation of a highly ordered structure at the interface between the T cell and the APC known as the immunological synapse or the supramolecular activation cluster (SMAC) (Grakoui et al., 1999; Leitenberg et al., 2001; Monks et al., 1998). The formation of SMACs may enhance TCR signalling by bringing positive signalling effectors into close proximity, while excluding negative signalling molecules (Freiberg et al., 2002; Janes et al., 1999). SMACs may also be important in integrating costimulatory signals with TCR stimulation (Balamuth et al., 2004; Fragoso et

al., 2003; Gaus et al., 2005; Janes et al., 2000). Several lines of evidence suggest that clustering or aggregation of lipid rafts contributes to the formation of SMACs and that lipid rafts are important in TCR signalling (Balamuth et al., 2004; Fragoso et al., 2003; Gaus et al., 2005; Janes et al., 1999; Janes et al., 2000; Viola, 2001; Viola et al., 1999). It is not clear whether the TCR is constitutively associated with lipid rafts, as different studies have shown that TCR complexes are excluded from, or only weakly associated with isolated raft fractions in unstimulated T cells; however, upon TCR activation, the concentration of TCR complexes associated with lipid raft fractions greatly increases (Drevot et al., 2002; Janes et al., 2000; Montixi et al., 1998; Viola, 2001). Key signalling effectors downstream of the TCR, including Lck, Fyn, LAT, ZAP-70, Vav, PLCγ, PKCθ, PI3K and Grb2 have been found in detergent-resistant raft fractions upon activation of the TCR (Bi and Altman, 2001; Brdicka et al., 1998; Janes et al., 2000; van't Hof and Resh, 1999; Xavier et al., 1998; Zhang et al., 1998a; Zhang et al., 1998b). Disruption of lipid rafts by treatment with methyl-β-cyclodextrin or polyunsaturated fatty acids (PUFAs) caused these proteins to dissociate from lipid rafts and inhibited TCR signalling (Moran and Miceli, 1998; Webb et al., 2000; Xavier et al., 1998). Similarly, raft localization of Lck, and Fyn is essential for their role in TCR signalling, as mutants that localize outside of rafts are unable to participate in signalling (Kabouridis et al., 1997; van't Hof and Resh, 1999). A LAT mutant protein that was unable to be palmitoylated failed to localize to lipid rafts, and was unable to support signalling downstream of ITAM phosphorylation (Zhang et al., 1998b). However, a recent study using a transmembrane domain mutant of LAT concluded that raft localization of LAT was not essential for its signalling function (Zhu et al., 2005). More work is needed to clarify the role of rafts in

LAT-mediated signalling downstream of the TCR. Immunofluorescence studies examining localization of a raft marker, ganglioside GM1, suggest that signalling by the costimulatory molecule CD28 may amplify TCR signalling by promoting the redistribution and clustering of lipid rafts at the site of TCR engagements (Viola et al., 1999). Similarly, PKCθ, which translocates to low density detergent-insoluble membrane fractions in activated T cells (Bi et al., 2001), also translocates to the site of cell contact between T cells and APCs, where it co-localizes with the TCR in the central core of the SMAC upon TCR-induced T cell activation (Monks et al., 1998; Monks et al., 1997). In unstimulated T cells, immunofluorescence data showed that GM1-enriched lipid rafts are distributed homogenously around most of the plasma membrane, while PKCθ was localized in the cytoplasm (Bi et al., 2001). In T cells activated by incubation with APCs pulsed with antigenic peptides, clustering of both GM1 and PKCθ at the site of SMAC formation between T cells and APCs was observed (Bi et al., 2001), suggesting that PKCθ translocates to lipid rafts, which become clustered at the immunological synapse. Raft localization of PKCθ was shown to be important in PKCθ-mediated NFκB activation, providing evidence that association of PKCθ with rafts is important for its signalling functions downstream of the TCR (Bi et al., 2001). The actin cytoskeleton has been implicated in controlling the composition and redistribution of lipid rafts (Leitenberg et al., 2001; Penninger and Crabtree, 1999) (Figure 1.2b). In the case of PKCθ, a pathway involving Vav and Rac appears to mediate the reorganization of the actin cytoskeleton that regulates the translocation of PKCθ observed upon TCR-induced T cell activation (Villalba et al., 2000). As many other lipid raft-associated molecules are

also localized at the immunological synapse (Bromley et al., 2001; Janes et al., 2000; Leitenberg et al., 2001; Montixi et al., 1998), this suggests that lipid rafts are important in the formation and organization of SMACs (Leitenberg et al., 2001). However, the exact relationship between lipid rafts and SMACs has not been clearly established (discussed in (Leitenberg et al., 2001)). The involvement of lipid rafts in early TCR signalling events is uncertain, as some have suggested that initial signalling may occur independently of lipid rafts, with lipid rafts instead acting at a later stage to sustain and amplify TCR signalling pathways (Kabouridis, 2006; Leitenberg et al., 2001). In addition, portions of the immunological synapse may form by raft-independent mechanisms (van der Merwe et al., 2000). Despite this uncertainty, the available evidence suggests that lipid rafts do have a significant role in signal transduction downstream of the TCR. One means by which lipid rafts might regulate TCR signalling is by controlling the segregation of positive and negative signalling effectors (a mechanism also proposed for SMACs, as mentioned previously). An example is the role of the raft-associated transmembrane adaptor protein Cbp/PAG, which binds the tyrosine kinase Csk, a major negative regulator of Src family kinases (Brdicka et al., 2000; Takeuchi et al., 2000). In resting T cells Csk is constitutively present in lipid rafts, due to its association with Cbp/PAG (Brdicka et al., 2000). After activation of peripheral blood T cells, PAG becomes rapidly dephosphorylated and dissociates from Csk, leading to loss of Csk from lipid rafts (Torgersen et al., 2001). This is consistent with a model in which Csk negatively regulates the activity of raft-associated Src family kinases in unstimulated T cells, while loss of Csk from rafts following TCR activation enables activation of Src family kinases required for signalling downstream of the TCR. The raft association of the tyrosine

phosphatase CD45, which has both positive and negative roles in TCR signalling, also seems to be tightly controlled (see (Kabouridis, 2006) and references therein). A small fraction of CD45 appears to be present within lipid rafts when TCR signalling is initiated, where it functions to dephosphorylate and activate Lck. However, later on CD45 appears to be excluded from rafts, and this may be critical for sustained signalling downstream of the TCR.

In addition to their role in TCR signalling, lipid rafts appear to aggregate in a polarized fashion at the site of target recognition upon formation of conjugates between natural killer cells and sensitive tumour cells (Inoue et al., 2002; Lou et al., 2000). Lipid rafts in resting mast cells and subsequent clustering of rafts during FcεRI signalling have been observed by immunogold labeling of raft-associated signalling molecules and electron microscopy (Wilson et al., 2000; Wilson et al., 2001) and cholesterol depleting agents inhibit FcεRI signalling (Shakarjian et al., 1993; Sheets et al., 1999). The FcεRI appears to translocate into lipid rafts upon ligand-binding (Field et al., 1997; Field et al., 1999). Engagement of the B cell protein CD20 by antibody cross-linking also causes it to rapidly redistribute to lipid rafts where signalling events are likely to occur (Deans et al., 2002; Deans et al., 1998; Janas et al., 2005; Unruh et al., 2005) (Figure 1.1b). A membrane-proximal sequence in the cytoplasmic carboxyl tail of CD20 is required for translocation to rafts following cross-linking (Polyak et al., 1998). Similarly, upon cross-linking the BCR translocates rapidly into a lipid raft containing the Src family kinase Lyn, which is involved in the initial phosphorylation events in the BCR signal cascade (Cheng et al., 1999; Petrie et al., 2000). CD45 was excluded from lipid rafts in both resting B cells, and B cells following BCR cross-linking (Cheng et al., 1999). This

observation is reminiscent of the segregation of positive and negative signalling components seen in TCR signalling and illustrates the fact that some signalling molecules are excluded from lipid rafts. In immature B cells, the BCR does not translocate into lipid rafts after cross-linking and signalling initiated outside of rafts leads to apoptosis instead of activation (Sproul et al., 2000). In mature B cells infected with Epstein-Barr virus, the presence of the latent viral protein LMP2A in lipid rafts prevents BCR translocation into rafts and blocks BCR signalling (Dykstra et al., 2001). These two studies indicate that controlling the access of the BCR to lipid rafts can dramatically affect the signalling capability of antigen-bound BCR.

Lipid rafts also appear to be involved in regulation of signalling by a number of cytokine receptors, including the interleukin-2 (IL-2) and interleukin-15 (IL-15) receptors (Marmor and Julius, 2001; Matko et al., 2002; Vamosi et al., 2004). Antibody or ligand-mediated immobilization of multiple different raft components, including GPI-anchored proteins and the GM1 ganglioside, was shown to inhibit IL-2-induced proliferation in murine T cells. IL-2 receptor α (IL-2Rα) was enriched in purified raft fractions, whereas most of the IL-2Rβ and IL-2Rγ was localized to detergent-soluble membranes. IL-2R signalling also appeared to occur in soluble membranes as IL-2 induced tyrosine phosphorylation of JAK1 and JAK3 occurred exclusively in soluble membrane fractions and was not inhibited by cholesterol depletion with methyl-β-cyclodextrin (MβCD). In addition, cross-linking experiments showed that IL-2Rα bound to radioactively labelled IL-2 formed a heterotrimeric receptor complex with IL-2Rβ and IL-2Rγ in detergent-soluble membranes but not in lipid rafts (Marmor and Julius, 2001). Immobilization of

raft components was associated with increased enrichment of IL-2Rα in lipid rafts, suggesting that immobilization of raft components affected the ability of IL-2Rα to dissociate from lipid rafts and form an active signalling complex with the IL-2Rβ and IL-2Rγ chains in detergent-soluble membranes (Marmor and Julius, 2001), consistent with Figure 1.1c). While it is possible that the binding of IL-2 to raft-associated IL-2Rα causes its translocation to detergent-soluble membranes, it is also possible that IL-2Rα is in a dynamic equilibrium between lipid rafts and soluble membranes, and that IL-2 binds to IL-2Rα in soluble membranes to initiate signalling. Modulation of raft components that affected the mobility of the IL-2Rα and/or shifted the equilibrium between rafts and soluble membranes would therefore be expected to affect IL-2-dependent signalling. In contrast to these results, studies using FRET, confocal microscopy, and biochemical fractionation showed that IL-2Rα, IL-2Rβ, and IL-2Rγ are constitutively localized to lipid rafts in human T cell lymphoma and leukemia cell lines, and that cholesterol depletion inhibited IL-2 dependent tyrosine phosphorylation of STATs (Matko et al., 2002; Vamosi et al., 2004). It is possible that the regulatory role of lipid rafts in IL-2R signalling may be cell- or species-specific, and more studies in the future are needed to clarify the function of rafts in IL-2R signalling. In general however, lipid rafts appear to have a key regulatory function in the control of intermolecular interactions between signalling components of the IL-2 pathway.

Overall, the studies of immunoreceptor signalling in hematopoietic cells confirm and extend the information gained from studies of compartmentalized signalling by growth factors and GPI-anchored proteins—namely, that lipid rafts are highly organized

yet dynamic structures and that regulated changes in their composition, size, and spatial localization can dramatically affect signalling responses to a wide variety of stimuli.

1.3.4 Specificity in Signalling

Although many different signalling pathways are compartmentalized in lipid rafts, it is equally clear that many other signalling events are not associated with rafts. This suggests that lipid rafts have specialized functions in signal transduction. One of these functions may be regulation of the specificity of signalling responses. Several experimental observations support this idea. Inhibition of the FGF-2 induced phosphorylation events within lipid rafts of LAN-1 cells by the Src family kinase inhibitor PP1, did not affect FGF-2 induced cell cycle progression (Davy et al., 2000). This suggests that FGF-2 initiates at least two distinct signalling pathways in LAN-1 cells—one response requiring Src family kinases and a second signal leading to cell proliferation. Although the Src family kinase-dependent pathway is localized to lipid rafts, it is not known whether the signal leading to cell cycle progression occurs in non-raft membranes, or whether it is also compartmentalized in lipid rafts. In the latter case, it is possible that the signalling pathways are localized in the same lipid rafts or alternatively, that each pathway is compartmentalized in distinct lipid rafts with unique protein and lipid compositions (Figure 1.2a). Ridyard and Robbins have further shown that FGF-2 stimulation of LAN-1 cells leads to lipid raft-dependent activation of MEK1/2 through multiple mechanisms that may lead to different cellular responses (Ridyard and Robbins, 2003). Overall these observations support the idea that signalling in lipid rafts can provide an additional level of specificity by enabling a single cell to have multiple distinct responses to a single growth factor. Signalling by GDNF family members also

illustrate a central role of lipid rafts in signalling specificity. GDNF and its related factors—neurturin, artemin, and persephin—bind to the GPI-anchored proteins GFRα1, GFRα2, GFRα3, and GFRα4 respectively (Saarma, 2000; Sariola and Saarma, 2003). While the four GDNF family members mediate similar biological effects, both tissue-specific and factor-specific physiological responses are also observed, even though all four growth factors appear to signal using Ret as a common transmembrane receptor. It is likely that signalling specificity in this instance is obtained through the different GFRα receptors, which are all located in lipid rafts (Saarma, 2000; Sariola and Saarma, 2003). It is not known whether the various GFRα receptors are localized within a homogenous population of lipid rafts, or whether they are found in distinct subpopulations of lipid rafts with unique compositions. A separate study examining the function of the GPI-anchored carcinoembryonic antigen (CEA) suggests that protein-specific modifications to the GPI-anchor moiety might direct different GPI-anchored proteins to separate lipid rafts, and therefore determine their biological specificity (Screaton et al., 2000). Ectopic expression of CEA in murine myocytes blocks myogenic differentiation (Eidelman et al., 1993), whereas overexpression of the GPI-anchored NCAM molecule normally accelerates myogenic differentiation (Dickson et al., 1990). Attaching the NCAM protein specifically to a CEA GPI anchor converted it into a differentiation-blocking protein (Screaton et al., 2000). NCAM and CEA did not co-localize by immunofluorescence, indicating that they may be present in distinct types of lipid rafts, where signalling components unique to the CEA-specific raft confer the ability for GPI-linked proteins with self-adhesive domains to block differentiation (Screaton et al., 2000).

Other evidence supporting the existence of distinct subpopulations of lipid rafts includes incomplete colocalization of caveolin and a raft-associated protein in immunofluorescence and/or electron microscopy experiments, which indirectly suggests that the raft protein exists in a lipid raft that does not contain caveolin (Chigorno et al., 2000; Davy et al., 1999). In MDCK cells, a polarized epithelial cell line, two distinct types of lipid rafts appear to be present on the apical plasma membrane—one population localized to microvilli containing the raft-associated transmembrane protein prominin, and a second population containing the GPI-anchored protein PLAP, which did not co-localize with prominin by immunofluorescence (Roper et al., 2000). Interestingly, while cholesterol depletion with methyl-β-cyclodextrin resulted in the loss of prominin's localization to microvilli and its redistribution more evenly over the plasma membrane, it still did not completely intermix with PLAP. Surprisingly, the distribution of PLAP did not change following cholesterol depletion, suggesting that the prominin-containing lipid rafts were more susceptible to removal of cholesterol with this particular agent than the PLAP-containing lipid rafts. Previous studies have shown that caveolae are normally present on the basolateral membrane of MDCK cells, but are not found on the apical membrane (Scheiffele et al., 1998; Vogel et al., 1998). This suggests that at least three distinct types of lipid rafts may be present in MDCK cells.

Electron microscopy studies of signalling molecules downstream of FcεRI in resting and activated mast cells suggest that distinct membrane domains with unique protein compositions organized around FcεRIβ and LAT respectively are formed in activated mast cells (Holowka et al., 2005; Wilson et al., 2001). While the signalling molecules present in each type of membrane domain do not intermix, the membrane

domains themselves did intersect one another, suggesting that direct interactions between different lipid rafts are functionally important in FcεRI signalling. Since cross-linked FcεRI are internalized relatively rapidly through coated pits, in contrast to LAT, the authors propose that the more stable LAT-containing domains are important in sustaining and amplifying signalling downstream of FcεRI (Wilson et al., 2001). It had previously been shown that the FcεRI sequentially associates with Lyn, Syk, and coated pits in topographically distinct membrane domains (Wilson et al., 2000), although it is not clear at present whether such transient associations result from dynamic movement of individual signalling components in and out of lipid rafts (Figure 1.1b, 1.1c), alterations in the interactions between multiple distinct lipid raft subpopulations (Figure 1.2), or a combination of both mechanisms.

Purification of caveolae from rat lung endothelial cells by in situ coating with cationic silica particles isolated two distinct populations of membrane vesicles—one enriched in GM1 and caveolin, and the other enriched in GPI-anchored proteins (Liu et al., 1997a). Caveolin-rich rafts have been successfully separated from rafts devoid of caveolin using anti-caveolin antibodies to selectively immunoisolate rafts enriched in caveolin from purified membrane fractions (Oh and Schnitzer, 1999; Waugh et al., 1998). Biochemical analysis of the two subpopulations of rafts revealed significant differences in protein and lipid composition. Similarly, GM3-enriched rafts were separated from caveolin-containing rafts isolated from B16 mouse melanoma cells using an anti-GM3 monoclonal antibody (Iwabuchi et al., 1998). The protein and lipid composition of the two subpopulations was also shown to be distinct, and signalling via GM3 upon cell

adhesion was shown to occur specifically in only one type of raft. Taken together, these experiments suggest the presence of lipid rafts that are distinct from caveolae in cells expressing caveolin.

Distinct subpopulations of lipid rafts are also required for the acquisition of polarity during T cell chemotaxis, in which the protruding leading edge and the rear uropod of lymphocytes are enriched in specific signalling molecules but lack others (Gomez-Mouton et al., 2001). In polarized migrating T cells, raft molecules GM1 and CD44 colocalize by immunofluorescence at the uropod, whereas rafts enriched in GM3, talin, the chemokine receptor CXCR4, and uPAR were detected at the leading edge (Gomez-Mouton et al., 2001). Raft association of membrane proteins was required for their asymmetric distribution, as non-raft-associated mutant forms of two raft proteins normally present in GM1-enriched uropod rafts were homogenously distributed along the cell surface. The idea that rafts are functionally important in T cell polarization and chemotaxis is supported by the observation that cholesterol depletion with MβCD reduces the number of cells with a polarized phenotype and inhibits uropod function (indicated by a decreased ability to recruit bystander T cells) as well as leading-edge function (indicated by decreased cell migration towards a CXCR4-specific chemokine) (Gomez-Mouton et al., 2001). Notably, replenishment of cholesterol levels by incubation of MβCD-treated cells with free cholesterol restored normal polarization and chemotaxis function, demonstrating that the inhibitory effect was limited to cholesterol removal. Asymmetric distribution of the leading rafts and uropod rafts required an intact actin cytoskeleton, and disruption of the actin cytoskeleton with latrunculin-B not only caused loss of the asymmetric distribution of L-rafts and U-rafts, it also prevented colocalization

of CD44 and GM1 (Gomez-Mouton et al., 2001). Thus, not only does the actin cytoskeleton appear to have an important role in maintaining the spatial localization of specific rafts on the cell surface, it is also important in regulating the association of individual molecules with lipid rafts. Overall, the asymmetric distribution of two different signalling domains in polarized T cells allows localized activation of signalling pathways required for distinct uropod- and leading-edge-specfic functions. Currently, there is evidence for asymmetric distribution of lipid raft domains in a variety of different types of migrating cells in addition to T cells, including carcinoma cells, nerve growth cones, epithelial cells, fibroblasts, and neutrophils (Manes and Viola, 2006).

Differences in signalling by different isoforms of Ras are also suggestive of the potential of distinct subpopulations of lipid rafts. Expression of a dominant-negative caveolin mutant or cholesterol depletion with cyclodextrin inhibits Raf activation in cells expressing a constitutively active form of H-Ras, but Raf activation is not inhibited in cells expressing an activated K-Ras4B allele (Roy et al., 1999). The inhibitory effect of the dominant-negative caveolin was completely reversed by incubating cells with a cyclodextrin/cholesterol mix that replenished plasma membrane cholesterol. H-Ras and K-Ras4B are targeted to the plasma membrane via CAAX box motifs—while both proteins are modified with lipids by farnesylation, H-Ras is also palmitoylated whereas K-Ras4B contains a polybasic domain which helps to anchor it to the membrane through charge interactions with negatively charged phospholipid headgroups (Hancock et al., 1990). Both H-Ras and K-Ras4B were present in purified lipid raft fractions (Roy et al., 1999). Previous studies suggest that activation of different Ras isoforms results in different signalling outcomes (Bos, 1989; Roy et al., 1999; Yan et al., 1998). These

signalling differences might be explained if the different Ras isoforms were localized to different lipid rafts. Alternatively, Raf activation might occur in a single raft, which both H-Ras and K-Ras4B would have to access. Association of farnesylated and palmitoylated H-Ras with this raft might be more sensitive to changes in cholesterol content, than K-Ras4B, where membrane targeting is partly achieved by its polybasic domain (Roy et al., 1999).

1.4 A Role for Cholesterol and Lipids?

The ability of dominant-negative caveolin to disrupt H-Ras-mediated Raf activation by affecting plasma membrane cholesterol levels suggests that physiological regulation of membrane cholesterol by lipid rafts may be linked to the regulation of compartmentalized signalling pathways (Fielding and Fielding, 2000; Roy et al., 1999). A variety of cholesterol-depleting agents (such as filipin, MβCD, nystatin, and lovastatin) have been extensively used as experimental tools to disrupt lipid rafts, causing loss of morphology of invaginated caveolae, and dispersion of GPI-anchored proteins into the bulk plasma membrane (Pralle et al., 2000; Smart et al., 1999). Disruption of rafts by cholesterol depletion is known to block many different compartmentalized signalling pathways (Simons and Toomre, 2000). The cholesterol-depleting agents are fairly crude tools, which may give different results due to different mechanisms of action (for example, cholesterol binding versus inhibition of cellular cholesterol synthesis). Treatment of B cells with MβCD (a carbohydrate molecule containing a cholesterol-binding pocket that extracts membrane cholesterol) prevented BCR redistribution and enhanced the release of intracellular calcium induced in response to BCR stimulation (Awasthi-Kalia et al., 2001). In contrast, stimulated B cells treated with filipin (an

antibiotic that sequesters cholesterol within membranes) resulted in a potent inhibition of the normal increase in intracellular calcium levels (Aman and Ravichandran, 2000; Awasthi-Kalia et al., 2001). These agents can also affect other cellular processes such as clathrin-dependent endocytosis (Kjersti Rodal et al., 1999) and may give different effects based on the type of cells and the specific receptor signalling systems investigated (Awasthi-Kalia et al., 2001). Hence, experimental strategies using these compounds require cautious interpretation and consideration of appropriate controls. Despite these limitations, there is merit in studying the effects of these compounds on cell physiology, as at least one (lovastatin) is used clinically in humans for long-term treatment of elevated cholesterol levels (Berger et al., 1996).

Treatment of cells with exogenous gangliosides and PUFAs alters lipid raft structure by causing some proteins to dissociate from rafts and affects signalling (Inokuchi, 2006; Simons et al., 1999; Stulnig et al., 1998; Webb et al., 2000). Overall, it is possible that modulation of the lipid composition of lipid rafts leading to changes in the structure or protein composition of rafts could be involved in the regulation of compartmentalized signalling. This is particularly relevant in the case of cholesterol, considering that lipid rafts have already been implicated in cholesterol homeostasis, and that the expression of at least one raft protein, caveolin, is transcriptionally regulated by cholesterol levels (Fielding and Fielding, 2000; Hailstones et al., 1998). However, because many of these observations have been made using non-physiological experimental models, the physiological significance of this mechanism remains to be determined for endogenous raft lipids.

1.5 Lipid Rafts and Human Disease

Complex signalling networks are responsible for controlling important cellular functions such as growth, differentiation, adhesion, and motility, and unregulated signalling can lead to many different diseases. Due to their importance in regulating signal transduction, it is not surprising that lipid rafts have been implicated in a wide variety of disorders. Mutations in an isoform of caveolin (caveolin-3) have been linked to a form of limb girdle muscular dystrophy (Minetti et al., 1998). Generation of the β-amyloid peptide from the amyloid precursor protein in Alzheimer's disease has been shown to occur in lipid rafts in a cholesterol-dependent manner (Ikezu et al., 1998). Similarly, efficient processing of the scrapie isoform of the prion protein requires its targeting to lipid rafts by GPI anchors (Kaneko et al., 1997).

Many oncogenes and tumour suppressors are proteins involved at all levels of signalling pathways that promote carcinogenesis when their normal function is altered or lost. There is some evidence that the structure and function of lipid rafts is altered significantly in cancer. Normally, attenuation of EGF signalling requires internalization of EGFRs by clathrin-dependent endocytosis (Vieira et al., 1996). Several mutant oncogenic EGFRs fail to down-regulate in this manner and remain in lipid rafts for abnormally prolonged periods of time (Mineo et al., 1999). Because these receptors remain in an activated state, it is possible that this results in unregulated stimulation of EGF signalling pathways leading to transformation.

The caveolin-1 isoform of caveolin has been proposed to have tumour suppressor-like properties due to its proposed ability to negatively regulate signalling by modulating the function of signalling molecules (Okamoto et al., 1998). Caveolin-1 was originally

identified as a major tyrosine-phosphorylated protein in chick embryo fibroblasts transformed by v-Src (Glenney and Soppet, 1992). Caveolin-1 mRNA and protein expression was lost and caveolae are absent in NIH 3T3 fibroblasts transformed with v-Abl or H-Ras (Koleske et al., 1995). Induction of caveolin-1 expression in these transformed cells abrogated anchorage-independent growth of the cells in soft agar (Engelman et al., 1997). Downregulation of caveolin-1 in NIH 3T3 cells by an antisense approach caused anchorage-independent growth, enabled the cells to form tumours in immunodeficient mice, and hyperactivated the MAPK pathway (Galbiati et al., 1998). Caveolin-1 expression in human lung and breast cancer cell lines was found to be reduced compared to normal tissue (Lee et al., 1998; Racine et al., 1999). When caveolin-1 cDNA was transfected into caveolin-1 negative breast cancer cells, there was a substantial decrease in growth rate and anchorage-independent growth (Lee et al., 1998). Others have found elevated levels of caveolin-1 in glioblastoma cell lines and primary tumours, as well as prostate and breast cancer cell lines and primary tumours (Abulrob et al., 2004; Yang et al., 1998). Hurlstone *et al.* analyzed the human caveolin-1 gene in primary human tumours and tumour cell lines and found no evidence of mutation or methylation of the caveolin-1 gene in human cancer (Hurlstone et al., 1999). Caveolin-1 expression was retained in primary tumours derived from breast myoepithelium (Hurlstone et al., 1999). Similarly, although primary human T cells do not express caveolin and do not have caveolae, caveolin-1 expression is detected in some constitutively activated adult T cell leukemia cell lines (Hatanaka et al., 1998). Multidrug resistant cancer cells also show dramatically increased expression of caveolin-1 and increased numbers of caveolae (Lavie et al., 1999). Some caution is required in

interpreting results obtained from cultured cell lines, as growth conditions (for example, cholesterol level) can significantly affect expression of caveolin-1 (Hailstones et al., 1998). However, because analysis of primary tumour specimens also found aberrant caveolin expression (Abulrob et al., 2004; Yang et al., 1998) it is possible that caveolae and the expression of caveolin-1 are altered during tumour progression. Alternatively, even though caveolin-1 expression levels might not vary considerably, its subcellular localization could be differentially affected, as has been previously observed in cells that have undergone senescence (Wheaton et al., 2001). Despite this, the evidence as a whole does not provide strong support for the initially proposed tumour suppressor model for caveolin. Recently, Williams and Lisanti have proposed a more sophisticated model of caveolin-1's role in cancer, in which it can act as a tumour suppressor in some contexts, but as a tumour promoter in other settings (Williams and Lisanti, 2005).

A number of lipids and proteins other than caveolin also appear to be affected in cancer cells. For example, glycosphingolipids are enriched in lipid rafts and are capable of inducing and modulating signal transduction (Hakomori et al., 1998). There are many cancer-associated glycosphingolipid antigens, which would be expected to be enriched in lipid rafts of cancer cells (Hakomori, 1998). Interestingly, these glycosphingolipids are also found in normal cells, but show differences in expression level and membrane organization in tumour cells (Hakomori, 1998). Differences in the expression or compartmentalization of GPI-anchored proteins may also play a role. Patients suffering from the acquired hematopoietic disorder paroxysmal nocturnal hemoglobinuria (PNH) lack the ability to synthesize GPI anchors, and express no GPI-anchored proteins on the cell surface of affected hematopoietic cells (Boccuni et al., 2000; Hall et al., 2002). PNH

cells seem to have a growth advantage over normal cells, possibly due to their increased resistance to apoptosis, and patients are more susceptible to leukemias (Boccuni et al., 2000; Brodsky et al., 1997; Hall et al., 2002). In general, it is likely that there are multiple routes through which abnormal structure and function of lipid rafts could contribute to the development of cancer or other diseases.

1.6 Conclusion

Lipid rafts are specialized liquid-ordered membrane microdomains with unique protein and lipid compositions that are present in both the plasma membrane and intracellular membranes in eukaryotic cells. Biochemical, microscopic, and functional studies have demonstrated that these membrane microdomains have important roles in diverse pathways of signal transduction. The high degree of organization observed in these structures coupled with their dynamic nature appears to be important in modulating and integrating signals, by acting to provide a signalling microenvironment that is tailored to produce specific biological responses. The overall hypothesis of this thesis is that changes in protein or lipid composition, size, structure, number, or membrane localization of lipid rafts affect the functional capabilities of these domains in signalling with important physiological consequences. Thus, differentiating cells might be able to alter their responsiveness to various growth factors in a cell type-specific manner by manipulating one or more of these properties of lipid rafts. Similarly, abnormal alterations in the structure and function of lipid rafts may contribute to the development of disease, if these changes result in the dysregulation of signalling pathways controlling cell growth and behaviour.

Much of the research performed in the Robbins' laboratory at the outset of my studies was directed towards the further characterization of the biology of lipid rafts in hematopoietic cells. Since these cells do not express caveolins or have caveolae on their cell surface, it was thought that non-caveolar rafts might have unique properties and functions. At the outset of these studies, substantial insight into lipid raft structure and function had already been derived from studies of known raft markers in a number of different hematopoietic cell types. In order to extend this knowledge, the initial objective of the studies described in Chapter 3 was to develop proteomic approaches to analyze and compare the protein composition of lipid rafts isolated from a number of different hematopoietic cell types. It was anticipated that this approach would allow the identification of novel lipid raft markers that could provide insight into the structure and function of non-caveolar rafts in hematopoietic cells. In addition, by comparing the lipid raft proteome in different cell types, it was hoped that one or more proteins that were differentially raft-associated in a particular physiological or pathological context could be identified and targeted for further analysis to determine the functional significance of the observed change in raft structure. In particular, the identification of novel raft-dependent signalling proteins was anticipated, since rafts were known to contain many signalling receptors and downstream effectors. Although many known and novel raft proteins were identified by this approach, providing significant insights into the properties and function of lipid rafts in hematopoietic cells, the studies described in Chapter 3 were unsuccessful in identifying specific raft proteins whose differential association with rafts in either a physiological or pathological context impacted either known or novel raft signalling pathways. Instead, in order to test the hypothesis that lipid raft structure is intimately

linked to its function in signal transduction, the experiments described in Chapter 4 were designed in order to examine the effects of an experimentally defined change in lipid raft structure—loss of expression of GPI-anchored proteins—on known raft-dependent signalling pathways. The results of these experiments provide further insight into the role of GPI-anchored proteins in raft-dependent signal transduction and the molecular pathogenesis of a human disease, paroxysmal nocturnal hemoglobinuria. Collectively, the work described in this thesis is a systematic attempt to further elucidate the specific relationships between lipid raft structure and function in hematopoietic cells in the hope of enhancing our understanding of the physiological and pathological significance of these extensively studied, yet still enigmatic membrane microdomains.

Chapter Two: Materials and Methods

2.1 Solutions

Mes-buffered saline (MBS): 25 mM morpholineethanesulfonic acid (MES; Sigma) pH 6.5, 150 mM NaCl.

Phosphate-buffered saline (PBS): 1.5 mM KH_2PO_4 (Sigma), 5 mM Na_2HPO_4 (Sigma), 154 mM NaCl (Sigma).

1% Triton X-100/MBS lysis buffer: 1% (v/v) Triton X-100 in MBS, with the following added immediately before use (final concentrations indicated): 1mM Na_3VO_4, 0.01 mg/mL aprotinin, 0.01 mg/ml leupeptin, and 1mM phenylmethylsulfonyl fluoride (PMSF).

1% Brij58/MBS lysis buffer: 1% (v/v) Brij58 in MBS, with the following added immediately before use (final concentrations indicated): 1mM Na_3VO_4, 0.01 mg/mL aprotinin, 0.01 mg/ml leupeptin, and 1mM PMSF.

1% Triton X-100/Tris lysis buffer: 1% (v/v) Triton X-100 in 10 mM Tris, 150 mM NaCl, pH 7. 5, with the following added immediately before use (final concentrations indicated): 1mM Na_3VO_4, 0.01 mg/mL aprotinin, 0.01 mg/ml leupeptin, and 1mM PMSF.

2% Triton X-100/Tris lysis buffer: 2% (v/v) Triton X-100 in 10 mM Tris, 150 mM NaCl, pH 7. 5, with the following added immediately before use (final concentrations indicated): 1mM Na_3VO_4, 0.01 mg/mL aprotinin, 0.01 mg/ml leupeptin, and 1mM PMSF.

30% sucrose: 30% (w/v) sucrose in MBS, with the following added immediately before use (final concentrations indicated): 1mM Na_3VO_4, 1mM PMSF.

5% sucrose: 5% (w/v) sucrose in MBS, with the following added immediately before use (final concentrations indicated): 1mM Na_3VO_4, 1mM PMSF.

Acrylamide: 29.2% (w/v) acrylamide (BioRad), 0.8% (w/v) bis-acrylamide (ICN) in double-distilled (dd)H_2O, filtered.

Thiourea lysis buffer: 7 M urea (Sigma), 2 M thiourea (Sigma), 4% (v/v) CHAPS (Sigma), 1% (w/v) dithiothreitol (DTT) (ICN), 2% (v/v) carrier ampholytes (BioRad; mix of 80% pH 5-7 ampholyte stock and 20% pH 3-10 ampholyte stock) in ddH_2O.

Gel equilibration buffer: 0.05 M Tris-HCl, pH 6.8, 6 M urea, 30% (v/v) glycerol, 2% (w/v) sodium dodecyl sulphate (SDS), trace of bromophenol blue for colour. Just before using, DTT to a final concentration of 65 mM was added.

4x Lower gel buffer: 1.5 M Tris-HCl, 0.4% (w/v) (SDS) (Sigma), pH 8.8.

4x Upper gel buffer: 0.5 M Tris-HCl (Sigma) pH 6.8, 0.4% (w/v) SDS.

Polyacrylamide gel running buffer: 25 mM Tris base (Sigma), 192 M glycine (Sigma), 0.1% (w/v) SDS.

2x SDS Laemmli sample buffer: 10% (v/v) glycerol (EM science), 5% (v/v) β-mercaptoethanol (Sigma), 2.3% (w/v) SDS, 62 mM Tris-HCl pH 6.8, trace of bromophenol blue for colour.

6x SDS sample buffer: 60% (w/v) glycerol, 13.8% (w/v) SDS, 0.65 M DTT, 375 mM Tris-HCl pH 6.8, trace of bromophenol blue for colour.

Tris-buffered saline (TBS): 5 mM Tris base, 135 mM NaCl (Sigma), 5 mM KCl (Sigma).

High detergent wash buffer: 1x TBS, 0.5% (v/v) Nonidet-P40 (NP40; Fluka), 0.1% (v/v) Tween-20 (Sigma).

Low detergent wash buffer: 1x TBS, 0.1% (v/v) NP40, 0.1 % (v/v) Tween-20.

Extra-low detergent wash buffer: 1x TBS, 0.1% (v/v) Tween-20.

Towbin transfer buffer: 25 mM Tris base, 192 mM glycine, 20% methanol, 0.1% SDS.

ECL: Solution 1: 30% (v/v) H_2O_2 10 mM Tris, pH 8.5; Solution 2: 2.5 mM luminol (Sigma), 0.4 mM coumaric acid (Sigma).

Calcium Buffer: 20 mM HEPES, pH 7.4 (free acid, adjusted to pH 7.4 using 1 M NaOH); 125 mM NaCl; 15 mM KCl; 1 mM Mg_2Cl_2; 1 mM $CaCl_2$.

2.2 Antibodies

The antibodies used in this thesis are described in the table below. They are listed as monoclonal (mAb) or polyclonal (pAb) antibodies. The concentrations of the stock solutions (if known) are provided, along with the dilutions and wash buffers used for Western blotting (WB), and the dilutions used for flow cytometry (FC). Antibody dilutions/concentrations used in other applications are described in other sections of this chapter, in the context of the specific experiments performed.

Antibody	Dilution	Application	Source
mIgG2a-FITC	20 μL/1 x 10^6 cells	FC (isotype control for α-CD59-FITC)	BD Biosciences
α-CD59-FITC (p282(H19); mIgG2a mAb)	20 μL/1 x 10^6 cells	FC	BD Biosciences
mouse IgG1 (1 mg/mL)	1 μg antibody/ 1 x 10^6 cells	FC (isotype control for α–CD48 (MEM102)	BD Biosciences
α–CD48 (MEM102; mIgG1 mAb) (1 mg/mL)	1 μg antibody/ 1 x 10^6 cells	FC	Abcam
mIgG2a-PE	20 μL/1 x 10^6 cells	FC (isotype control for α–CD55-PE)	BD Biosciences
α–CD55-PE (IA10; mIgG2a mAb)	20 μL/1 x 10^6 cells	FC	BD Biosciences

α-CD55 (H-319; rabbit pAb)	1:100 (low wash)	WB	Santa Cruz
α-phosphotyrosine (4G10; mAb)	1:1000 (high wash)	WB	in lab (available through UBI)
α-Hck (rabbit pAb)	1:1000 (low wash)	WB	in lab
goat anti-human IgM ($Fc_{5\mu}$ specific) (1.3 mg/mL; pAb)	1:240 (low wash)	WB	Jackson Immunoresearch
$F(ab')_2$ goat anti-human IgM ($Fc_{5\mu}$ specific) (1.3 mg/mL; pAb)		apoptosis, calcium, signalling experiments	Jackson Immunoresearch
FITC-conjugated $F(ab')_2$ goat anti-human IgM ($Fc_{5\mu}$ specific) (1.3 mg/mL; pAb)	1 μg antibody/ 1 x 10^6 cells	FC	Jackson Immunoresearch
whole human IgG (11.1 mg/mL)	1 μg antibody/ 1 x 10^6 cells	FC apoptosis, calcium, signalling experiments	Jackson Immunoresearch
rituximab	1 μg antibody/ 1 x 10^6 cells	FC apoptosis, calcium, signalling experiments	Dr. Julie P. Deans
α-CD20 (GST-77; rabbit pAb)	1:1000 (extra-low wash)	WB	Dr. Julie P. Deans
α-CD20 (2H7; mIgG2a mAb)	1 μg antibody/ 1 x 10^6 cells	FC	Dr. Julie P. Deans
α-actin (mAb1501; mouse mAb)	1:10 000 (low wash)	WB	Chemicon
α-Lyn (44; rabbit pAb)	1:200 (low wash)	WB	Santa Cruz
α-Cbp (rabbit pAb)	1:1000 (low wash)	WB	in lab
α-$G\alpha_{i3}$ (Ab-5; rabbit pAb)	1:300 (high wash)	WB	Oncogene Research
Secondary Reagents	**Dilution**	**Application**	**Source**
streptavidin-HRP	1:30 000	WB	BioRad
α–mouse IgG-HRP	1:10 000	WB	GE Healthcare (Amersham), Santa Cruz

α–rabbit IgG-HRP	1:10 000	WB	GE Healthcare (Amersham), Santa Cruz
α-goat IgG-HRP	1:20 000	WB	Pierce
protein A-HRP	1:5000	WB (α-CD20 blots)	BioRad
$F(ab')_2$ goat anti-mouse IgG-Alexa488	1:500	FC	Invitrogen (Molecular Probes)
$F(ab')_2$ goat anti-human IgG (Fc_γ specific) (1.3 mg/mL)		apoptosis, calcium, signalling experiments (hypercrosslinking of CD20)	Jackson Immunoresearch
FITC-conjugated $F(ab')_2$ goat anti-human IgG (Fc_γ specific) (1.3 mg/mL)	1:200	FC	Jackson Immunoresearch

2.3 Cell culture

2.3.1 Maintenance of hematopoietic cell lines in culture

U937, THP-1, HL60, K562, IVEE, and Ramos cells were maintained in RPMI (Invitrogen) supplemented with 10% heat-inactivated fetal bovine serum (Invitrogen), 1% penicillin/streptomycin (Invitrogen), 1 mM sodium pyruvate (Invitrogen), and 50 μM β-mercaptoethanol (hereafter this medium is referred to as RPMI complete) at 37°C in a 5% CO_2 atmosphere. U937 cells were differentiated towards a more mature macrophage-like phenotype by culturing them in RPMI complete supplemented with 20 ng/mL of 12-*O*-tetradecanoylphorbol-13-acetate (TPA) at a density of 1×10^6 cells/mL for 48 hours (Harris and Ralph, 1985). IVEE/GPI8 cells were grown in RPMI complete supplemented with 300 μg/mL hygromycin B (Sigma) when initially thawed from frozen stocks or to obtain cells to freeze down as stocks. For routine experimental use, IVEE/GPI8 cells were grown in drug-free RPMI complete, and GPI-anchored protein expression was

monitored every 1-3 weeks to ensure that hGPI8 expression was not lost. The presence or absence of GPI-anchored proteins in K562, IVEE and IVEE/GPI8 cells was confirmed by flow cytometry and Western blotting (Figure 2.1).

GPI-deficient Raji26/vector and GPI-expressing Raji26/pigL cell lines (Harris and Morgan, 1995) (the kind gift of Dr. Taroh Kinoshita, Osaka University) were maintained in RPMI complete supplemented with 100 μg/mL hygromycin B when initially thawed from frozen stocks, or to obtain cells for frozen stocks. For routine experimental use, the cells were maintained in drug-free RPMI complete, and cell surface GPI-anchored protein expression was monitored by flow cytometry every 1-3 weeks. When the cells were first received in the lab, initial flow cytometry analysis confirmed that GPI-anchored proteins were not expressed on the cell surface of Raji26/vector cells (Figure 2.2). However, analysis of Raji26/pigL cells showed that only 20% of the cells expressed CD59 (data not shown). To obtain a pure population of GPI-expressing cells, viable Raji26/pigL cells were stained with a FITC-conjugated CD59 antibody, and a pure population of CD59-positive cells was obtained by fluorescence-activated cell sorting (FACS) performed by staff at the University of Calgary Flow Cytometry Facility. This population of sorted GPI-positive Raji26/pigL cells was used for the experiments described in this thesis (Figure 2.2).

GPI-deficient Ramos517/vector and GPI-expressing Ramos/pigM cells (Maeda et al., 2001) (the kind gift of Dr. Taroh Kinoshita, Osaka University) were cultured in RPMI complete supplemented with 200 μg/mL hygromycin B when initially thawed from frozen stocks, or to obtain cells to freeze down as stocks. For routine experimental use, the Ramos517 cell lines were maintained in drug-free RPMI complete, and cell surface

Figure 2.1. GPI-anchored protein expression on K562, IVEE, and IVEE/GPI8 cells.

(A) Intact, unfixed cells were labelled with a FITC-conjugated anti-CD59 antibody or a PE-conjugated anti-CD55 antibody, and analyzed by flow cytometry. CD55 and CD59 staining is shown in red. The staining of corresponding isotype controls is shown in black. **(B)** Cells were lysed in 1% Triton X-100/MBS, and cell lysates were fractionated by sucrose density gradient centrifugation. Equal amounts of protein from raft and soluble fractions were separated by SDS-PAGE, transferred to nitrocellulose, and the blots were probed with an anti-CD55 antibody.

A

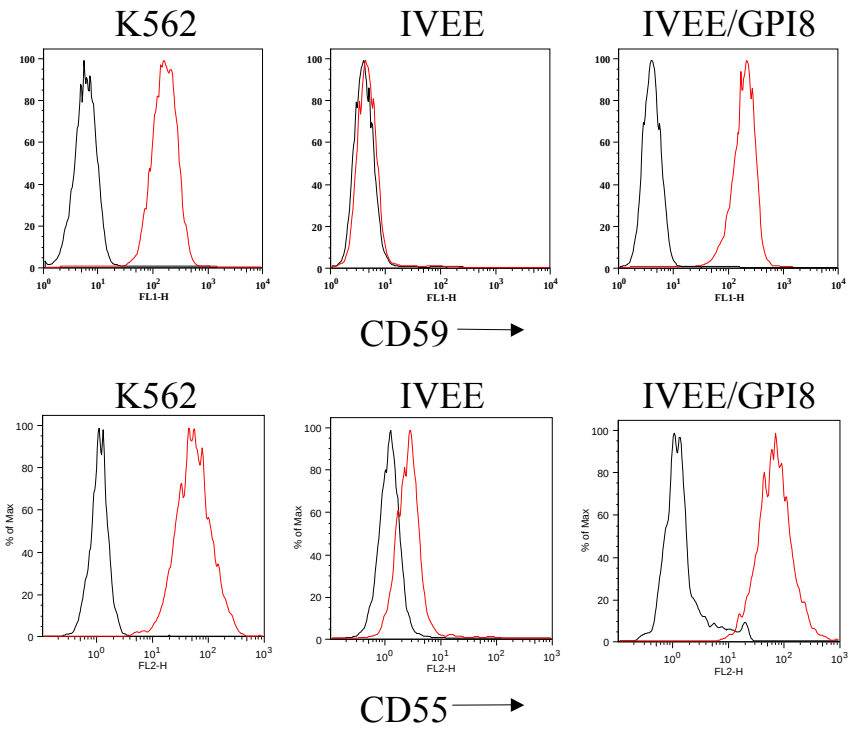
K562
IVEE
IVEE/GPI8
FL1-H
CD59
K562
IVEE
IVEE/GPI8
% of Max
FL2-H
CD55

B

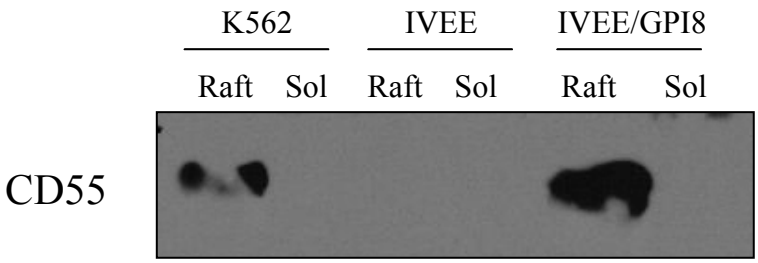
K562
IVEE
IVEE/GPI8
Raft
Sol
Raft
Sol
Raft
Sol
CD55

Figure 2.2. Cell surface GPI-anchored protein expression on Raji26, Ramos, and Ramos517 cell lines.

Intact, unfixed cells were labelled with a FITC-conjugated anti-CD59 antibody, a PE-labelled CD55 antibody, or indirectly with a mouse anti-CD48 antibody recognized by an $F(ab')_2$ goat anti-mouse-Alexa488 secondary antibody and analyzed by flow cytometry. The red line indicates staining with the above antibodies, whereas the black line shows the staining of the appropriate isotype control.

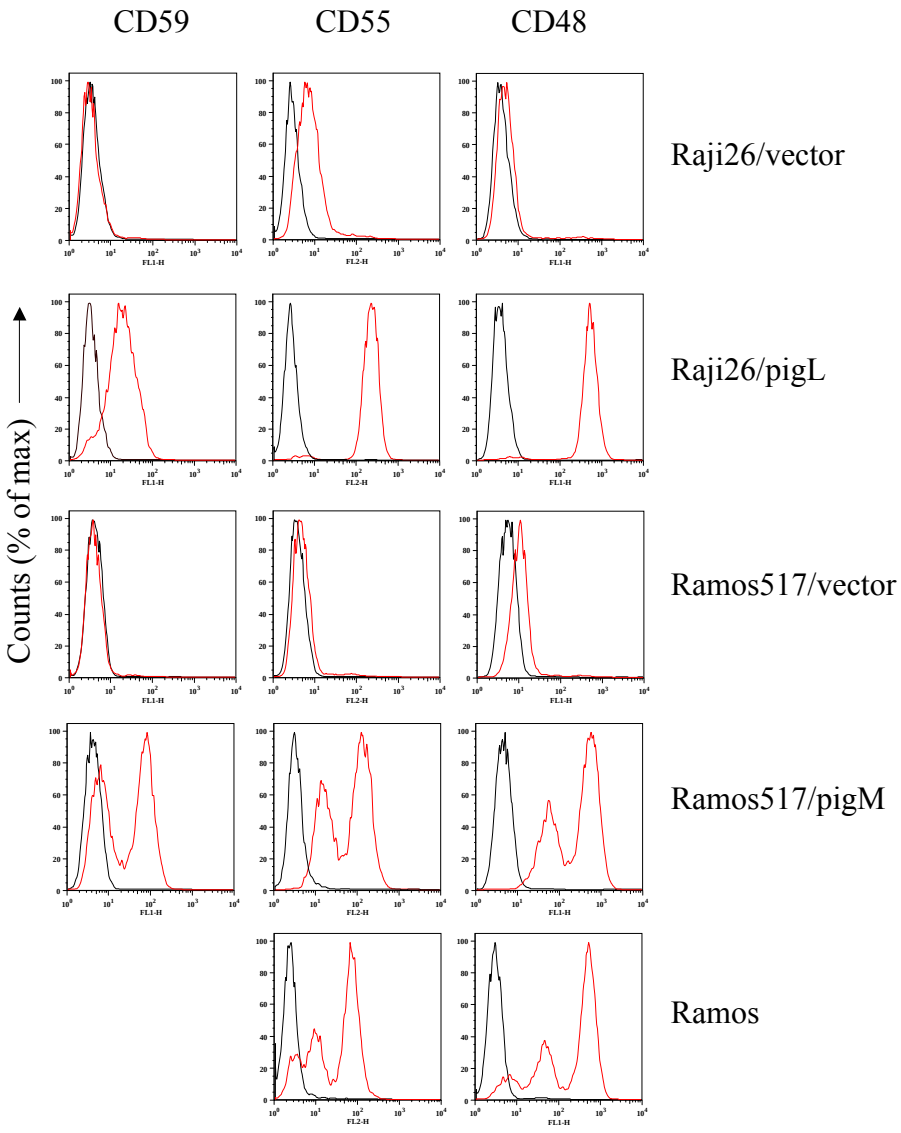
CD59
CD55
CD48
Raji26/vector
Raji26/pigL
Ramos517/vector
Ramos517/pigM
Ramos
Counts (% of max)
FL1-H
FL2-H

GPI-anchored protein expression was monitored every 1-3 weeks by flow cytometry. When the cells were first received in the lab, initial flow cytometry analysis confirmed that the GPI-anchored protein CD59 was not expressed on the cell surface of Ramos517/vector cells (Figure 2.2). However, approximately 40% of the Ramos517/pigM cells also appeared CD59-negative (Figure 2.2). All of the Ramos517/pigM cells stained positively for two other GPI-anchored proteins, CD55 and CD48 (Figure 2.2), but showed two distinct subpopulations, a subpopulation with low levels of GPI expression ("low GPI") and a subpopulation with high levels of GPI expression ("high GPI"). In a separate experiment Ramos517/pigM cells were costained for CD59 and CD55, or for CD48 and CD55, and analyzed by two-colour flow cytometry. This demonstrated that the "high GPI" population was double-positive for the two GPI markers in both cases (data not shown), and that the "high GPI" subpopulation observed likely expressed all three GPI-anchored proteins. Multiple FACS attempts failed to obtain a pure population of the "high GPI" Ramos517/pigM cells, as a population of "low GPI" cells always reappeared days to weeks after sorting (data not shown). The parental Ramos517 cell line was initially derived from the Burkitt's lymphoma Ramos cell line as a GPI-deficient clone following limiting dilution (Maeda et al., 2001). Analysis of CD48 and CD55 cell surface staining on Ramos cells showed corresponding "low GPI" and "high GPI" subpopulations, but also showed an additional third subpopulation of cells as a small peak that matched the staining of the isotype control (Figure 2.2). This peak likely corresponds to the true GPI-negative population from which the Ramos517 cells were derived. Based on these observations, unsorted Ramos517/pigM cells containing both "low GPI" and "high GPI" expressing

subpopulations were considered GPI-positive cells and used for the experiments described in this thesis.

2.3.2 Establishment of IVEE/GPI8 cells

IVEE cells were transfected with the plasmid pMEEB-hGPI8-GST-FLAG containing the *hGPI8* cDNA and a hygromycin B resistance gene (the kind gift of Dr. Taroh Kinoshita of Osaka University) by electroporation as follows. IVEE cells were harvested from actively growing cultures (less than 7 x 10^5 cells/mL), and washed once in serum-free RPMI. 1 x 10^7 washed cells were resuspended in 5 mL of RPMI and 0.5 mL of cell suspension was aliquoted into each of ten 0.4 cm electroporation cuvettes. Twenty μg of plasmid DNA were added to the cell suspension in the cuvette, and the mixture was incubated at RT for 5-10 minutes. Cells were pulsed at 350 V and 1050 μF, with a resistance setting of ∞ using a BioRad Gene Pulser II. After electroporation, 1 mL of RPMI complete was added to the cuvette, and the contents of each cuvette were transferred to one well of a 6-well tissue culture plate containing 1.5 mL of RPMI complete. Cells were cultured for 48 hours, then diluted into RPMI complete containing 300 μg/mL hygromycin B for selection of *hGPI8*-expressing cells. Surviving colonies were expanded and screened for cell surface CD59 expression by flow cytometry.

2.4 Cell surface biotinylation

Cells were washed three times in PBS, pH 8.0 (2x10^7 cells/mL of buffer), resuspended at 2.5x10^7 cells/mL in 0.5 mg/mL Sulfo-NHS-LC-Biotin (Pierce) in PBS, pH 8.0, and incubated at room temperature for 30 minutes with gentle rocking. To remove excess biotinylation reagent, cells were washed three times with ice-cold PBS,

pH 8.0 ($2x10^7$ cells/mL of buffer), and then lysed in 1% Triton X-100/MBS lysis buffer prior to isolation of lipid raft fractions.

2.5 Apoptosis assays

The day before experiments, separate cultures of Ramos517/vector and Ramos517/pigM cells were set up at equal density (5×10^5 cells/mL) in fresh RPMI complete. The next day 1.5×10^6 cells were plated in 2 mL of fresh RPMI complete or fresh RPMI complete containing antibodies or H_2O_2, as indicated in the figures, and incubated at 37°C in a 5% CO_2 atmosphere. At the indicated times following the addition of antibodies to the cells, an aliquot of approximately 1×10^6 cells from each well was stained with annexin V-FITC and propidium iodide (PI) and analyzed by flow cytometry, as described in section 2.9.2.

To examine apoptosis induced by ultraviolet (UV) radiation, separate cultures of Ramos517/vector and Ramos517/pigM cells were set up at equal density (5×10^5 cells/mL) in fresh RPMI complete the day before the experiment. 2×10^6 cells per treatment were harvested, pelleted by centrifugation, and resuspended in 0.5 mL of PBS in 1 well of a six well dish, with care taken to spread the cell suspension evenly in a thin layer over the bottom of the well. Cells were irradiated with 0, 5, 10, 20, or 40 J/m^2 with a UV-C germicidal lamp (Phillips) inside the tissue culture flow hood, with the lid of the dish removed. Doses were calculated by measuring the level of UV radiation at this location using a Blak-Ray Model J225 UV meter. After irradiation, 2.5 mL of RPMI complete and 0.05 mL of heat-inactivated FBS were added to each well, and the cells were cultured 24 hours prior to annexin V/PI staining.

2.6 Growth curves after anti-IgM or rituximab hyper-crosslinking

The day before experiments were initiated, separate cultures of Ramos517/vector and Ramos517/pigM cells were set up at equal density (5 x 10^5 cells/mL) in fresh RPMI complete. The following day, 5 x 10^5 cells were plated in 2 mL of fresh RPMI complete with or without the indicated antibodies in 1 well of a 24 well plate. Three wells were plated per treatment condition in each experiment. Cells treated with 50 μg of F(ab')$_2$ anti-human IgM (per well) were compared to cells cultured in the absence of antibody. Cells treated with 2 μg of rituximab + 20 μg of F(ab')$_2$ anti-human IgG per well were compared to both untreated cells and cells cultured with 2 μg of hIgG + 20 μg of F(ab')$_2$ anti-human IgG per well. The number of viable cells in each well was determined by hemacytometer counting using trypan blue exclusion 24, 48, 72, and 96 hours following the addition of antibodies.

2.7 BCR translocation to Triton-insoluble rafts and raft phosphotyrosine signalling experiments

The evening before the experiment was performed, Ramos517/vector and Ramos517/pigM cells were set up at equal density (1 x 10^6 cells/mL) in fresh RPMI complete. The next day, 5 x 10^8 cells of each cell line were washed once in 5 mL of warm (37°C) RPMI, aliquoting 1 mL of cell suspension into each of 5 microfuge tubes prior to centrifuging the cells. The resulting cell pellet was resuspended in 500 μL of warm RPMI. Cells were stimulated by the addition of 500 μL of warm RPMI alone or RPMI containing 100 μg of F(ab')$_2$ anti-human IgM, and incubated at 37°C for 0, 1, 5, 15, or 60 minutes. One minute prior to the end of the incubation period, the cells were pelleted by centrifugation at 3000 x g for 1 minute. The supernatant was discarded, and

the cells were lysed in 1 mL of 1% Triton X-100/MBS lysis buffer. The lysates were subjected to sucrose density gradient centrifugation to isolate raft and soluble fractions as described in section 2.10. Raft pellets were resuspended in 60 μL of MBS containing 1mM Na_3VO_4, 0.01 mg/mL aprotinin, 0.01 mg/ml leupeptin, and 1mM PMSF. Protein in raft and soluble fractions was quantitated, and equal amounts of protein were separated by SDS-PAGE, transferred to nitrocellulose, and subjected to Western blotting for the μ heavy chain of the IgM receptor, anti-phosphotyrosine, $G\alpha_{i3}$, and actin. A parallel SDS-PAGE gel was used to separate equal amounts of raft protein and processed by silver staining.

2.8 CD20 translocation to Triton-insoluble rafts

Initially, CD20 association with Triton-insoluble rafts was analyzed by crude fractionation of cells into Triton-soluble and Triton-insoluble fractions, as Triton-insoluble CD20 has previously been shown to associate entirely with low density Triton-insoluble fractions (Deans et al., 1998). The day before an experiment, Ramos517/vector and Ramos517/pigM cells were set up at equal density (5 x 10^5 cells/mL) in fresh RPMI complete. On the following day, the cells were washed once in warm (37°C) RPMI, aliquoting 2 x 10^6 cells into one microfuge tube for each treatment condition, prior to centrifuging cells to remove the medium after the wash. Each cell pellet was resuspended in 50 μL of warm RPMI. To each tube, 50 μL of RPMI alone, or RPMI containing hIg, rituximab, hIg + $F(ab')_2$ anti-hIgG, or rituximab + $F(ab')_2$ anti-hIgG was added, as indicated in the figure legends. The cell/antibody suspension was lysed immediately (untreated control cells with no antibody added) or incubated at 37°C for 30 seconds, 1 min, 5 min, 15 min, or 60 min and then lysed by the addition of 100 μL of 2%

Triton X-100/Tris lysis buffer on ice. Twenty minutes after lysis of the last sample in the timecourse, the samples were centrifuged at 14 000 x g for 15 minutes at 4°C. The supernatant (soluble fraction), was saved in a fresh microfuge tube and 40 μL of 6 x SDS sample buffer was added. The Triton X-100-insoluble pellet was washed three times with 250 μL volumes of 1% Triton/Tris lysis buffer, and then resuspended in 100 μL of 2 x SDS sample buffer. The pellet fraction was heated at 95°C for 5 minutes, vortexed, and frozen at -80°C. The heat/vortex/freeze/thaw procedure was repeated two more times, and both the soluble and pellet fractions were heated at 95°C, prior to loading equal volumes of each sample (5×10^5 cell equivalents) on SDS-PAGE gels, prior to Western blotting for CD20 and actin.

Several experiments were also performed using sucrose density gradient centrifugation to examine CD20 association with low density, Triton-insoluble membranes. Ramos517/vector and Ramos517/pigM cells were set up at equal density (1×10^6 cells/mL) in fresh RPMI complete the evening before the experiment. The next day, 2×10^7 cells per treatment were washed in warm RPMI, and aliquoted into microfuge tubes, prior to centrifugation at 3000 x g for 1 min to remove the medium. The cell pellet was resuspended in 500 μL of warm RPMI. Another 500 μL of warm RPMI alone, or RPMI containing hIg, rituximab, hIg + $F(ab')_2$ anti-hIgG, or rituximab + $F(ab')_2$ anti-hIgG was added to the cells, and the mixture was incubated at 37°C for 15 minutes. Cells were pelleted by centrifugation at 3000 x g for 1 minute and then lysed in 1 mL of 1% Triton X-100/MBS lysis buffer. Lysates were fractionated into raft, soluble, and pellet fractions using sucrose density gradient centrifugation as described in section 2.10. Raft pellets were resuspended in 50 μL of 2 x SDS sample buffer. The high

density pellet was washed twice in PBS and then solubilized in 200 μL of 2 x SDS sample buffer followed by two cycles of heating at 95°C, freezing at -80°C and thawing. Equal amounts of protein were separated by SDS-PAGE and analyzed by Western blotting for CD20, $G\alpha_{i3}$, and actin.

2.9 Flow cytometry

2.9.1 Staining for cell surface antigens

Viable unfixed cells (1 x 10^6/sample) were washed three times in 1 mL of PBS, and then resuspended in 100 μL of PBS containing the primary antibody. Cells were incubated on ice for 30 minutes, and then washed three times with 1 mL of cold PBS. Cells stained with a fluorophore-conjugated primary antibody were resuspended in 1 mL of cold PBS and analyzed by flow cytometry. Samples requiring indirect staining were resuspended in 100 μL of cold PBS containing the appropriate fluorophore-conjugated secondary antibody and incubated on ice for 30 minutes. The cells were washed 3 times in 1 mL of cold PBS, and resuspended in 1 mL cold PBS for analysis by flow cytometry. The amount of each antibody used is given in the table in section 2.2**.**

2.9.2 Annexin V/PI Apoptosis Assay

Cells were treated with apoptosis-inducing stimuli as described in section 2.5. At the indicated time points post-treatment, cells were stained with annexin V-FITC and propidium iodide (PI) using the BD ApoAlert Annexin V-FITC Apoptosis Kit (Clontech). Briefly, 1 x 10^6 cells from each sample were washed one time with 1 mL of serum-free RPMI, and resuspended in 100 μL of 1 x binding buffer containing 5 μL of 20 μg/mL annexin V-FITC and 10 μL of 50 μg/mL PI. The cell suspension was gently mixed, and then incubated in the dark at RT for 15 minutes. After addition of an

additional 400 μL of 1 x binding buffer, the cells were immediately analyzed by two-colour flow cytometry. Cells staining positive for annexin V and negative for PI were considered apoptotic. Cells staining positive for both annexin V and PI were considered to be late apoptotic and/or necrotic cells.

2.9.3 Ratiometric Calcium Assay

Intracellular calcium concentrations were measured using a ratiometric flow cytometric assay essentially as described by Novak and Rabinovitch (Novak and Rabinovitch, 1994). The day before each experiment, the cell lines to be used were set up at equal density (5 x 10^5 cells/mL) in fresh RPMI complete. The following day, cells were washed once in warm serum-free RPMI, and then resuspended in warm serum-free RPMI containing 4 μM fluo-3, AM (Invitrogen) and 10 μM fura red, AM (Invitrogen) at 1 x 10^7 cells/mL. The cell/dye suspension was incubated at 37ºC for 30 minutes in the dark, and then washed once with warm serum-free RPMI. 2 x 10^6 cells/sample were aliquoted into 5 mL round-bottom tubes prior to centrifuging the cells after washing. In experiments in which cells were stimulated with $F(ab')_2$ goat anti-human IgM, the cell pellet was resuspended in 2 mL of calcium buffer for subsequent flow cytometric analysis. In experiments in which cells were stimulated by hypercrosslinking of CD20, the cells were first resuspended in 100 μL of calcium buffer containing 0.02 μg/μL of rituximab or control hIg and incubated for 15 minutes. Excess primary antibody was removed by washing cells twice in 2 mL volumes of calcium buffer. The cell pellet was resuspended in 2 mL of calcium buffer for flow cytometric analysis.

Flow cytometry was performed on a Becton Dickinson FACScan flow cytometer (BD Bioscience) with a 488 nm laser excitation source. Green (fluo-3) and red (fura red)

fluorescence emission was collected in linear mode over a total period of ten minutes. Baseline fluorescence was measured for the first 60 seconds of the experiment. At this time, the tube was removed from the sample injection port (SIP), the stimulating antibody ($F(ab')_2$ goat anti-human IgM or $F(ab')_2$ goat anti-hIgG as indicated in the figure legends) was added in 50 μL of calcium buffer, and the cell-antibody suspension was quickly mixed by inverting the capped tube a total of three times. The tube was replaced on the SIP and data was collected for the remaining period of time. The data was analyzed using FlowJo (Tree Star Inc, San Carlo, CA).

2.10 Isolation of lipid raft fractions

Low-density detergent-resistant membrane fractions (raft fractions) were isolated essentially as described by Robbins *et al.* (Robbins et al., 1995). A maximum of 1×10^8 (for U937, $U937_{tpa}$, THP-1, HL60, K562, IVEE, IVEE/GPI8 cells) or 2×10^8 (for Raji26 and Ramos517 cells) cells were lysed in 1 mL of 1% Triton X-100/MBS lysis buffer and incubated on ice for 30 minutes. Lysates were dounce homogenized using approximately 25 strokes, and adjusted to a final concentration of 40% sucrose by the addition of 1 mL of 80% sucrose in 1% Triton X-100/MBS lysis buffer. Samples were transferred to ultracentrifuge tubes (Beckman), overlaid with a 10 mL linear 30% to 5% sucrose gradient, and centrifuged at 37 000 rpm for 16 hours at 4°C in an SW41 rotor (Beckman). The top 7 mL of the gradient was harvested as the raft fraction, diluted 1:3 with MBS, and insoluble material was pelleted by centrifugation at 37 000 rpm for 1 hour at 4°C in an SW41 rotor. An aliquot of the bottom 2 mL of the gradient was reserved for analysis of soluble material (soluble fraction). The high-density insoluble pellet was washed three times with PBS and resuspended in 200 μL of 2 x SDS sample buffer. In specific

experiments analyzing 1% Brij58 raft fractions, the same protocol was used except that 1% Brij58/MBS lysis buffer was used in place of 1% Triton X-100/MBS lysis buffer.

2.11 *In vitro* kinase assay of raft fractions

Raft fractions were isolated as described above. The final pellet of raft material was resuspended in 50 μL of kinase assay buffer without ATP and split into two equal aliquots. Five μL of 300 μM ATP in kinase assay buffer was added to one sample, giving a final concentration of 50 μM ATP. Five μL of kinase assay buffer without ATP was added to the second sample, and the samples were incubated at room temperature for 15 min. Prior to two-dimensional gel electrophoresis, the samples were pelleted by centrifugation at 100 000 x g for 20 minutes at 4°C, resuspended in 30 μL of thiourea lysis buffer, and processed as described below.

2.12 Protein quantitation

Total protein in detergent lysates of whole cells, or in raft or soluble fractions was measured using a bicinchoninic acid (BCA) assay for the colorimetric detection and quantitation of total protein according to the manufacturer's protocol (Pierce), using bovine serum albumin (BSA) standards.

2.13 Polyacrylamide gel electrophoresis

2.13.1 Two-dimensional gel electrophoresis

Two-dimensional (2D) gels were run as described by O'Farrell (O'Farrell, 1975) with some modifications. Fifteen cm long glass tubes with a 1.5 mm inside diameter or a 3.4 mm inside diameter (BioRad) were sealed at one end with Parafilm and used for first dimension isoelectric focusing (IEF). Polyacrylamide tube gels containing a final concentration of 4.73% acrylamide, 0.27% bis-acrylamide, 5% carrier ampholytes

(BioRad; a mix of 70% pH 5-7 ampholyte mixture and 30% pH 3-10 ampholyte mixture), 2% NP-40, and 9 M urea were poured using 0.0015 vol of a 10% APS stock solution and 0.001 vol of TEMED, and overlaid with 8 M urea during polymerization. After polymerization was complete, the parafilm was removed, and the top and bottom of each gel was rinsed three times with ddH_2O, and once with thiourea lysis buffer immediately prior to sample loading. Prior to 2D gel analysis, raft membrane pellets were directly solubilized in a small volume of thiourea lysis buffer (30 μL per tube gel) and then stored at -20°C. Approximately three hours prior to loading onto the IEF gels, samples were thawed and kept at room temperature to promote protein solubilization. Samples were centrifuged at 100 000 x g for 15 min to remove insoluble particulate matter, and the supernatant was loaded onto tube gels installed in a vertical tube gel electrophoresis apparatus (BioRad). Samples were overlaid with an equal volume of thiourea lysis buffer diluted 1:4 with ddH_2O to prevent contact with the catholyte (0.1 M NaOH) filling the upper chamber. The lower chamber was filled with anolyte (0.01 M H_3PO_4). Both anolyte and catholyte were degassed prior to use. Isoelectric focusing was performed by applying 800 V overnight.

Tube gels were removed from the glass tubes at the completion of IEF by gentle mechanical pressure with an 18 cm long needle against a small plug of clean Kimwipe inserted into the tube at the basic end of the gel. The tube gels were stored frozen at -80°C or processed immediately for second dimension SDS-PAGE by soaking in 2 mL of gel equilibration buffer for 30 minutes. For 1.5 mm diameter tube gels, the tube gels were placed between the vertical glass plates of a 10% SDS-PAGE vertical slab gel (with stacking gel omitted), directly on top of the resolving gel, ensuring that no air bubbles

were present between the tube gel and the slab gel. For 3.4 mm diameter tube gels, the 10% SDS-PAGE gel was topped with stacking gel poured to the top edge of the plates, and the tube gel was sealed to the top of the stacking gel with 0.7% agarose to hold it in place. SDS-PAGE, Western blotting, and silver staining were performed as described in the following sections.

2.13.2 One-dimensional SDS-PAGE

Protein samples were solubilized by boiling in 1x SDS sample buffer and loaded onto 10% polyacrylamide vertical slab gels. The resolving gels were 13 cm high and 15 cm wide. Electrophoresis was performed in an Aladdin polyacrylamide gel electrophoresis apparatus for 1000 volt·hours.

2.13.3 Silver staining of polyacrylamide gels

Silver staining was performed based on the protocols described by Rabilloud *et al.* (Rabilloud et al., 1988) and Blum *et al.* (Blum et al., 1987). All solutions were freshly prepared on the day of use. A volume of 100 mL of solution was used per gel, and gels were processed in separate glass dishes. Gels were fixed overnight in 10% acetic acid/30% ethanol, and then washed three times, for 20 minutes per wash, with 30% ethanol. Gels were sensitized in 0.2 g/L sodium thiosulfate for 1 minute, rinsed in ddH_2O three times, for 20 seconds per wash, and incubated at room temperature for 30 minutes in 0.2% silver nitrate and formaldehyde (75 μL of 37% stock per 100 mL of solution). Following two 20 second washes in ddH_2O, gels were developed in 6% sodium carbonate containing formaldehyde (50 μL of 37% stock per 100 mL) and sodium thiosulfate ($4x10^{-3}$ mg/mL). The reaction was stopped by the addition of 3.5 mL of glacial acetic

acid to the developer. To avoid increased background staining, the gels were then washed four times, for 30 minutes each wash, with ddH_2O to remove acetic acid.

2.13.4 Western blotting

Following electrophoresis, proteins were transferred to nitrocellulose (Schleicher & Schuell) by sandwich blotting using Towbin transfer buffer in a wet transfer apparatus (BioRad) for 2 hours at 800 mA. For CD20 Western blots, samples were transferred onto polyvinyldifluoride (PVDF) instead of nitrocellulose. The membranes were dried at room temperature, and then blocked using 5% BSA (Roche Applied Science, in the case of CD20, phosphotyrosine and streptavidin blots) or 5% non-fat dry milk (Carnation, for all other blots) in the wash buffer indicated in the table in section 2.2 for at least 30 minutes. Membranes were incubated in primary antibody diluted in blocking buffer for 1 hour at room temperature, or overnight at 4°C, and then washed three times for 10 minutes in wash buffer. Blots were incubated for 30 minutes in HRP-conjugated secondary reagents diluted in blocking buffer, washed as described above, and developed using an enhanced chemiluminescence substrate (ECL).

2.14 Protein identification by mass spectrometry

Spots excised from 2D gels and bands excised from 1D gels were stored frozen at -80°C prior to MS analysis at the Alberta Cancer Board (ACB) Proteome Mass Spectrometry Facility at the University of Alberta, Edmonton, Alberta, Canada. Personnel at the ACB Proteomics laboratory prepared the samples and conducted the MS analysis according to standard in-house protocols. Gel spots or bands were subjected to washing, reduction, alkylation, tryptic digestion, and extraction of tryptic peptides from the gel pieces. MALDI-MS of peptide extracts was carried out using a Bruker REFLEX

III TOF mass spectrometer (Bremen/Leipzig, Germany). Peptide masses obtained by MALDI-MS were used for peptide mass fingerprinting by database searching with Mascot (Matrix Science). For certain samples, 1-3 selected peptides were fragmented by MALDI-MS/MS analysis performed on a PE Sciex API-QSTAR pulsar (MDS-Sciex, Toronto, Ontario, Canada). The obtained partial sequence information for each peptide was used to confirm the previously obtained results from the peptide mass search. In some experiments, LC-MS/MS analysis was performed on samples extracted from bands cut from 1D gels. In this case, peptide extracts obtained as described above were desalted using C-18 ZipTips, followed by capillary LC-MS/MS experiments on a Finnigan LCQ^{deca} ion-trap mass spectrometer coupled with a capillary C-18 HPLC system.

Raft pellets isolated from 2.25 x 10^8 IVEE or IVEE/GPI8 cells were resuspended in a total of 150 μL of PBS, and protein levels were quantitated prior to shotgun proteomics analysis. The samples were given to Ella Ng in the laboratory of Dr. David Schriemer at the University of Calgary, who performed a shotgun proteomics analysis as follows. Raft samples were solubilized and digested with trypsin essentially as described by Blonder *et al.* (Blonder et al., 2004a). The raft pellet was washed in ddH_2O, and resuspended in 25 mM NH_4HCO_3, pH 7.9 with intermittent vortexing and sonication. The membrane vesicles were pelleted by ultracentrifugation, and the supernatant was discarded. These steps were repeated five times to remove residual Triton X-100. The final membrane pellet was resuspended in 60% methanol/40% 50 mM NH_4HCO_3 buffer, pH 7.9 to solubilize integral and membrane-bound proteins. Trypsin was directly added to this solution to a final ratio of 1:50 (trypsin:protein) to digest solubilized proteins, and

the peptide digest was stored at -80°C prior to MS analysis. Chromatographic separation was performed with a Zorbax 300 SB-C18 analytical column (Zorbax 300 SB-C18, 3.5 μm, 75 μm ID x 15 cm long) using the Agilent 1100 nanoLC system (Agilent Technologies). Two μg of sample in a 2 μL volume was loaded onto an enrichment column (Zorbax 300 SB-C18, 5 μm, 5 x 0.3 mm) using an Agilent binary pump starting with a flow rate of 5 μL/min and ramped to 40 μL/min over 8 minutes. The analytical column was equilibrated for 5 minutes with 97% mobile phase A (0.05% formic acid, 3% acetonitrile in water) and peptides were eluted using a linear gradient from 3% to 90% mobile phase B (0.0%% formic acid, 3% water in acetonitrile) over 100 minutes with a constant flow rate of 0.3 μL/minute. The analytical column was connected online to an ion-trap Agilent LC/MSD Trap XCT mass spectrometer using a nanoelectrospray source with an applied electrospray potential of 1.8 kV. The three most abundant peptide molecular ions in each full MS scan were selected for MS/MS fragmentation. The MS scan range was between 400 and 2200. Database searching was performed using the Agilent Spectrum Mill MS Proteomics Workbench software (Agilent Technologies).

2.15 Cholesterol Assay

For measurement of total cholesterol, 1.5 x 10^6 cells/sample were plated in 3 mL of fresh RPMI complete in one well of a 6 well dish, and cultured overnight. The following day, all of the cell suspension was collected and spun down, and the cell pellet was washed twice in 5 mL PBS. After the second wash, the cells were resuspended in 5 mL of RPMI, 5 mL of RPMI + 10 mM methyl-β-cyclodextrin (MβCD; Sigma), or 5 mL of RPMI + 10 mM MβCD + 1.4 mM cholesterol (Sigma), and incubated at 37°C for 15

minutes. The cells were then washed twice in 5 mL volumes of PBS, and each cell pellet was lysed by addition of 300 μL of cold 1% Triton X-100/Tris lysis buffer. Lysates were kept on ice for 30 minutes and mixed well by pipetting prior to protein and cholesterol quantitation.

For measurement of raft cholesterol levels, 1 x 10^8 cells were plated in 100 mL of fresh RPMI complete the evening before the experiment. The next day, Triton-insoluble raft fractions were prepared as described in section 2.10 using 1 x 10^8 cells/gradient and one gradient/cell line. The pellet of raft material was resuspended in 60 μL of PBS, and the solution was mixed vigorously by repeated pipetting prior to protein and cholesterol quantitation.

Cholesterol levels were measured using the Amplex Red Cholesterol Assay Kit (Invitrogen) based on the manufacturer's supplied protocols. In this enzyme-based fluorometric assay, both free cholesterol and cholesteryl esters are quantitated. Cholesteryl esters are first hydrolyzed to cholesterol by cholesterol esterase. Cholesterol is oxidized by cholesterol oxidase to yield H_2O_2 and a ketone product. The H_2O_2 produced is detected using 10-acetyl-3,7-dihydroxyphenoxazine (Amplex Red reagent), which reacts with H_2O_2 in the presence of HRP with a 1:1 stoichiometry to produce highly fluorescent resorufin. Raft and total cholesterol samples were diluted 1:25 and 1:5, respectively, in the supplied reaction buffer. 50 μL of cholesterol-containing sample or 50 μL of cholesterol reference standards (0, 1, 2, 10, and 20 μM cholesterol in reaction buffer) were added to each well of a 96 well plate. Each sample or standard was assayed in triplicate within a given experiment. Fifty μL of 300 μM Amplex Red reagent in

reaction buffer containing 2 U/mL horseradish peroxidase (HRP), 2 U/mL cholesterol oxidase, and 0.2 U/mL cholesterol esterase was added to each well to initiate the reaction. The plate was incubated at 37°C in the dark for 30 minutes, followed by measurement of fluorescence in a fluorescence microplate reader using excitation at 560 nm and emission detection at 590 nm. Background fluorescence was corrected for by subtracting the average number of counts from the three 0 μM cholesterol wells from the reading for each sample well.

2.16 Statistical analysis

All statistical analyses were performed using Graphpad Prism v.4. Comparison of raft cholesterol levels in GPI-deficient and wildtype cells was performed using a paired, two-tailed t-test. The levels of total cholesterol in GPI-deficient and wildtype cells were compared using one-way analysis of variance (ANOVA) with blocking of each experimental replicate. Multiple comparisons were carried out using the Bonferroni post test. All other experimental data sets in Chapter 4 were analyzed using two-way ANOVA with blocking of each experimental replicate and Bonferroni post tests. Statistical significance was defined using the critical value $\alpha = 0.05$.

Chapter Three: Proteomic Analysis of Non-Caveolar Lipid Rafts from Hematopoietic Cells

3.1 Introduction

In the last decade, techniques for the systematic large-scale study of genes and gene expression have been firmly established in the field of genomics. The complete or almost complete sequencing of the genomes of more than 150 organisms, from bacteria to humans, has tremendously influenced biology and medicine (Baggerman et al., 2005; Woodage and Broder, 2003). This has provided a wealth of new information about the structure and composition of these genomes, including a multitude of previously unknown genes. These successes have also motivated the development of techniques for the large-scale study of proteins, which are, for the majority of genes, the real mediators of biological function (Pandey and Mann, 2000). Marc Wilkins introduced the term proteome in 1994 to refer to "the proteins expressed by a genome or tissue" (Huber, 2003). In contrast to the genome, which is the same in all cells of a single organism, there are in fact many different proteomes. The complement of proteins expressed in a particular cell at a particular time and place is highly context dependent, varying not only with cell type, but also dynamically in response to differing physiological and/or disease states (Huber, 2003). The proteome is also far more complex than the genome for several reasons. Alternative splicing of mRNAs can give rise to multiple distinct protein products derived from a single gene (Newman, 1998). Each of these protein products can undergo further post-translational processing, including more than three hundred different post-translational modifications that have been identified (Krishna and Wold, 1993), some of which are reversibly regulated in response to biological stimuli. Proteomics can

be defined as the large-scale determination of the sequence, quantity, structure, modification state, activity, subcellular localization, and interaction partners of the proteins in a given cell type at a particular time (Pandey and Mann, 2000). Most proteomic studies to date have focused on analyzing only one, or at most a few, of the above properties at a time in the context of a specific biological question. For example, some studies have focussed on identifying proteins with particular modifications such as methylation (Ong et al., 2004), or phosphorylation (Nuhse et al., 2003), while others have identified proteins in a particular organelle (Yates et al., 2005), or compared changes in protein expression between benign and malignant human tumours to identify tumor markers (Alaiya et al., 2000). A number of different protein analysis techniques are used in proteomics experiments, depending on the question of interest. One of the most common core techniques identified with proteomics is two-dimensional (2D) gel electrophoresis (Gorg et al., 2000; O'Farrell, 1975). However, by far the most influential development in proteomics has been the application of mass spectrometry-based approaches to protein analysis (Domon and Aebersold, 2006; Pandey and Mann, 2000).

First introduced in 1975 (O'Farrell, 1975), 2D gel electrophoresis has been extensively used in proteomics experiments due to its unparalleled ability to both resolve and display complex mixtures of proteins. In this technique, proteins are resolved in the first dimension using isoelectric focusing (IEF) in a thin tube or strip gel, which separates proteins based on their differing isoelectric points. In the second dimension, the IEF gel is placed horizontally across the top of a slab gel, in which proteins are separated according to their molecular weight by SDS-PAGE. The slab gel is then subjected to conventional protein staining methods or Western blotting to analyze the pattern of

resolved proteins. Using this strategy under ideal conditions, up to several thousand proteins can be resolved on a single gel (Gorg et al., 2000; O'Farrell, 1975). In the original procedure described by O'Farrell (O'Farrell, 1975), IEF was carried out in tube gels where soluble carrier ampholytes migrated under the influence of an electric field to create the necessary pH gradient. More recently the use of immobilized pH gradient (IPG) gel strips, in which the acidic and basic buffering groups that create the pH gradient are covalently integrated into the gel matrix, has increased the stability and range of pH gradients that are available (Hanash, 2000). Additional improvements include more efficient protocols for protein solubilization prior to electrophoresis (Molloy, 2000; Pasquali et al., 1997), different methods of sample application onto the IEF gel (Gorg et al., 2000), and improved protein staining methods with increased sensitivities and linear dynamic ranges (Patton, 2000). The 2D gel profiles observed are sufficiently reproducible to allow the comparison of two or more different samples, and any differences observed in spot intensity can be compared quantitatively using commercially available software for spot detection (Englbrecht and Facius, 2005; Kakhniashvili et al., 2005). Once spots of interest have been resolved and defined, they can be identified using mass spectrometry (MS).

The development of biological MS techniques has become a central platform supporting an ever-increasing number of proteomics strategies. In the late 1980s, two soft ionization techniques were developed that allowed the routine formation of molecular ions from intact biomolecules without excessive fragmentation, electrospray ionization (ESI) (Fenn et al., 1989) and matrix assisted laser desorption/ionization (MALDI) (Karas and Hillenkamp, 1988). Using these techniques, the analysis of

polypeptides by MS became feasible. The increased sensitivity and speed of MS when compared to traditional microsequencing by Edman degradation has allowed MS-based strategies for protein identification and amino acid sequencing to become the mainstream method for polypeptide analysis (Domon and Aebersold, 2006). There are two major approaches to protein identification using MS. The first is referred to as "peptide mass mapping" or "peptide mass fingerprinting" (PMF) (Gevaert and Vandekerckhove, 2000; Pappin et al., 1993; Yates et al., 1993). In the most common manifestation of this technique, a purified protein is digested with a proteolytic enzyme of known specificity, usually trypsin, and the peptide extract is analyzed by MS to generate a spectrum of peaks representing the different masses of the individual peptides. Specifically designed database-searching software is able to compare this "fingerprint" of peptide masses to the virtual "fingerprints" obtained by theoretically cleaving the protein sequences found in databases, and the top-scoring proteins are retrieved as possible matches. The search programs allow for a limited amount of flexibility when matching peptides to account for uncleaved enzyme sites, or for posttranslational modifications to peptides that commonly occur *in vivo* or during sample processing (Englbrecht and Facius, 2005). Since PMF becomes less reliable in mixtures of proteins, for more confident and reliable protein identifications, tandem MS (or MS/MS) search strategies were designed (Wilm and Mann, 1996; Yates et al., 1996). Proteins or protein mixtures are extracted and proteolytically digested as for PMF. As its name suggests, tandem MS consists of two consecutive MS steps (Domon and Aebersold, 2006; Englbrecht and Facius, 2005). The first step is identical to that described for PMF. In the second step, significant peptides from the PMF are selected using mass filters, one at a time, and fragmented in a collision

chamber filled with argon gas. When the selected peptides collide with the relatively large argon atoms, the peptide breaks at or near a peptide bond into two ionized fragments, creating a series of different ion types depending on the site of cleavage (Englbrecht and Facius, 2005). This new set of peptide ions is analyzed in the second MS step, generating a peptide fragment mass fingerprint (PFMF). There are two general approaches used to interpret the fragmentation data from tandem MS using various search algorithms (Englbrecht and Facius, 2005). In the first case, all possible peptides are generated from a protein sequence database. Theoretical PFMFs for all of these peptides are generated using known fragmentation rules, and the search program attempts to find the best match to a given experimental PFMF. The second approach tries to directly interpret the PFMF to derive the full or partial amino acid sequence of the peptide, and the obtained sequence tag is then used for database-searching. This approach, also called *de novo* sequencing, depends on the correct identification of the different types of ions in the PFMF, as the difference between two neighbouring peaks of the same ion type gives the mass of a single amino acid [see (Englbrecht and Facius, 2005), and references therein].

Using both PMF and tandem MS approaches, many investigators have successfully identified proteins isolated from 2D gels, but despite its advantages, 2D gel electrophoresis has certain limitations. Very hydrophobic proteins, such as membrane proteins, are difficult to analyze by 2D gel electrophoresis because of the difficulty of solubilization in the IEF sample buffers and because, once solubilized, they are prone to precipitation at their isoelectric points (Santoni et al., 2000; Wu and Yates, 2003). Very acidic or extremely basic proteins falling outside the pH range of the 2D gel system being

used are also excluded--very basic proteins in particular have been more difficult to resolve on 2D gels due to cathodic drift of carrier ampholyte gradients. This problem has been somewhat ameliorated by the use of IPG strips for the first dimension (Gorg et al., 2000). In light of continuing improvements in the sensitivity and mass accuracy of mass spectrometers, combined with increasing use and refinement of tandem MS protein identification approaches that are more suitable for analyzing complex protein mixtures, many investigators have also turned to traditional 1D gel analyses coupled with MS protein identification, since it is easier to solubilize difficult samples for SDS-PAGE (Galeva and Altermann, 2002; Simpson et al., 2000; Wu and Yates, 2003). Gel-free methods have also become an important proteomics tool. In these "shotgun" proteomics approaches, complex protein samples are digested in solution, and the peptide extracts are then extensively fractionated by one or more chromatographic steps prior to analysis by high-throughput, rapidly scanning, automated MS/MS instruments (Domon and Aebersold, 2006; Wu and Yates, 2003). Shotgun proteomics experiments have the advantage of being easily adapted for accurate quantitation, and they exhibit increased proteomic coverage compared to gel-based techniques (Blonder et al., 2004a; Domon and Aebersold, 2006). An increasing number of methods are also available for the detection and analysis of a variety of post-translational modifications using MS (Larsen et al., 2006; Mann and Jensen, 2003). Overall, the optimization and development of both gel-based and gel-free MS-based methods for protein identification and characterization have provided powerful tools to cell biologists interested in specific biological questions.

At the outset of the research described in this thesis, the identification and study of different protein markers of lipid rafts through various biochemical and microscopic

approaches had already provided important insight into the structure, composition, organization, and functional roles of these membrane microdomains. When early studies of the protein composition of isolated raft fractions revealed that rafts appeared to be enriched in signalling molecules (Chang et al., 1994a; Hope and Pike, 1996; Lisanti et al., 1994b; Wu et al., 1997) (Table 1.2), a functional role for lipid rafts in mediating signal transduction was proposed (Lisanti et al., 1994a; Okamoto et al., 1998; Simons and Ikonen, 1997). It was also apparent that the protein composition of rafts varied in different cell types (Brown and London, 1997; Ilangumaran et al., 1997), as well as before and after the activation of a number of different receptors (Bi et al., 2001; Field et al., 1997; Gustavsson et al., 1996; Mineo et al., 1999; Montixi et al., 1998; Petrie et al., 2000). Furthermore, several studies suggested evidence of distinct subpopulations of rafts with different protein and lipid compositions in the same cell, which appeared to compartmentalize distinct signalling pathways (Gomez-Mouton et al., 2001; Iwabuchi et al., 1998; Roy et al., 1999). It was apparent that lipid rafts existed in hematopoietic cells, even though most hematopoietic cell types did not express caveolin or have morphologically identifiable caveolae (Fra et al., 1994; Fra et al., 1995; Parolini et al., 1996). The importance of these membrane microdomains in hematopoietic cell signalling was also established (Cheng et al., 1999; Field et al., 1997; Janes et al., 2000; Marmor and Julius, 2001). The Robbins' laboratory was interested in further characterizing the structure and function of non-caveolar lipid rafts in cells of hematopoietic origin, because we thought that these rafts might have unique properties or regulatory mechanisms. The overall hypothesis of this thesis is that the specific properties of a given lipid raft, including its protein composition, define its capacity in

cellular signalling, and that changes in raft properties such as protein composition, due to either physiological or pathological circumstances would substantially affect raft function as it relates to signal transduction. At that time, there were no published studies that attempted to systematically characterize the protein composition of lipid rafts in hematopoietic cells. Therefore I decided to utilize a novel and relatively unbiased proteomics approach to characterize and compare the protein composition of lipid rafts isolated from a number of different hematopoietic cell lines. The experiments described in this chapter encompass both gel-based and gel-free approaches to the proteomic analysis of detergent-resistant lipid raft fractions. Cell lines from both myeloid and lymphoid lineages were chosen as a model to investigate potential changes that might reflect the differentiation status of the cells. In addition, raft fractions from GPI-deficient cells were compared to wildtype GPI-expressing cells in order to model the effects of the human disease paroxysmal nocturnal hemoglobinuria (PNH) on lipid rafts as an example of a pathologically relevant change in lipid raft composition. By comparing the lipid raft proteomes in these cells and identifying novel raft-associated proteins, we hoped to gain insight into the organization and function of non-caveolar lipid rafts. It was also anticipated that identification of novel raft proteins would lead to the discovery of previously unknown raft-mediated signalling pathways and provide a greater understanding of known compartmentalized signalling pathways, in addition to an increased understanding of signalling-independent raft functions.

3.2 Results

3.2.1 Two-dimensional gel analysis of the non-caveolar lipid raft proteome

The initial strategy employed to analyze the lipid raft proteome utilized the high resolution of 2D gel electrophoresis, because this approach enabled the comparison of the protein composition of lipid raft fractions from different cell types in addition to the identification of proteins of interest by MS. Advances in 2D gel analysis of membrane proteins at that time (Molloy, 2000; Pasquali et al., 1997) suggested that this was a reasonable strategy to apply to raft proteins. For the purposes of these studies, low-density Triton X-100 insoluble membrane fractions were prepared from whole cell lysates of the cell lines of interest using sucrose density gradient centrifugation. The complete disaggregation, solubilization, denaturation, and reduction of proteins are necessary to achieve a clear and well-focused first-dimension separation (Berkelman and Stenstedt, 2001). To this end, the isolated raft membrane pellet was directly solubilized in IEF sample buffer containing the chaotropic agents urea and thiourea, DTT as a reducing agent to cleave disulfide bonds, carrier ampholytes, and the zwitterionic detergent CHAPS. This sample buffer composition had previously been shown to enhance the solubilization of membrane proteins for 2D gel electrophoresis (Molloy, 2000). In pilot experiments it was also found that incubation of the raft membrane pellet in IEF sample buffer at room temperature for three hours prior to IEF improved solubilization of the raft proteins, as judged by the increased number and intensity of silver-stained spots observed on the 2D gels (data not shown). In the experiments described in this section a standard ampholyte mixture, which resulted in a pH gradient that enabled the focusing and separation of proteins with pIs ranging from approximately

4.5 to 8.5, was used in the first dimension, and a 10% SDS-PAGE gel was used to resolve proteins by size in the second dimension.

In order to determine whether or not the protein composition of non-caveolar lipid rafts was different in hematopoietic cell lines of different origins, in a preliminary set of experiments raft fractions were isolated from a number of different hematopoietic cell lines (Figure 3.1), and total protein profiles were observed by silver staining after 2D gel electrophoresis. Representative 2D gels of four different cell lines are shown in Figure 3.2. The cell lines examined included U937 cells (a myelomonocytic human leukemia cell line), U937 cells cultured for 48 hours in the presence of 12-*O*-tetradecanoylphorbol-13-acetate (TPA) to induce a more macrophage-like phenotype (Harris and Ralph, 1985), K562 erythroleukemia cells, and a B lymphoma cell line, Raji26/pigL. A manual comparison of the 2D gel protein profiles obtained indicated that while there were similarities in the protein patterns across the different cell lines (representative examples are indicated by the red arrows and circle in Figure 3.2), there were also differences visible even at a qualitative level, with some proteins being present in some cell types but undetectable in others (representative examples are indicated by the blue arrows in Figure 3.2). Thus, this preliminary data was consistent with evidence in the literature that the protein composition of raft fractions differed in different cell types, and indicated that at least some of these differences could be detected by the 2D gel method used.

It is known that many signalling proteins are of low abundance, and this hampers their detection in many proteomics experiments (Huber, 2003; Pandey and Mann, 2000). In order to determine if at least some raft signalling proteins were successfully resolved on 2D gels, *in vitro* protein kinase assays were performed using isolated lipid raft

Figure 3.1. Differentiation of hematopoietic cells.

During hematopoiesis in the bone marrow, all types of red and white blood cells are produced by the proliferation and differentiation of pluripotent hematopoietic stem cells. Early in hematopoiesis, the pluripotent stem cells differentiate along one of two major pathways to become myeloid or lymphoid stem cells, which in turn further differentiate to form committed progenitor cells for each type of mature hematopoietic cell. Unlike stem cells, the progenitor cells lack the capacity for self-renewal and are committed to differentiation along a given cell lineage. The myeloid stem cells produce erythrocytes, neutrophils, eosinophils, basophils, monocytes, mast cells and platelets, whereas the lymphoid stem cells generate B and T cells. A simplified schematic of hematopoiesis is shown here, emphasizing the lineages corresponding to the human cell lines used in this study. The K562, IVEE (GPI-negative K562), and IVEE/GPI8 (GPI-positive K562) cells are erythroid leukemia cells with a general myeloid phenotype that have the potential to further differentiate along the erythroid or megakaryocytic pathways. U937 and THP-1 cells are monocytic cell lines that can be induced to acquire the expression of additional macrophage markers upon treatment with TPA or vitamin D_3. HL60 cells are a myeloid cell line with the potential to differentiate along the monocytic or granulocytic pathways after exposure to TPA or DMSO respectively. The GPI-positive and GPI-negative Raji26 and Ramos517 B cell lines are sublines derived from the Raji and Ramos Burkitt's lymphoma cells that have been extensively used as *in vitro* models of mature B lymphocytes.

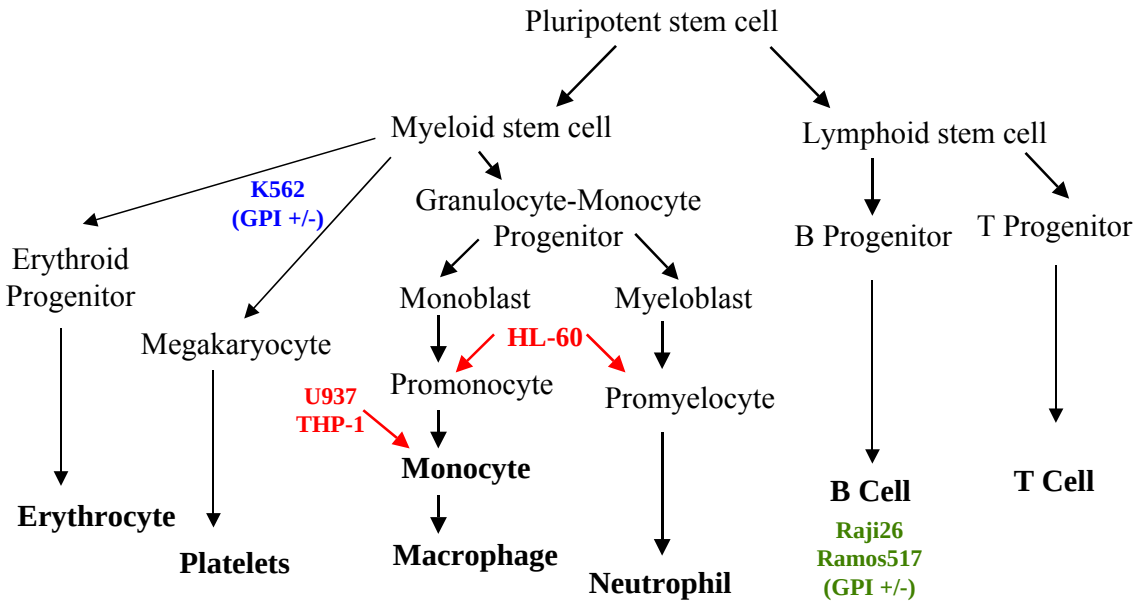
Pluripotent stem cell
Myeloid stem cell
Lymphoid stem cell
K562
(GPI +/-)
Granulocyte-Monocyte
Progenitor
B Progenitor
T Progenitor
Erythroid
Progenitor
Monoblast
Myeloblast
Megakaryocyte
HL-60
Promonocyte
U937
THP-1
Promyelocyte
Monocyte
Erythrocyte
Platelets
Macrophage
Neutrophil
B Cell
Raji26
Ramos517
(GPI +/-)
T Cell

Figure 3.2. Two-dimensional gel electrophoresis of lipid raft fractions isolated from hematopoietic cell lines.

Lipid raft fractions isolated from 1 x 10^8 U937, $U937_{tpa}$, or K562 cells, or from 2 x 10^8 Raji26/pigL cells were separated by 2D gel electrophoresis and silver stained. The red arrows and circle indicate several examples of spots that are similar in raft fractions isolated from these cell lines. The blue arrow indicates an example of spots that are unique to lipid rafts of that cell type. These results are representative of three independent experiments.

U937
(monocytic)

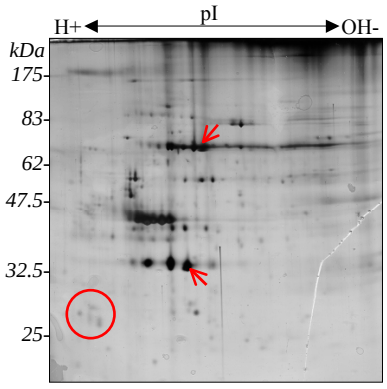

U937$_{tpa}$
(macrophage-like)

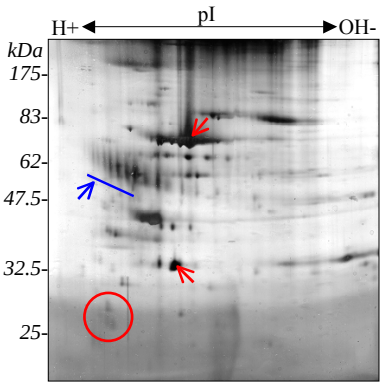

K562
(erythroid)

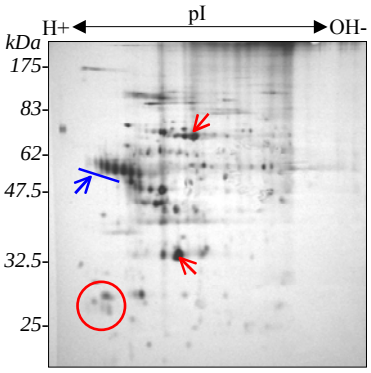

Raji26/pigL
(B cell)

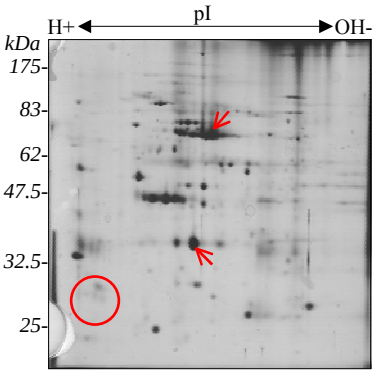

fractions from several different monocytic cell lines, followed by 2D gel analysis and immunoblotting with an anti-phosphotyrosine antibody, to detect potential protein tyrosine kinases and/or their substrates. A separate gel was processed in parallel by silver staining to determine whether the phosphorylated proteins identified by Western blotting could be putatively identified on silver-stained gels. As can be seen in a representative example using rafts isolated from THP-1 monocytic cells (Figure 3.3a), in the presence of ATP there is a significant increase in the amount of tyrosine phosphorylation detected by anti-phosphotyrosine immunoblotting. Some of the anti-phosphotyrosine signal overlapped with stained spots on the gel, though the immunoblot signal was so diffuse in some areas that it was difficult to correlate directly with a specific silver-stained spot or series of spots. This was not unexpected, as small populations of differentially phosphorylated forms of a given protein would exhibit slightly varying pIs from the major forms of the protein present in large enough amounts to be detectable by silver staining. However, a significant amount of the anti-phosphotyrosine signal in the immunoblot, corresponded to areas of the gel in which little or no protein was detectable, particularly in the more basic regions, indicating that a substantial amount of the tyrosine-phosphorylated raft proteins were present in amounts too low to be detected by the silver staining protocol used. In control raft samples in which ATP was omitted from the kinase assay buffer, most of the phosphotyrosine staining was present in the basic region between the 47.5 and 62.5 kDa markers, and staining in this region of the gel and in the basic region among proteins of higher molecular weight dramatically increased in raft samples incubated with ATP. This was also observed when the same experiment was conducted with raft samples isolated from U937 cells differentiated with TPA (data not

Figure 3.3. Many signalling proteins are of low abundance in raft fractions.

(A) Equal amounts of raft fractions isolated from THP-1 cells were subjected to an *in vitro* kinase assay in the presence and absence of ATP, and analyzed by 2D gel electrophoresis and Western blotting with an anti-phosphotyrosine monoclonal antibody. A parallel gel (in which no ATP was added to the raft fractions) was silver-stained. The results shown are representative of two independent experiments. (B) Equal amounts of raft proteins isolated from U937tpa cells were loaded on equivalent 2D gels. One gel was silver stained and the second gel was transferred to nitrocellulose for Western blot analysis with an anti-Hck polyclonal antibody. This experiment was performed once.

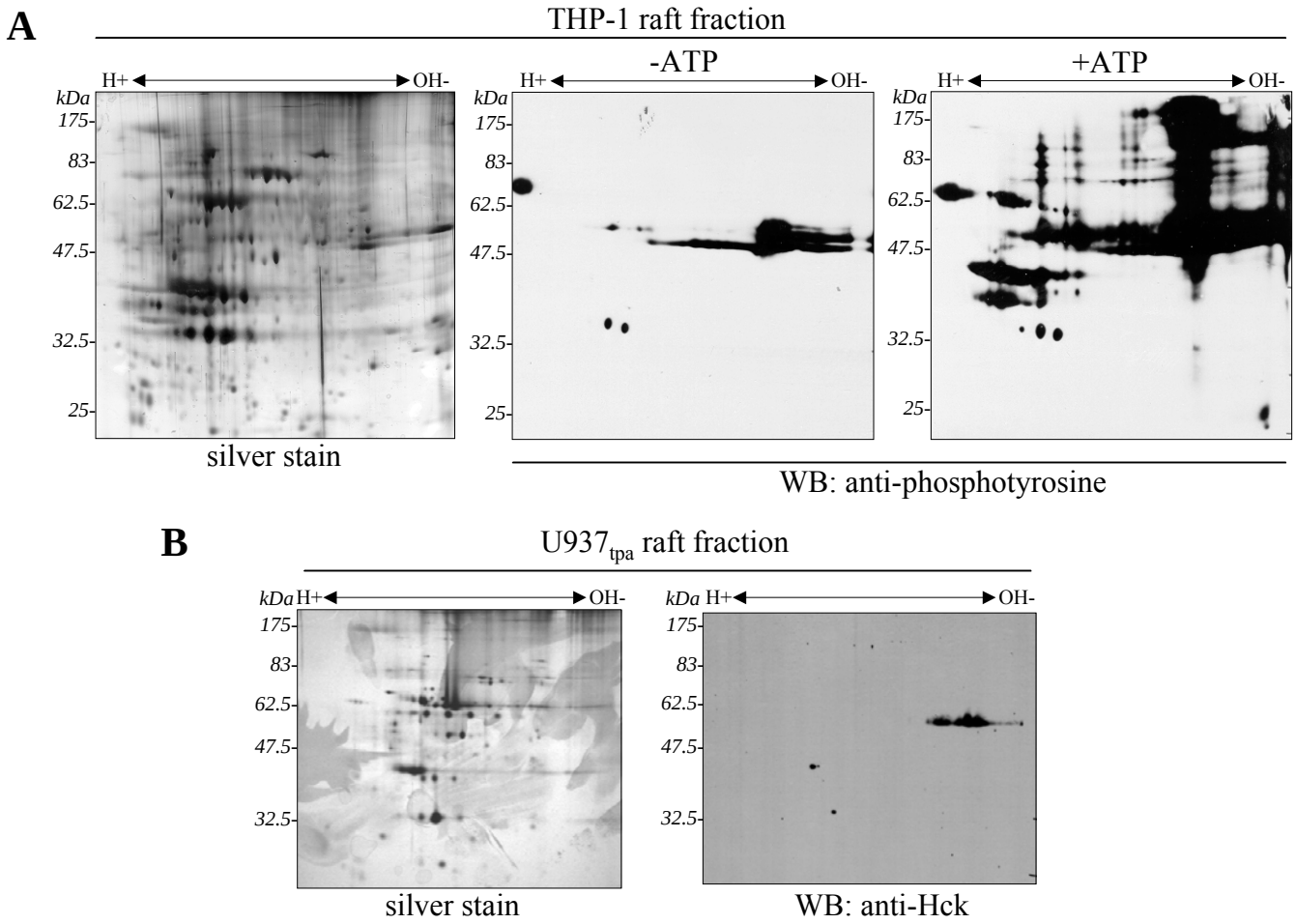
A
THP-1 raft fraction
-ATP
+ATP
H+
OH-
kDa
175
83
62.5
47.5
32.5
25
silver stain
WB: anti-phosphotyrosine
B
U937tpa raft fraction
WB: anti-Hck

shown). Many Src family kinases migrate in this molecular weight range and the Src family kinases are known to be both localized to lipid rafts and important in a number of different raft-compartmentalized signalling pathways (Cheng et al., 1999; Davy et al., 2000; Liu et al., 1997a; Robbins et al., 1995). Therefore a 2D Western blot of $U937_{TPA}$ raft proteins was probed with an antibody recognizing the Src family kinase Hck, which is abundantly expressed in lipid rafts in these cells (Murray and Robbins, 1998; Quintrell et al., 1987) (Figure 3.3b). This confirmed the presence of Hck in this region of the 2D gel, though in the accompanying silver stain there were no corresponding protein spots detected. Overall, these results suggest that 2D gel electrophoresis was successful in resolving at least some potential signalling molecules, but that many of these proteins were of relatively low abundance, and could not be detected by silver staining.

To further characterize the nature of the proteins resolved on the 2D gels, cell surface biotinylation of intact K562 cells was used to identify cell surface raft proteins that might also be potential signalling receptor candidates. As seen in Figure 3.4, immunoblotting with streptavidin-HRP detected a number of biotinylated proteins present in the 2D gel profile, indicating that cell surface proteins were successfully isolated and resolved in the 2D gels of raft fractions. Some of these protein spots, and series of spots, could be correlated to spots observed on the corresponding silver stain. However, other biotinylated proteins on the immunoblot were present in regions in which there were no proteins detectable by silver staining, indicating that some of the raft proteins present on the cell surface were of very low abundance. Notably, some of the most abundant proteins seen by silver staining were not biotinylated, suggesting that the

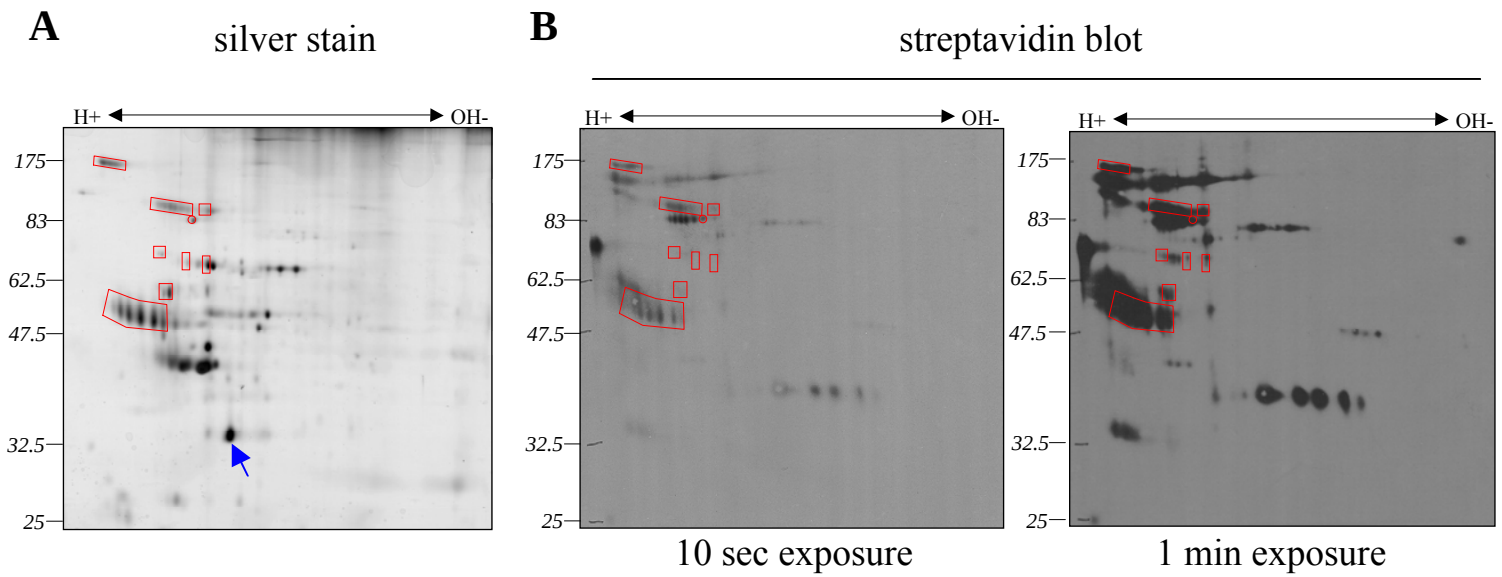

Figure 3.4. Identification of cell surface proteins in 2D gel profiles of raft fractions isolated from K562 cells.

Cell surface proteins on $2x10^8$ K562 cells were biotinylated with Sulfo-NHS-LC-biotin, excess biotinylation reagent was washed off, and cells were lysed in 1% Triton X-100/MBS. Raft fractions were isolated from the cell lysates using sucrose density gradient centrifugation. Raft protein from $1x10^8$ cells was run on two parallel 2D gels—one gel was silver-stained to visualize total protein (A), and the other was transferred to nitrocellulose and analyzed by Western blotting with streptavidin-HRP (A). The results shown are representative of two independent experiments.

biotinylation protocol was successful in selectively staining cell surface proteins (Figure 3.4).

GPI-anchored proteins are enriched in the lipid rafts of both hematopoietic and non-hematopoietic cells (Hooper, 1999; Murray and Robbins, 1998; Tansey et al., 2000). IVEE cells are a GPI-deficient cell line originally derived from K562 cells by chemical mutagenesis and phenotypic screening for the lack of surface expression of the GPI-anchored protein CD55 (Mohney et al., 1994). The genetic defect in these cells was discovered to be a defect in the *hGPI8* gene, which is a component of the GPI transamidase complex that attaches the preassembled GPI anchor to proteins with a GPI attachment signal peptide in the endoplasmic reticulum (Ohishi et al., 2000; Yu et al., 1997). This defect renders IVEE cells incapable of synthesizing mature GPI anchors, and they therefore lack surface expression of any proteins normally attached to the extracellular leaflet of the plasma membrane by a GPI anchor. There is evidence that the protein and lipid composition of the plasma membrane in general, or of rafts in particular, are specifically altered in GPI-deficient cells. In GPI-deficient CHO cells, which normally express caveolins and have caveolae, expression of caveolin-1 and caveolin-2 was upregulated, though levels of flotillin-1 and GM1 remained unchanged (Abrami et al., 2001). The upregulation of the caveolins was accompanied by an increase in the number of cell surface caveolae. Interestingly, in lymphocytes that did not express caveolin proteins, GPI-deficiency resulted in an increase in total cholesterol levels (Abrami et al., 2001). The loss of GPI-anchored proteins in a *GPI8* mutant strain of trypanosomes was accompanied by the expression of a subset of membrane proteins at a much higher level than was observed in either wildtype cells or complemented mutant

cells (Lillico et al., 2003). Analysis of total lipid extracts also showed an increase in the abundance of ethanolamine- and mannose-containing lipids in the GPI-deficient trypanosomes (Lillico et al., 2003). The protein composition of IVEE raft fractions was compared to that of K562 raft fractions in silver-stained 2D gels in order to identify putative GPI-anchored proteins in the K562 rafts, and to determine whether GPI-deficiency resulted in any additional changes to raft protein composition. Potential GPI-anchored proteins were expected to be spots visible on the K562 2D profile, but missing in the IVEE gel. Surprisingly, only one series of spots likely to be a GPI-anchored protein was observed when comparing the K562 rafts to the IVEE rafts. As can be seen in Figure 3.5**,** a prominent series of spots present in K562 cells at a relatively acidic pI, and migrating between the 47.5 and 62.5 kDa MW markers was absent in the IVEE cells. The same series of spots was shown to be on the cell surface by the cell surface biotinylation experiment in Figure 3.4, consistent with a GPI-anchored protein. Though it is possible that this series of spots could correspond to more than one GPI-anchored protein, it is probable that this series of spots of similar MW and pI represents a number of differentially modified forms of a single protein. It is known for instance, that many GPI-anchored proteins are extensively glycosylated, and are often detected as multiple, and sometimes faint, pI and MW isoforms on 2D gels (Fivaz et al., 2000). In addition, flow cytometry and Western blotting showed that K562 cells express at least two other GPI-anchored proteins of different sizes (Figure 2.1); CD55, which migrates at approximately 80 kDa; and CD59, which migrates as a series of bands between 20 and 30 kDa on 1D gels (Murray and Robbins, 1998). Differentially expressed spots that might correspond to these GPI-anchored proteins were not detected (Figure 3.5). Another

Figure 3.5. Comparison of 2D gel profiles of raft proteins from GPI-positive and GPI-negative K562-derived cell lines.

The protein composition of raft fractions isolated from $1x10^8$ K562 (GPI+), IVEE (GPI-), or IVEE/GPI8 (GPI+) cells was analyzed by 2D gel electrophoresis followed by silver staining. The spots indicated in red were identified by MALDI-MS peptide mass fingerprinting (Table 3.2). The blue line indicates the series of spots identified as the GPI-anchored protein dipeptidase 1 in K562 and IVEE/GPI8 raft fractions. A blue line marks the same position on the 2D gel of IVEE raft fractions, showing the absence of this series of spots in the GPI-deficient cell line. These results are representative of three independent experiments.

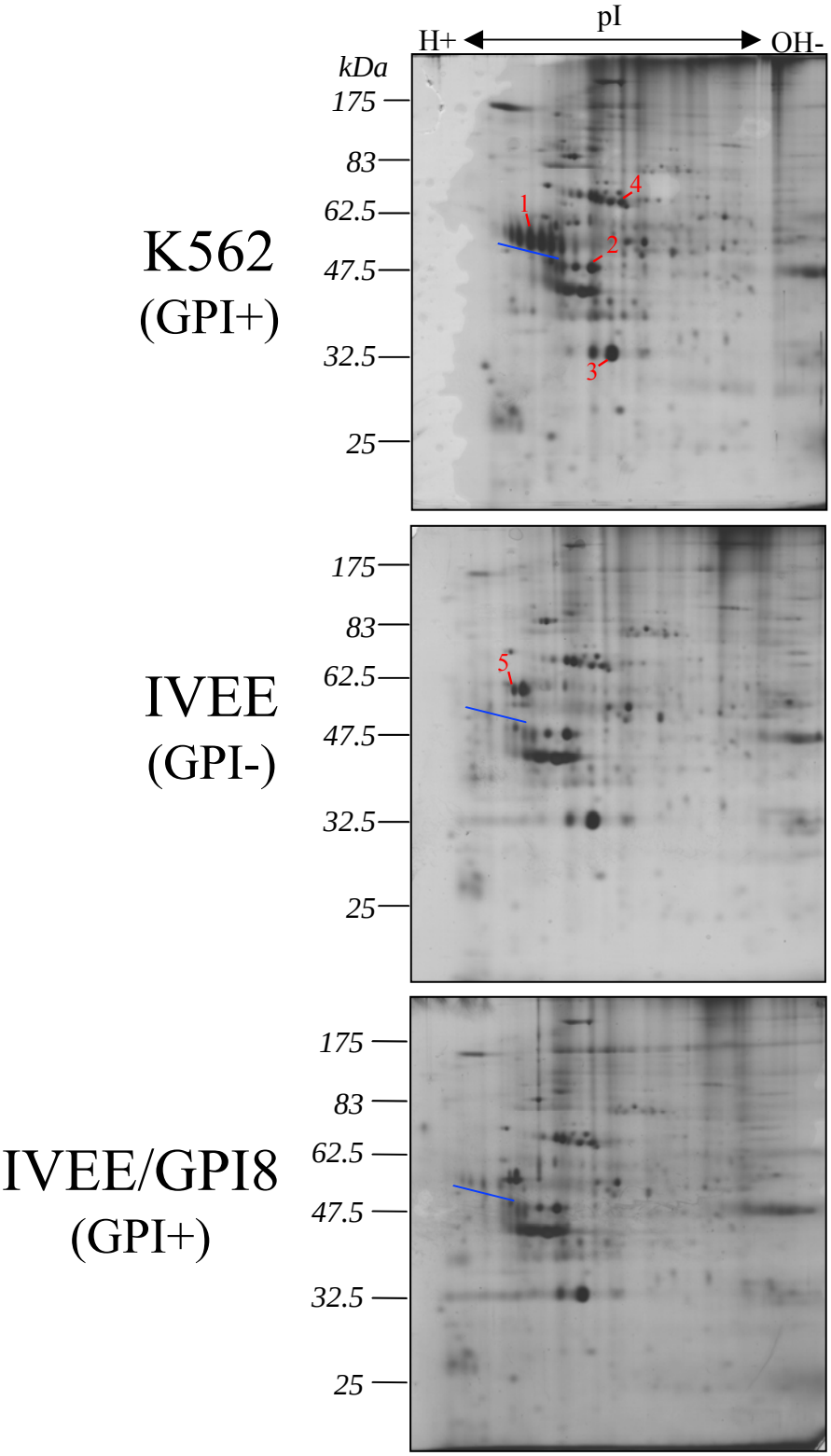
pI
H+
OH-
kDa
175
83
62.5
47.5
32.5
25
1
2
3
4
5
K562
(GPI+)
IVEE
(GPI-)
IVEE/GPI8
(GPI+)

group has shown that GPI-anchored proteins are often undetectable in 2D gels due to both low abundance and the interference of the hydrophobic GPI lipid anchor during IEF, and that enzymatic removal of the lipid anchor was required for effective 2D gel analysis of GPI-anchored proteins (Abrami et al., 2001; Fivaz et al., 2000). This may explain the apparent under-representation of GPI-anchored proteins in the 2D gels. With the exception of the putative GPI-anchored protein, the gel patterns of the GPI+ K562 cells and the GPI- IVEE cells were very similar by qualitative manual comparison. Since the IVEE cells were generated by random mutagenesis, the *hGPI8* cDNA was transfected into IVEE cells to complement the GPI biosynthesis defect and create a stable GPI-expressing cell line, IVEE/GPI8, as a control to confirm that the change observed between the K562 and the IVEE rafts was due to the difference in GPI status. The putative GPI-anchored protein was restored in the IVEE/GPI8 2D raft profile, but there appeared to be a significantly lower level of this protein in the IVEE/GPI8 rafts when compared to the K562 gel, though flow cytometry and western blotting showed similar expression levels of CD55 and CD59 in these cells (Figure 2.1). As with the IVEE 2D raft profile, the 2D raft protein profile for the IVEE/GPI8 cells was otherwise highly similar to both the GPI- IVEE and the GPI+ K562 cells.

In an initial set of experiments to see if spots cut from the silver-stained 2D gels could be readily identified by MS, 20 spots of varying staining intensity were cut from silver-stained 2D gels of $U937_{TPA}$ raft fractions and sent to the Alberta Cancer Board Proteome Mass Spectrometry Facility at the University of Alberta. There the spots were subjected to in-gel trypsin digestion, the resulting peptide extracts were analyzed by MALDI-MS, and protein identification was attempted using PMF. Only four of the

submitted spots were identified by this method. Many of the other spots either did not contain enough protein to obtain spectra, or the peptide peaks that were identified did not result in significant matches upon database searching (personal communication, Jing Zheng, ACB MS Facility). The identified proteins were GRP 78 (spot no. 1), annexin VI (spot no. 2), vacuolar ATP synthase subunit B2 (spot no. 4) and prohibitin (spot no. 11), as summarized in Table 3.1. Figure 3.6 indicates where the identified spots are located on a representative gel of $U937_{TPA}$ cells.

Because it was apparent that a major factor in the low success rate of MS identification was low protein abundance, 27 of the most abundant raft proteins present in K562 2D gels and 13 of the most abundant spots in IVEE 2D gels were selected and sent to the University of Alberta for MALDI-MS and PMF analysis. However, only 4 spots could be identified from K562 rafts, and only 1 spot was identified in IVEE cells (Figure 3.5 and Table 3.2). In many of the unidentified spots, a lack of sufficient protein sample meant that either no specific peaks were obtained, or that the few specific peaks that were measured were not able to be specifically matched with high scores to database proteins (personal communication, Jing Zheng, ACB MS Facility). The putative GPI-anchored protein in K562 rafts was identified as dipeptidase 1, which is a known GPI-anchored ectoenzyme with broad dipeptidase activity that may be involved in regulation of leukotriene activity (Adachi et al., 1989). Two signalling effector proteins were identified; a regulatory subunit of protein kinase A, and $G_{\beta}2$, a component of heterotrimeric G protein complexes that transduce signals from activated GPCRs. The identification of $G_{\beta 2}$, which is localized to the cytoplasmic leaflet of the plasma in tight association with prenylated G_{γ} subunits (Morris and Malbon, 1999), was consistent with

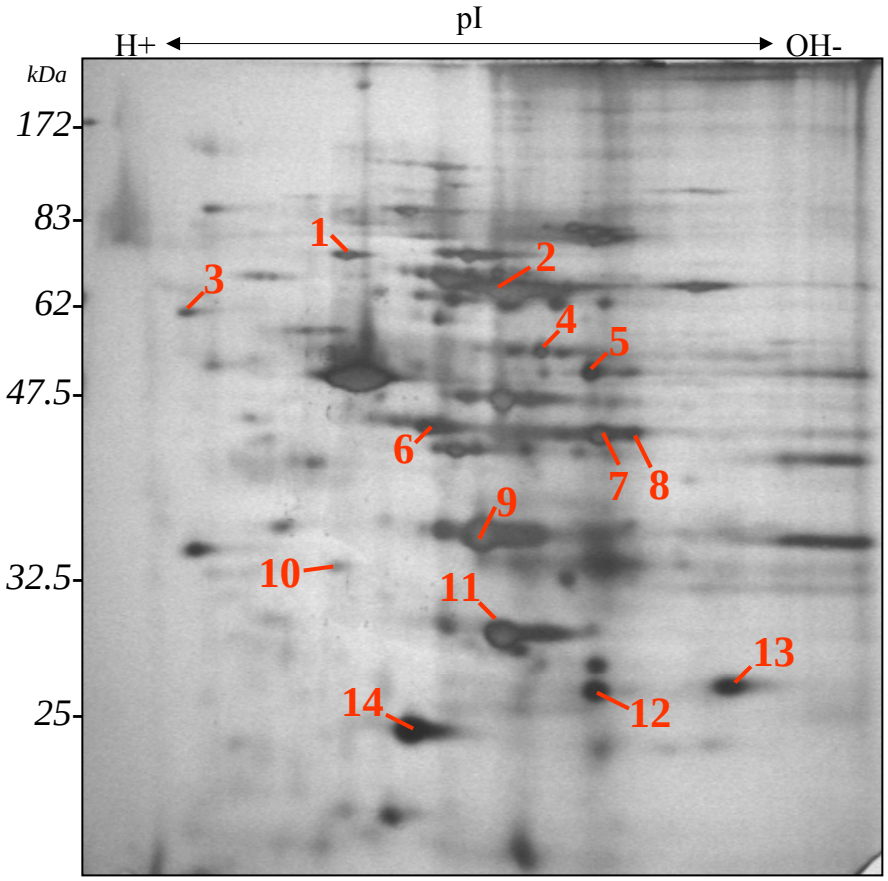

Figure 3.6. Two-dimensional gel electrophoresis of raft proteins isolated from differentiated U937 cells.

U937 cells were treated with TPA for 48 hours, lysed in 1% Triton X100/MBS and subjected to sucrose density gradient centrifugation as described in Materials and Methods to isolate low density raft fractions. Raft fractions from $2x10^8$ cells were separated by 2D gel electrophoresis and proteins were visualized by silver staining. The indicated spots were cut out and subjected to MALDI-MS and MALDI-MS/MS analysis to identify the proteins (Table 3.1).

Table 3.1. Identification of proteins in raft fractions isolated from differentiated U937 cells using 2D gel electrophoresis followed by MALDI peptide mass fingerprinting and MALDI-MS/MS.

Peptide extracts from spots cut from silver-stained 2D gels of $U937_{tpa}$ raft fractions (Figure 3.6) were analyzed by MALDI-MS and proteins were identified by database searching using the obtained peptide maps. For some samples, the protein identifications were further confirmed by sequencing 1-3 selected peptides by MALDI-MS/MS. Abbreviations: nd, not done; % seq cov, percentage sequence coverage. *mitochondrial protein; **endoplasmic reticulum protein

Spot No.	Protein Name	SwissProt/ Trembl Accession	% Seq Cov	Sequenced Peptides from MALDI-MS/MS
1	**78 kDa glucose-regulated protein (GRP 78)	P11021	15	nd
2	annexin VI	P08133	18	nd
3	**calreticulin	P27797	25	1. FYALSASFEPFSNK 2. EPAVYFKEQFLDGDGWTSR
4	vacuolar ATP synthase subunit B2	P21281	16	nd
5	*Dihydrolipoyllysine-residue succinyltransferase component of 2-oxoglutarate dehydrogenase complex	P36957	21	1. VEVRPMMYVALTYDHR
6	actin, cytoplasmic 2	P63261	37	1. GQVITIGNER 2. IWHHTFYNELR 3. SYELPDGQVITIGNER
7	*calcium-binding transporter	Q9P129	32	1. SGQWWR 2. MNIFGGFR
8	a) *calcium-binding transporter	a)Q9P129 b)O75306	a)22 b)21	a) 1. SGQWWR 2. DYFLFNPVTDIEEIIR

8	b) *NADH-ubiquinone oxidoreductase, 49 kDa subunit			b) signals too weak for MS/MS
9	G protein beta 2 subunit	P62879	33	1. Ac-SELEQLRQEAEQLR[1] 2. IYAMHWGTDSR
10	annexin V	P08758	47	1. FITIFGTR 2. WGTDEEKFITIFGTR
11	*prohibitin	P35232	28	nd
12	*NADH-ubiquinone oxidoreductase, 24 kDa subunit, mitochondrial	P19404	30	1. IPKPGPR 2. VAEVLQVPPMR 3. AAAVLPVLDLAQR
13	*Ubiquinol-cytochrome C reductase iron-sulfur subunit, mitochondrial	P47985	23	1. GKPLFVR 2. VPDFSEYR
14	*ATP synthase D chain, mitochondrial	O75947	74	1. PHQPIEN 2. YPYWPHQPIENL

[1]This is the N-terminus of the protein, with the initial M missing and evidence of acetylation. There was also peptide mass mapping evidence for the non-acetylated N-terminus, but this was not confirmed by MS/MS.

Table 3.2. Identification of raft proteins isolated from GPI-positive and GPI-negative K562-derived cell lines by 2D gel electrophoresis and MALDI-MS peptide mass fingerprinting.

Peptide extracts from spots cut from silver-stained 2D gels (Figure 3.5) were analyzed by MALDI-MS and proteins were identified by database searching using the obtained peptide maps.

Spot No.	Protein Name	SwissProt/ Tremble Accession	Exptl Mr/pI[1]	Calc Mr/pI[2]	# peptides	% Seq Cov[3]
1	dipeptidase 1	P16444	55-60/5.20	41/5.50	9	24
2	cAMP dependent protein kinase type I alpha regulatory subunit	P10644	50/5.55	43/5.27	15	34
3	G protein beta 2 subunit	P62879	35/5.60	37/5.60	8	22
4	annexin VI	P08133	70/5.65	76/5.42	12	16
5	vimentin	P08670	59/5.48	54/5.06	9	24

[1]Experimental protein molecular weights (Mr) are given in kDa. The experimental Mr and pI given are approximate, as they are estimated by comparison to the migration of known standards on the same or parallel gels.

[2]The calculated Mr and pI were obtained using the ProtParam program (Gasteiger et al., 2005) found at http://ca.expasy.org/tools/protparam.html.

[3]The percentage sequence coverage (% Seq Cov) refers to the percentage of the total protein sequence covered by the identified peptides.

the previous observation that this relatively abundant raft protein was not labelled after cell surface biotinylation of K562 cells (Figure 3.4 and Table 3.2**)**. Annexin VI, which had been previously identified in the $U937_{TPA}$ raft fractions, was also identified in K562 raft fractions migrating at a similar MW and pI. The intermediate filament protein vimentin was identified in IVEE raft fractions. The presence of vimentin in K562, IVEE, and IVEE/GPI8 raft fractions was confirmed by probing 2D Western blots of isolated raft proteins with an anti-vimentin antibody, which showed a single spot of approximately the same intensity in each cell type migrating at a similar MW and pI as the spot originally cut from the silver-stained gel (data not shown). In addition, the similarities between the theoretical MW and pI of the identified proteins and the experimentally determined MW and pI of the excised spots increased confidence in these identifications (Table 3.1 and Table 3.2).

It was obvious that more protein sample was needed for effective MALDI-MS and PMF analysis. Therefore, the 2D gel analysis was scaled up to enable the isolation of larger amounts of protein. While previous experiments had used tube gels of 1.5 mm diameter, tube gels of 3.4 mm diameter were now used, allowing the loading of up to twice as much raft material. Two identical 2D gels of $U937_{TPA}$ rafts were run in parallel, one with $2x10^8$ cell equivalents of raft material (Figure 3.6), and one with $1x10^8$ cell equivalents of raft material. This resulted in greater amounts of raft protein in the spots, but also decreased the resolution of the technique, as many spots began to overlap (Figure 3.6). Corresponding spots were excised from both gels and pooled for MALDI-MS and PMF analysis. A total of 15 spots were submitted for analysis. The ACB Proteome MS Facility had established MALDI-MS/MS protocols at this point, and MS/MS analysis of

1-3 peptides was used to confirm the initial PMF identification. The increase in protein amount combined with the increased confidence in identification by using MALDI-MS/MS as well as PMF enabled the identification of 11 of the submitted samples, as summarized in Table 3.1.

From all of the experiments described above, a total of 14 proteins from differentiated U937 raft fractions (Table 3.1) and 5 proteins from K562 raft fractions were identified (Table 3.2). Two of these proteins ($G_{\beta 2}$ and annexin A6) were identified in independent samples, one from each cell type, of a common spot in the 2D gel pattern. One protein (vimentin) was initially identified from IVEE raft fractions, but this spot was also common to both K562 and IVEE/GPI8 raft fractions, and Western blotting confirmed that these spots also contained vimentin. Even with the limited number of protein identifications from these experiments, these results suggest that the similarities observed in the 2D gel profiles of isolated raft fractions from a diverse set of hematopoietic cell lines correspond to a subset of lipid raft proteins that comprise a common lipid raft proteome. Some of the identified proteins were previously known to be raft-associated, or were closely related to other known raft proteins. These included the GPI-anchored protein dipeptidase 1 (Parkin et al., 2001), $G_{\beta 2}$ (Chang et al., 1994b; Oh and Schnitzer, 2001), annexin V (Parkin et al., 1996), and annexin VI (Babiychuk et al., 1999; Parkin et al., 1996; Schnitzer et al., 1995). Prohibitin shares an N-terminal SPFH domain (also known as a prohibitin domain) with the known raft markers flotillin-1 and flotillin-2 (Tavernarakis et al., 1999), and has since been shown to be a raft-resident protein (Mielenz et al., 2005; Sharma and Qadri, 2004), though it appears to localize mainly to the mitochondria (Nijtmans et al., 2002). Surprisingly, six other mitochondrial

proteins were also identified in raft fractions from differentiated U937 cells (Table 3.1), including a component of the 2-oxoglutarate dehydrogenase complex that functions in the TCA cycle (#5), two subunits of complex I (#8 and #12) and one subunit of complex III (#13) of the respiratory chain, a calcium-dependent aspartate and glutamate carrier (#7 and #8), and a subunit of ATP synthase (#14). Two ER-resident chaperones were also identified, GRP78 (#1) and calreticulin (#3), though the latter has also been localized to the plasma membrane and the extracellular matrix (Gardai et al., 2005; Stuart et al., 1997). Though the raft fractions were expected to be significantly enriched in signalling molecules, this limited survey identified only one signalling protein other than $G_{\beta 2}$, a regulatory subunit of PKA (#2, Table 3.2), as a component of K562 raft fractions.

In summary, a preliminary 2D gel analysis of lipid rafts from several different hemtopoietic cell lines supports the idea that the protein composition of lipid rafts differs according to cell type. While the experiments described above show that 2D gels can be used successfully to resolve a subset of proteins found in low-density detergent-resistant fractions, certain types of raft proteins, such as GPI-anchored proteins, may be underrepresented in this type of analysis. Furthermore, evidence from 2D *in vitro* protein kinase assays, as well as the inability to correlate Hck detection by Western blotting with spots on a corresponding silver-stained gel, indicates that many potential signalling molecules present in 2D gels are of such low abundance that they are undetectable by silver staining, and may therefore be extremely difficult or impossible to identify by MS. Similarly, a significant number of cell surface proteins, some of which might represent signalling receptor candidates, are also present in low abundance. Though some of the more abundant protein spots were identified by MALDI-MS, PMF, and MALDI-MS/MS,

it was apparent that it would be difficult to annotate many of the detectable spots using the MS protocols available at that time. In addition, the 2D gel system used showed a certain amount of variability (for example, compare $U937_{tpa}$ gels in Figure 3.2 and Figure 3.3b, and K562 gels in Figure 3.2 and Figure 3.4). Improved reproducibility, as well as increased resolution of basic proteins and coverage of a greater number of proteins with wider pH ranges, might have been obtained by switching to the use of IPG strips in the first dimension. However, initial experiments using IPG strips were significantly less successful than the tube gel system used in terms of the number and staining intensity of the protein spots (data not shown). Effective use of IPG strips would also have required extensive optimization. Other sources of variability likely included inter-experimental differences in the efficacy of solubilization prior to IEF, and effects on the efficiency of silver staining, due to subtle variations in timing, temperature, or solution composition on a day-to-day basis (Patton, 2000; Quadroni and James, 1999). These factors meant that quantitative comparisons of the different 2D raft profiles would require extensive work to further optimize the 2D gel protocol, and to perform enough replicates to gain statistically significant results. Though this would have been an interesting avenue to pursue, I was primarily interested in identifying one or more novel raft-associated signalling pathways to study, through which I might be able to mechanistically define a causal relationship between a specific change in raft protein composition and changes in raft signalling. Since it seemed likely that I would be unable to identify many of the differentially associated raft proteins that might be detected by this approach, I chose instead to use a 1D gel-based approach.

3.2.2 One-dimensional gel-based proteomic analyses of non-caveolar lipid rafts

Since the technical limitations of 2D gel analysis provided incomplete coverage of lipid raft proteins, and since the availability of MS/MS techniques improved the analysis of more complex protein mixtures, 1D SDS-PAGE was used to fractionate lipid raft proteins prior to MS protein identification. A preliminary examination of 1D silver-stained gels of several myelomonocytic cell lines showed distinct protein banding patterns in lipid raft fractions from different cell lines (Figure 3.7). Although 2D gel analysis had shown little difference in raft protein composition when GPI+ K562 and GPI- IVEE cells were compared, 1D gel analysis showed multiple differences in the silver-stained banding pattern of K562 and IVEE raft fractions (Figure 3.8). Bands that appeared enriched in either the K562 or the IVEE raft fractions were excised from the gels, as indicated in Figure 3.8, and sent to the ACB Proteome Mass Spectrometry Facility for analysis by either PMF followed by MALDI-MS/MS confirmation, or by LC-MS/MS. Successfully identified proteins are summarized in Table 3.3**.** A total of 14 proteins were identified in 12 bands excised from 1D gels of K562 raft fractions. Some of these proteins had previously been identified from 2D gels of K562 and $U937_{tpa}$ raft proteins, including the type I regulatory subunit of PKA, $G\beta_2$, annexin VI, actin, and the GPI-anchored protein dipeptidase 1. As expected, the band containing dipeptidase 1 was greatly reduced in IVEE raft fractions (Figure 3.8). The raft markers flotillin-1 and flotillin-2 were identified, together with two other prohibitin family members—stomatin and a novel member of this family erlin-2, which localizes to the ER (Browman et al., 2006). Stomatin has previously been described as a major component of lipid rafts in erythrocytes, together with flotillin-1 and flotillin-2 (Salzer and Prohaska, 2001). Several

Figure 3.7. Lipid raft fractions from four different myelomonocytic cell lines have significant differences in protein composition.

Equal amounts of lipid raft fractions (10 μg of protein/sample) from U937, $U937_{tpa}$, THP-1, and HL60 cell lines were separated by SDS-PAGE and silver-stained to visualize total protein. This experiment was performed once.

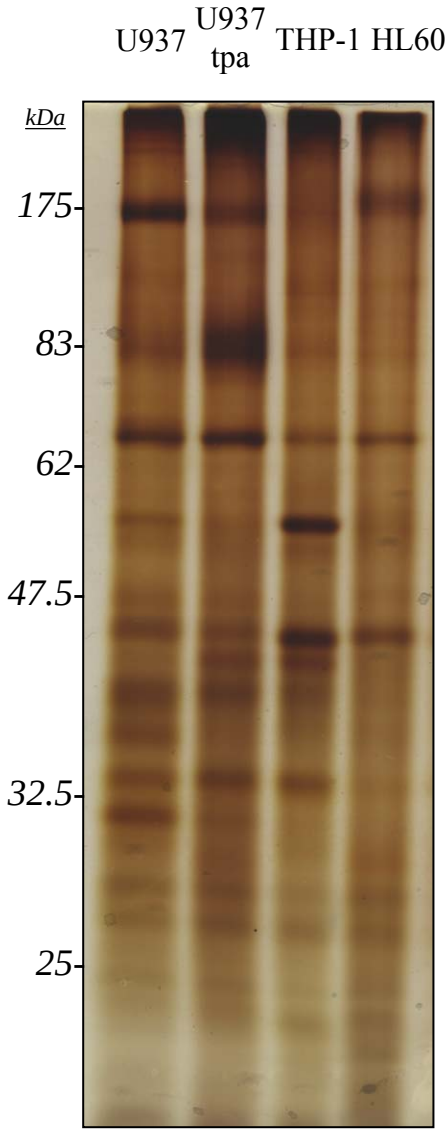
U937
U937 tpa
THP-1
HL60
kDa
175
83
62
47.5
32.5
25

Figure 3.8. Comparison of lipid raft protein composition in GPI+/- K562 cells.

Equal amounts of lipid raft fractions were separated by SDS-PAGE and total protein was visualized with silver staining. The indicated bands from each cell line were cut out and proteins were identified after analyis by MALDI-MS, MALDI-MS/MS, and/or LC-MS/MS, as summarized in Table 3.3. Note that in this gel, samples from parental GPI-positive K562 cells, GPI-negative IVEE cells, and GPI-positive IVEE/GPI8 cells were run in three adjacent lanes. For clarity when labelling protein bands identified by MS, the gel is shown here in two overlapping panels—the IVEE sample in both panels is the identical lane. This experiment is representative of 4 independent experiments.

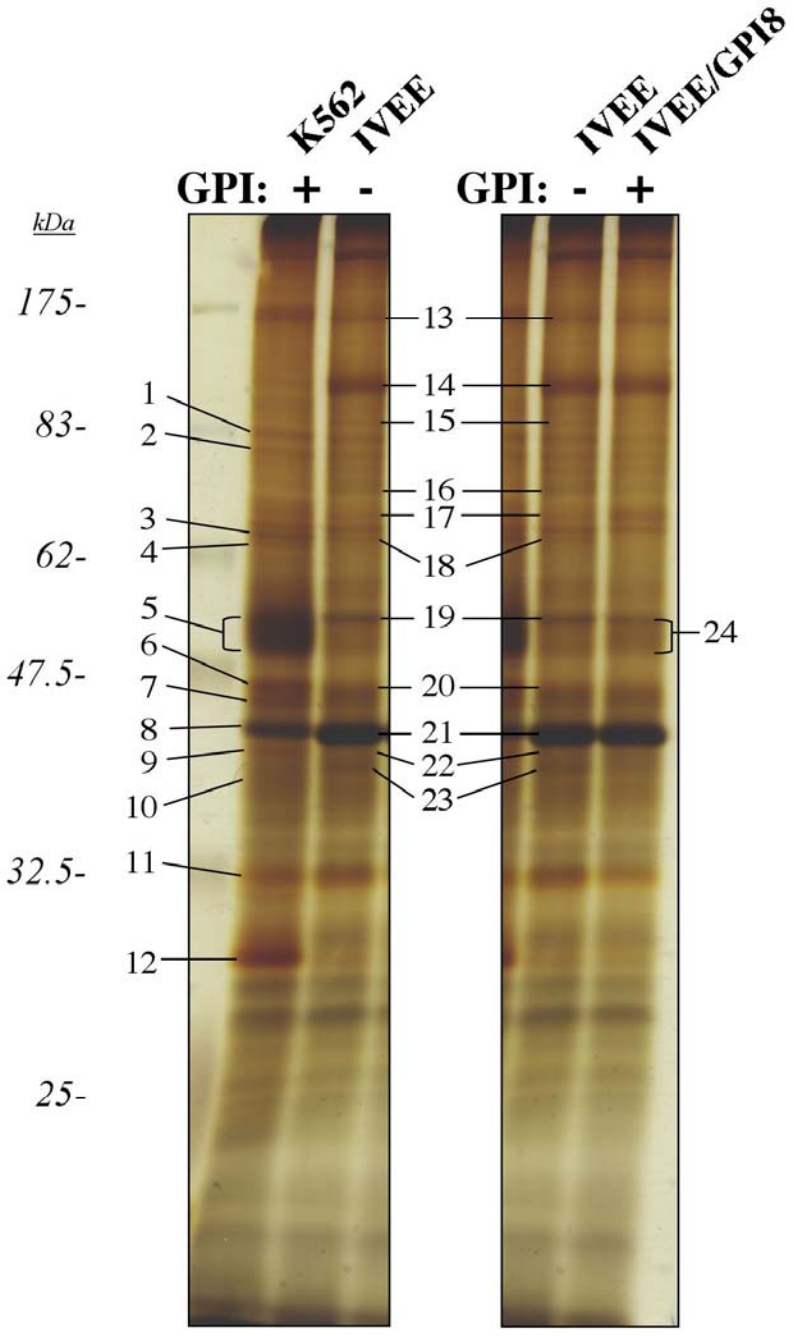
K562
IVEE
IVEE
IVEE/GPI8
GPI: + -
GPI: - +
kDa
175-
83-
62-
47.5-
32.5-
25-
1
2
3
4
5
6
7
8
9
10
11
12
13
14
15
16
17
18
19
20
21
22
23
24

Table 3.3. Identification of proteins in lipid raft fractions isolated from GPI+/- K562 cells by MALDI-MS, MALDI-MS/MS and LC-MS/MS.

Peptide extracts from bands cut from silver-stained and Coomassie Blue- stained gels (Figure 3.8) were analyzed by MALDI-MS peptide mass fingerprinting, followed by sequencing of 1-3 peptides with MALDI-MS/MS to confirm identifications (method A), or by LC-MS/MS (method B) as indicated. This table summarizes results obtained from 4 independent MS experiments. Note: K, K562; I, IVEE; 8, IVEE/GPI8. *mitochondrial protein; **endoplasmic reticulum protein

Band No. (Cell Line)	Protein Name	SwissProt or NCBI Accession	Calc MW (kDa)	MS Method Used
1 (K)	**calnexin	P27824	68	A
2 (K)	heat shock protein 90-beta (and possibly heat shock protein 90-alpha)	P08238	83	A
3 (K)	heat shock cognate 71 kDa protein	P11142	71	A
4 (K)	annexin VI	P08133	76	A
5 (K)	dipeptidase I	P16444	46	A
	tubulin alpha-6 chain	Q9BQE3	51	B
	flotillin-2	Q14254	42	B
6 (K)	cAMP dependent protein kinase type I alpha regulatory subunit	P10644	43	A
7 (K)	flotillin-1	O75955	47	A
	flotillin-2	Q14254	42	A
8 (K)	actin, cytoplasmic 1 (beta-actin) and/or actin, cytoplasmic 2 (gamma-actin)	P60709 and/or P63261	42	A
9 (K)	**C8orf2 (erlin-2)	O94905	38	A
10 (K)	G (i) alpha-3	P08754	41	A
11 (K)	G protein beta 2 subunit	P62879	38	A[1]
12 (K)	stomatin	P27105	32	A
13 (I)	beta-II spectrin	Q01082	28	B
	desmoglein 2	Q14126	123	B
	band 4.1-like protein 2	O43491	113	B
14 (I)	myosin Id	O94832	117	B
	beta-II spectrin	Q01082	28	B

15 (I)	myosin Id	O94832	117	B
	AP-2 complex subunit alpha-1	O95782	109	B
	AP-2 complex subunit beta-1	P63010	105	B
16 (I)	serum albumin precursor	P02769	71	A
17 (I)	protein 4.1	P11171	98	B
	ezrin	P15311	69	B
	myosin Id	O94832	117	B
18 (I)	moesin	P26038	68	B
19 (I)	vimentin	P08670	54	A
20 (I)	flotillin-1	O75955	47	B
	flotillin-2	Q14254	42	B
	cAMP dependent protein kinase type I alpha regulatory subunit	P10644	43	B
21 (I)	actin, cytoplasmic 1 (beta-actin))	P60709	42	A
	actin, cytoplasmic 2 (gamma-actin)	P63261	42	A
	actin, alpha skeletal muscle	P68133	42	B
22 (I)	**C8orf2 (erlin-2)	O94905	38	A
23 (I)	G (i) alpha-3	P08754	41	B
	G (i) alpha-2	P04899	41	B
	G (i) alpha-1	P63096	41	B
24 (8)	*ATP synthase alpha chain	P25705	60	B
	tubulin beta-5 chain	P05218	50	B
	tubulin alpha-1 chain	P05209	51	B
	dipeptidase I	P16444	46	B
	T-complex protein 1, beta subunit	P78371	58	B
	flotillin-2	Q14254	42	B

[1]Analysis of MS/MS peptide fragmentation data shows that both the non-acetylated and the acetylated N-terminus are present.

chaperone proteins, actin, tubulin, and the heterotrimeric G protein subunit $G\alpha_{i3}$ were also identified. Twenty-one proteins were identified in 11 bands excised from IVEE samples (Table 3.3). Several of these proteins were also identified in K562 samples, including erlin-2, $G\alpha_{i3}$, flotillin-1, and flotillin-2. Two AP-2 complex subunits, which are involved in clathrin-mediated endocytosis, were also identified in IVEE fractions, along with numerous cytoskeletal proteins were also identified in IVEE samples. In some cases, a given protein was identified in more than one band, for example myosin Id, and βII-spectrin in the IVEE cells.

When IVEE/GPI8 cells became available for analysis as a control for the GPI-dependency of the observed changes, it was clear that transfection of the IVEE cells with the *hGPI8* cDNA did not complement the changes observed in the IVEE cells, as the IVEE/GPI8 banding pattern was very similar to the IVEE pattern (Figure 3.8). Notably, the 50-55 kDa band (containing the GPI-anchored protein dipeptidase 1) that is highly enriched in K562 cells was not restored in the IVEE/GPI8 cells. However, MS analysis of peptides extracted from the corresponding band in IVEE/GPI8 cells confirmed that dipeptidase 1 was present in the IVEE/GPI8 cells (Table 3.3), and flow cytometry and immunoblotting demonstrated that CD59 and CD55 were present in IVEE/GPI8 cells at levels similar to those in K562 cells (Figure 2.1). When considering these observations in concert with the 2D gel data previously discussed, it is likely that the IVEE/GPI8 cells have less raft-associated dipeptidase 1, and presumably, express lower levels of this particular GPI-anchored protein than the K562 cells.

It is possible that GPI-deficiency caused irreversible changes in the IVEE cells, perhaps by an epigenetic mechanism that could not be complemented by transfection of

hGPI8, but it is equally possible that the observed changes are unrelated to GPI status and instead reflect a secondary mutation or event that occurred during the original mutagenesis and isolation of this cell line. As K562 cells can be induced to undergo further megakaryocytic or erythroid differentiation upon treatment with a variety of agents (Alitalo, 1990; Gahmberg and Andersson, 1981), expression of 35 cell surface differentiation markers on K562, IVEE, and GPI8 cells was compared by flow cytometry to see if the differences observed between the K562 cells, and the IVEE and IVEE/GPI8 cells could be correlated with a differentiation event. There was no change in the majority of markers between any of the cell lines, though there was a difference observed in the CD13 staining profile (Figure 3.9). Although the majority of the cell populations in all three cell lines stained positive for the multilineage myeloid marker CD13 (Figure 3.9), a significant subpopulation of K562 cells expressed higher levels of CD13 than IVEE or IVEE/GPI8 cells. However, all three cell lines are negative for the megakaryocyte markers CD41, CD61, and CD42b, and show similar expression profiles for the erythroid marker CD235a. Overall, there was no conclusive evidence supporting the idea that a differentiation event was responsible for the changes in raft protein composition observed in the IVEE cells.

As I was creating the stable IVEE/GPI8 cell line as a control for the K562/IVEE model, I also began studies to characterize raft fractions from two sets of GPI+/- B cell lines, Raji26 and Ramos517, to see if the changes that I had thought were due to GPI deficiency were also found in rafts isolated from other types of GPI-deficient cells. Raft fractions prepared from these cell lines were compared by 1D SDS-PAGE and silver staining (Figure 3.10). In contrast to the IVEE cells that were created by random

Figure 3.9. Expression profiles of cell surface differentiation markers on K562, IVEE, and IVEE/GPI8 cells are similar.

Cells were labelled with antibodies against 36 different cell surface proteins and analyzed by Calgary Lab Service's Flow Cytometry Facility using standard protocols for their acute leukemia panel. Samples and controls stained with FITC-conjugated (A), PE-conjugated (B), ECD-conjugated (C), PC5-conjugated (D) or PC7-conjugated (E) antibodies are shown together in the indicated panels.

A

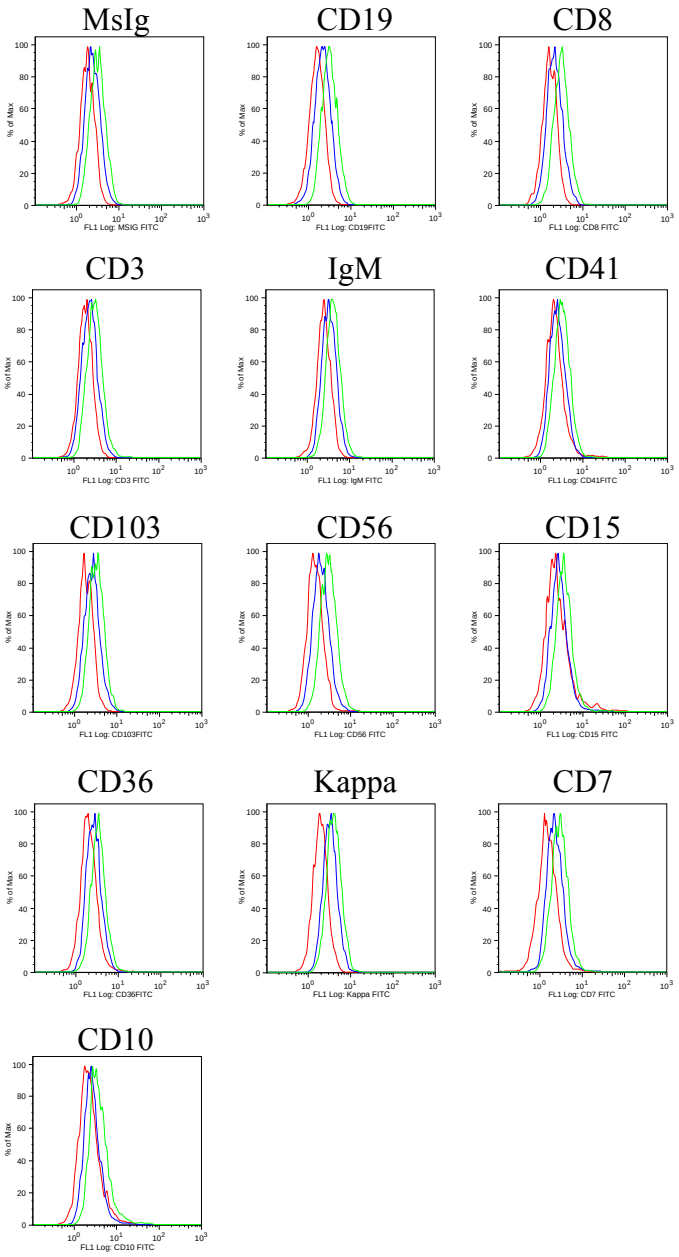
MsIg
CD19
CD8
CD3
IgM
CD41
CD103
CD56
CD15
CD36
Kappa
CD7
CD10
% of Max
FL1 Log: MSIG FITC
FL1 Log: CD19FITC
FL1 Log: CD8 FITC
FL1 Log: CD3 FITC
FL1 Log: IgM FITC
FL1 Log: CD41FITC
FL1 Log: CD103FITC
FL1 Log: CD56 FITC
FL1 Log: CD15 FITC
FL1 Log: CD36FITC
FL1 Log: Kappa FITC
FL1 Log: CD7 FITC
FL1 Log: CD10 FITC

B

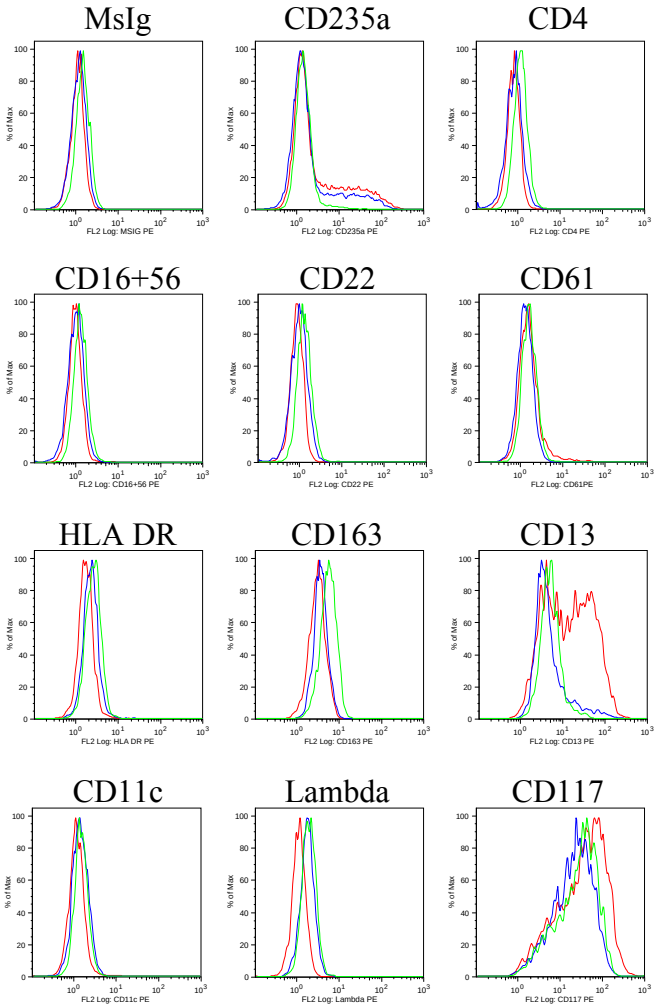
MsIg
CD235a
CD4
CD16+56
CD22
CD61
HLA DR
CD163
CD13
CD11c
Lambda
CD117
% of Max
FL2 Log: MSIG PE
FL2 Log: CD235a PE
FL2 Log: CD4 PE
FL2 Log: CD16+56 PE
FL2 Log: CD22 PE
FL2 Log: CD61PE
FL2 Log: HLA DR PE
FL2 Log: CD163 PE
FL2 Log: CD13 PE
FL2 Log: CD11c PE
FL2 Log: Lambda PE
FL2 Log: CD117 PE

C

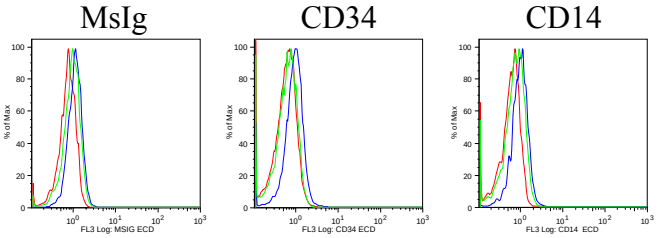
MsIg
CD34
CD14
% of Max
FL3 Log: MSIG ECD
FL3 Log: CD34 ECD
FL3 Log: CD14 ECD

D

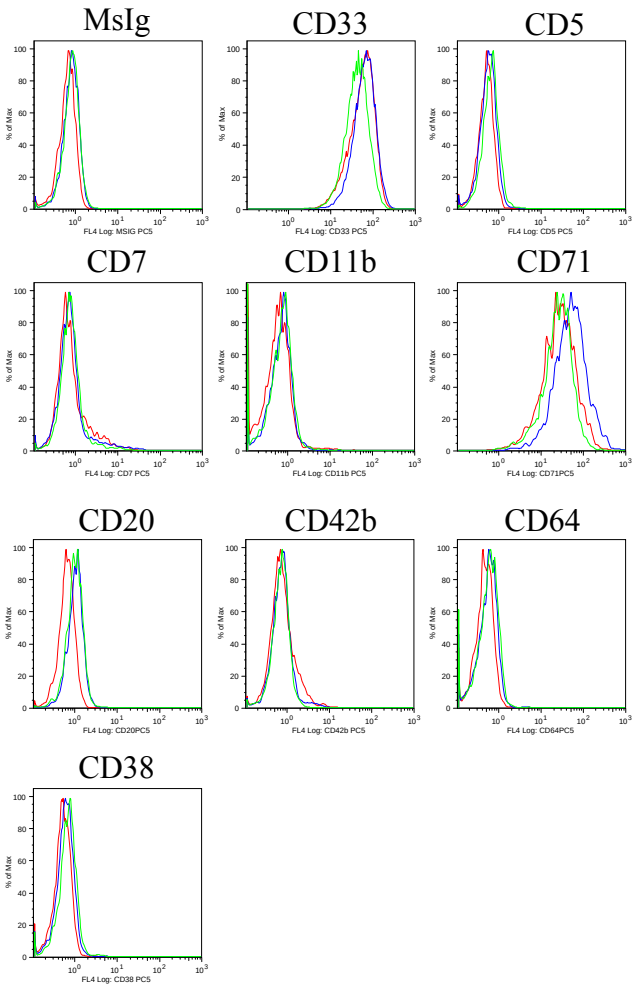
MsIg
CD33
CD5
CD7
CD11b
CD71
CD20
CD42b
CD64
CD38
% of Max
FL4 Log: MSIG PC5
FL4 Log: CD33 PC5
FL4 Log: CD5 PC5
FL4 Log: CD7 PC5
FL4 Log: CD11b PC5
FL4 Log: CD71PC5
FL4 Log: CD20PC5
FL4 Log: CD42b PC5
FL4 Log: CD64PC5
FL4 Log: CD38 PC5

E

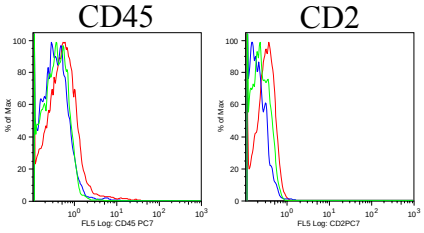
CD45
CD2
% of Max
FL5 Log: CD45 PC7
FL5 Log: CD2PC7

Figure 3.10. Comparison of lipid raft protein composition in GPI+/- B cells.

Equal amounts of lipid raft fractions were separated by SDS-PAGE and total protein was visualized by silver staining. Selected bands were cut out and proteins were identified by LC-MS/MS analysis of peptide extracts. See Table 3.4 and Table 3.5 for details. The gel shown is representative of the results of three independent silver stains.

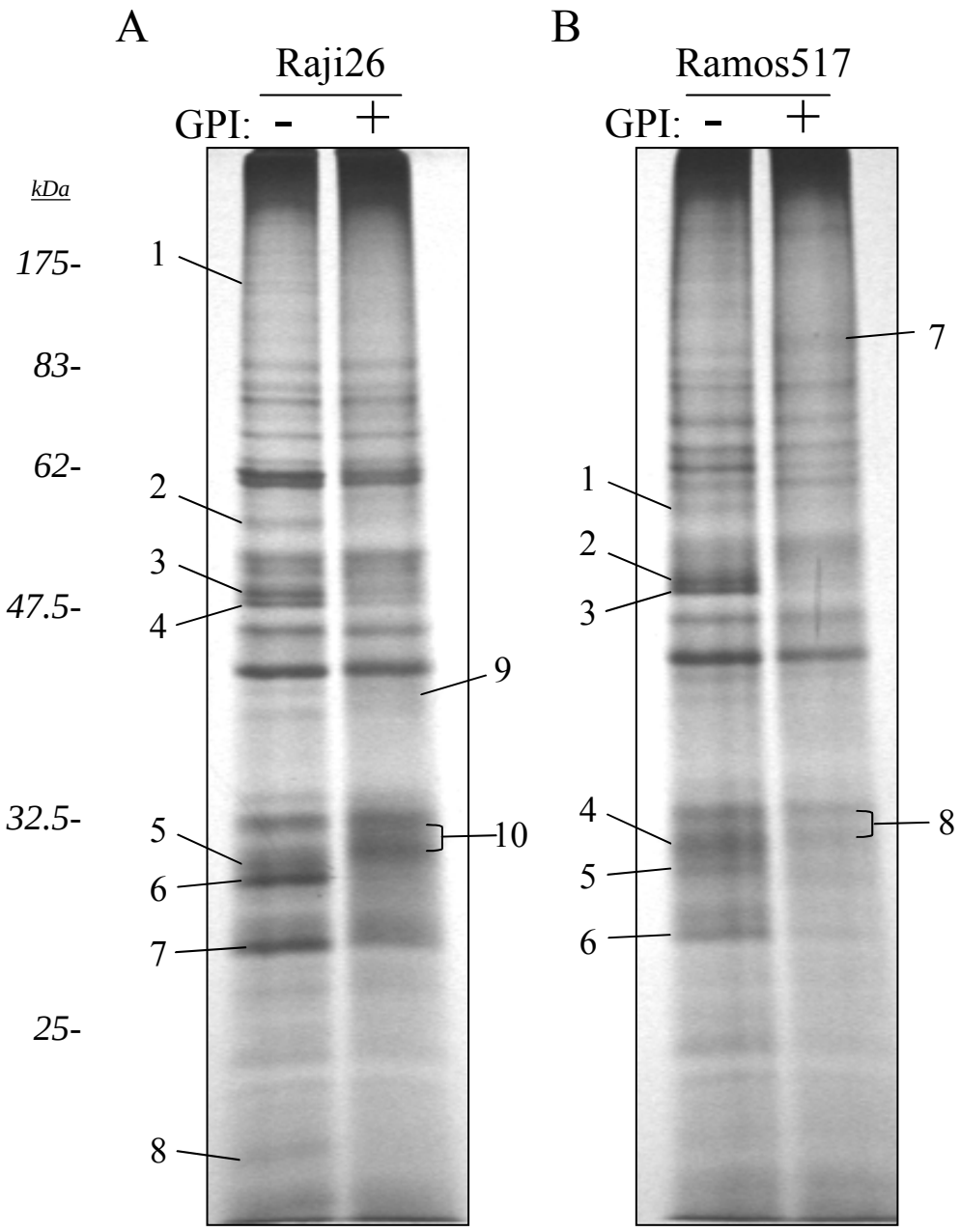
A
Raji26
GPI: - +
kDa
175-
83-
62-
47.5-
32.5-
25-
1
2
3
4
5
6
7
8
9
10
B
Ramos517
GPI: - +
1
2
3
4
5
6
7
8

mutagenesis, the GPI-deficient B cell lines were isolated as spontaneously occurring mutants, and purified by fluorescence-activated cell sorting (see Chapter 2, section 2.3.1). The mutation in their GPI biosynthesis pathway was characterized, and then the original cell line was transfected with a vector control, or a cDNA encoding the mutated protein to restore GPI-anchored protein expression (Figure 2.2). There were a number of visible differences in the protein banding patterns of rafts from the GPI-positive and GPI-negative cell lines, including some bands that were specifically upregulated in the GPI-deficient cells. Some of these differences were present in both the Raji26 and the Ramos517 raft fractions. Selected bands that appeared to be enriched in either the vector control or the GPI-positive cell lines were cut out and sent to the ACB Proteome Mass Spectrometry Facility for LC-MS/MS analysis.

A total of 26 proteins from the Raji26 cell lines, and 20 proteins from the Ramos517 cell lines were successfully identified, with multiple proteins identified in each band (Table 3.4 and Table 3.5). The GPI-anchored protein CD48 was identified in a band enriched in GPI-positive Raji26 cells as expected (#9, Table 3.4). Strikingly, 10 of 26 proteins in the Raji26 cell lines, and 10 of 20 proteins identified in the Ramos517 cell lines were mitochondrial, including components of ATP synthase, the voltage-dependent anion-selective channel (VDAC), prohibitin, several mitochondrial transporter proteins, and a mitochondrial heat shock protein. Class I and class II MHC subunits were identified, which is consistent with their previously characterized localization to raft domains in the context of antigen presentation (Anderson et al., 2000; Lebedeva et al., 2004; Mielenz et al., 2005). The plasma membrane glycoprotein CD147 was also identified. This transmembrane receptor is expressed in many cell types, where it is

Table 3.4. Identification of raft proteins isolated from GPI+/- Raji26 cells by 1D SDS-PAGE and LC-MS/MS.

Peptide extracts from bands cut from a silver-stained gel (Figure 3.10) were analyzed by LC-MS/MS and identified by database searching using the obtained fragmentation spectra. *mitochondrial protein

Band No.	Protein Name	SwissProt or NCBI Accession	Calc MW (kDa)
1	complement C3	P01024	189
2	*60 kDa heat shock protein, mitochondrial	P10809	61
	pyruvate kinase, isozymes M1/M2	P14618	58
	*ATP synthase alpha chain, mitochondrial	P25705	60
	CD147	P35613	43
3	*ATP synthase alpha chain, mitochondrial	P25705	60
	*ATP synthase beta chain, mitochondrial	P06576	57
	CD147	P35613	43
	Lyn	P07948	59
4	*ATP synthase beta chain, mitochondrial	P06576	57
	CD147	P35613	43
5	*voltage-dependent anion-selective channel protein 1	P21796	31
	*voltage-dependent anion-selective channel protein 2	P45880	39
	HLA class II histocompatibility antigen, gamma chain	P04233	34
	*sideroflexin 1	Q9H9B4	36
	*ATP synthase gamma chain, mitochondrial	P36542	33
6	*voltage-dependent anion-selective channel protein 1	P21796	31
	*voltage-dependent anion-selective channel protein 2	P45880	39
	*ATP synthase gamma chain, mitochondrial	P36542	33
7	*ADP/ATP translocase 2	P05141	33
	*prohibitin	P35232	30
	60S ribosomal protein L7	P18124	30
	HLA class II histocompatibility antigen, DRB1-11 beta chain	P20039	30

8	HLA class I histocompatibility antigen, B-53 alpha chain and/or its homologs (may be a fragment)	P30491	41
	*cytochrome c oxidase polypeptide II	P00403	26
	60S ribosomal protein L18a	Q02543	21
	unknown protein	3283893	27
9	guanine nucleotide-binding protein G(s), alpha subunit	P63092	46
	guanine nucleotide-binding protein G(i), alpha-2 subunit	P04899	41
	CD48	P09326	28
10	voltage-dependent anion-selective channel protein 1	P21796	31
	voltage-dependent anion-selective channel protein 2	P45880	39
	HLA class II histocompatibility antigen, DR alpha chain	P01903	29
	HLA class II histocompatibility antigen, gamma chain	P04233	34
	syntaxin-6	O43752	29
	membrane-associated transporter protein	Q9UMX9	59

Table 3.5. Identification of raft proteins isolated from GPI-positive and GPI-negative Ramos517 cells by 1D SDS-PAGE and LC-MS/MS.

Peptide extracts from bands cut from a silver-stained gel (Figure 3.10) were analyzed by LC-MS/MS and identified by database searching using the obtained fragmentation spectra. *mitochondrial protein;

Band No.	Protein Name	SwissProt or NCBI Accession	Calc MW (kDa)
1	CD147	P35613	43
	*acyl-CoA dehydrogenase family member 9, mitochondrial	Q9H845	69
	alpha-(1,6)-fucosyltransferase	Q9BYC5	67
2	*ATP synthase alpha chain, mitochondrial	P25705	60
	*ATP synthase beta chain, mitochondrial	P06576	57
3	ATP synthase alpha chain, mitochondrial	P25705	60
	ATP synthase beta chain, mitochondrial	P06576	57
4	*voltage-dependent anion-selective channel protein 1	P21796	31
	*voltage-dependent anion-selective channel protein 2	P45880	39
	*ATP synthase gamma chain, mitochondrial	P36542	33
	*sideroflexin 1	Q9H9B4	36
	*phosphate carrier protein, mitochondrial	Q00325	41
	protein KIAA0152	Q14165	32
5	voltage-dependent anion-selective channel protein 1	P21796	31
	voltage-dependent anion-selective channel protein 2	P45880	39
	40S ribosomal protein S3	P23396	27
	ATP synthase gamma chain, mitochondrial	P36542	33
	vacuolar ATP synthase subunit E	P36543	33
	HLA class II histocompatibility antigen, DRB1-9 beta chain	Q9TQE0	30
6	*prohibitin	P35232	30
	*ADP,ATP translocase 2	P05141	33
	60S ribosomal protein L7	P18124	29
	HLA class II histocompatibility antigen, DRB1-9 beta chain	Q9TQE0	30
7	neprilysin	P08473	86

8	voltage-dependent anion-selective channel protein 1	P21796	31
	voltage-dependent anion-selective channel protein 2	P45880	39
	HLA class II histocompatibility antigen, gamma chain	P04233	34
	HLA class II histocompatibility antigen, DR alpha chain	P01903	29

involved in numerous pathophysiological processes including reproduction, neural function, inflammation, and tumour invasion, through its involvement in intracellular signalling and stimulation of extracellular matrix metalloproteinase (MMP) activity (Gabison et al., 2005; Muramatsu and Miyauchi, 2003). CD147 has previously been identified by MS in Triton-insoluble raft fractions in myelomonocytic cells (Browman et al., 2006; Li et al., 2004b), and Western blotting showed that a pool of CD147 is found in Brij96-insoluble raft fractions in epithelial cells cells (Tang and Hemler, 2004), and in Brij58-insoluble raft fractions in T cells (Staffler et al., 2003). CD147 is heavily glycosylated and different glycoforms range from approximately 32-60 kDa (Gabison et al., 2005; Tang and Hemler, 2004), which likely explains why it was identified in three different bands ranging from about 47.5 to 60 kDa in GPI- Raji26 cells. With respect to signalling molecules, in addition to heterotrimeric G proteins and CD147, the Src family protein kinase Lyn was identified in band 3 from GPI- Raji26 samples, but not in the corresponding band 2 that was excised from the GPI- Ramos517 gel, though it is also found in raft fractions in these cells (see Chapter 4, Figure 4.17). Somewhat surprisingly, several ribosomal proteins were also identified in both Raji26 and Ramos517 raft fractions. Foster *et al.* also identified ribosomal proteins in Triton-insoluble raft fractions by MS, and showed that their association with the raft fractions was cholesterol-dependent, though the significance of these findings is presently unknown (Foster et al., 2003).

The proteins identified from bands in 1D gels provide further qualitative information about the protein composition of rafts in these cells, but can only be regarded as potential candidates for proteins that might be differentially associated with lipid rafts

in the two cell lines. The reduced resolution obtained using 1D gels rather than 2D gels is offset by the increased solubilization and coverage of hydrophobic proteins in 1D gels. In this respect, more differences were observed in K562 versus IVEE raft fractions in 1D banding patterns, than in 2D gel spot profiles, which likely results from the solubilization and display of a greater number of raft proteins in 1D gels. However, as these 1D gel-based experiments also showed, multiple proteins can contribute to the staining of a single band. This makes it impossible to conclude on the basis of qualitative MS identification alone that a given protein is responsible for differences in the intensity of a given band. Quantitation of the amount of a specific protein in raft fractions from different cells by Western blotting is required before any conclusions regarding differential raft association can be made following MS identification of proteins in 1D gel bands. Though this is not an issue when the desire is to merely catalogue the contents of a protein sample, the time-consuming individual validation of each protein candidate in a given experiment is a significant limitation of this approach to differential proteomics. Instead of the 1D gel approach followed by individual Western blots, a quantititative gel-free MS approach could be adopted, which would be far more efficient in identifying specific proteins whose raft association was altered. Since I wanted to compare the protein composition of rafts from wildtype and GPI-deficient cells, I therefore chose to focus on the development of a gel-free proteomic approach that could eventually be adapted to allow quantitation of individual peptides. Nevertheless, the proteins identified from 1D gels of raft fractions confirm and extend the findings of the previously described experiments with respect to the general protein composition of lipid rafts, in addition to

providing potential candidate proteins that are altered in GPI-deficient cells, which might be of interest for future studies.

3.2.3 Shotgun proteomics of non-caveolar lipid rafts

The experiments above, and the results of other groups (Li et al., 2003b; von Haller et al., 2001), indicated that 1D gel-based approaches to raft proteomics constituted an improvement over 2D gels, but identification of membrane-associated proteins was still challenging. Several studies had reported improvements in overall coverage of membrane proteins, including raft fractions, by adopting solution-based methods to analyze complex protein mixtures (Blonder et al., 2004a; Foster et al., 2003; Li et al., 2004b; Wu and Yates, 2003). Shotgun proteomics experiments, in which isolated raft fractions are solubilized, digested in solution, and the resulting peptides subjected to liquid chromatography coupled to tandem mass spectrometry, also have the advantage of being much faster and cheaper to perform than a complete gel-based analysis (Baggerman et al., 2005). Such analyses can also provide rudimentary information about gross changes in protein composition when comparing different samples (Blonder et al., 2004a), and with further optimization can be converted to a more rigorous quantitative approach by the addition of stable isotope labelling by amino acids in cell culture (SILAC) (Ong et al., 2004) or other quantitative MS techniques.

In collaboration with the laboratory of Dr. David Schriemer at the University of Calgary, the method of Blonder et al. (Blonder et al., 2004a) was chosen to compare raft fractions from IVEE and IVEE/GPI8 cells in order to further test the hypothesis that the protein composition of rafts was altered in GPI-deficiency. Pellets of Triton X-100-insoluble raft material were washed to remove detergent, solubilized by sonication in

60% buffered methanol, and tryptically digested in solution. The peptide digestate was then analyzed by LC-ESI-MS/MS.

The results of the single preliminary experiment performed are given in Table 3.6 and Table 3.7. A total of 61 proteins in IVEE/GPI8 raft fractions and 52 proteins in IVEE raft fractions were identified, confirming that this technique enables more rapid and large-scale protein identification than the gel-based approaches. The proteins identified in IVEE and IVEE/GPI8 cells were very similar, and were also generally reminiscent of previous MS protein identifications. Proteins with the highest number of identified peptides included cytoskeletal proteins, and the raft markers flotillin-1 and flotillin-2. Other members of the prohibitin family (stomatin, erlin-1 and erlin-2) were also identified. A large number of cytoskeletal and related proteins were identified, including components of actin, intermediate filament and microtubule-based networks, and annexins, in addition to proteins involved in vesicular trafficking, such as SNAP-23. Polyubiquitin was identified in both IVEE and IVEE/GPI8 raft fractions, and in IVEE raft fractions the polyubiquitin-binding protein sequestosome-1 (Seibenhener et al., 2004) was identified, which is consistent with reports that certain raft proteins, including Src family kinases and growth factor receptors, are regulated by polyubiquitination (Howlett and Robbins, 2002; Huang et al., 2006). In contrast to both $U937_{tpa}$ and B cell raft fractions, few mitochondrial proteins were identified in K562, IVEE, or IVEE/GPI8 cells using 2D and 1D gel-based MS approaches, and shotgun analysis of IVEE and IVEE/GPI8 raft fractions further suggests that raft fractions from these cell lines contain relatively few, or smaller amounts of mitochondrial proteins.

Table 3.6. IVEE lipid raft proteins identified following in-solution tryptic digest of methanol-solubilized raft proteins and LC-MS/MS.

Triton X-100 insoluble lipid raft fractions were isolated from IVEE cells. After detergent removal, sonication in 60% buffered methanol was used to extract and solubilize the raft proteins, which were then digested with trypsin. The peptides were analyzed by LC-MS/MS and database searching was performed using the Agilent Spectrum Mill MS Proteomics workbench software. Scores greater than 13 are considered excellent matches. Proteins identified in shotgun analysis of IVEE raft fractions that were not identified in the corresponding shotgun analysis of IVEE/GPI8 raft fractions (Table 3.7) are indicated in red.

#	SwissProt or NCBI Accession	Protein Name	Score	# of Peptides
1	Q01082	beta-II spectrin	631.93	40
2	Q13813	alpha-II spectrin	350.45	14
3	P08670	vimentin	341.12	21
4	NP_149043	myosin IG	293.79	18
5	BAA23486	polyubiquitin	233.6	16
6	O75955	flotillin 1	233.4	14
7	NP_001422	erythrocyte membrane protein band 4.1-like 2	188.28	12
8	Q14254	flotillin 2	169.65	10
9	NP_001611.1	AHNAK	161.89	13
10	P07355	annexin II	146.08	32

11	P60709	actin, cytoplasmic 1 (beta-actin)	117.26	8
12	P07948	tyrosine-protein kinase Lyn	117.18	8
13	O00161	synaptosomal-associated protein 23	115.81	6
14	21749456	unnamed protein product	107.83	8
15	Q13727	AHNAK-related protein (fragment)	99.1	8
16	P11142	heat shock cognate 71 kDa protein	94.3	7
17	P10644	cAMP dependent protein kinase type I alpha regulatory subunit	92.21	6
18	P08754	guanine nucleotide-binding protein G (k) subunit alpha (G(i) alpha-3)	89.51	6
19	P63092	guanine nucleotide-binding protein G(s), subunit alpha	82.73	6
20	P04899	guanine nucleotide-binding protein G(i), alpha-2 subunit	81.27	6
21	P08238	heat shock protein 90-beta	62.17	4
22	Q9BQE3	tubulin alpha-6 chain	59.26	4
23	P27105	stomatin	59.18	4
24	Q53X12	vacuolar-type H(+)-ATPase	50.85	4
25	O00214	galectin-8	47.32	3
26	P17661	desmin	46.22	3
27	P63096	guanine nucleotide-binding protein G(i), alpha-1 subunit	44.72	3
28	Q5TB33	erythrocyte membrane protein band 4.1	43.15	3
29	Q14126	desmoglein-2	40.5	3
30	P68104	elongation factor 1-alpha 1	40.19	3
31	P61224	Ras-related protein Rap-1b	40.18	3

32	P54652	heat shock-related 70 kDa protein 2	39.37	3
33	P08133	annexin VI	33.48	3
34	P07437	tubulin beta-2 chain	33.37	2
35	P62070	Ras-related protein R-Ras2	32.42	2
36	P80723	brain acid soluble protein 1 (NAP-22)	31.91	2
37	Q13501	sequestosome 1	31.35	2
38	P14923	junction plakoglobin	31.02	2
39	P29777	guanine nucleotide-binding protein G(o), subunit alpha-2	30.88	2
40	P07900	heat shock protein 90-alpha	30.64	2
41	Q9NY65	tubulin alpha-8 chain	28.11	2
42	O60726	mutant guanine nucleotide-binding protein G(s), alpha subunit	28.07	2
43	O94905	C8orf2 (erlin-2)	26.9	2
44	O75477	protein KE04 (erlin-1)	26.71	2
45	Q6IAA8	hypothetical protein FLJ20625	25.74	2
46	P62873	guanine nucleotide-binding protein G(I)/G(S)/G(T) subunit beta 1	24.31	2
47	Q13509	tubulin beta-3 chain	18.29	1
48	Q12931	heat shock protein, 75 kDa, mitochondrial	17.2	1
49	Q03113	guanine nucleotide-binding protein alpha-12 subunit	17.05	1
50	Q14344	guanine nucleotide-binding subunit alpha-13 subunit	17.05	1
51	Q13748	tubulin, alpha-2 chain	15.28	1
52	Q14160	protein LAP4 (hScrib)	14.41	1

53	Q9HAV0	guanine nucleotide-binding subunit beta 4	14.29	1

Table 3.7. IVEE/GPI8 lipid raft proteins identified following in-solution tryptic digest of methanol-solubilized raft proteins and LC-MS/MS.

Triton X-100 insoluble lipid raft fractions were isolated from IVEE/GPI8 cells. After detergent removal, sonication in 60% buffered methanol was used to extract and solubilize the raft proteins, which were then digested with trypsin. The tryptic peptides were subsequently analyzed by LC-MS/MS and database searching was performed using the Agilent Spectrum Mill MS Proteomics workbench software. Scores greater than 13 are considered excellent matches. Proteins identified by shotgun analysis of IVEE/GPI8 raft fractions, but not by shotgun analysis of IVEE raft fractions (Table 3.6), are indicated in red.

#	SwissProt or NCBI Accession	Protein Name	Score	# of Peptides
1	Q01082	beta-II spectrin	643.57	42
2	NP_149043	myosin IG	390.21	23
3	P08670	vimentin	346.3	21
4	Q13813	alpha-II spectrin	266.61	18
5	O75955	flotillin 1	255.03	16
6	Q14254	flotillin 2	214	13
7	BAA23486	polyubiquitin	146.08	8
8	NP_001422	erythrocyte membrane protein band 4.1-like 2	144.49	8
9	O00161	synaptosomal-associated protein 23	127.38	7
10	P60709	actin, cytoplasmic 1 (beta-actin)	122.46	8

11	P10644	cAMP dependent protein kinase type I alpha regulatory subunit	113.97	8
12	P08754	guanine nucleotide-binding protein G(k) subunit alpha (Gαi3)	112.53	7
13	P07948	tyrosine-protein kinase Lyn	107.44	7
14	Q14126	desmoglein-2	93.69	7
15	Q9BQE3	tubulin alpha-6 chain	85.85	6
16	NP_001611.1	AHNAK	79.86	6
16	Q15149	plectin-1	75.26	6
17	P63092	guanine nucleotide-binding protein G(s), subunit alpha	70.82	5
18	P14923	junction plakoglobin	70.71	5
19	O00214	galectin-8	66.22	5
20	P16444	dipeptidase I	62.93	4
21	Q14160	protein LAP4 (hScrib)	60.99	5
22	P07355	annexin II	58.23	4
23	P27105	stomatin	58.05	3
24	P07437	tubulin beta-2 chain	55.47	4
25	O94905	C8orf2 (erlin-2)	49.53	3
26	O75477	protein KE04 (erlin-1)	47.43	3
27	P17661	desmin	46.22	3
28	P63096	guanine nucleotide-binding protein G(i), alpha-1 subunit	45.69	3
29	Q13748	tubulin, alpha-2 chain	40	3
30	O60726	mutant guanine nucleotide-binding protein G(s), alpha subunit	37.56	3

31	Q14156	hypothetical protein KIAA0143	37.55	3
32	Q6IAA8	hypothetical protein FLJ20625	37.38	3
33	O75781	paralemmin	36.92	2
34	P08238	heat shock protein 90-beta	36.03	2
35	Q07020	60S ribosomal protein L18	34.37	2
36	P80723	brain acid soluble protein 1 (NAP-22)	34.12	2
37	Q9NY65	tubulin alpha-8 chain	29.82	2
38	P11142	heat shock cognate 71 kDa protein	29.63	2
39	Q13509	tubulin beta-3 chain	29.61	2
40	Q16891	mitofilin	29.06	2
41	Q5TB33	erythrocyte membrane protein band 4.1	28.83	2
42	Q00013	55 kDa erythrocyte membrane protein	27.7	2
43	P31321	cAMP-dependent protein kinase type I-beta regulatory subunit	27.44	2
44	P61224	Ras-related protein Rap-1b	27.2	2
45	P29777	guanine nucleotide-binding protein G(o), subunit alpha-2	26.95	2
46	P55084	trifunctional enzyme beta subunit, mitochondrial (precursor)	26.47	2
47	Q53X12	vacuolar-type H(+)-ATPase	25.37	2
48	Q9Y6M4	casein kinase I isoform gamma 3	25.13	2
49	Q9C0B5	probable palmitoyltransferase ZDHHC5	23.35	2
50	P58107	epiplakin	22.96	2
51	Q96RT1	protein LAP2	22.71	2
52	P68104	elongation factor 1-alpha 1	22.49	2

53	P54652	heat shock-related 70 kDa protein 2	16.17	1
54	Q03113	guanine nucleotide-binding protein alpha-12 subunit	16.08	1
55	Q14344	guanine nucleotide-binding subunit alpha-13 subunit	16.08	1
56	Q12931	heat shock protein, 75 kDa, mitochondrial	15.94	1
57	P07900	heat shock protein 90-alpha	15.94	1
58	Q9HCP0	casein kinase I isoform gamma 1	14.85	1
59	P78368	casein kinase I isoform gamma 2	14.85	1
60	Q13727	AHNAK-related protein (fragment)	13.7	1

The proteins identified uniquely in either IVEE or IVEE/GPI8 fractions are highlighted in red in the indicated tables (Table 3.6 and Table 3.7). Some authors have suggested that the number of unique peptides identified in a global proteome analysis is related to the abundance of a protein within a complex mixture, though the information is very rudimentary, and likely only to be of value in detecting large differences among abundant proteins (Blonder et al., 2004a; Tirumalai et al., 2003). Most of the proteins identified with relatively high numbers of peptides were the same in both cell types, and were identified with similar numbers of peptides. The GPI-anchored protein dipeptidase 1 was identified only in IVEE/GPI8 raft fractions as expected, by identification of 4 unique peptides, which is a relatively high number (by comparison, 28 out of 61 of the proteins were identified with only 1 or 2 peptides). Annexin VI was found only in IVEE raft fractions, but had previously been identified in K562 raft fractions in 1D and 2D gels (Table 3.2 and Table 3.3). Since the 2D gel spot in which annexin VI was identified is also present in the 2D raft protein profiles of K562, IVEE, and IVEE/GPI8 cells, annexin VI is likely to be present in IVEE/GPI8 cells, but happened to be missed in this particular experiment. Based on these observations, it is difficult to assign any kind of significance to unique hits, as most may simply represent differences in protein coverage in this single experiment. Nevertheless, some of the identified proteins are of interest with respect to general raft protein composition. Two protein kinases were also identified: the Src family tyrosine kinase Lyn and the serine/threonine kinase casein kinase I, which is involved in many different signalling pathways (Knippschild et al., 2005), was putatively identified in IVEE/GPI8 raft fractions, and had not been detected in raft fractions previously in this study. Another protein that might have a signalling function is the

prenylated and palmitoylated protein paralemmin, which is highly expressed in neurons, but also less abundantly in other cell types (Kutzleb et al., 1998). Paralemmin localizes to the cytoplasmic face of the plasma membrane and to a pool of intracellular vesicles, where it may localize to lipid rafts based on immunofluorescence and detergent extraction experiments (Kutzleb et al., 2006; Kutzleb et al., 1998). In neurons paralemmin has recently been shown to interact directly with the D3 dopamine receptor, to modulate adenylate cyclase activity downstream of dopamine and other GPCR agonists (Basile et al., 2006). Since palmitoylation often targets proteins to lipid rafts, it was interesting to note that a probable palmitoyltransferase was also identified in IVEE/GPI8 samples (protein#50, Table 3.7), consistent with an earlier report that palmitoyltransferase activity was present in low density membrane preparations (Dunphy et al., 2001). One of the few mitochondrial proteins identified in IVEE/GPI8 cells was mitofilin, which localizes to the mitochondrial inner membrane where it appears to have a role in the controlling the morphology of cristae (John et al., 2005). Mitofilin has previously been identified in raft fractions by the Robbins' laboratory (Browman et al., 2006), and by others (Mielenz et al., 2005).

In conclusion, the 1D and 2D gel experiments provide preliminary evidence that, while many protein components of rafts appear to be similar in diverse cell types, there are also distinct differences that may be related to cell type or stage of differentiation, or the pathological condition of GPI deficiency. The gel-based and gel-free proteomics experiments described here have provided a great deal of information about general raft protein composition, but unfortunately, they have at best only provided the names of candidate proteins that might be differentially associated with rafts depending on a cell's

GPI status. Definitive conclusions regarding differentially associated raft proteins await independent validation and/or the application of quantitative MS screens. Unfortunately, due to time constraints in my program of study, I was unable to pursue these avenues of investigation. Nevertheless, the experiments described here confirm the presence of known raft proteins and were successful in identifying novel raft proteins, including the unexpected finding of numerous mitochondrial and ER proteins in lipid rafts. Taken together, these results identify many potential raft markers, which could be used in the future to further characterize these microdomains, and provide additional insight into lipid raft structure and function.

3.3 Discussion

Cell membranes are characterized by their complexity at many levels, in terms of both the diversity of their lipid and protein constituents and the dynamic but regulated interactions between these membrane components. The plasma membrane is the gatekeeper of the cell, controlling the passage of materials into and out of the cell, responding to extracellular signals, and physically interacting with adjacent cells and the extracellular matrix to maintain tissue integrity, or permit cell adhesion or migration. In eukaryotic cells, the extensive intracellular membrane networks of organelles are the sites of many different signalling, biosynthetic, transport, and metabolic processes, in addition to their role in compartmentalizing organellar contents. All of these biological events are dependent on organized yet highly dynamic lipid and protein assemblies within membranes.

It is now widely accepted that spatial and temporal segregation of membrane proteins and lipids in lipid rafts is an important cellular mechanism underlying the

organization and regulation of many membrane functions. The structural properties of lipid rafts, including their morphology, subcellular localization, and protein and lipid composition, have been intimately linked to their function in specific cellular systems. A key experimental approach that has been used to define the molecular composition of rafts has been the study of raft proteins and lipids isolated by virtue of their insolubility in non-ionic detergents and the low buoyant density of the detergent-resistant membranes in sucrose density gradients (Sargiacomo et al., 1993; Shogomori and Brown, 2003). As discussed in Chapter 1, these purified lipid raft fractions cannot be considered equivalent to lipid rafts *in vivo*, but they do appear to be derived from *bona fide* raft domains present in unperturbed cell membranes. Early analyses of the composition of low-density detergent-resistant raft fractions suggested that rafts were enriched in a number of different signalling molecules, including G proteins, Src family kinases, and certain transmembrane receptors. These initial observations led to the proposal that rafts had a central function in the regulation of signal transduction by acting as platforms that could control the assembly of signalling complexes. This hypothesis has since been expanded and confirmed as a general paradigm in many different cellular contexts using detergent-independent techniques, including studies of the segregation of raft components in living cells (Hancock, 2006; Zajchowski and Robbins, 2002). Given that relatively limited knowledge of the protein composition of rafts has provided much of the foundation for the current understanding of the functional relevance of rafts, a more comprehensive knowledge of the molecular composition of lipid rafts is expected to substantially increase our understanding of the role of lipid rafts in signalling and other raft-mediated processes. The relatively simple procedure for the biochemical isolation of enriched lipid

raft fractions based on low buoyant density and detergent insolubility is ideally suited to proteomic analysis. Therefore, in the experiments described in this chapter, the protein composition of low density, Triton X-100-insoluble raft fractions isolated from various hematopoietic cells was investigated using both gel-based and gel-free proteomics approaches. These experiments were successful in identifying a large number of raft proteins, including both novel proteins and known raft markers. These results are both confirmed and extended by independent studies in the literature describing proteomic analyses of raft fractions isolated from neutrophils (Nebl et al., 2002), T cells (Bini et al., 2003; Tu et al., 2004; von Haller et al., 2001), B cells (Gupta et al., 2006; Mielenz et al., 2005; Saeki et al., 2003), neurons (Ledesma et al., 2003), kidney tissue (Bonnin et al., 2003), HeLa cells (Foster et al., 2003), monocytes (Li et al., 2003b; Li et al., 2004b), Vero cells (kidney epithelium) (Blonder et al., 2005; Blonder et al., 2004a), endothelial cells (Karsan et al., 2005; Sprenger et al., 2004), rat liver (Bae et al., 2004), Schwann cells (Yu et al., 2005), mouse sperm (Sleight et al., 2005), smooth muscle cells (MacLellan et al., 2005), rat intestinal brush border (Nguyen et al., 2006), human heart tissue (Banfi et al., 2006), yeast (*Candida albicans*) (Insenser et al., 2006) and plants (*Arabidopsis thaliana* callus cultures) (Borner et al., 2005). Despite the wide array of tissue types examined, taken together the data in this chapter and studies in the literature provide insight into lipid raft biology in several areas including: 1) the presence and functional significance of rafts in intracellular membranes including the ER and mitochondria, 2) the association of rafts with the cytoskeleton, and 3) the apparent existence of a common lipid raft proteome. The data also illustrate current challenges in

lipid raft proteomics with respect to the identification and analysis of signalling proteins, and the special considerations necessary in differential proteomics studies.

Extraction of whole cells with Triton X-100 prior to isolation of low-density raft fractions has the potential to isolate raft components from any subcellular localization, although knowledge of the original subcellular origin (or origins) of a particular lipid raft protein is lost. The identification of numerous ER and mitochondrial proteins in raft proteomics studies, both in this work and by others, was unexpected given that rafts had not been reported within these organelles. Nevertheless, these observations, when considered in light of other available evidence in the literature, support the presence of lipid raft microdomains in novel intracellular locations including the ER and mitochondria.

An important caveat of using biochemically purified protein preparations is the issue of contamination. Even the best of fractionation and affinity purification techniques will have some level of contamination due to inefficient separation of other cellular components, or non-specific protein-protein or other interactions. The simple identification of a protein in a raft fraction does not necessarily mean that this identification is biologically significant with respect to rafts in the absence of corroborating functional data. This is especially important to consider in mass spectrometry protein identification experiments, where the excellent sensitivity of the technique is capable of detecting very low amounts of protein, including trace contaminants. Therefore it is possible that some or all of the mitochondrial and ER proteins identified may simply be present in raft fractions due to contamination by non-raft components. However, it is also possible that some of these proteins have important

functional roles at locales outside of these organelles, where rafts are known to exist. A third possibility is that rafts do exist within ER and mitochondrial membranes. Studies of the localization and function of some of the ER and mitochondrial proteins identified to date in raft fractions have provided evidence for both of the latter two possibilities.

There is strong evidence for functionally important rafts in the plasma membrane, and in the Golgi complex (Galbiati et al., 2001; Gkantiragas et al., 2001; Nichols et al., 2001; Zajchowski and Robbins, 2002). For example, caveolin-1 was shown to be a structural component of plasma membrane caveolae (Rothberg et al., 1992) and was also found in raft fractions isolated from transport vesicles derived from the trans-Golgi network (Kurzchalia et al., 1992). Early studies that developed protocols for the biochemical isolation of lipid rafts found that GPI-anchored proteins associated with low-density detergent-resistant membranes after transport from the ER to the Golgi (Brown and Rose, 1992; Fra et al., 1994). Since the ER contains very low levels of cholesterol and sphingolipids, it was thought that rafts were absent from this organelle (Prinz, 2002; Simons and Ikonen, 1997; van Meer and Lisman, 2002). However, ER-resident proteins, including the calcium-binding chaperone proteins calnexin, calreticulin, and GRP78, as well as the proapoptotic molecule BAP31, have been identified in raft fractions from a variety of different sources (Table 3.1 and Table 3.3) (Banfi et al., 2006; Browman et al., 2006; Foster et al., 2003; Karsan et al., 2005; Li et al., 2003b; Li et al., 2004b; McMahon et al., 2006; Sprenger et al., 2004).

Calnexin and calreticulin are two ER-resident chaperone proteins with critical functions in protein folding, quality control, and calcium homeostasis in the ER (Michalak et al., 2002). Both proteins are also found on the cell surface of cultured and

primary cells (Gardai et al., 2005; Okazaki et al., 2000; Stuart et al., 1997). There is evidence that cell surface calreticulin (also called ecto-calreticulin) may have functional importance as a C1q receptor (Stuart et al., 1997) or in initiating clearance of apoptotic cells by phagocytes (Gardai et al., 2005). Interestingly, ecto-calreticulin on the surface of purified human neutrophils uses the raft-localized GPI-anchored protein CD59 as an adaptor molecule, and both cholesterol depletion and treatment with PI-PLC dramatically reduced the amount of ecto-calreticulin (Ghiran et al., 2003). Cross-linking of ecto-calreticulin induced a calcium flux, suggesting that it is capable of initiating signalling (Ghiran et al., 2003). Neutrophils stimulated by immobilized C1q produce extracellular superoxide and pretreatment of neutrophils with antibodies against CD59 and other GPI-anchored proteins inhibited C1q-triggered superoxide release, as did cholesterol depletion with MβCD (Otabor et al., 2004). Taken together these results are consistent with a model in which ecto-calreticulin serves as a C1q receptor in plasma membrane rafts enriched in GPI-anchored proteins, generating a raft-mediated signal that initiates superoxide production. Moreover, it is strong evidence that the identification of calreticulin in raft fractions is not simply the result of contamination, but in fact has functional significance.

It is possible that calreticulin is also present in rafts in the ER itself, although further study is needed to validate this. However, the existence of ER lipid rafts is supported by new information about two proteins, erlin-1 and erlin-2 (for **e**ndoplasmic **r**eticulum **li**pid raft prote**in**), which have only recently been characterized (Browman et al., 2006). These proteins have been identified directly in raft fractions by our lab (Table 3.3, Table 3.6, Table 3.7 (Browman et al., 2006) and by others (Blonder et al., 2005;

Ledesma et al., 2003; Li et al., 2004b; Sprenger et al., 2004) using MS-based proteomics screens. The erlins are expressed widely in both hematopoietic and non-hematopoietic cells, and are significantly enriched in lipid raft fractions when compared to the detergent-soluble fraction, an association that was shown to be cholesterol-dependent (Browman et al., 2006). Erlin-1 and erlin-2 share a high degree of sequence similarity and both contain a prohibitin (PHB) domain, identifying them as members of the prohibitin family, whose other members include the known raft markers stomatin, flotillin-1, and flotillin-2 (Morrow and Parton, 2005). The relatively high degree of enrichment in raft fractions combined with the cholesterol-dependence of the association and the sequence similarity with other known raft markers argues against the idea that erlin-1 and erlin-2 are non-specific contaminants of the raft fraction. Immunofluorescence microscopy of endogenous erlin-1 revealed a perinuclear staining pattern similar to that seen with other ER markers and when GFP-tagged erlin-1 and erlin-2 were expressed in HeLa cells, they showed a high level of colocalization with ER markers (Browman et al., 2006). The specific functional role of the erlins is currently unknown. Based on their similarity to prohibitin, which is reported to function as a molecular chaperone for mitochondrial membrane proteins, protecting them from degradation by the *m*-AAA-protease (Steglich et al., 1999), it is speculated that the erlins, and the proposed ER rafts in which they are localized, may have a role in regulating the stability of proteins by protecting them from degradation by ER-resident proteases (Browman et al., 2006).

Other reports also support the existence of lipid rafts in the ER. GPI-anchor biosynthesis is a multi-step pathway that occurs within the ER (Takeda and Kinoshita,

1995). Several GPI biosynthesis enzymes as well as intermediate forms of the GPI anchor that are formed during this process were identified in raft fractions isolated from both whole cell lysates and purified ER membranes (Pielsticker et al., 2005; Sevlever et al., 1999). Additionally, in contrast to some earlier studies (Brown and Rose, 1992; Fra et al., 1994), the GPI-anchored prion protein has been found to associate with rafts in the ER (Paladino et al., 2004; Sarnataro et al., 2004). Collectively, all of these observations provide strong evidence that lipid raft microdomains exist within the ER, and suggest that rafts may be functionally important in the regulation of some of the diverse biosynthetic, trafficking, and signalling events that take place in this organelle.

If rafts within the ER were unexpected, the possible existence of rafts within the mitochondria is another novel insight into raft biology provided by proteomics. A striking and unexpected finding was the identification of numerous mitochondrial proteins in raft fractions. For example, 7 of 14 proteins identified in raft fractions from differentiated U937 cells (Table 3.1), 10 of 26 proteins from GPI+/- Raji26 raft fractions (Table 3.4) and 10 of 20 proteins identified in GPI+/- Ramos517 raft fractions (Table 3.5) were known mitochondrial proteins. Other raft proteomics studies have also reported identification of substantial numbers of mitochondrial proteins (Bae et al., 2004; Banfi et al., 2006; Bini et al., 2003; Foster et al., 2003; Ledesma et al., 2003). For example, of 196 proteins identified in rat liver raft fractions, 24% were mitochondrial (Bae et al., 2004). Components of the ATP synthase complex and mitochondrial respiratory proteins are commonly observed in raft fractions and it is tempting to speculate that raft microdomains act as platforms to spatially organize the multiprotein complexes of the respiratory assembly, facilitating ATP synthesis within mitochondria. However, some

authors have interpreted these findings as being the result of contamination of raft fractions by abundant mitochondrial proteins, a possibility that cannot be definitively excluded. For example, Foster *et al.* (Foster et al., 2003) considered most of the mitochondrial proteins identified in raft fractions from HeLa cells to be contaminants based on the observation that cholesterol depletion of cells with MβCD did not drastically affect their association with raft fractions. However, certain types of rafts appear to be resistant to cholesterol depletion (Hansen et al., 2001; Morrow et al., 2002), and cholesterol-dependence may be difficult to demonstrate for certain raft proteins. This may be particularly relevant when considering intracellular rafts as, depending upon the specific conditions used, MβCD often extracts cholesterol primarily from the plasma membrane (Neufeld et al., 1996). A case in point is that of the erlins. Depletion of plasma membrane cholesterol by treatment of intact cells with MβCD did not alter the association of erlin-1 and erlin-2 with detergent-insoluble raft fractions. However, depleting cholesterol from both plasma membranes and intracellular membranes by hypotonically lysing cells prior to treatment of pelleted membranes with MβCD caused the erlins to shift to the high-density soluble fraction (Browman et al., 2006). In addition, it is unlikely that the raft fractions are contaminated by intact mitochondria because although proteins of the inner and outer mitochondrial membranes are often identified, soluble proteins of the mitochondrial matrix are not (Bini et al., 2003). Based on these observations, the existence of mitochondrial rafts deserves serious consideration.

Like the ER, mitochondria contain low levels of cholesterol and sphingolipids when compared to the plasma membrane (van Meer and Lisman, 2002). Nevertheless,

cholesterol and gangliosides are present in mitochondria in detergent-resistant membrane fractions, and alterations of the levels of these components can affect mitochondrial function. The ganglioside GD3 has been observed to redistribute from the plasma membrane to mitochondria in hepatocytes exposed to TNF-α via a vesicular trafficking pathway regulated by the actin cytoskeleton (Garcia-Ruiz et al., 2002). Depletion of plasma membrane cholesterol prevented trafficking of GD3 to mitochondria, suggesting a possible role for rafts in intracellular transport of GD3. Cholesterol depletion also protected cells from TNF-α-mediated cell death (Garcia-Ruiz et al., 2002). Similarly, in human lymphoblastoid CEM cells, isolated mitochondria contained GD3 and GM3, and triggering of the CD95 death receptor caused a significant increase in mitochondrial GD3 content (Garofalo et al., 2005). Immunoelectron microscopy showed that GD3 was found mainly at the plasma membrane in untreated control cells, but after CD95 cross-linking GD3 was primarily associated with well-organized structures in the internal cristae of mitochondria (Garofalo et al., 2005). GD3 is hypothesized to induce opening of the permeability transition pore in the mitochondrial outer membrane during apoptotic cell death (Scorrano et al., 1999). The voltage-dependent anion-selective channel (VDAC) proteins are candidate components of the permeability transition pore (Cheng et al., 2003) and have been identified in raft fractions in this work (Table 3.4 and Table 3.5) and by others (Bae et al., 2004; Banfi et al., 2006; Bini et al., 2003; Foster et al., 2003). Confirming these observations, Garafalo *et al*. (Garofalo et al., 2005) found that VDAC-1 was constitutively present in detergent-resistant raft fractions isolated from whole cell lysates, and in Triton X-100-insoluble fractions from isolated mitochondria. The active truncated form of Bid (t-Bid) and Bax

(two pro-apoptotic Bcl-2 family members) associated with raft fractions from whole cells, and with Triton X-100-insoluble fractions from isolated mitochondria, but only after CD95 cross-linking (Garofalo et al., 2005). Incubation of isolated mitochondria in the presence of GD3 or t-Bid caused a significant loss of mitochondrial membrane potential and release of cytochrome *c*, but these effects were reduced by half when the mitochondria were pre-incubated with MβCD to deplete cholesterol (Garofalo et al., 2005). Overall, these studies suggest a model in which mitochondrial lipid rafts enriched in GD3 and VDAC-1 recruit Bax and t-Bid upon triggering of CD95, initiating the mitochondrial apoptotic program. More generally, they provide an example of how lipid raft domains in the mitochondria might be important for the proper coordination of mitochondrial responses with signals from the plasma membrane. Independent support for this idea comes from a separate study examining protein association with lipid rafts at several time points following TCR engagement, in which raft association of ten different mitochondrial proteins showed a similar profile of temporal variation (Bini et al., 2003), suggesting that lipid rafts may also be involved in the reorganization of mitochondrial membranes in response to TCR signals.

Prohibitin is the archetypal protein of the prohibitin protein family, and this protein has been consistently identified in raft fractions in this work and in other studies (Table 3.1, (Bae et al., 2004; Banfi et al., 2006; Bini et al., 2003; Foster et al., 2003)). Prohibitin is ubiquitously and abundantly expressed (Nijtmans et al., 2002). Most studies report a predominantly mitochondrial localization for prohibitin, where it is proposed to act as a chaperone in the mitochondrial inner membrane (Ikonen et al., 1995; Nijtmans et al., 2000; Steglich et al., 1999), though there are reports of prohibitin in the nucleus

(Fusaro et al., 2003; Wang et al., 1999), at the plasma membrane (Terashima et al., 1994; Thomas et al., 1994), and in phagosomes (Garin et al., 2001). Other PHB domain-containing proteins are enriched in rafts, but occupy different cellular locations (see (Morrow and Parton, 2005) and references therein). As discussed earlier, erlin-1 and erlin-2 are widely expressed in different cell types and localize to the ER. Stomatin is highly expressed in red blood cells, but is also expressed in other cell types, where it is found at the plasma membrane, and in endosomes, phagosomes and lipid bodies. The flotillins appear to be ubiquitously expressed, and localize to the plasma membrane, endosomes, phagosomes, Golgi, and the nucleus. The PHB protein family member podocin is a 42 kDa integral membrane protein that is almost exclusively expressed in a subset of highly specialized kidney epithelial cells called podocytes. Podocin where it localizes to the plasma membrane of specialized podocyte processes called foot processes, and regulates signalling by the protein nephrin, which is vital for proper kidney function. A striking commonality of all of the PHB domain-containing proteins in higher eukaryotes is their raft association (as defined by their enrichment in purified raft fractions), which contrasts with their significant diversity with respect to subcellular localization, tissue expression profile, and putative functions (Morrow and Parton, 2005). A general role for the PHB domain in lipid raft association is supported by a recent study in which the PHB domain of flotillin was able to target GFP to the plasma membrane and impart partial lipid raft properties on the fusion protein (Morrow et al., 2002). Taken together, these observations suggest that lipid rafts containing prohibitin may exist within mitochondria.

An alternative explanation for the existence of mitochondrial proteins in raft fractions is their presence in plasma membrane rafts. Components of the respiratory chain, ATP synthase and VDAC are commonly identified in raft fractions, and were thought to be restricted to the mitochondria. However, these proteins, as well as other mitochondrial proteins, have also been identified in proteomics studies examining purified plasma membrane preparations (Blonder et al., 2004b; Zhao et al., 2004) and raft fractions derived from plasma membranes (Man et al., 2005; McMahon et al., 2006; Sprenger et al., 2004). ATP synthase α and β were detected on the extracellular surface of the plasma membrane in hepatocytes and adipocytes by immunofluorescence, cell surface biotinylation, and Western blotting of purified plasma membrane fractions (Bae et al., 2004; Kim et al., 2004a). In mouse kidney tissue, respiratory chain components and ATP synthase α and β subunits were detected in lipid raft fractions derived from purified plasma membrane (Kim et al., 2006). ATP synthase α and β and the ubiquinol-cytochrome c reductase core I subunit almost exactly colocalized with the GPI-anchored protein 5'-nucleotidase on the surface of 293 cells by immunofluorescence. Immunohistochemistry of mouse kidney cortex confirmed cell surface as well as mitochondrial expression of ATP synthase α and β, ubiquinol-cytochrome c reductase core I subunit, and the NADH-ubiquinone oxidoreductase 17 kDa subunit (Kim et al., 2006). In rat natural killer (NK) cells, ATP synthase α and β were identified in a proteomic analysis of detergent-resistant raft fractions isolated from purified plasma membranes and cell surface expression of these proteins was confirmed by flow cytometric analysis of unpermeabilized cells (Man et al., 2005). The ability of the NK

cells to kill target cells was inhibited by pre-treatment with antibodies against ATP synthase α and β, though the mechanisms through which this might occur were not investigated further (Man et al., 2005). Lipid rafts aggregate at the site of target recognition between NK cells and sensitive tumour cells and are required for activation of signalling pathways downstream of CD2 (Inoue et al., 2002; Lou et al., 2000). These observations support the possibility that ATP synthase localized in plasma membrane rafts might affect NK cell function. It is possible that respiratory chains and ATP synthase in plasma membrane rafts are involved in the generation of extracellular ATP (Champagne et al., 2006). Addition of ADP and P_i to the culture media of adipocytes expressing cell surface ATP synthase resulted in a high rate of ATP synthesis, which was inhibited by ATP synthase inhibitors and uncouplers (Kim et al., 2004a). Extracellular ATP and its metabolites (ADP and adenosine) are agonists of purinergic receptors including P2Y GPCRs and ATP-gated P2X receptor cation channels, whose activation leads to signalling responses that control diverse cellular responses including proliferation, differentiation, and inflammation (Schwiebert and Zsembery, 2003). Certain P2Y and P2X receptors are known to localize to rafts (Becher and McIlhinney, 2005; Quinton et al., 2005; Vial et al., 2006). The GPI-anchored protein 5'-nucleotidase is a raft-associated enzyme that converts extracellular ATP into adenosine. Recent work indicates that 5'-nucleotidase activity is regulated by a Ca^{2+}-dependent, annexin-mediated stabilization of rafts (Babiychuk and Draeger, 2006), providing additional support for a role for rafts in extracellular ATP metabolism. Other raft-associated proteins that might require ATP to function at the cell surface are hsp70 and hsp90, which were observed in raft fractions in this work (Table 3.3, Table 3.6, and Table 3.7) and by others (Bini et al.,

2003; Karsan et al., 2005; Li et al., 2003b; Li et al., 2004b; McMahon et al., 2006). These proteins have intrinsic ATPase activity, and function in protein folding at both intracellular and extracellular sites by binding to specific protein substrates and altering their conformation through cycles of ATP binding and hydrolysis (Pratt and Toft, 2003; Schmitt et al., 2007). Many hsp70/hsp90 substrates are signalling proteins and receptors (Pratt and Toft, 2003). Recent work describes clustering of hsp70 and hsp90 with Toll-like receptor 4 in lipid rafts following stimulation with bacterial lipopolysaccharide (Triantafilou and Triantafilou, 2004), providing one example of a raft signalling event that might require extracellular ATP for proper function. The main source of extracellular ATP is thought to be ATP produced in mitochondria and then secreted outside of the cell (Schwiebert and Zsembery, 2003). Extracellular ATP synthesis by ATP synthase in rafts would constitute a previously unrecognized source of ATP at the cell surface. Since ATP is rapidly degraded outside of the cell (Schwiebert and Zsembery, 2003), raft-centred ATP synthesis might be important for localized generation of ATP, facilitating its interaction with ATP-binding signalling molecules.

Overall, the observation of numerous ER and mitochondrial proteins in raft fractions isolated from whole cell lysates suggest the presence of rafts in ER and mitochondrial membranes, where these microdomains had not previously been reported. Structural and functional characterization of a number of the identified proteins supports the existence of lipid rafts in the ER and in mitochondria. In the future, proteomic analysis of raft fractions isolated from purified ER and mitochondrial membranes should prove useful in further characterizing the specific roles of lipid rafts within these organelles. However, it is also apparent that proteins previously thought to function

specifically in the ER or the mitochondria may have raft-dependent functions outside of these locations, and particularly at the plasma membrane. Some of these functions are likely to be specific to the plasma membrane microenvironment. However, the observation of mitochondrial and ER proteins in plasma membrane rafts might also indicate a role for rafts in facilitating inter-organelle communication. Components of membrane fusion machinery, including SNARE proteins, vacuolar-ATPase subunits, and Rab family members have been observed in rafts in this study and by others (Table 3.1, Table 3.4, Table 3.5, Table 3.6 and Table3.7 (Dermine et al., 2001; Li et al., 2003b; Mielenz et al., 2005; von Haller et al., 2001)), and functional evidence suggests that rafts are involved in vesicular trafficking pathways (Dermine et al., 2001; Garcia-Ruiz et al., 2002; Lafont et al., 1999; Sharma et al., 2003; Shaw and Li, 2003). In macrophages, the ER has been shown to fuse with the plasma membrane underneath phagocytic cups, providing a source of membrane for phagosome formation and a possible mechanism for the introduction of ER proteins into the plasma membrane (Gagnon et al., 2002). Proteomic analysis of phagosome preparations shows that many raft proteins are enriched in phagosomes (Garin et al., 2001) and independent biochemical and immunofluorescence data demonstrate that flotillin-1-enriched lipid rafts accumulate on maturing phagosomes (Dermine et al., 2001), a finding consistent with the observation that 27 of 52 proteins identified in a proteomic analysis of monocyte lipid rafts were also found in the phagosome proteome (Li et al., 2003b). Lipid rafts are also thought to exist in lysosomal and endosomal membranes (Bagshaw et al., 2005; Helms and Zurzolo, 2004; Parton and Richards, 2003), and it seems reasonable to think that rafts may have an important role in coordinating the interaction of the plasma membrane, ER, lysosomes

and endosomes during phagocytosis. By extension, since rafts in other cell types also contain similar membrane fusion and trafficking components, other biological trafficking processes requiring coordination between different membrane compartments might also be raft-dependent (such as, for example, the internalization of gangliosides and receptors in response to extracellular signals). Rafts might also be important at membrane contact sites between different organelles. In both yeast and mammalian cells, subcompartments of the ER are physically associated with both mitochondria and the plasma membrane (Achleitner et al., 1999; Ardail et al., 1993; Pichler et al., 2001). Both the plasma-membrane associated and the mitochondria-associated ER seem to have a common function in the synthesis and inter-membrane transfer of phospholipids (Achleitner et al., 1999; Pichler et al., 2001), and ER-mitochondrial contacts are also implicated in intracellular calcium signalling and apoptosis (Goetz and Nabi, 2006; Rutter, 2006). A possible role for rafts in coordinating inter-organelle communication in these biological contexts would be an interesting area to study in the future.

Actin, tubulin, and intermediate filament proteins, as well as proteins that bind to and regulate the function and assembly of the cytoskeleton were identified in lipid raft fractions isolated from all of the cell types examined in this study. Cytoskeletal proteins are also commonly identified in other published raft proteomes (Foster et al., 2003; Li et al., 2003b; Li et al., 2004b; Nebl et al., 2002; Sprenger et al., 2004; Tu et al., 2004; von Haller et al., 2001). Although the possibility that some of these identifications result from contamination by abundantly expressed cytoskeletal proteins cannot be completely ruled out, a large amount of evidence supports functionally important associations between the cytoskeleton and lipid rafts. Studies of raft-cytoskeleton interactions in both

hematopoietic and non-hematopoietic cells illustrate several basic themes that appear to be conserved in diverse cell types (Harder and Simons, 1999; Head et al., 2006; Holowka et al., 2000; Kamiguchi, 2006; Leitinger and Hogg, 2002; Lisanti et al., 1994b; Manes and Viola, 2006; Oliferenko et al., 1999; Rodgers and Zavzavadjian, 2001; van Deurs et al., 2003). Association of rafts with the cytoskeleton may be important in the general regulation of raft-mediated vesicular trafficking events involved in protein sorting, endocytosis, and phagocytosis (Garcia-Ruiz et al., 2002; Li et al., 2003b; Li et al., 2004b; van Deurs et al., 2003; Yoon et al., 2003). There is also strong evidence indicating that cytoskeletal interactions are important for controlling the spatial distribution of lipid rafts in the plasma membrane, promoting their clustering or segregation depending on the particular cellular context, as well as controlling the association of individual proteins with rafts (Golub and Caroni, 2005; Holowka et al., 2000; Leitinger and Hogg, 2002; Rodgers and Zavzavadjian, 2001; Runembert et al., 2002; Setterblad et al., 2004; Simpson-Holley et al., 2002; Valensin et al., 2002; Watzl and Long, 2003). Cytoskeleton-raft interactions have been particularly well studied in the context of lymphocyte activation and/or migration following the engagement of integrins, adhesion molecules, or other immune receptors, and subsequent receptor localization to lipid rafts where compartmentalized signals are initiated (Gupta et al., 2006; Hao and August, 2005; Leitinger and Hogg, 2002; Manes and Viola, 2006; Oliferenko et al., 1999; Villalba et al., 2001). Actin microfilaments accumulate at the membrane at sites enriched in raft markers, where they colocalize with activated signalling molecules following engagement of antigen receptors in T and B cells (Gupta and DeFranco, 2003; Harder and Simons, 1999). Treatment of B and T lymphocytes

with actin-depolymerizing agents prevents the induced clustering of raft markers on the plasma membrane as well as the association of specific downstream signalling effectors with detergent-insoluble membrane fractions following antigen receptor engagement, and these changes correlate with alterations in signalling and cellular responses (Gupta et al., 2006; Hao and August, 2005; Leitinger and Hogg, 2002; Manes and Viola, 2006). A general paradigm emerging from these studies suggests that the association of the actin cytoskeleton with rafts is dynamically regulated following the engagement of raft-associated receptors. The Arp2/3-binding protein hematopoietic lineage cell-specific protein 1 (HS1) is rapidly phosphorylated by Syk on two tyrosine residues upon BCR activation. This phosphorylation event was necessary for the translocation of HS1 to rafts along with Arp2/3 complex and the Wiskott-Aldrich syndrome protein (WASP), where they may be responsible for actin assembly (Hao et al., 2004). In addition, in response to a diverse set of extracellular signals, lipid rafts appear to transiently disengage from the actin cytoskeleton, thus enabling relocalization and clustering of rafts at defined cellular locations (Gupta et al., 2006; Manes and Viola, 2006). Gupta *et al*. (Gupta et al., 2006) have shown that ezrin localized to lipid rafts in resting B cells quickly becomes dephosphorylated after BCR engagement, causing it to detach from actin and to dissociate from lipid rafts. However, loss of ezrin from rafts is only temporary, as 30 minutes following receptor stimulation, ezrin phosphorylation and raft association was re-established. Constitutively active ezrin mutants interfered with the clustering of lipid raft markers normally observed following BCR engagement, suggesting that transient uncoupling of rafts from the actin cytoskeleton via dissociation of ezrin is necessary for activation-induced lipid raft coalescence in B cells. In Jurkat T

cells, death receptors and associated downstream signalling molecules, along with ezrin, moesin, RhoA and RhoGDI, associated with lipid rafts following induction of apoptosis with the antitumor drug Aplidin, which was itself rapidly incorporated in rafts (Gajate and Mollinedo, 2005). In a separate study, transient up-regulation of the level of raft-associated actin was observed following TCR engagement in Jurkat cells (Bini et al., 2003). In smooth muscle cells, annexins II and VI associate with lipid rafts where they interact with actomyosin to form a calcium-dependent cytoskeleton-membrane complex that both aggregates rafts and links them to the cytoskeleton in response to the increase in intracellular free calcium that occurs upon muscle contraction (Babiychuk et al., 1999; Babiychuk et al., 2000). Annexin II is also present in raft-based vesicles participating in other actin-dependent processes, including apical sorting of proteins in polarized epithelial cells (Jacob et al., 2004) and calcium-dependent exocytosis in neuroendocrine cells (Chasserot-Golaz et al., 2005). All members of the annexin protein family have in common the ability to bind to both phospholipids and actin-based cytoskeletal elements in a calcium-dependent manner (Hayes et al., 2004). Multiple annexins also localize to lipid rafts and it is tempting to speculate that the annexins could regulate interactions between lipid rafts and the actin cytoskeleton in response to calcium signalling in hematopoietic cells as well, since annexins II, V, and VI were identified in raft fractions in myeloid and erythroid cell lines in this study. In general, the temporally regulated association of cytoskeletal molecules with rafts after exposure to specific stimuli that are known to provoke functionally important cytoskeletal rearrangements argues against the idea that these proteins are merely non-specific contaminants of the raft fractions. Rather, it is likely that closely coordinated interactions between lipid rafts and the actin

cytoskeleton occur in diverse biological contexts through a number of different conserved mechanisms.

Though many of the cytoskeletal proteins identified in this study are associated with the actin cytoskeleton, tubulin was also identified in raft fractions, suggesting that rafts also interact with microtubules. Li et al. (Li et al., 2004b) identified not only tubulin, but also tubulin-binding regulatory proteins in monocyte lipid rafts, an observation that supports the idea that tubulin in raft fractions is representative of functional microtubule/raft interactions, and is not merely due to contamination (Li et al., 2004b). Several additional lines of evidence support the existence of regulated interactions of microtubules with lipid rafts in diverse contexts. In neurons palmitoylated tubulin associates with GM1 gangliosides at the plasma membrane, and both GM1 and tubulin were present in low-density detergent-resistant membrane fractions, suggesting that the lipid-anchored tubulin was specifically targeted to lipid rafts on the cell surface (Palestini et al., 2000). Depolymerization of microtubules in cardiac myocytes resulted in the loss of β-adrenergic GPCRs, $G\alpha_s$, and adenylyl cyclase from buoyant raft fractions, a reduction in the number of cell surface caveolae, as well as increased production of cAMP in response to agonist stimulation, suggesting that microtubule-based stabilization of rafts regulates cAMP formation by controlling the raft localization of adenylyl cyclase signalling components (Head et al., 2006). Raft interactions with microtubules are also implicated in the regulation of cell motility. Integrin-mediated cell adhesion causes microtubules to become stabilized at the leading edge of migrating fibroblasts, where they colocalize with the raft marker GM1 (Palazzo et al., 2004). Since cholesterol depletion inhibited microtubule accumulation, rafts may be important in the

reorganization of microtubules following integrin activation in these cells (Palazzo et al., 2004). In PC12 cells, NGF-induced motility results in the clustering of PI(4,5)P_2-enriched rafts at sites of ruffling lamellopodia (Golub and Caroni, 2005). In addition to promoting changes in the actin cytoskeleton necessary for protrusive motility, the PI(4,5)P_2-enriched raft patches captured and stabilized microtubule plus ends through the raft-localized protein IQGAP1. Disruption of microtubules with nocodazole prevented raft clustering and altered the organization and polarization of cell motility. The authors further showed that PKA was delivered to raft patches at the plasma membrane via microtubules and that PKA activity promoted raft clustering and focussed motility. In contrast to these studies, another raft-localized microtubule-binding protein, CLIPR-59, has high affinity for unpolymerized tubulin and can prevent microtubule polymerization (Lallemand-Breitenbach et al., 2004), suggesting that in some rafts interactions with microtubules are actively inhibited. Similarly, the microtubule-destabilizing factor SCG10 was enriched in brain-derived rafts, where it may inhibit polymerization of tubulin in a phosphorylation-dependent manner (Maekawa et al., 2001). These observations further imply that the presence of tubulin subunits in raft fractions may not necessarily indicate the association of rafts with polymerized microtubules, and that the significance of tubulin in the K562, IVEE, and IVEE/GPI8 raft fractions requires further investigation to determine whether microtubules associate with rafts in these cells.

Components of intermediate filament networks, including vimentin, desmin, and epiplakin, were also observed in raft fractions in several cell types in this study. In contrast to microfilaments and microtubules, there has been very little investigation of interactions between intermediate filaments and rafts. Vimentin was identified as a

component of a raft-associated membrane skeleton at neutrophil plasma membranes (Nebl et al., 2002). Vimentin was also reported to affect the raft localization and activity of the sodium-glucose cotransporter SGLT1 in renal proximal tubular cells (Runembert et al., 2002). Interestingly, in addition to their structural roles, there is evidence to suggest that intermediate filament proteins have specific roles in signal transduction, although in most cases the molecular mechanisms underlying their effects on cell signalling have not yet been defined (Paramio and Jorcano, 2002). Given the consistent proteomic identification of intermediate filament proteins in raft fractions, the existence of raft-intermediate filament interactions might explain some of these observations, and is an area worthy of further study.

It is striking that many of the proteins identified in raft fractions isolated from diverse cell types are the same, suggesting that a common lipid raft proteome may exist. In this study, qualitative 2D gel analysis of raft fractions isolated from myeloid, erythroid, and lymphoid cells demonstrated that, while there were specific differences observed in the protein profiles of each cell type, there was also a significant degree of overlap. This data is consistent with other 2D gel studies of raft fractions. A quantitative 2D gel analysis that compared the protein profiles of detergent-resistant raft fractions isolated from an epithelial and a lymphoma cell line found that of the approximately 150 protein spots reproducibly observed in raft fractions from each cell type, 66 (~44%) were present in both cell types (Matousek et al., 2003). McMahon *et al.* compared the composition of a detergent-free caveolae preparation isolated from four different cell types (normal human fibroblasts, ovine pulmonary aortic endothelial cells, MA104 cells, and Jurkat T cells) and found that 62% of spots were common to all four

cell types (McMahon et al., 2006). Similarly, Kim et al. qualitatively compared 2D gel profiles of detergent-resistant raft fractions from different mouse organs, including the liver, lung, brain, and kidney, and found that, in addition to some tissue-specific differences, many of the protein spots were present in all types of rafts (Kim et al., 2006). In both of the latter two studies, of the common raft proteins identified by mass spectrometry, most were cytoskeletal, mitochondrial or ER proteins, members of the prohibitin family, proteins involved in vesicular trafficking, or heterotrimeric G proteins, which is consistent with the results obtained in this study and in the overwhelming majority of raft proteomes currently published. The existence of a common lipid raft proteome implies that rafts share similar structural and functional roles in many different cell types. These commonalities may reflect the presence of conserved regulatory interactions between the cytoskeleton and rafts, conserved raft-based mechanisms of vesicular trafficking, and/or the involvement of rafts generally in the regulation or organization of "housekeeping" metabolic processes or conserved signalling pathways.

Surprisingly, relatively few signalling molecules were identified in the raft fractions analyzed in this study, or in other lipid raft proteomes (Banfi et al., 2006; Blonder et al., 2005; Blonder et al., 2004a; Foster et al., 2003; Mielenz et al., 2005; Tu et al., 2004), and those that have been identified are mostly heterotrimeric G proteins and Src family kinases. The identification of numerous subunits of heterotrimeric G proteins is consistent with a well-established role for lipid rafts in the regulation of GPCR signalling (Becher and McIlhinney, 2005; Head et al., 2006). Similarly, Src family kinases, which were among the first signalling molecules discovered in rafts (Furuchi and Anderson, 1998; Liu et al., 1997a; Robbins et al., 1995), are also commonly identified in

raft fractions. Despite ample evidence of the involvement of lipid rafts in kinase-dependent signalling pathways, other than Src family kinases, only one other kinase and one kinase regulatory subunit were identified in raft fractions in this study. These were the monomeric serine/threonine protein kinase, casein kinase I (CKI), and the type I regulatory subunit of the cAMP-dependent protein kinase (PKA). The PKA holoenzyme is a serine/threonine kinase that is composed of two cAMP-binding regulatory subunits (of type I or type II) complexed to two catalytic subunits (Sim and Scott, 1999). Despite the consistent identification of type I regulatory subunits, the catalytic subunit was not detected in raft fractions in the proteomic experiments described in this chapter. However, in other cell types, both type I and type II regulatory and catalytic subunits of PKA have been detected in lipid raft fractions by immunoblotting (Noyama and Maekawa, 2003; Vang et al., 2001), and, as discussed previously, type II PKA colocalizes with clustered raft markers on the plasma membrane during NGF-induced cell motility in PC12 cells (Golub and Caroni, 2005). Interestingly, though both CKI and PKA are involved in a vast number of different cellular processes, specificity in substrate targeting in PKA- or CKI-mediated signalling is often achieved by the targeting of the kinases to specific subcellular locales, which controls the access of the kinases to upstream activating signals and/or substrates (Knippschild et al., 2005; Sim and Scott, 1999; Smith and Scott, 2006). In the case of PKA, such targeted localization occurs primarily via the interaction of the regulatory subunits with different A-kinase anchoring proteins (AKAPs) targeted to specific subcellular locations (Smith and Scott, 2006). It is tempting to speculate that compartmentalization of specific pools of CKI or PKA to rafts might provide a general cellular mechanism to provide additional specificity to CKI or

PKA signalling pathways. To the best of my knowledge, there have been no studies to date reporting a raft-localized signalling pathway involving CKI, though it has been identified independently by MS in raft fractions isolated from Raji B cells (Saeki et al., 2003), HeLa cells (Foster et al., 2003), and Vero cells (Blonder et al., 2005). Further localization and functional studies are necessary to investigate potential raft-based regulation of CKI signalling. However, there is evidence that rafts compartmentalize PKA-mediated signalling. Since at least some types of rafts are sites of cAMP production (Head et al., 2006; Martin and Cooper, 2006), the localization of PKA to raft microdomains would effectively couple the kinase to cAMP-generating signals. In addition to the previously mentioned role of type II PKA in promoting raft clustering during cAMP-dependent cell motility in PC12 cells, raft-localized type I PKA appears to be function in the regulation of Src family kinase activity. In T cells, type I PKA localizes to lipid rafts by interaction with an as-yet unidentified AKAP (Tasken and Stokka, 2006), where it phosphorylates and activates Csk in a cAMP-dependent manner downstream of both physiological and pharmacological cAMP-generating agents (Vang et al., 2001). Csk phosphorylates the negative regulatory C-terminal tyrosine residue of Lck, leading to decreased Lck activity, and inhibition of proximal TCR signalling, cytokine production, and proliferation (Vang et al., 2001). Though experimental evidence for this pathway exists only for T cells, it seems reasonable to suggest that this might represent a general mechanism of regulation of Src family kinase activity in other Src-dependent signalling pathways and/or in other cell types, including K562 cells, though further work is needed to confirm this. Since PKA has many known substrates, it will also be of interest in the future to determine whether other raft-localized proteins are

substrates of PKA in specific experimental settings. Another open question is whether or not PKA-containing rafts constitute a homogeneous population. It is possible that more than one type of PKA-containing raft exists, differing in their protein composition and/or localization, with each raft subtype responding to distinct signals upstream of PKA, providing an additional means by which the cell can introduce specificity into PKA signalling in order to generate discrete cellular responses to signals mediated by cAMP.

Despite the sensitivity of MS-based protein identification methods, and technical improvement in both gel-based and gel-free proteomics approaches, the expectation that proteomic analysis of raft fractions would lead to identification and elucidation of receptor-based signalling pathways in rafts remains largely unfulfilled. The results of this and other studies indicate that many signalling proteins that are known to be present in rafts, according to classical biochemical and colocalization experiments, are not detected by current proteomics approaches (Banfi et al., 2006; Blonder et al., 2005; Blonder et al., 2004a; Foster et al., 2003; Mielenz et al., 2005; Shaw and Li, 2003; Tu et al., 2004). In general, only relatively abundant cell surface receptors were identified in this study (for example, GPI-anchored proteins generally, and class I MHC, class II MHC, and CD147 in B cell raft fractions), and most of these proteins were previously identified in rafts using more traditional approaches (Anderson et al., 2000; Garnett et al., 1993; Lebedeva et al., 2004; Parkin et al., 2001; Tang and Hemler, 2004). Though the gel-based experiments described here are not comprehensive in their coverage of spots and bands in 1D and 2D gels, which is an obvious reason for this finding, even the less biased shotgun proteomics experiment examining the entire raft fraction identified only a

limited number of signalling components, mainly heterotrimeric G proteins and Src family kinases. Based on these results, it is likely that these signalling molecules are among the most abundant in raft fractions. Similar trends are evident even in larger shotgun raft proteomes in which hundreds of proteins were identified (Blonder et al., 2005; Blonder et al., 2004a; Foster et al., 2003), and in more recent and more comprehensive gel-based studies that have the advantage of access to improved MS protocols, instrumentation, search engines, and databases (Banfi et al., 2006; Mielenz et al., 2005; Tu et al., 2004). In some cases technical limitations may explain such reduced coverage of the raft fractions. For example, in gel-based methods, a protein may fail to enter the gel under the given electrophoresis conditions, might be resistant to trypsinization, or the resulting peptides might not be efficiently recovered from the gel. As noted in this work and by others, GPI-anchored proteins often fail to enter 2D gels (Abrami et al., 2001; Fivaz et al., 2000). Similarly, the transmembrane protein LAT is easily detectable by Western blotting in 1D gels, but cannot be detected in 2D gels (Bini et al., 2003). It is also clear that one reason many signalling molecules fail to be identified is their relatively low abundance compared to other raft proteins. In this work, 2D gel profiling of raft proteins following *in vitro* kinase assays demonstrated that a number of potential tyrosine kinases and/or their substrates were detectable by Western blotting using sensitive anti-phosphotyrosine antibodies, but could not be correlated with spots on a silver-stained gel. Similarly, as described here, in agreement with data from other groups (Bini et al., 2003; Mielenz et al., 2005), certain Src family kinases can be detected by immunoblotting in 2D gels of raft fractions, but cannot be matched with silver-stained spots, indicating their relatively low abundance. Cell surface biotinylation

of K562 cells identified a number of surface-exposed raft proteins present in 2D gels, which might include a number of signalling receptors, however a significant number of these proteins were also undetectable by silver staining. An independent group recently reported essentially identical findings when examining 2D gel profiles of detergent-resistant membranes isolated after cell surface biotinylation of endothelial cells (Sprenger et al., 2006), further supporting the idea that the low levels of receptors and signalling effectors in raft fractions is an important limiting factor in raft proteomics directed towards the analysis of raft-based signalling. It will be important in the future to continue to improve the resolution and sensitivity of MS-based proteomic techniques, as well as to further fractionate the raft membranes examined prior to MS analysis (for example, according to their subcellular location or by using affinity-based purification techniques) to obtain a more complete picture of the signalling and other proteins present in relatively low abundance in rafts.

All of the experiments described in this chapter analyzed raft fractions isolated using 1% Triton X-100 lysis buffer, which is considered to be a very stringent detergent extraction protocol that efficiently solubilizes non-raft membrane (Schuck et al., 2003). However, it is apparent that some raft proteins (including immune receptors and downstream signalling effectors), while soluble in 1% Triton X-100, are only found in insoluble raft fractions after cross-linking, or in preparations isolated using lower concentrations of Triton X-100 or weaker detergents (Deans et al., 1998; Field et al., 1997; Li et al., 2004a; Montixi et al., 1998). These results can be interpreted in several different ways. It is possible that these proteins localize to rafts with distinct lipid and protein subsets that interact differently with a given concentration or type of detergent. It

is also possible that these observations reflect a weak association of specific proteins with rafts at the periphery of raft domains. In addition, some models of raft organization suggest that progressively less ordered (and increasingly detergent-soluble) peripheral raft domains surround more highly ordered Triton-insoluble core raft domains (Braccia et al., 2003; Draeger et al., 2005; Edidin, 2003a; Edidin, 2003b; Madore et al., 1999). This is consistent with evidence that raft fractions isolated using weaker detergents tend to contain a greater number of proteins than Triton-insoluble raft fractions (Kim et al., 2004b; Schuck et al., 2003). Thus, using different detergent extraction conditions might enable the detection of raft signalling molecules that are excluded from the more stringent Triton X-100 raft preparations, but nevertheless reside in ordered membrane domains *in vivo.* However, these studies would have to be evaluated and interpreted with great care, and in concert with other independent approaches, since less stringent detergent extraction conditions increase the chances of incompletely solubilizing non-raft membrane. Another valuable approach would be to analyze raft fractions isolated from cells at various time points after stimulation of a receptor of interest, since it is also apparent that a substantial number of receptors and signalling proteins associate with rafts only upon cellular activation (see (Lucero and Robbins, 2004; Zajchowski and Robbins, 2002) for review).

The work described here also illustrates the specific challenges associated with differential proteomics studies. The 2D gel experiments suggest that, although there appears to be a significant number of raft proteins that belong to a conserved lipid raft proteome, there are also specific differences in raft protein composition in different cell types. Because of the difficulty in identifying proteins from 2D gel spots at that time, I

chose not to further characterize those differences. However, given the substantial improvements in MS protocols, instrumentation, search algorithms, and databases that are currently available, this avenue would be worth revisiting in the future using optimized IPG-based 2D gels, and sensitive fluorescent protein stains with a much larger linear range than silver staining that facilitate accurate quantitation. Indeed, several recent studies have successfully used 2D gels, in combination with other MS approaches, to compare lipid raft fractions and identify proteins of interest in resting versus stimulated T cells (Tu et al., 2004), in immature versus mature B cell lines (Mielenz et al., 2005), and in raft fractions derived from failing versus non-failing human hearts (Banfi et al., 2006). Quantitative gel-free proteomics strategies will also greatly facilitate differential raft proteomics experiments in the future by enabling investigators to immediately target proteins that undergo quantitative changes in raft association for validation and subsequent functional and localization studies. An example of the utility of this approach is the study of Gupta *et al.*, who recently examined lipid raft composition using a quantitative MS approach to compare raft fractions isolated from resting B cells and B cells activated by engagement of the BCR (Gupta et al., 2006). This analysis identified the transient dissociation of ezrin from rafts in stimulated B cells, which appears to be important in the reorganization of rafts and the cytoskeleton during B cell activation.

The 1D gel experiments summarized here also demonstrate the existence of differences in raft protein composition in different cell types. A preliminary examination of several myeloid cell lines and of the GPI-deficient and wildtype erythroid cell lines IVEE and K562 illustrated differences in the raft protein profiles obtained in different cell types. The effect of GPI deficiency on raft structure and function is of interest in the

context of the human disease paroxysmal nocturnal hemoglobinuria (PNH), which is an acquired disorder of hematopoietic stem cells. A mutation in the GPI anchor biosynthesis pathway in PNH stem cells abrogates biosynthesis of the GPI anchor, preventing cell surface expression of the any of the proteins normally modified in this manner. Several studies suggest that the expression levels of several raft components are altered in GPI-deficient cells, and that signalling in these cells is affected (Abrami et al., 2001; Hazenbos et al., 2004a; Hazenbos et al., 2004b; Lillico et al., 2003; Romagnoli and Bron, 1997; Romagnoli and Bron, 1999; Ruggiero et al., 2004; Samuel et al., 2001; Terrazzano et al., 2005). Based on these observations, I focussed on comparing the protein composition of rafts isolated from both wildtype and GPI-deficient cells. Initial comparison of raft protein profiles from K562 and IVEE cells suggested that, though certain bands were downregulated in IVEE raft samples (consistent with the loss of GPI-anchored proteins, but potentially involving other proteins), certain protein bands were upregulated in GPI-deficient cells. However, because complementation of the GPI anchor biosynthesis defect in the IVEE cells by transfection with the *hGPI8* gene failed to alter the observed raft protein profile to that seen in GPI+ K562 cells, there is no evidence to support the hypothesis that the differences in raft protein composition observed in K562 versus IVEE cells are due to changes in GPI expression. The possibility that GPI deficiency in K562 cells leads to irreversible changes in raft phenotype was considered, but attempts to test this possibility proved inconclusive. K562 cells were treated with the GPI-anchor cleaving enzyme phosphatidylinositol phospholipase C (PI-PLC) to remove surface GPI-anchored proteins prior to isolation of raft fractions (data not shown). Even when the majority of cell surface CD59 was

removed following PI-PLC treatment, the protein profile of K562 cells was essentially unchanged. However, some GPI-anchored proteins are resistant to cleavage with PI-PLC (Sharom and Lehto, 2002), and the intensity of the band corresponding to the GPI-anchored protein dipeptidase 1 was not reduced in PI-PLC-treated cells. Given the uncertainty of the effectiveness of GPI depletion using this approach, the results are at best inconclusive. In order to examine K562 raft protein composition before, and at various time points after the loss of GPI-anchored protein expression, I also attempted to develop an siRNA that could effectively knock down an enzyme in the GPI anchor biosynthesis pathway. However, I was unable to find an siRNA sequence that was effective even after screening four different siRNA sequences over a timecourse of 0 to 96 hours, using both RT-PCR and flow cytometry to monitor surface GPI-anchored protein expression. It is also possible that the differences observed in the K562 versus IVEE raft samples reflect secondary GPI-independent changes that occurred during the original mutagenesis and cloning of the IVEE cells. The ability of K562 cells to undergo megakaryocytic or erythrocytic differentiation in response to specific agents is well known (Tsiftsoglou et al., 2003), and the 1D gel analysis of different myeloid cell lines supported the idea that raft protein profiles vary with cell type. To determine whether some of the observed differences might be due to a differentiation event that occurred during the original mutagenesis and isolation of the IVEE cells, the K562, IVEE, and IVEE/GPI8 cells were analyzed by flow cytometry against a panel of differentiation markers. However, this analysis detected no significant alteration in any of the differentiation markers examined. To date, the only difference in phenotype in K562 versus IVEE and IVEE/GPI8 cells that I have observed is a noticeably increased

tendency for K562 cells to adhere to the sides of the flask in culture, suggesting that these cells exhibit altered adhesive properties, though it is not known whether this property is raft-dependent. The proteins identified in the differentially stained bands from K562 and IVEE cells are generally common to many lipid raft proteomes, and are not immediately suggestive of an explanation for the difference in raft protein composition that is observed. At the present time, the underlying factor responsible for the differences in raft phenotype between K562 and the IVEE /IVEE/GPI8 cells remains unknown. Nevertheless, the differences in raft protein profiles seen in the GPI+/- B cell lines examined do support the idea that the loss of GPI-anchored proteins can have other secondary effects on raft protein composition and, presumably, function. In contrast to the K562 and IVEE cells, the parental Raji26 and Ramos517 cells were isolated as spontaneously occurring GPI-deficient clones of the commonly utilized Raji and Ramos cell lines. The GPI+/- Raji 26 and GPI +/- Ramos517 cell lines used in this study were derived by transfection of these GPI-deficient clones with a vector control construct, or with a construct expressing the defective GPI anchor biosynthesis component, providing a more robust model in which to investigate changes that might be due to GPI deficiency. Though a number of proteins were identified in the differentially expressed bands excised from these cell lines, quantitative evaluation of levels of these proteins in raft fractions by immunoblotting or other techniques is required before any definitive conclusions regarding the nature of specific differences can be made. Further development of the shotgun proteomic approach to enable quantitation of proteins identified by MS should also be undertaken in the future to efficiently compare rafts isolated from wildtype and

GPI-deficient cells under resting conditions, and after stimulation of signalling pathways of particular interest.

In conclusion, a number of novel and known raft proteins have been identified in non-caveolar rafts isolated from several types of hematopoietic cells, using both gel-based and gel-free proteomics approaches. In particular, the discovery of numerous mitochondrial and ER-localized proteins within the lipid raft proteome suggests that lipid rafts exist in previously unrecognized intracellular locales, and is also consistent with potential raft-based models of inter-organelle communication. The presence of numerous cytoskeletal elements in raft fractions is consistent with the steadily increasing evidence of regulatory interactions between rafts and the cytoskeleton in diverse biological contexts. It is also striking to observe that the lipid raft proteomes examined in an exceptionally diverse array of tissue types share many commonalities, suggesting that many mechanisms that regulate rafts and/or processes in which rafts are involved are highly conserved. Of the specific differences in raft protein composition that were observed using both 1D and 2D gel profiling of raft fractions, while candidate proteins that might be responsible for these differences were successfully identified by MS, differential association of these proteins with rafts awaits independent verification. To date, proteomics has not provided the type of insight into raft signalling processes that was expected at the outset of these studies. However, it is likely that the continued improvement and development of sensitive and quantitative MS screens that can be applied to very specific and focussed biological questions will enable investigators to begin to overcome these limitations in the future.

Chapter Four: GPI Deficiency Alters the Function of Lipid Rafts in B Cell Signalling

4.1 Introduction

The general hypothesis of this thesis is that the distinct structural properties of a given lipid raft (such as its protein or lipid composition, size, or morphology) are directly related to its specific functions in cellular processes, including signal transduction. The previous chapter focussed on analyzing one component of lipid raft structure in hematopoietic cells by utilizing a proteomics approach to investigate raft protein composition. In this chapter, the effect of a defined change in raft protein composition, GPI-anchored protein deficiency, on lipid raft function in hematopoietic cell signalling is investigated in order to directly address the hypothesized link between lipid raft structure and function.

GPI deficiency is of interest in the context of the human disease paroxysmal nocturnal hemoglobinuria (PNH). This relatively rare hematopoietic disorder causes hemolytic anemia, venous thrombosis, bone marrow failure, and possibly, an increased risk of leukemia (Boccuni et al., 2000; Hall et al., 2002). The underlying molecular defect in this disease is an acquired mutation of the *hPIGA* gene in hematopoietic stem cells (Miyata et al., 1993; Takeda et al., 1993). This gene encodes an enzyme that catalyzes an early step in the GPI anchor biosynthesis pathway. Because of this mutation, hematopoietic cells derived from the PNH clone lack cell surface expression of any of the proteins normally tethered to the plasma membrane by GPI anchors. Some of the symptoms of PNH can be linked directly to the lack of expression of specific GPI-anchored proteins. For example, hemolytic anemia is thought to result from uncontrolled

complement lysis of GPI-deficient erythrocytes lacking cell surface expression of the GPI-anchored proteins CD55 and CD59, which protect the plasma membrane of normal cells from damage by activated complement (Boccuni et al., 2000; Hall et al., 2002). However, the pathological mechanisms that allow preferential expansion of the PNH clone and that are involved in the other symptoms of PNH are not well understood. In this context, it is interesting to note that studies of GPI-deficient cells isolated from mouse knockout models or PNH patients demonstrate that signalling and associated downstream phenotypic responses are altered in GPI-deficient cells. GPI-deficient myeloid cells isolated from myeloid-specific GPI anchor-deficient mice show impaired FcγR effector functions upon IgG-immune complex binding, including decreased TNF-α release, impaired dendritic cell maturation, and defects in antigen presentation (Hazenbos et al., 2004a). These defects are accompanied by decreased tyrosine phosphorylation of the FcR γ chain (Hazenbos et al., 2004a). Similarly, GPI-deficient monocytes isolated from PNH patients exhibit impaired dendritic cell differentiation *in vitro* and have severe defects in their ability to provide costimulatory signals necessary for TCR-dependent T cell proliferation (Ruggiero et al., 2004). Differences in signalling in GPI-deficient T cells have also been described. GPI-deficient murine T cells isolated from T lymphocyte-specific GPI-anchor knockout mice had an enhanced proliferative response to the mitogenic lectin concanavalin A and to allogeneic (but not antigenic) stimulation (Hazenbos et al., 2004b). Reduced TCR-dependent proliferation and interferon-γ production have also been reported in GPI-deficient T lymphocytes isolated from PNH patients (Terrazzano et al., 2005). A possible molecular basis for some of these observations is suggested by an earlier study of proximal TCR signalling in several GPI-

deficient T lymphoma cell lines, which showed that TCR stimulation in GPI-deficient cells decreased tyrosine phosphorylation of the TCR ζ chain and ZAP-70, and this correlated with a decrease in the kinase activity of Fyn and Lck coprecipitating with activated TCR complexes (Romagnoli and Bron, 1997; Romagnoli and Bron, 1999).

These functional studies did not directly examine the involvement of lipid rafts, though rafts have previously been implicated in both FcγR and TCR signalling (Janes et al., 2000; Kabouridis, 2006; Kwiatkowska and Sobota, 2001). Other evidence also suggests that GPI-anchored proteins can modulate raft-dependent signals through both direct and indirect mechanisms. As discussed in Chapter 1, certain GPI-anchored proteins are capable of directly initiating signalling in response to crosslinking by antibodies or natural ligands. Other GPI-anchored proteins appear to function in signalling by acting as coreceptors. For example, there is evidence that TNF-α binds to the GPI anchor glycan moiety in U937 cells to form a high affinity complex with the TNF-α receptor that enhances TNF-α-induced apoptosis (Fukushima et al., 2004). Similarly, IL-18 complexed with the IL-18 receptor α subunit binds to both the GPI anchor glycan and the peptide portion of CD48(Fukushima et al., 2005). This interaction is functionally important in the formation of active IL-18 receptor complexes as PI-PLC treatment inhibited IL-18-dependent tyrosine phosphorylation and IFN-γ production (Fukushima et al., 2005). The GPI-anchored protein CD14 functions as a lipopolysaccharide coreceptor by forming raft-localized receptor complexes with toll-like receptors and other membrane proteins that are critical for activation of monocytes and macrophages (Schmitz and Orso, 2002). Certain peptide hormones have been shown to

activate endogenous PI-PLC enzymes, leading to the cleavage of GPI anchors and the production of free inositolphosphoglycans, which are thought to act as second messengers in the propagation of intracellular signals (Lazar et al., 1994; Marquez et al., 1998; Rademacher et al., 1994). Other effects of GPI-anchored proteins on signalling might be more indirect. GPI-deficient T cells and erythrocytes have been shown to have elevated total and raft cholesterol levels (Abrami et al., 2001; Samuel et al., 2001), and cholesterol has been shown to bind noncovalently to certain receptors, affecting their signalling function (Fahrenholz et al., 1995; Gimpl et al., 2000; Gimpl et al., 2002; Jones and McNamee, 1988; Klein et al., 1995; Narayanaswami and McNamee, 1993). In addition, evidence that the expression of non-GPI membrane and raft proteins is altered by GPI deficiency (Chapter 3, (Abrami et al., 2001; Lillico et al., 2003)) suggests that levels of key raft signalling effectors might also be altered in rafts in GPI-deficient cells.

Based on the evidence outlined above, I hypothesized that the loss of GPI-anchored protein expression alters the composition and/or organization of lipid rafts, resulting in differences in raft-mediated signalling that contribute to the aberrant cellular responses observed in GPI-deficient cells. In order to test this hypothesis, I chose to characterize two raft-dependent signalling pathways in GPI-deficient and wildtype Ramos517 B cells: 1) signalling downstream of the BCR, and 2) signalling that occurs following hypercrosslinking of CD20.

Ligand-induced oligomerization of the BCR generates multiple intracellular signals that are propagated by protein phosphorylation, modification, and interaction, phosphoinositide turnover, and the release of intracellular calcium (Figure 4.1). The nature of the antigen, as well as the presence or absence of positive and negative

Figure 4.1. B cell receptor-induced signal transduction pathways.

The BCR is composed of an antigen-binding membrane immunoglobulin subunit and a signal transducing subunit, the Igα/Igβ heterodimer. Antigen-induced BCR oligomerization activates the Src family kinase Lyn, which phosphorylates ITAM motifs on Igα/Igβ, leading to the recruitment and activation of additional tyrosine kinases such as Syk, Btk, and PI3K. Adaptor molecules such as BLNK and BAM32 facilitate interaction of the kinases with other downstream effectors. Activation of PLCγ2 leads to the release of intracellular calcium and activation of PKC—both of which are important for activation of MAPKs such as Erk, Jnk and p38. The dynamic reorganization of the cytoskeleton that occurs upon BCR stimulation is mediated in part by activation of Rac, Rho, and cdc42. Though not shown, additional positive and negative regulatory coreceptors such as CD19 and CD22 can influence BCR signalling at multiple levels in the signalling pathways initiated after receptor ligation. Ultimately, all of the signals activated downstream of the BCR coordinately regulate the activation of transcription factors such as NFκB, NFAT, and c-myc. The resulting gene expression profiles direct B cell fate towards activation, proliferation, anergy, or apoptosis depending on the nature of the antigenic stimulus and its associated downstream signals. This figure is modified from (Niiro and Clark, 2002).

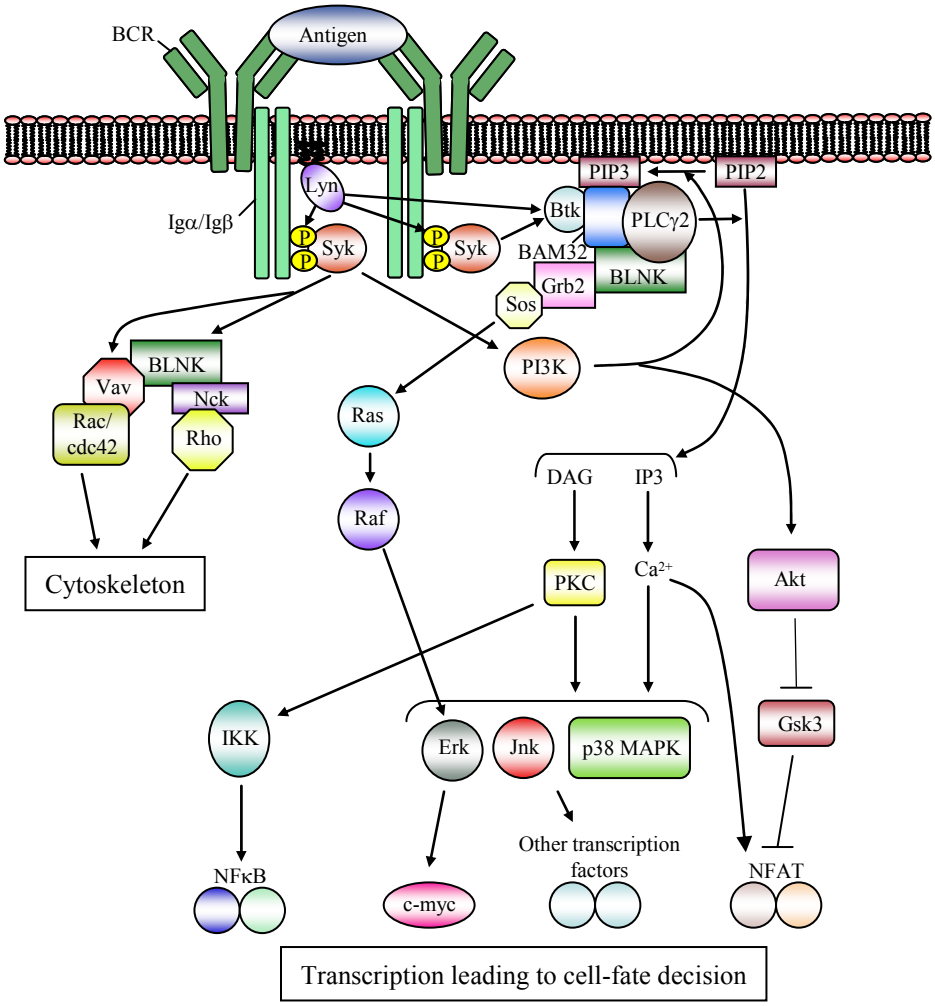
BCR
Antigen
Igα/Igβ
Lyn
Syk
Syk
PIP3
PIP2
Btk
PLCγ2
BAM32
BLNK
Grb2
Sos
PI3K
BLNK
Vav
Nck
Rac/
cdc42
Rho
Ras
Raf
DAG
IP3
PKC
Ca2+
Akt
Gsk3
Cytoskeleton
IKK
Erk
Jnk
p38 MAPK
Other transcription
factors
NFκB
c-myc
NFAT
Transcription leading to cell-fate decision

costimulation, affects the quality and strength of the BCR signal and ultimately determines the functional outcome of the BCR signal—which may be proliferation, differentiation, anergy, or apoptosis, depending on the specific biological context and the type of B cell that is stimulated. As discussed in Chapter 1, the ability (or inability) of the BCR to translocate to lipid rafts correlates with specific downstream biological responses and is regulated in physiological (*e.g.* in immature versus mature B cells) and in pathological (*e.g.* by the viral protein LMP2A) contexts. A number of signalling effectors that are important in BCR signalling are found either constitutively or inducibly in raft fractions, including Lyn, PI3K, SHIP, and the adaptor protein LAB (Awasthi-Kalia et al., 2001; Janssen et al., 2003; Petrie et al., 2000). Cholesterol depletion is capable of altering BCR-induced calcium mobilization and tyrosine phosphorylation, implying a role for lipid rafts in regulating these BCR-mediated signalling events (Aman and Ravichandran, 2000; Awasthi-Kalia et al., 2001). In Ramos cells, crosslinking of the B cell receptor causes its translocation to lipid rafts, where multiple intracellular signalling cascades are initiated, as shown in Figure 4.1, that lead to growth arrest and the induction of apoptosis. Though relatively little is known about the mechanisms that link receptor proximal signalling to apoptosis execution, apoptosis in Ramos cells appears to involve the mitochondrial death pathway and activation of caspases 3, 9 and 7, as well as the targeted upregulation and downregulation of the expression of numerous proteins involved in the regulation of the cell cycle and apoptosis, including c-myc, Bcl-2, Bim, Bik, Daxx, DAD-1, and p21(An et al., 2003a; An et al., 2003b; Awasthi-Kalia et al., 2001; Eldering and VanLier, 2005; Jiang et al., 2003; Luciano et al., 2003; Ollila and Vihinen, 2003; Petrie et al., 2000).

The second raft dependent signalling pathway examined involves CD20, a tetraspan membrane protein that is abundantly expressed on most B cells (Cragg et al., 2005; Deans et al., 2002). CD20 is thought to form part of a store-operated calcium channel in lipid rafts that regulates the calcium flux induced by BCR stimulation (Li et al., 2003a). Because it is not internalized upon antibody binding, and because it is abundantly expressed on both normal and transformed B cells, immunotherapy using the humanized anti-CD20 antibody rituximab has been successful in the treatment of B cell lymphoma and autoimmune disorders (Cragg et al., 2005; Smith, 2003). Depletion of B cells after rituximab binding is thought to occur through multiple mechanisms *in vivo*, including antibody-dependent cytotoxicity, complement-mediated lysis, and direct signalling of apoptosis (Deans et al., 2002; Smith, 2003). An interesting property of most anti-CD20 antibodies, including rituximab, is their ability to promote the association of CD20 with Triton X-100 insoluble raft fractions upon antibody binding (Deans et al., 2002; Deans et al., 1998; Janas et al., 2005; Unruh et al., 2005). Depending on the specific experimental system, crosslinking of CD20 by rituximab alone, or hypercrosslinking of CD20 by rituximab and anti-hIgG or FcR-bearing cells causes growth inhibition and apoptosis in B cells (Bezombes et al., 2004; Flieger et al., 2000; Hofmeister et al., 2000; Janas et al., 2005; Jazirehi and Bonavida, 2005; Liu et al., 2004; Shan et al., 2000; Unruh et al., 2005). In Ramos cells, hypercrosslinking of CD20 initiates a Src family kinase-dependent pathway that results in PLCγ activation and calcium release, culminating in apoptosis (Figure 4.2) (Hofmeister et al., 2000; Janas et al., 2005; Shan et al., 2000; Unruh et al., 2005). This pathway is thought to be raft-

Figure 4.2. Hypercrosslinking of CD20 initiates intracellular signalling leading to apoptosis.

This figure depicts the proposed mechanism of anti-CD20-mediated apoptosis (Deans et al., 2002; Unruh et al., 2005). In unstimulated B cells, CD20 constitutively associates with lipid rafts containing Src family kinases and the transmembrane adaptor Csk-binding protein (Cbp) with low affinity. Cbp recruits Csk (not shown) to lipid rafts where it phosphorylates Src family kinases and maintains them in an inactive state. Hypercrosslinking of anti-CD20 antibodies stabilizes CD20's association with rafts and leads to aggregation of the rafts, trans-activating Src family kinases. Src family kinase-dependent activation of PLC-γ leads to calcium mobilization and ultimately apoptosis. This pathway is thought to be independent of CD20's proposed function as a store-operated calcium channel. The figure shown is modified from (Deans et al., 2002).

Unstimulated Cells

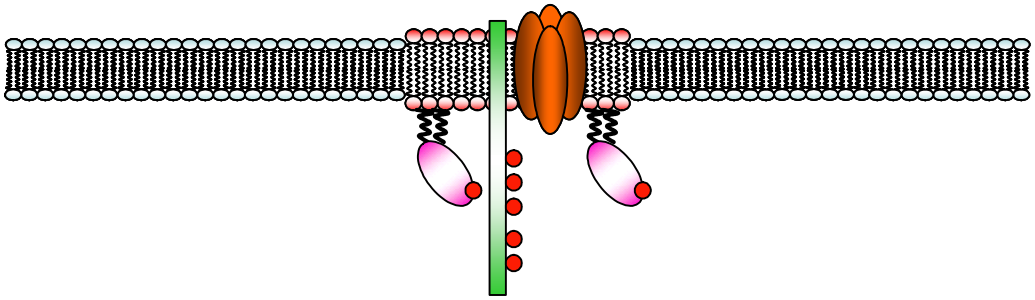

Antibody crosslinking of CD20

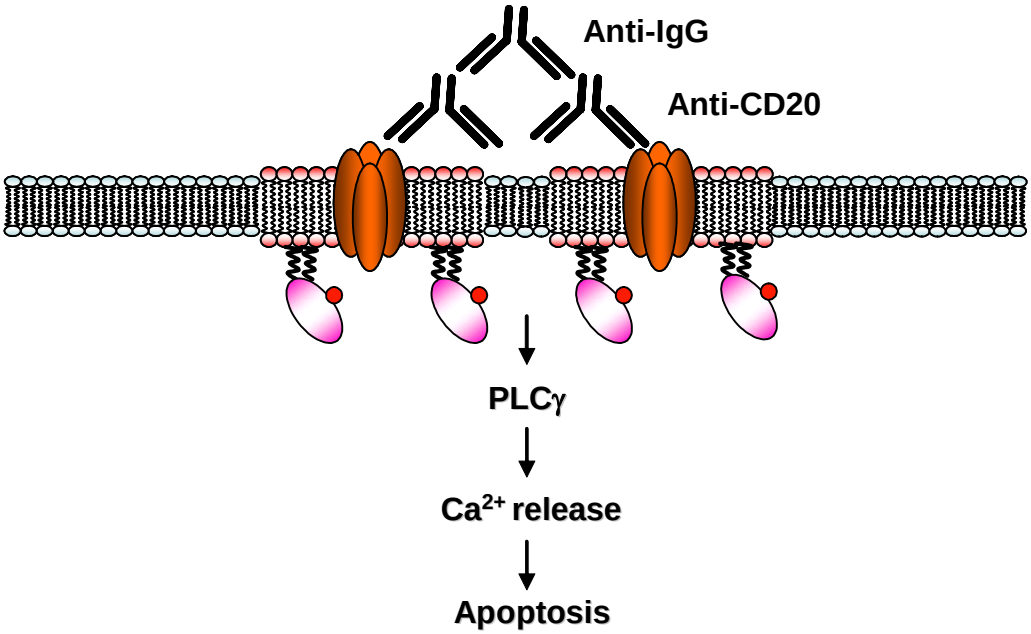

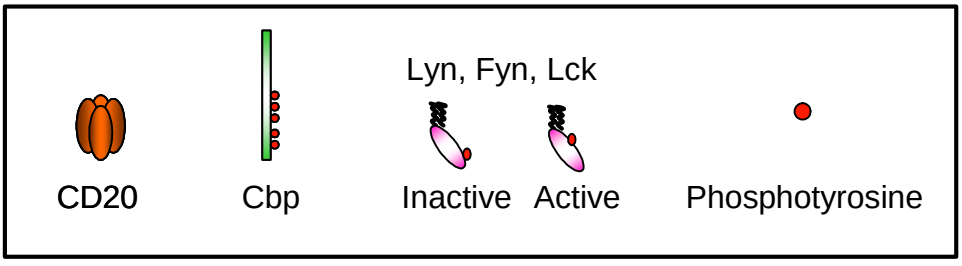

dependent, since cholesterol depletion inhibits antibody-induced CD20 raft association, calcium mobilization and apoptosis (Janas et al., 2005; Unruh et al., 2005).

The experiments described in this chapter test the hypothesis that alterations in lipid raft structure or organization, caused directly or indirectly by GPI deficiency, alter the function of lipid rafts in signalling induced by hypercrosslinking of CD20 or by stimulation of the BCR. If this hypothesis is true, there should be a difference in the amount of apoptosis observed in GPI-deficient and wildtype Ramos517 B cells following initiation of each of these signals. After initial experiments demonstrated that the extent of BCR- and CD20-mediated apoptosis was decreased in GPI-deficient B cells compared to GPI-expressing cells, subsequent experiments were designed to identify and characterize the specific alterations in raft-dependent signalling caused by GPI deficiency.

4.2 Results

4.2.1 Effect of GPI deficiency on B cell apoptosis induced by crosslinking of the B cell receptor.

4.2.1.1 GPI-deficient B cells are resistant to anti-IgM-induced growth inhibition and apoptosis

In Ramos cells, engagement of the BCR causes it to translocate to lipid rafts, where it initiates signalling that ultimately leads to growth inhibition and apoptosis in the absence of other costimulation (Awasthi-Kalia et al., 2001; Jiang et al., 2003; Luciano et al., 2003; Petrie et al., 2000). If GPI-deficiency affects the raft-mediated signal downstream of the BCR, there should be a difference in the amount of apoptosis observed following crosslinking of the BCR in GPI-deficient cells. To determine whether this was indeed the case, GPI-deficient and wildtype Ramos517 cells were

treated with various doses of crosslinking anti-IgM antibody, and the percentage of apoptotic and nonviable cells was determined after 24 hours by staining cells with annexin V-FITC and propidium iodide (PI) (Figure 4.3). Cells in the early stages of apoptosis externalize phosphatidylserine (which is bound by annexin V), but maintain their membrane integrity and therefore exclude PI, which fluoresces only when bound to nucleic acids inside cells. Cells that bind annexin V and stain positively with PI have lost their membrane integrity, and are either cells in the later stages of apoptosis or cells dying by necrosis. As shown in Figure 4.3a, there was a dose-dependent increase in the amount of cells in the early stages of apoptosis (annexin V-positive/PI-negative cells) in GPI-positive and GPI-negative Ramos517 cells treated with anti-hIgM, when compared to untreated control cells. In particular, there was a significant difference in the amount of apoptosis detected in GPI-negative cells compared to GPI-positive cells at doses of anti-hIgM between 5 μg and 60 μg. Similar trends were apparent when the percentage of nonviable cells (all cells staining positively with annexin V, including both PI-negative and PI-positive cells) in GPI-positive and GPI-negative cells were compared (Figure 4.3b), which is consistent with an increase in apoptotic cell death following BCR stimulation in both GPI-negative and GPI-positive Ramos517 cells. However, the GPI-deficient Ramos517 cells appeared to have a decreased amount of cell death compared to the wildtype cells.

Since apoptosis is a rapid and dynamic process, and the kinetics of the apoptotic response have been observed to vary in different B cell lines in response to factors that affect BCR signalling (Trujillo and Eberhardt, 2003), it was possible that the apoptotic program in the GPI-deficient cell lines was delayed, and that levels of apoptosis in GPI-

Figure 4.3. GPI-deficient B cells are resistant to apoptosis induced by various doses of anti-human IgM.

2×10^6 Ramos517/vector (GPI-) or Ramos517/pigM (GPI+) cells were cultured for 24 hours in the presence of the indicated amounts of $F(ab')_2$ anti-human IgM, and then stained with annexin V-FITC/PI to detect (A) early apoptotic cells, and (B) nonviable cells lacking membrane integrity (including early and late apoptotic and necrotic cells). Results are expressed as the means of three independent experiments and the error bars represent the standard error of the mean. Asterisks indicate statistically significant differences in results from GPI-positive and GPI-negative cells at the indicated dose of crosslinking antibody. *P<0.05, **P<0.01, ***P<0.001.

A. Early apoptotic

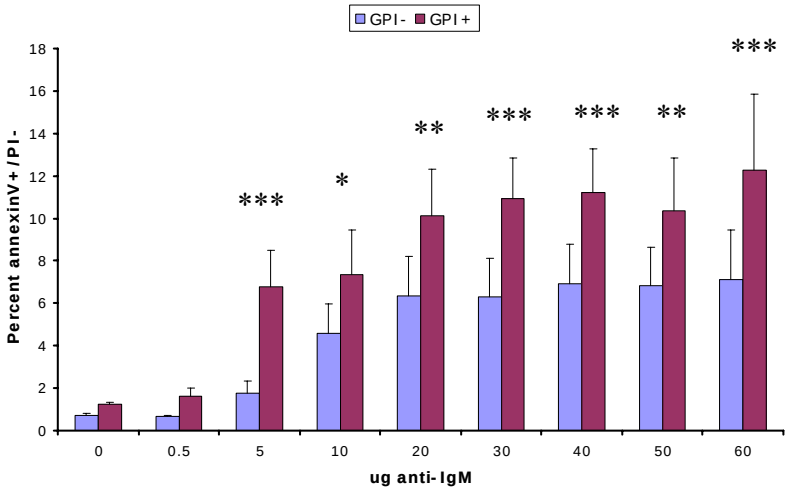

B. Apoptotic/Necrotic

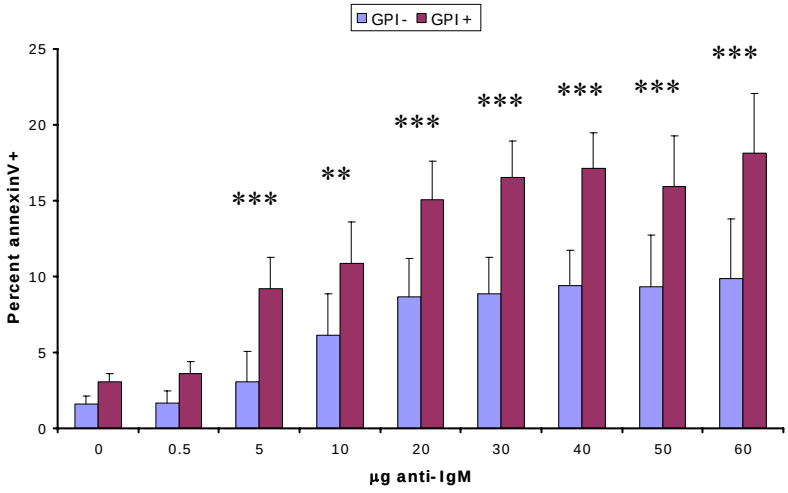

deficient cells would increase at later timepoints. To test this possibility, the extent of apoptosis was examined at various timepoints ranging from 6 hours to 48 hours following crosslinking with anti-hIgM, to see if the kinetics of apoptosis induction were altered in GPI-deficient cells. The results shown in Figure 4.4 demonstrate that the kinetics of the apoptotic response is similar in GPI-positive and GPI-negative Ramos517 cells. An increase in the percentage of early apoptotic cells is observed as early as 6 hours after BCR crosslinking in GPI-positive cells when compared to untreated control cells, although the increase is less pronounced when comparing control and stimulated GPI-negative cells (Figure 4.4a). The percentage of apoptotic cells at 36 and 48 hours is similar to that observed at 24 hours in treated and control GPI-positive cells. Similarly, though the magnitude of anti-hIgM-induced apoptosis is decreased in GPI-negative cells, the amount of apoptosis detected at the 36 and 48 hour timepoints is similar to that seen at 24 hours. The fact that the percentage of apoptotic and nonviable cells fails to increase at these later timepoints in GPI-deficient cells suggests that the apoptotic program is not merely delayed in these cells, but rather that there is a consistent decrease in the amount of apoptosis observed in GPI-deficient compared to wildtype cells.

To further characterize and confirm the biological significance of these findings, the growth of untreated and anti-IgM-treated Ramos517 cells was monitored over a total of four days. As seen in Figure 4.5**,** both the GPI-negative and GPI-positive B cells showed essentially identical growth properties in the absence of BCR crosslinking. Over the entire timecourse examined, the growth of GPI-positive Ramos517 cells was dramatically inhibited by treatment with anti-hIgM. However, the GPI-deficient Ramos517 cells were relatively resistant to the growth inhibitory effects of BCR

Figure 4.4. GPI-deficient B cells are resistant to apoptosis 6 to 48 hours after crosslinking of the B cell receptor.

2×10^6 Ramos517/vector (GPI-) or Ramos517/pigM (GPI+) cells were cultured in the presence (IgM) or absence (untreated (UT)) of 50 μg of $F(ab')_2$ anti-human IgM for 6, 12, 24, 36, or 48 hours, and then stained with annexin V-FITC/PI and analyzed by flow cytometry to detect (A) early apoptotic cells, and (B) nonviable cells lacking membrane integrity (including early and late apoptotic and necrotic cells). Results are expressed as the means of three independent experiments, with the error bars representing the standard error of the mean.

A. Early apoptotic

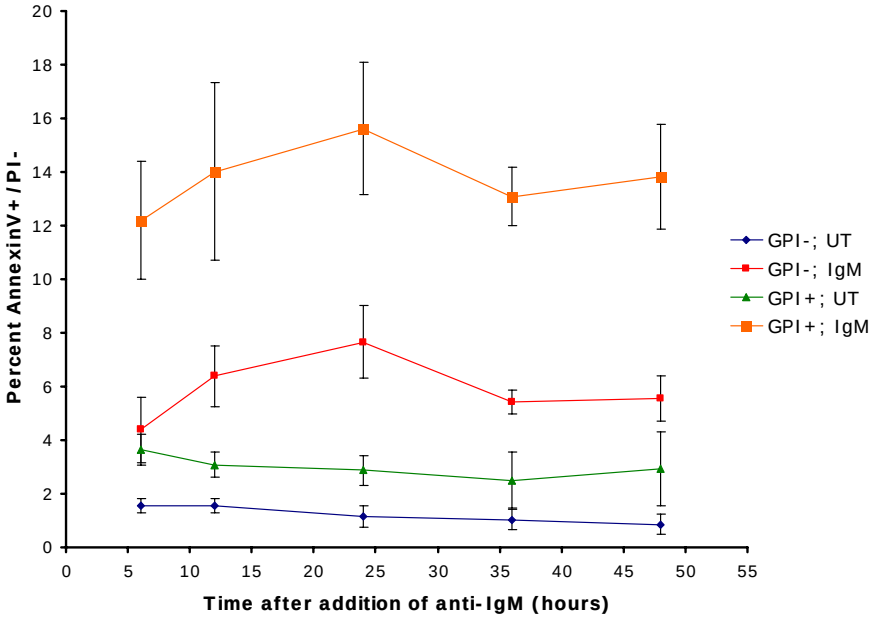

B. Apoptotic/Necrotic

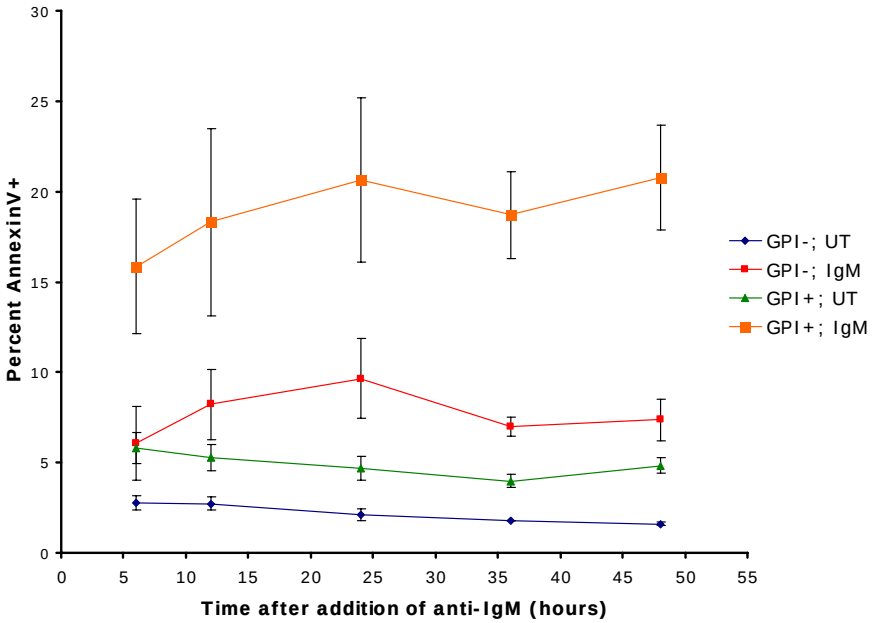

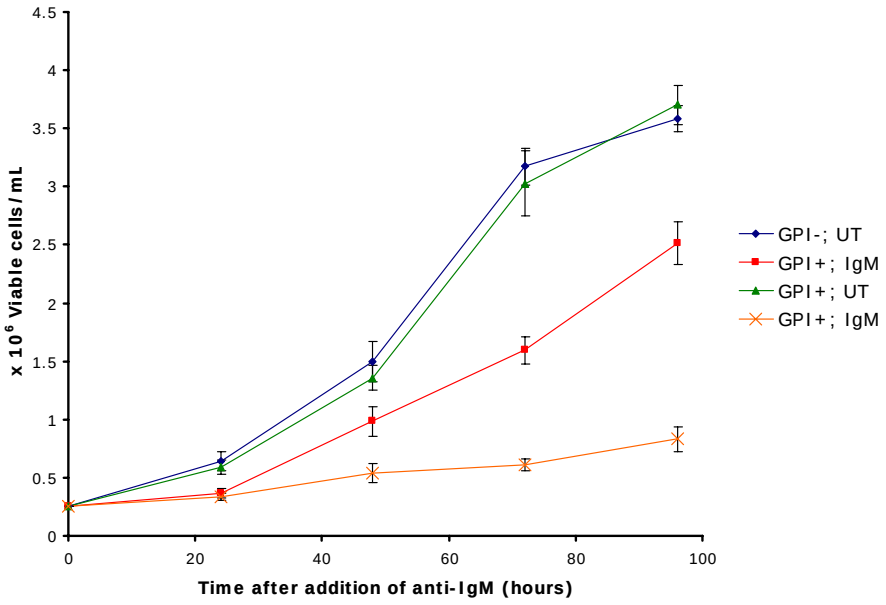

Figure 4.5. GPI-deficient B cells are resistant to growth inhibition induced by crosslinking of the B cell receptor.

5 x 10^5 Ramos517/vector (GPI-) or Ramos517/pigM (GPI+) cells were cultured in the presence (IgM) or absence (untreated (UT)) of 50 µg of F(ab')$_2$ anti-human IgM for a total of 96 hours. At 24 hour intervals, the number of viable cells/mL was determined by hemacytometer counting using trypan blue exclusion. Results are expressed as the means of three independent experiments, with the error bars representing the standard error of the mean.

crosslinking, and continued to grow, albeit at a reduced rate. Interestingly, the difference in the degree of growth inhibition in GPI-negative versus GPI-positive cells only became apparent after 48 hours, as at the 24 hour timepoint, both the GPI-negative and the GPI-positive cells showed a similar degree of growth inhibition. Taken together, the above results indicate that GPI-deficiency causes Ramos517 cells to become resistant to growth inhibition and apoptosis induced by raft-dependent BCR signals.

4.2.1.2 Cell surface expression of the B cell receptor is similar in wildtype and GPI-deficient B cells

The regulation of B cell fate in response to antigen receptor signals is extremely complex and BCR signalling is fine-tuned by the differential expression and activation of key signalling molecules (Niiro and Clark, 2002). Some studies have indicated that changes in surface BCR levels can significantly affect B cell responses downstream of BCR engagement (George et al., 1993; Trujillo and Eberhardt, 2003). Since expression levels of non-GPI cell surface membrane proteins are affected in GPI-deficient cells (Abrami et al., 2001; Lillico et al., 2003), it was possible that the decrease in apoptosis and growth inhibition observed in the GPI-deficient Ramos517 cells was caused by downregulation of surface IgM receptors. To test this possibility, the levels of cell surface IgM in GPI-deficient and wildtype cells were analyzed by flow cytometry of unpermeabilized cells stained with a FITC-conjugated anti-hIgM antibody. As seen in Figure 4.6, the levels of surface IgM on GPI-deficient and wildtype cells were similar. Thus, GPI status has no detectable effect on the levels of BCR on the surface of Ramos517 cells, and the decrease in BCR-mediated apoptosis and growth inhibition

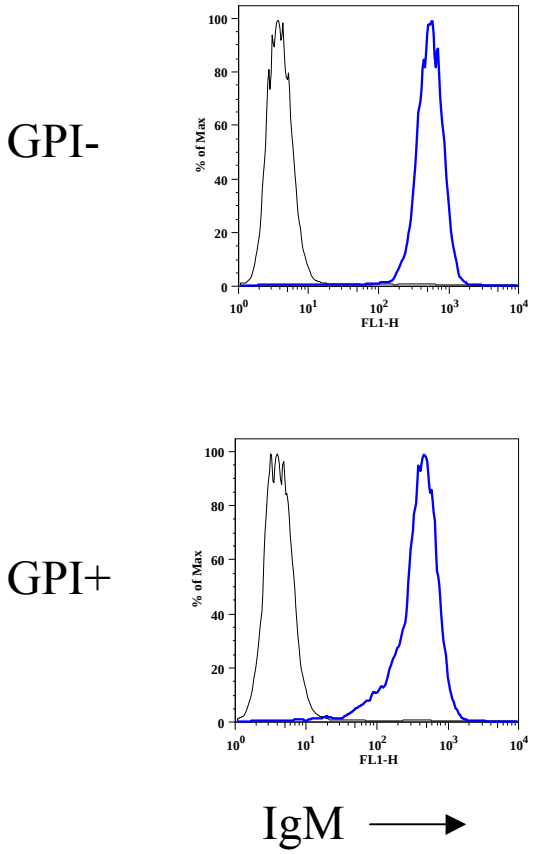

Figure 4.6. Cell surface expression of the B cell receptor is similar in GPI-deficient and wildtype cells.

1 x 10^6 Ramos517/vector (GPI-) or Ramos517/pigM (GPI+) cells were stained with FITC-conjugated F(ab')$_2$ anti-human IgM and analyzed by flow cytometry. Blue lines indicate IgM staining, while black lines indicate autofluorescence of unstained cells. Results are representative of 3 independent experiments.

observed in GPI-deficient cells is not the result of a GPI-dependent downregulation of cell surface B cell receptors.

4.2.1.3 B cell receptor translocation to lipid rafts occurs normally in GPI-deficient B cells

In Ramos517 cells, crosslinking of the BCR results in its translocation to lipid rafts (Petrie et al., 2000). Although the levels of B cell receptor on the cell surface are not altered in GPI-deficient cells, it was possible that the ability of the receptors to access lipid rafts was compromised, and that this was responsible for the decrease in apoptosis observed in GPI-deficient B cells. Therefore, the ability of the BCR to translocate to lipid rafts following anti-IgM crosslinking was examined. As seen in Figure 4.7a, BCR stimulation induces the accumulation of bands at approximately 80 and 25 kDa, consistent with the heavy and light chains of IgM, in silver-stained raft fractions isolated from both GPI-deficient and wildtype Ramos517 cells. Western blotting analysis confirmed that the μ heavy chain was inducibly associated with raft fractions in GPI+ and GPI- Ramos517 cells after BCR crosslinking, and this was accompanied by its concurrent loss from the detergent-soluble fraction (Figure 4.7b). The kinetics of IgM translocation to raft fractions did not appear to be affected by GPI deficiency, as the heavy and light chains were observed in raft fractions as early as 1 minute and as late as 60 minutes after stimulation of both GPI-deficient and GPI-expressing Ramos517 cells. The amount of heavy and light chain observed in raft fractions upon BCR stimulation was similar in both GPI-deficient and wildtype cells at most timepoints examined. In the experiment shown in Figure 4.7, there appears to be a slight decrease in the amount of heavy and light chain present in raft fractions after 60 minutes, however due to variability in silver staining and

Figure 4.7. B cell receptor translocation to lipid rafts after antibody crosslinking is not affected by the absence of GPI-anchored proteins.

GPI-positive and GPI-negative Ramos517 cells were incubated with $F(ab')_2$ anti-human IgM for the indicated amount of time at 37°C, prior to lysis in 1% Triton X-100 and sucrose density gradient centrifugation. Equal amounts of protein from the raft and soluble fractions were separated by SDS-PAGE and the gels were analyzed by silver staining (A) or by Western blotting for the μ heavy chain (B). The results shown are representative of 4 independent experiments.

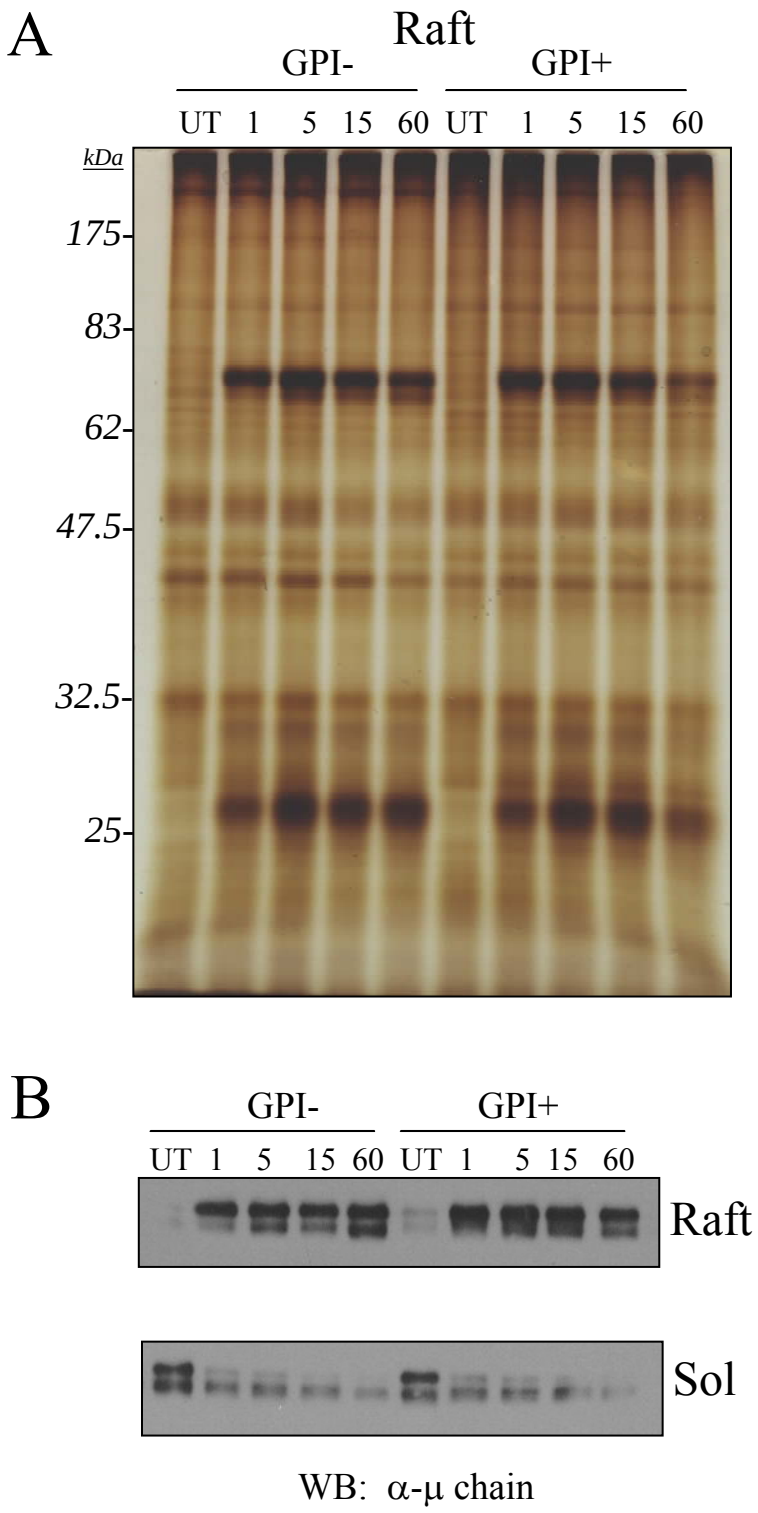
A
Raft
GPI-
GPI+
UT 1 5 15 60 UT 1 5 15 60
kDa
175
83
62
47.5
32.5
25
B
GPI-
GPI+
UT 1 5 15 60 UT 1 5 15 60
Raft
Sol
WB: α-μ chain

Western blotting in separate experiments, it is unclear whether this difference is biologically significant, and additional experiments would need to be performed to address this. Taken together, these observations suggest that the ability of the B cell receptor to translocate to lipid rafts is not significantly affected by GPI deficiency.

4.2.1.4 B cell receptor-induced phosphotyrosine signalling in rafts is decreased in GPI-deficient B cells

Some of the earliest signalling events upon engagement of the B cell receptor result in the activation of protein tyrosine kinases and phosphorylation of immunoreceptor tyrosine-based activation motifs (ITAMs) in the cytoplasmic tails of the Igα and Igβ subunits, which in turn recruit and activate other protein tyrosine kinases and their substrates (Niiro and Clark, 2002). Some of these phosphotyrosine-based signalling events appear to take place within lipid rafts, as a number of tyrosine-phosphorylated proteins are observed in raft fractions isolated from Ramos and tonsillar B cells following engagement of the B cell receptor (Petrie et al., 2000). It is possible that alterations in the constitutive or induced raft association of downstream signalling effectors and/or effects of GPI deficiency on the activity of a raft-localized signalling molecule in GPI-deficient cells might be responsible for altering BCR signalling, leading to the observed decrease in apoptosis and growth inhibition exhibited by these cells. Such changes might affect the magnitude or nature of the phosphotyrosine signalling cascade observed downstream of the BCR. Therefore, the phosphotyrosine signalling induced by BCR crosslinking in isolated raft and soluble fractions was compared at various timepoints following anti-IgM treatment of GPI-positive and GPI-negative Ramos517 cells. As can be seen in Figure 4.8, the basal level of tyrosine phosphorylation is higher in raft fractions isolated from

Figure 4.8. The level of tyrosine phosphorylation on raft proteins induced following BCR crosslinking is reduced in GPI-deficient B cells.

1×10^8 Ramos517/vector or Ramos517/pigM cells were treated with 100 μg of $F(ab')_2$ anti-human IgM to crosslink the BCR for 1, 5 15, or 60 minutes at 37°C, or left untreated (no exposure to antibody) and lysed in 1% Triton X-100/MBS lysis buffer. The detergent lysates were subjected to sucrose density gradient centrifugation to isolate raft and soluble fractions, which were separated by SDS-PAGE, transferred to nitrocellulose and examined by Western blotting using anti-phosphotyrosine, anti-Gαi3, or anti-actin antibodies. Results are representative of 4 independent experiments.

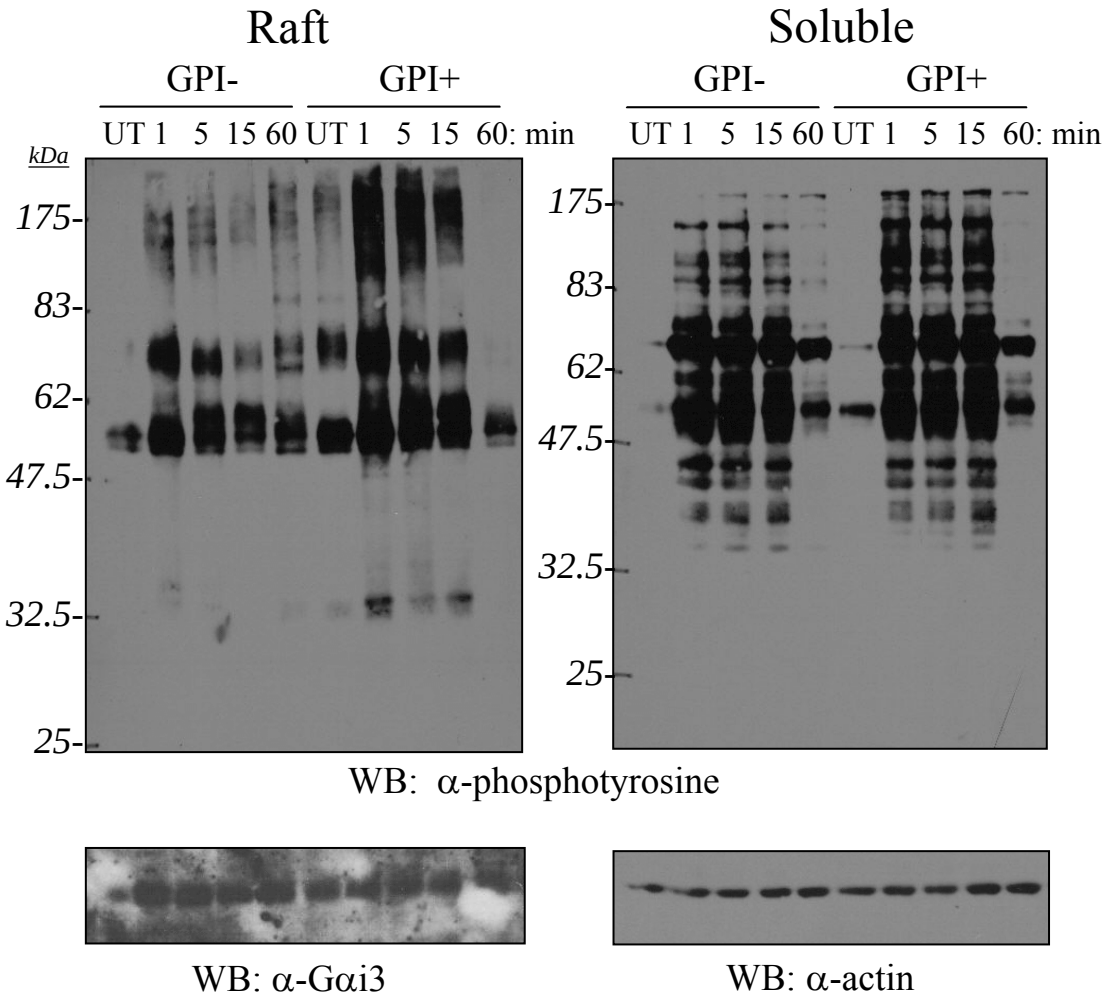
Raft
Soluble
GPI-
GPI+
GPI-
GPI+
UT 1 5 15 60 UT 1 5 15 60: min
UT 1 5 15 60 UT 1 5 15 60: min
kDa
175
83
62
47.5
32.5
25
175
83
62
47.5
32.5
25
WB: α-phosphotyrosine
WB: α-Gαi3
WB: α-actin

GPI-positive cells, with a number of additional tyrosine-phosphorylated bands visible that are not detected in GPI-deficient cells. Up to 15 minutes after crosslinking with anti-hIgM, though a similar pattern of tyrosine-phosphorylated bands is induced in raft fractions isolated from both GPI-positive and GPI-negative cells, the general level of tyrosine phosphorylation was consistently observed to be significantly reduced in raft fractions in GPI-deficient cells. In the experiment shown, the amount of tyrosine phosphorylation in raft fractions remained steady 60 minutes after crosslinking of the BCR in GPI-deficient cells, but in contrast, is significantly reduced again at this timepoint in GPI-expressing cells. However, in the only other experiment in which a 60 minute timepoint was examined, the opposite effect was observed and phosphotyrosine levels in GPI-expressing cells were higher after 60 minutes (data not shown). Thus, definitive conclusions regarding the effect of GPI-deficiency on the regulation of phosphotyrosine signalling at later timepoints cannot be made at this time. Nevertheless, a general reduction in early phosphotyrosine signalling in raft fractions isolated from GPI-deficient cells suggests that alterations in early raft-specific phosphotyrosine signalling may be responsible for the decreased response to BCR crosslinking observed in the GPI-deficient cells. There is also a general decrease in the level of basal and BCR-induced tyrosine phosphorylation on proteins present in the soluble fractions of GPI-deficient cells when compared to GPI-expressing samples, but the effect is much less dramatic than that observed in the raft fraction, further supporting the idea that the changes in phosphotyrosine signalling cascades in GPI-deficient cells are largely due to specific alterations in raft structure or function.

4.2.1.5 Calcium signalling downstream of the BCR is not affected by GPI deficiency

Engagement of the BCR in Ramos cells is associated with an elevation in intracellular calcium levels that is thought to be important in B cell responses such as apoptosis (Awasthi-Kalia et al., 2001; Petrie et al., 2000). BCR calcium signalling appears to be regulated at least in part by lipid rafts, as perturbation of cellular cholesterol (and presumably lipid rafts) using MβCD or filipin has been found to respectively enhance or inhibit BCR-mediated calcium release (Aman and Ravichandran, 2000; Awasthi-Kalia et al., 2001). Therefore, I examined calcium signalling downstream of BCR crosslinking as another example of a raft-dependent signalling readout that might be affected by changes in the structure or function of GPI-deficient rafts. As shown in Figure 4.9, in both GPI-deficient and GPI-expressing Ramos517 cells, crosslinking of the BCR with anti-IgM induced a calcium flux whose magnitude was dose-dependent. However, at each of the three antibody doses examined, the kinetics and magnitude of the calcium response in GPI-positive and GPI-negative cells was similar, indicating that GPI status does not affect calcium signalling induced by BCR activation.

In conclusion, the above studies have shown that, as in Ramos cells, wildtype Ramos517 cells undergo growth inhibition and apoptosis in response to engagement of the B cell receptor. However, the loss of GPI-anchored protein expression in Ramos517 cells causes them to become partially resistant to BCR-mediated growth inhibition and apoptosis. The altered phenotypic response to BCR stimulation observed in GPI-deficient cells suggests that the nature of the signal downstream of the BCR has changed. I hypothesized that GPI deficiency would introduce changes in raft structure and/or function that would affect raft function in signalling. In support of this hypothesis, a

Figure 4.9. The increase observed in intracellular calcium following crosslinking of the B cell receptor is similar in GPI-deficient and wildtype cells.

Intracellular calcium levels in 2 x 10^6 Ramos517/vector (GPI-; blue line) or Ramos517/pigM (GPI+; red line) preincubated with the calcium indicator dyes fluo-3 AM and fura red AM were measured using a ratiometric flow cytometry assay. The arrows indicate the time point (60 seconds) at which the indicated doses of $F(ab')_2$ anti-human IgM were added to each sample. Results are representative of three independent experiments.

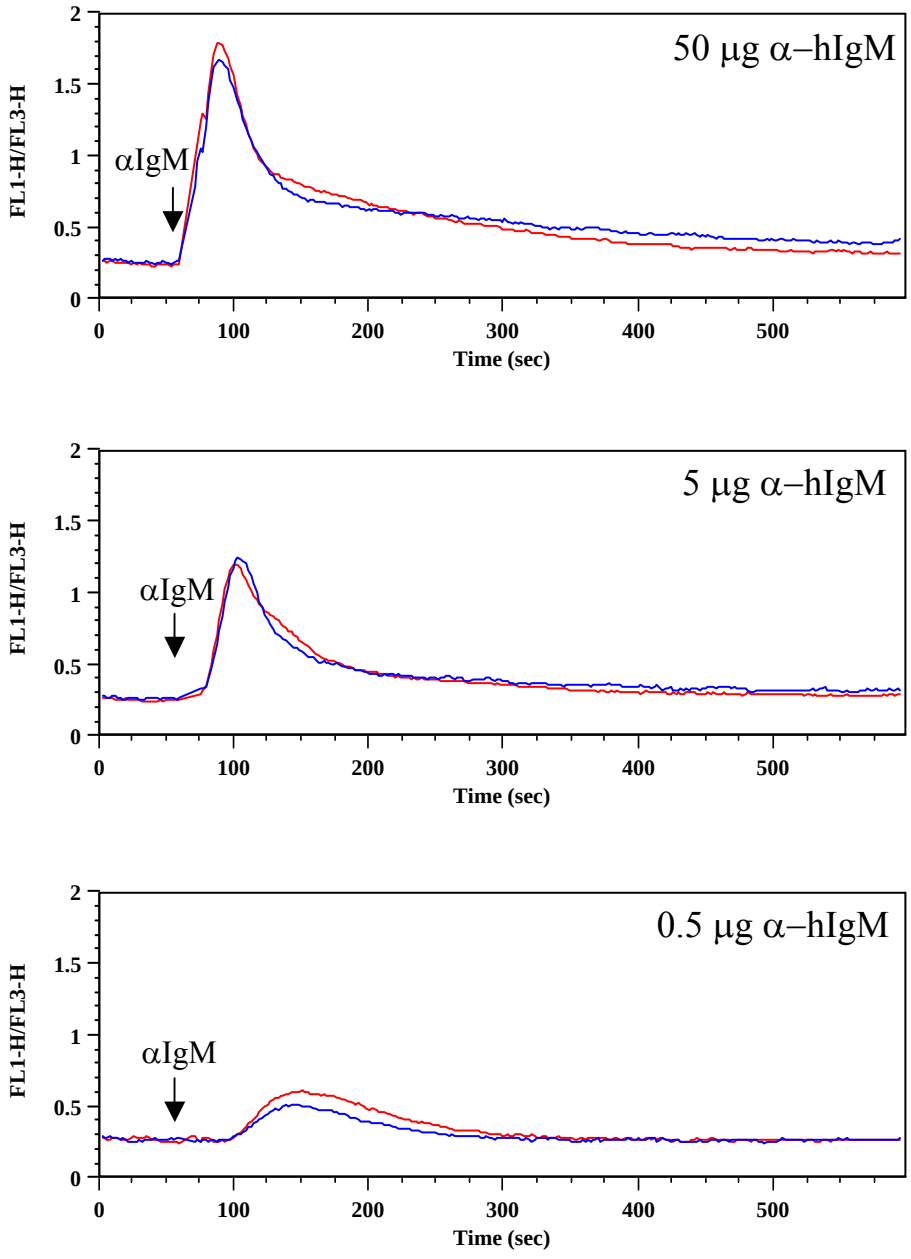
50 µg α–hIgM
αIgM
FL1-H/FL3-H
Time (sec)
5 µg α–hIgM
αIgM
FL1-H/FL3-H
Time (sec)
0.5 µg α–hIgM
αIgM
FL1-H/FL3-H
Time (sec)

significant reduction in phosphotyrosine signalling in raft fractions was observed in GPI-deficient cells. However, other parts of the BCR signal, such as the mobilization of intracellular calcium, are unchanged in GPI-deficient cells.

4.2.2 Effect of GPI deficiency on B cell apoptosis induced by hypercrosslinking of CD20

4.2.2.1 GPI-deficient B cells are resistant to apoptosis induced by hypercrosslinking of CD20

Hypercrosslinking of CD20 in Ramos and other B cell lines is known to activate Src family kinases upstream of a calcium-dependent signalling pathway that leads to apoptosis (Hofmeister et al., 2000; Shan et al., 2000), and there is evidence that this signalling pathway is raft-dependent in Ramos cells (Janas et al., 2005; Unruh et al., 2005). If changes in raft structure or function due to GPI deficiency alter this raft-dependent signal, one would expect to see a difference in the extent of apoptosis observed after CD20 hypercrosslinking. Therefore, cells were treated with no antibody, with hIg and anti-hIgG secondary antibody, or with rituximab and anti-hIgG, using the assay conditions optimized in Ramos cells by Unruh *et al.* (Unruh et al., 2005). As seen in Figure 4.10, treatment with rituximab and secondary antibody caused a small but consistent increase in the percentage of early apoptotic and nonviable (apoptotic and necrotic) cells in GPI-positive Ramos517 cells. This response was CD20 specific and was not caused by rituximab binding to Fc receptors, as the hIg control did not show any increase in apoptosis compared to untreated cells. In both untreated and hIg control cells, there was a significant increase in the percentage of early apoptotic and total annexin V-positive cells in GPI-positive cells when compared to the GPI-deficient cells. A similar, but not statistically significant trend was observed in untreated control cells in Figure 4.3,

Figure 4.10. GPI-deficient cells are resistant to apoptosis induced by hypercrosslinking of CD20 after 24 hours.

2×10^6 Ramos517/vector or Ramos517/pigM cells were cultured in the presence of no antibody (no Ab), 2 μg hIg and 20 μg $F(ab')_2$ anti-hIgG (hIg), or with 2 μg rituximab and 20 μg $F(ab')_2$ anti-hIgG (Rtx) for 24 hours, and then stained with annexin V-FITC/PI and analyzed by flow cytometry to detect (A) early apoptotic cells, and (B) nonviable cells lacking membrane integrity (including both early and late apoptotic and necrotic cells). Results are expressed as the means of three independent experiments with the error bars representing the standard error of the mean. Asterisks indicate a statistically significant difference when comparing results for GPI-positive cells to GPI-negative cells for a given treatment. $^{*}P<0.05$, $^{***}P<0.001$.

A. Early apoptotic

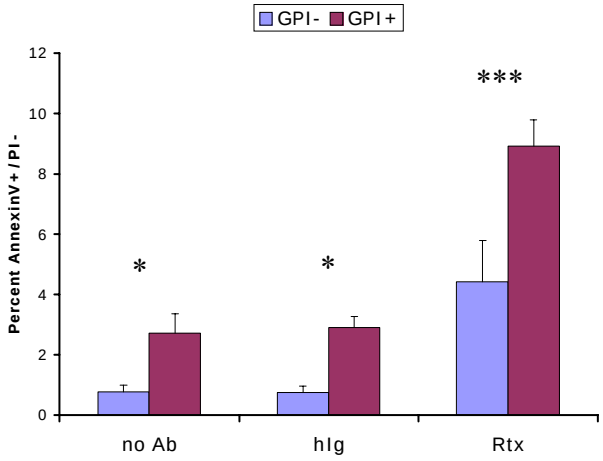

B. Apoptotic/Necrotic

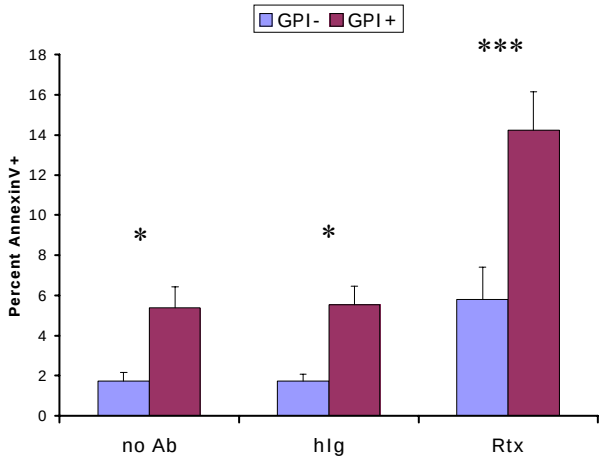

however, this difference is unlikely to be biologically significant, since untreated GPI-deficient and wildtype Ramos517 cells grow at similar rates (Figure 4.5), and cell cycle analysis of untreated GPI-positive and GPI-negative Ramos517 cell populations showed no significant differences in the amount of sub-G1 material (apoptotic cells), or in the distribution of cells in the G1, S, or G2 phases of the cell cycle (data not shown). Therefore, it seems unlikely that there is a significant difference in basal amounts of apoptosis. More notably, in cells in which CD20 was hypercrosslinked with rituximab, there was a significant reduction in the percentage of early apoptotic and total apoptotic and necrotic cells in GPI-deficient cells compared to GPI-positive cells.

To further characterize the effect of GPI deficiency on apoptosis induced by CD20 hypercrosslinking, the kinetics of the apoptotic response were examined over timepoints between 6 hours and 48 hours after antibody stimulation. As seen in Figure 4.11, as early as 6 hours after CD20 hypercrosslinking, the amount of apoptotic and nonviable cells seen in GPI-positive Ramos517 cells compared to Ig-treated controls is significantly increased and already reaching maximal levels. Over the entire timecourse examined, this level of apoptosis is maintained at similar levels, in the case of total apoptotic/necrotic cells (Figure 4.11b), or shows a slight decrease over time, in the case of early apoptotic cells (Figure 4.11a). The kinetics of the response to CD20 hypercrosslinking are similar but not identical in GPI-deficient cells, which appear to exhibit a slightly slower induction of apoptosis, requiring 12 hours to reach maximal levels of apoptosis and cell death, after which the levels of cell death steadily decrease (Figure 4.11).

Figure 4.11. GPI-deficient B cells are resistant to apoptosis induced 6 to 48 hours after hypercrosslinking of CD20.

2×10^6 Ramos517/vector (GPI-) or Ramos517/pigM (GPI+) cells were cultured in the presence of 2 μg of hIg and 20 μg of $F(ab')_2$ anti-hIgG (Ig), or 2 μg of rituximab and 20 μg of $F(ab')_2$ anti-hIgG (Rtx), for the indicated amount of time prior to staining with annexin V-FITC/PI and analysis by flow cytometry to detect (A) early apoptotic cells, and (B) nonviable cells lacking membrane integrity (including early and late apoptotic and necrotic cells). Results are expressed as the means of three independent experiments, with the error bars representing the standard error of the mean.

A. Early apoptotic

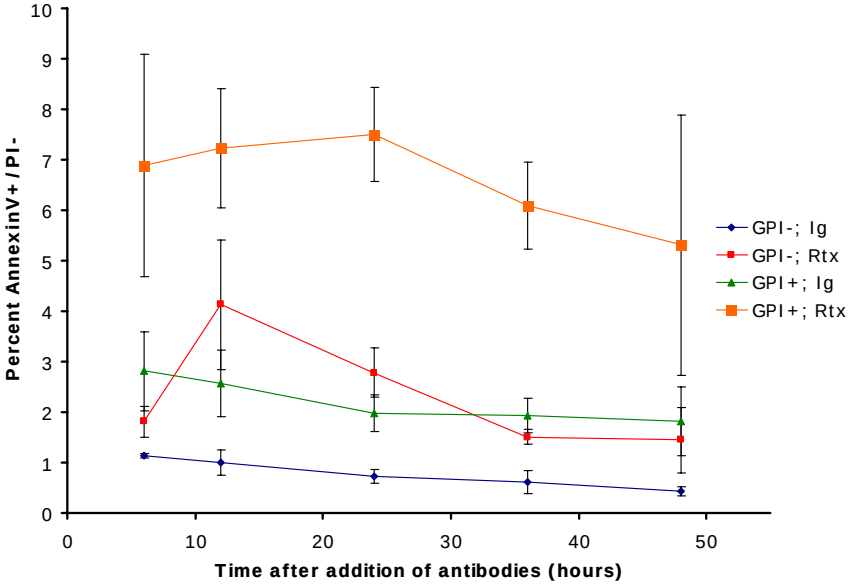

B. Apoptotic/Necrotic

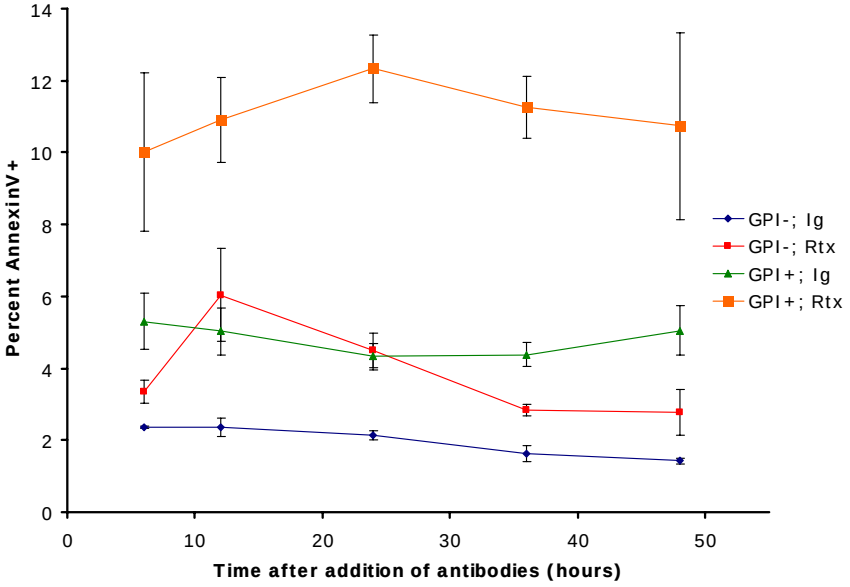

The increases in annexin V staining observed in these experiments were relatively small, and though the differences observed between the GPI-deficient and wildtype Ramos517 cells were both consistently observed and statistically significant, I wanted to further examine the biological significance of these results. Therefore, I examined the growth of GPI-positive and GPI-negative Ramos517 cells over a period of four days after hypercrosslinking of CD20 with rituximab. As shown in Figure 4.12, GPI-positive cells exhibit reduced growth after hypercrosslinking of CD20, whereas GPI-deficient cells are resistant to CD20-induced growth inhibition, growing at a rate that is similar to untreated and Ig treated control cells. Taken together with the previous data, this evidence demonstrates that GPI-deficient Ramos517 cells are resistant to growth inhibition and apoptosis following hypercrosslinking of CD20 with rituximab.

4.2.2.2 Cell surface expression of CD20 is similar in wildtype and GPI-deficient B cells

In Molt-4 T cells transfected with CD20, lower levels of cell surface expression of CD20 were correlated with lower levels of apoptosis following CD20 hypercrosslinking (Unruh et al., 2005). Because GPI-deficiency has been shown to affect the expression levels of cell surface membrane proteins and raft markers in other cell types (Abrami et al., 2001; Lillico et al., 2003), we compared the levels of CD20 expressed on the cell surface of GPI-deficient and wildtype Ramos517 cells to see if downregulation of CD20 was responsible for the decreased response to CD20 hypercrosslinking in GPI-deficient cells. As shown in Figure 4.13, flow cytometric analysis of unpermeabilized cells using the 2H7 anti-CD20 antibody shows that the expression of cell surface CD20 is not affected by GPI deficiency. Since different anti-CD20 antibodies exhibit heterogeneity in their biological effects that is related to small differences in their epitope binding

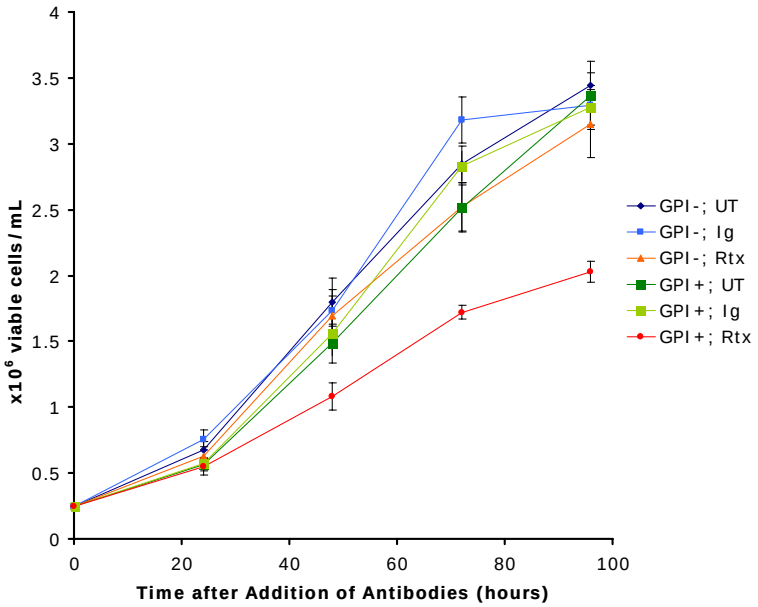

Figure 4.12. GPI-deficient B cells are resistant to growth inhibition following hypercrosslinking of CD20.

5 x 10^5 Ramos517/vector (GPI-) or Ramos517/pigM (GPI+) cells were cultured in 2 mL of RPMI complete containing no antibody (UT), 2 μg of hIg + 20μg of F(ab')$_2$ anti-hIgG (Ig) or 2 μg of rituximab + 20 μg of F(ab')$_2$ anti-hIgG (Rtx) for a total of 96 hours. At 24 hour intervals, the number of viable cells/mL was determined by hemacytometer counting with trypan blue exclusion. Results are expressed as the means of three independent experiments, with the error bars representing the standard error of the mean.

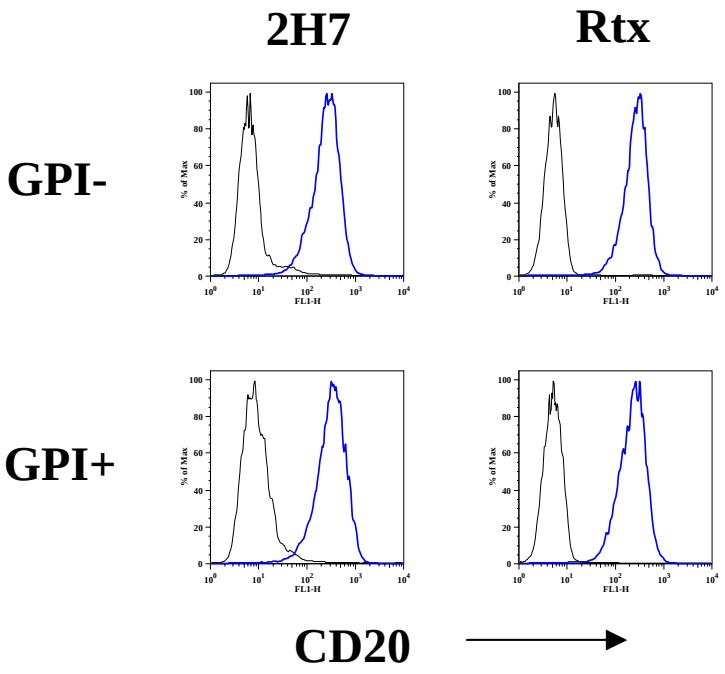

Figure 4.13. Cell surface expression of CD20 is unaltered in GPI-deficient cells.

1 x 10^6 Ramos517/vector (GPI-) or Ramos517/pigM (GPI+) cells were stained with anti-CD20 antibodies (2H7 and Alexa488-conjugated F(ab')$_2$ anti-mouse IgG or rituximab (Rtx) and Alexa488-conjugated F(ab')$_2$ anti-human IgG) and analyzed by flow cytometry. Blue lines indicates staining of CD20, while the black lines indicate staining of isotype controls. Results are representative of three independent experiments.

specificity (Polyak and Deans, 2002), I confirmed this result by staining cells with rituximab, since that was the reagent used in the signalling and functional studies described in this chapter. As with the 2H7 antibody, rituximab staining showed no differences in the levels of cell surface CD20 in GPI-positive and GPI-negative Ramos517 cells, indicating that rituximab binding to CD20 is not specifically affected in GPI-deficient cells.

4.2.2.3 CD20 raft association is not affected by GPI deficiency

An important property of most CD20 antibodies, including rituximab, is their ability to induce a change in the Triton X-100 insolubility of CD20 that is thought to indicate its translocation to or stabilization in rafts (Cragg et al., 2003; Deans et al., 1998; Janas et al., 2005; Unruh et al., 2005). Failure of CD20 to translocate to Triton-insoluble raft fractions correlates with inhibition of apoptosis in Ramos cells (Janas et al., 2005; Unruh et al., 2005). Binding of rituximab alone is sufficient to induce CD20 association with Triton X-100-insoluble raft fractions and hyperrcrosslinking of CD20 with both rituximab and anti-hIgG also causes CD20 to become stabilized in Triton X-100-insoluble raft fractions (Janas et al., 2005; Unruh et al., 2005). Though similar levels of CD20 are expressed on the cell surface of GPI-deficient and wildtype Ramos517 cells, it was possible that antibody-induced CD20 translocation to Triton-insoluble rafts was inhibited in GPI-deficient cells, and this might be responsible for the resistance to CD20-mediated apoptosis and growth inhibition observed in GPI-deficient cells. To test this possibility, antibody-induced raft association of CD20 in GPI-deficient and wildtype Ramos517 cells was examined by subjecting 1% Triton X-100 detergent lysates to low-speed centrifugation to separate crude Triton-soluble and Triton-insoluble pellet

fractions. This procedure was faster than sucrose density gradient experiments, required fewer cells and less antibody, and is considered to be a good approximation of CD20 raft association, as all of the Triton-insoluble CD20 has previously been shown to reside in low density raft fractions (Deans et al., 1998). Using this approach, it was apparent that binding of rituximab alone was sufficient to induce the redistribution of a significant proportion of CD20 to the Triton-insoluble pellet, and this redistribution was CD20 specific, as treatment with hIg failed to induce Triton insolubility (Figure 4.14). The relative amounts of CD20 present in the pellet and soluble fractions before and after rituximab crosslinking were similar in GPI-deficient and GPI-positive cells at both 5 minute and 15 minute timepoints. A similar experiment was performed, examining a more extensive timecourse, with the addition of secondary cross-linking anti-hIgG to further cluster and hypercrosslink CD20. Consistent with the results observed in the experiment using rituximab alone, hypercrosslinking of CD20 with rituximab and anti-hIgG also induced Triton-insolubility of CD20 in both GPI-deficient and wildtype cells (Figure 4.14). The kinetics and magnitude of the response were similar in both GPI-negative and GPI-positive cells with a subset of CD20 redistributing to the insoluble pellet as early as 30 seconds, and remaining insoluble after as long as 60 minutes of antibody treatment. As in the previous experiment, though there was a decrease in the amount of CD20 detected in the soluble fraction, a substantial portion of CD20 still remained soluble under the experimental conditions used, although this occurred in both cell types and was not related to GPI status.

In order to confirm that the crude Triton-insolubility observed above was indeed indicative of raft association, several sucrose density gradient experiments were

Figure 4.14. CD20 association with Triton X-100 insoluble fractions following antibody crosslinking is similar in GPI-deficient and wildtype B cells.

Ramos517/vector (GPI-) and Ramos517/pigM (GPI+) cells were treated with hIg (Ig) or rituximab (Rtx) alone (A), or with hig + anti-hIgG (Ig) or rituximab + anti-hIgG (Rtx) (B) for various lengths of time, prior to lysis in 1% Triton X-100/Tris lysis buffer. The detergent lysates were separated into crude Triton X-100-soluble (soluble) and Triton X-100-insoluble (pellet) fractions by centrifugation at 14 000 x g for 15 minutes. Equal amounts of protein from the soluble and pellet fractions were separated by SDS-PAGE and the corresponding Western blots were probed with antibodies recognizing CD20 and actin. Results in (A) are representative of two independent experiments. Results in (B) are representative of 3 independent experiments.

A. Rituximab alone

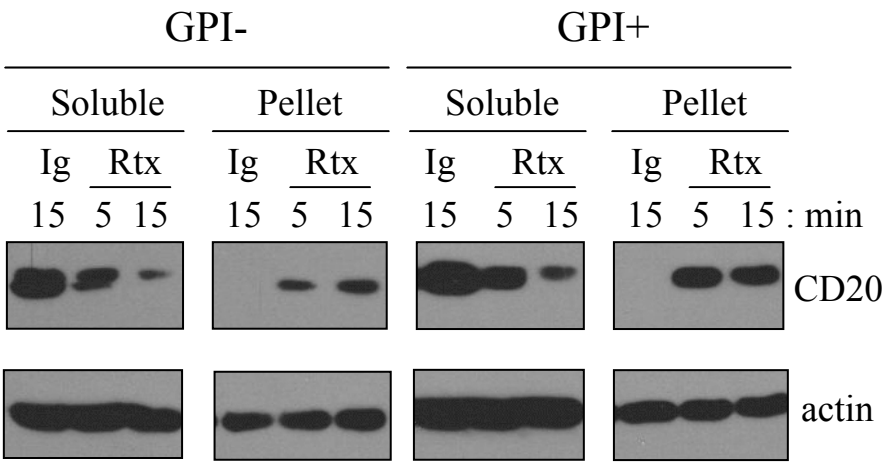

B. Rituximab + anti-hIgG

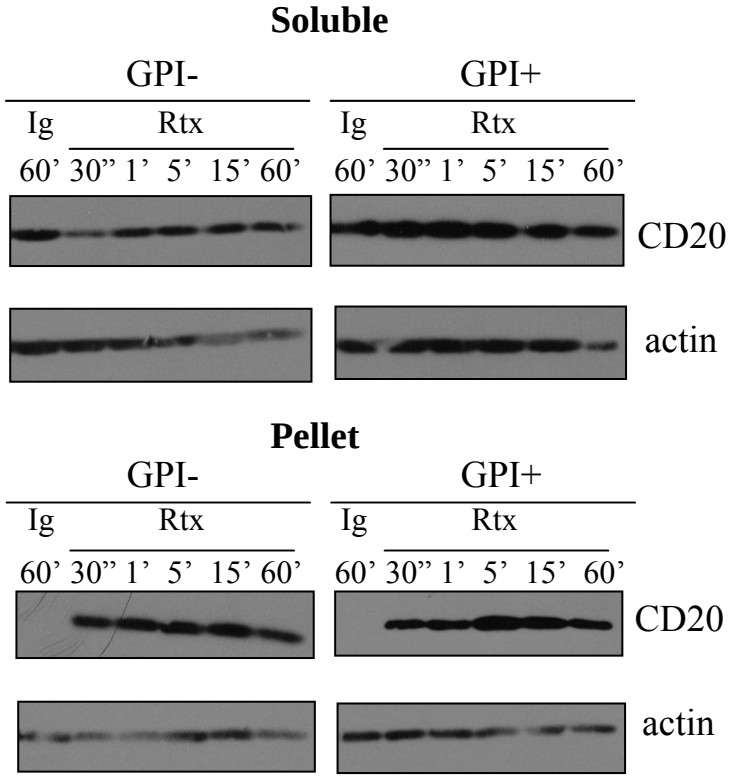

performed to isolate low density raft fractions after treatment of cells with rituximab alone, or after hypercrosslinking of CD20 with rituximab and anti-hIgG. As seen in Figure 4.15, the vast majority of insoluble CD20 redistributed to low density Triton-insoluble raft fractions following binding of rituximab alone in both GPI-deficient and GPI-positive cells. This was accompanied by a substantial decrease in the amount of CD20 detected in the detergent-soluble fraction. Surprisingly, the results observed following hypercrosslinking of CD20 proved to be more complex. In the first of two independent experiments, a significant amount of CD20 redistributed to low density raft fractions in an antibody-dependent manner in both GPI-deficient and GPI-positive Ramos517 cells (Figure 4.16). A small amount of CD20 was also detected in the high density pellet in this experiment, though the amount in the pellet did not appear to change in response to CD20 hypercrosslinking. Surprisingly, in the second experiment, which was performed in exactly the same manner as the first experiment, most of the hypercrosslinking-induced Triton-insoluble CD20 was found in the high density insoluble pellet, with little to no CD20 observed in the low density raft fractions (Figure 4.16). The reasons for this variability are currently unknown. It is tempting to speculate that in this particular experiment, the CD20 in the high density pellet is raft-associated, but that these rafts are tightly associated with the cytoskeleton, preventing their flotation in the sucrose gradients. Further experiments are needed to investigate this possibility and investigate the factors that might be responsible for the variability seen upon hypercrosslinking. Nevertheless, the variability in the density gradient results upon CD20 hypercrosslinking does not appear to be related to GPI status and taken together, the above data suggest that antibody-induced CD20 translocation to Triton-insoluble raft

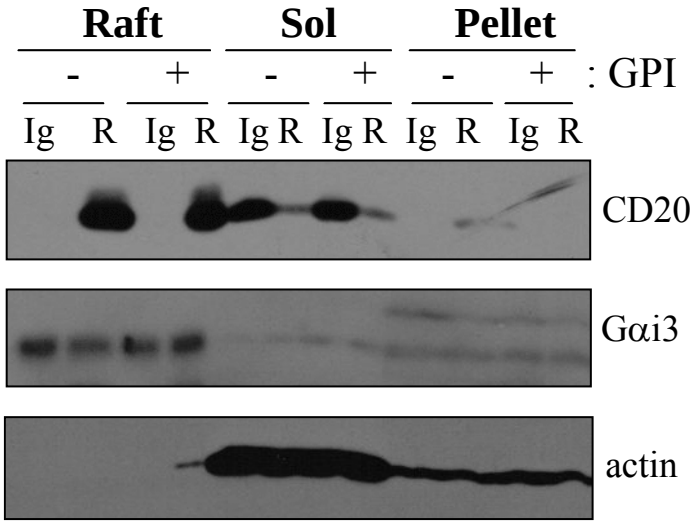

Figure 4.15. CD20 translocation to Triton X-100 raft fractions is not affected by GPI deficiency.

Ramos517/vector (GPI-) and Ramos517/pigM (GPI+) cells were incubated with hIg (Ig) or rituximab (R) for 15 minutes prior to lysis in 1% Triton X-100/MBS lysis buffer and fractionation by sucrose density gradient centrifugation. Equal amounts of protein from raft, soluble, and high density pellet fractions were separated by SDS-PAGE and analyzed by Western blotting with anti-CD20 and anti-Gαi3 antisera. The results shown are representative of two independent experiments.

Figure 4.16. CD20 association with Triton-insoluble raft fractions following hypercrosslinking of CD20 is similar in GPI-deficient and wildtype B cells.

Ramos517/vector (GPI-) and Ramos517/pigM (GPI+) cells were treated with hIg + anti-hIgG (Ig) for 60 minutes, or with rituximab + anti-hIgG (Rtx + 2ndary) for 1, 15, or 60 minutes, and lysed in 1% Triton X-100/MBS lysis buffer. The lysates were subjected to sucrose density gradient centrifugation, and equal amounts of protein from the raft, soluble, and high density pellet fractions obtained were separated by SDS-PAGE and analyzed by Western blotting for CD20. Equal protein loading was confirmed by Western blotting for $G\alpha_{i3}$ and actin (data not shown). Two independent experiments are shown.

Experiment 1:

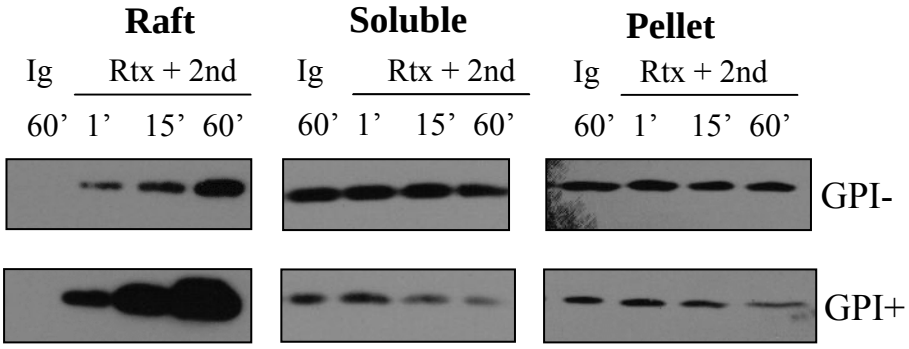

WB: α-CD20

Experiment 2:

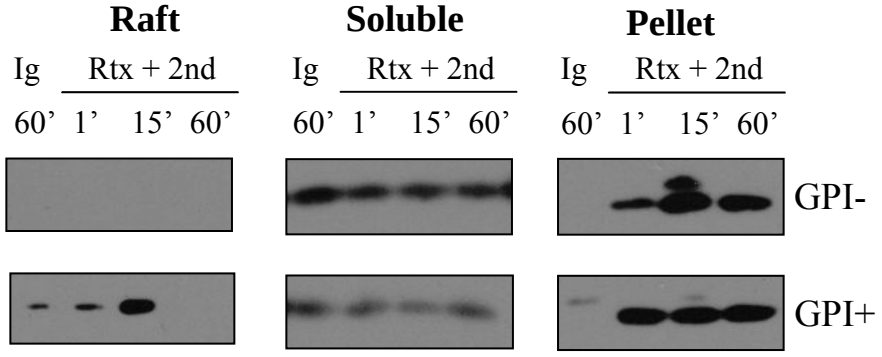

WB: α-CD20

domains is not affected by the loss of GPI-anchored protein expression in Ramos517 cells.

Though CD20 is only found in Triton-insoluble raft fractions after antibody crosslinking, it is constitutively present in raft fractions isolated using the non-ionic detergent Brij58 (Janas et al., 2005; Li et al., 2004a). This may be due to a constitutive low affinity association of CD20 with rafts that is sensitive to solubilization by Triton X-100 but not by Brij58 (Janas et al., 2005; Li et al., 2004a). As a further probe to determine whether any differences in CD20 association with membrane rafts exist in GPI-deficient cells, the association of CD20 with Brij58 raft fractions was examined. As shown in Figure 4.17, Western blotting of raft fractions isolated from GPI-negative and GPI-positive cells showed similar levels of the adaptor protein Cbp, and the Src family kinase Lyn. The GPI-negative raft fractions appeared to contain slightly less CD20 than the GPI-positive raft fractions, however this difference reflects experiment-to-experiment variability that was independent of GPI status, as in other experiments the reverse was observed (*i.e.* more CD20 in GPI-negative raft fractions and less CD20 in GPI-positive raft fractions; data not shown). Silver staining of equivalent amounts of raft protein from GPI-deficient and wildtype cells confirmed equal protein loading, and illustrated that, while the raft protein profiles of the two cell types were very similar, several noticeable differences in the banding pattern were also evident, which is consistent with the data regarding Triton-insoluble raft fractions from Ramos517 cells discussed in Chapter 3. As with the raft fractions, Western blotting of aliquots of the detergent-soluble fraction, and of the total detergent lysate prior to density gradient centrifugation, showed similar amounts of CD20 (Figure 4.17). Together with the flow cytometry data presented in section 4.2.2.3, these

Figure 4.17. CD20 is still constitutively associated with Brij 58-insoluble raft fractions in GPI-deficient B cells.

Raft fractions were isolated from 1 x 10^8 Ramos517/vector (GPI-) or Ramos517/pigM (GPI+) cells lysed with 1% Brij 58/MBS lysis buffer. Equal amounts of raft protein were separated by SDS-PAGE and analyzed by silver staining to visualize total protein, and by Western blotting to compare levels of CD20, Cbp, and Lyn. CD20 levels in Brij58-soluble fractions and in total Brij58 detergent lysates prior to sucrose density gradient centrifugation were also analyzed by Western blotting. Results are representative of 4 independent experiments.

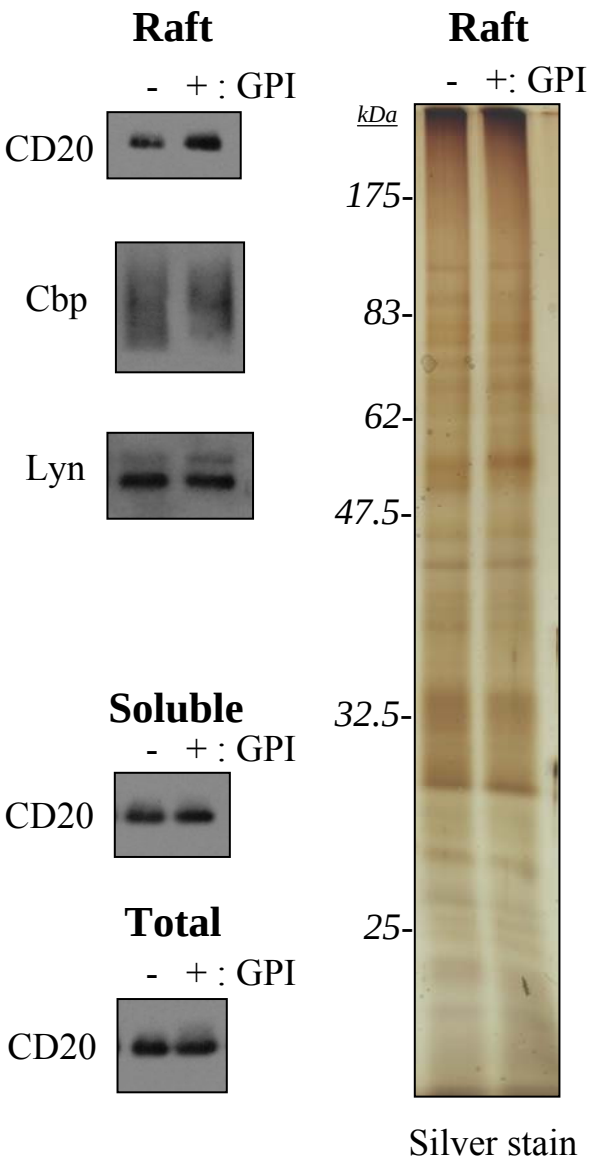
Raft
- + : GPI
CD20
Cbp
Lyn
Soluble
- + : GPI
CD20
Total
- + : GPI
CD20
Raft
- +: GPI
kDa
175-
83-
62-
47.5-
32.5-
25-
Silver stain

data further suggest that total expression levels as well as the extent of CD20 raft association in untreated Ramos517 cells are similar in both GPI-deficient and wildtype cells. Thus, the constitutive association of CD20 with Brij58-insoluble raft fractions does not appear to be affected by GPI-deficiency, and overall these observations suggest that both low and high affinity CD20 association with lipid raft microdomains are unaffected by the loss of GPI-anchored protein expression.

4.2.2.4 Calcium signalling is altered in GPI-deficient B cells following hypercrosslinking of CD20

Chemical inhibitors of Src family kinase or phospholipase-C γ activity and cholesterol depletion with MβCD strongly inhibit both calcium mobilization and apoptosis following rituximab-mediated CD20 hypercrosslinking, (Janas et al., 2005; Unruh et al., 2005). Chelation of calcium with EGTA is also sufficient to almost completely abrogate apoptosis following CD20 crosslinking (Janas et al., 2005). Therefore, the calcium flux induced by hypercrosslinking of CD20 was compared in GPI-deficient and GPI-positive Ramos517 cells, to determine whether GPI deficiency affected the raft-dependent calcium signal downstream of CD20 hypercrosslinking. As shown in Figure 4.18a, initial studies comprising four independent experiments performed over a period of 3.5 months consistently demonstrated a delay of approximately 30 seconds in CD20 hypercrosslinking-induced calcium release in GPI-deficient cells when compared to GPI-positive cells, suggesting that GPI-dependent changes in calcium signalling downstream of CD20 hypercrosslinking might be responsible, at least in part, for the decrease in CD20-mediated apoptosis and growth inhibition observed in GPI-deficient cells. These experiments utilized antibody doses and conditions that were optimized by Unruh *et al.*

Figure 4.18. Calcium signalling differs in GPI-deficient and wildtype B cells after hypercrosslinking of CD20, but the response has changed over time.

GPI-deficient Ramos517/vector cells (blue lines) and wildtype Ramos517/pigM cells (red lines) were loaded with the calcium indicator dyes fluo-3 AM and fura red AM, and preincubated with 2 μg of rituximab. Baseline calcium levels were measured by flow cytometry, and then CD20 was hypercrosslinked by the addition of 5 μg of $F(ab')_2$ anti-human IgG (indicated by arrows), and fluorescence was measured for an additional 9 minutes. (A) Initially, the calcium flux was delayed in GPI-deficient cells, though the magnitude of the flux was similar. These results are representative of 4 independent experiments performed between July 12, 2005 and Sept. 24, 2005. (B) In 3 independent experiments performed in April of 2006, cells were preincubated with 2 μg of rituximab, and hypercrosslinked with 1.25, 5, or 20 μg of $F(ab')_2$ anti-human IgG. At this time, the kinetics of thecalcium response were similar in both GPI-deficient and wildtype cells, but the magnitude of the response in GPI-expressing cells was now significantly reduced compared to the GPI-deficient cells. One representative experiment is shown .

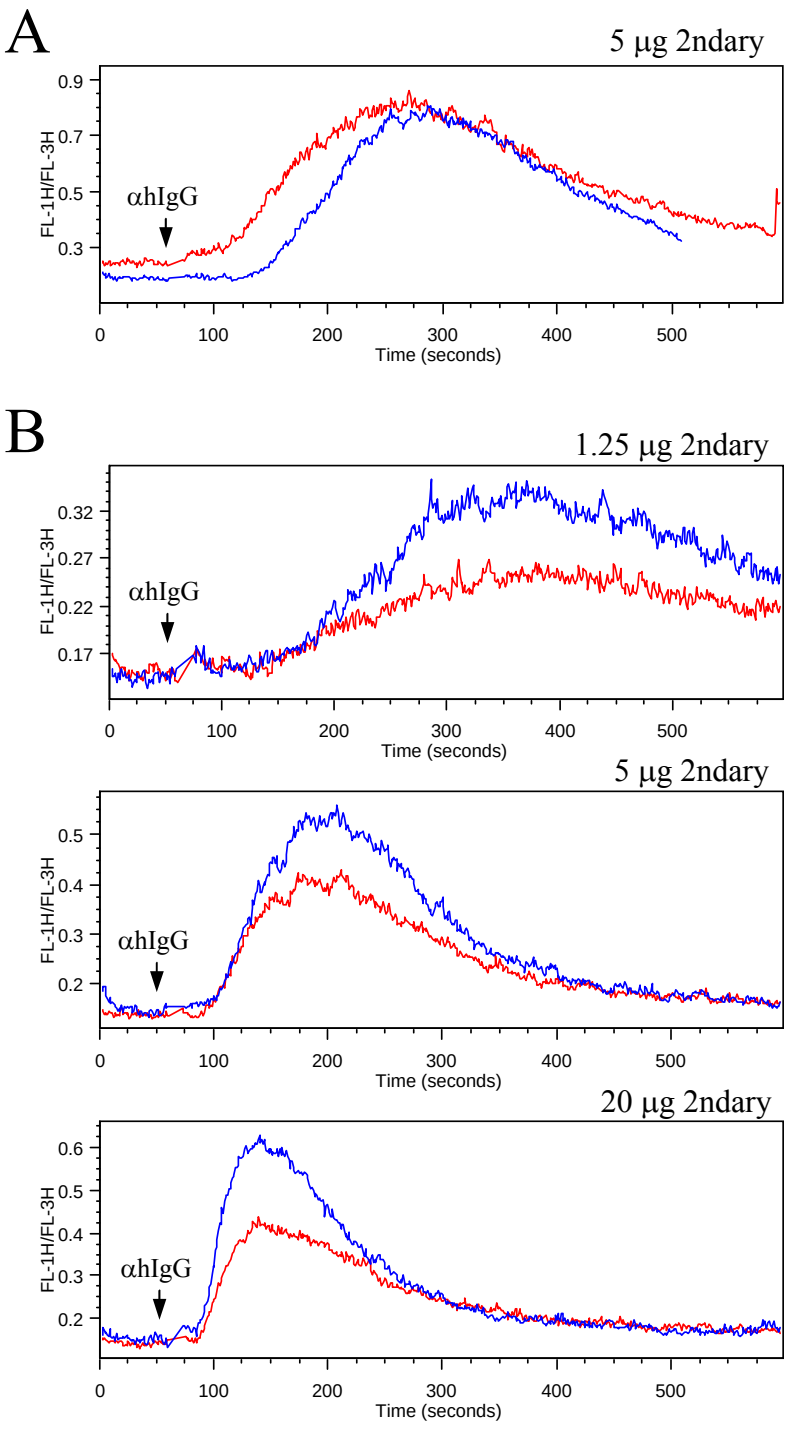
A
5 µg 2ndary
FL-1H/FL-3H
αhIgG
Time (seconds)
B
1.25 µg 2ndary
FL-1H/FL-3H
αhIgG
Time (seconds)
5 µg 2ndary
FL-1H/FL-3H
αhIgG
Time (seconds)
20 µg 2ndary
FL-1H/FL-3H
αhIgG
Time (seconds)

(Unruh et al., 2005) in Ramos cells. To further characterize the GPI-dependent change in CD20-mediated calcium signalling, several months later a series of experiments were performed using additional doses of secondary crosslinking antibody, to determine whether or not the difference observed was dose-dependent. Surprisingly, as seen in Figure 4.18b, at this time the results were different. In four independent experiments the kinetics of the calcium response was similar in both GPI-deficient and GPI-positive cells, but now the magnitude of the calcium response was substantially and reproducibly reduced in GPI-positive cells when compared to GPI-negative cells. The calcium assay is performed on the flow cytometer at ambient room temperature. At the time of the latter set of experiments, it was apparent that the room was noticeably colder than it was when the first set of experiments was performed (in the summer and early fall, when the room was quite hot). GPI-deficient hematopoietic cells have previously been reported to have elevated cholesterol levels (Abrami et al., 2001; Samuel et al., 2001), and differences in cholesterol levels of GPI-positive and negative Ramos517 cells could result in differences in membrane fluidity that might explain temperature-dependent changes in signalling. However, a series of experiments in which cells were equilibrated for 20 minutes at temperatures of 19°C ("cold room"), 25°C ("warm room"), and 37°C prior to analysis indicated that temperature was not responsible for the observed change in calcium signalling (data not shown). Prior to the second set of calcium experiments, our laboratory had begun to use a new lot of fetal bovine serum, and it is possible that uncharacterized differences between the two lots of serum were responsible for the change in calcium signalling. It is also important to note that the annexin V staining data described above was all obtained prior to time that the CD20-mediated calcium responses

were observed to change. One of the growth curves summarized in Figure 4.12 was performed during the same period of time as the second set of calcium experiments, and was consistent with the two earlier growth curve experiments performed concurrently with the first set of calcium experiments. Unfortunately, it is unclear which lot of serum was utilized for this particular growth curve experiment, and therefore, the annexin V staining and growth curve experiments must be repeated in the future in order to assess whether the responses to CD20 hypercrosslinking in the Ramos517 B cell lines have been altered by unexplained variables in the experimental system. It is also important to note that the calcium response to anti-IgM in both GPI-positive and GPI-negative cells remained consistent with the data in Figure 4.9 throughout this entire period of time.

In conclusion, the data presented in section 4.1.2 demonstrates that GPI-deficient Ramos517 cells were resistant to apoptosis and growth inhibition induced by rituximab-mediated hypercrosslinking of CD20. Although CD20 expression levels and raft association were not affected by GPI deficiency, a GPI-dependent delay in the kinetics of the calcium flux induced by CD20 hypercrosslinking could be correlated with the observed resistance to growth inhibition and apoptosis. Although the responses in these cell lines may have changed recently, requiring additional experiments to re-evaluate the effect of GPI deficiency in this model system, the initial results reported here support the hypothesis that alterations in raft structure or organization induced by the loss of GPI-anchored proteins alters signalling responses downstream of a raft compartmentalized signalling pathway.

4.2.3 GPI-deficient B cells are resistant to apoptosis induced by ultraviolet radiation but are equally susceptible to apoptosis induced by hydrogen peroxide

The above data support the idea that GPI-deficient cells are resistant to apoptosis induced by two receptor-dependent raft-compartmentalized signalling pathways. However, it was unclear whether these results illustrate resistance to apoptosis induced by specific stimuli, or whether they indicate that GPI-deficient Ramos517 cells exhibit a generalized resistance to apoptosis. To further investigate this question, the extent of apoptosis induced by two additional stimuli—ultraviolet (UV) radiation and hydrogen peroxide (H_2O_2)--was compared in GPI-deficient and wildtype Ramos517 cells. As shown in Figure 4.19a, treatment of GPI-positive cells with doses of UV-C ranging from 5 to 40 J/m^2 caused a significant dose-dependent increase in the percentage of early apoptotic cells, and this was accompanied by an even more dramatic increase in the percentage of nonviable apoptotic/necrotic cells (Figure 4.19b). In comparison, there was a much smaller increase in the percentage of early apoptotic and nonviable cells in GPI-deficient cells at all doses of UV-C examined, indicating that GPI-deficient cells showed a remarkable degree of resistance to UV-induced apoptosis.

Treatment of DT40 B cells with various concentrations of H_2O_2 leads to different cellular responses—at lower concentrations of H_2O_2 (10 –100 μM) cell cycle arrest and apoptosis is observed, but at H_2O_2 concentrations of 1 mM and higher, necrotic cell death is induced (Tohyama et al., 2004). The extent of apoptotic and necrotic cell death induced by various concentrations of H_2O_2 was determined in GPI-deficient and wildtype Ramos517 cells. As shown in Figure 4.20a, there was a similar increase in the percentage of early apoptotic cells in GPI-negative and GPI-positive cells treated with

Figure 4.19. GPI-deficient B cells are resistant to apoptosis induced by ultraviolet radiation.

Ramos517/vector (GPI-) or Ramos517/pigM (GPI+) cells were treated with the indicated doses of UV-C, and then cultured for 24 hours prior to staining with annexin V-FITC/PI and analysis by flow cytometry to detect (A) early apoptotic cells, and (B) nonviable cells lacking membrane integrity (including early and late apoptotic cells and necrotic cells). Results are expressed as the means of three independent experiments, with the error bars representing the standard error of the mean. Asterisks indicate statistically significant differences between the results from GPI-positive and GPI-negative cells at the indicated doses of UV. *P<0.05, **P<0.01, ***P<0.001.

A. Early apoptotic

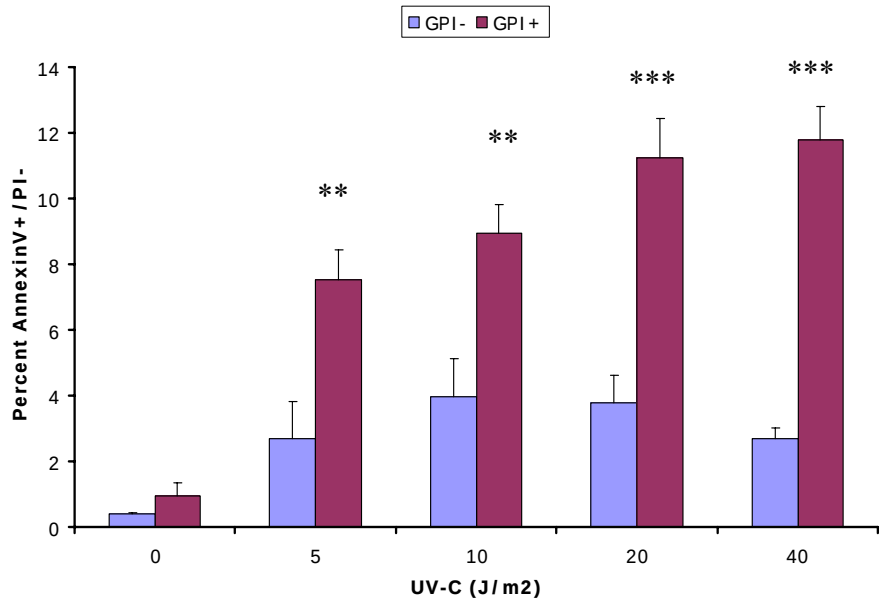

B. Apoptotic/Necrotic

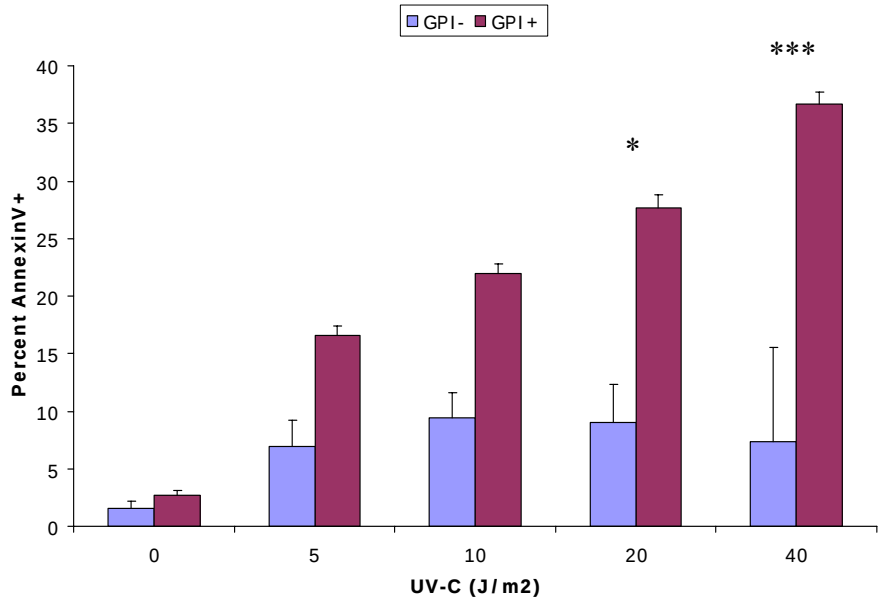

Figure 4.20. GPI-deficient B cells are resistant to cell death induced by hydrogen peroxide.

2×10^6 Ramos517/vector (GPI-) or Ramos517/pigM (GPI+) cells were cultured for 24 hours in the presence of the indicated concentrations of hydrogen peroxide. Annexin V-FITC/PI staining and analysis by flow cytometry was used to detect (A) early apoptotic cells, and (B) nonviable cells lacking membrane integrity (including both early and late apoptotic cells and necrotic cells). Results shown are the means of three independent experiments, with the error bars representing the standard error of the mean.

A. Early apoptotic

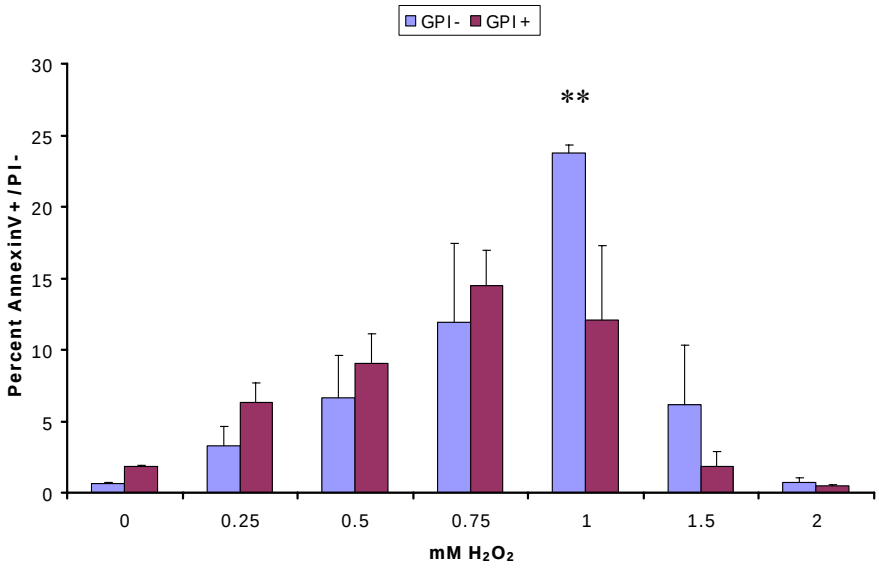

B. Apoptotic/Necrotic

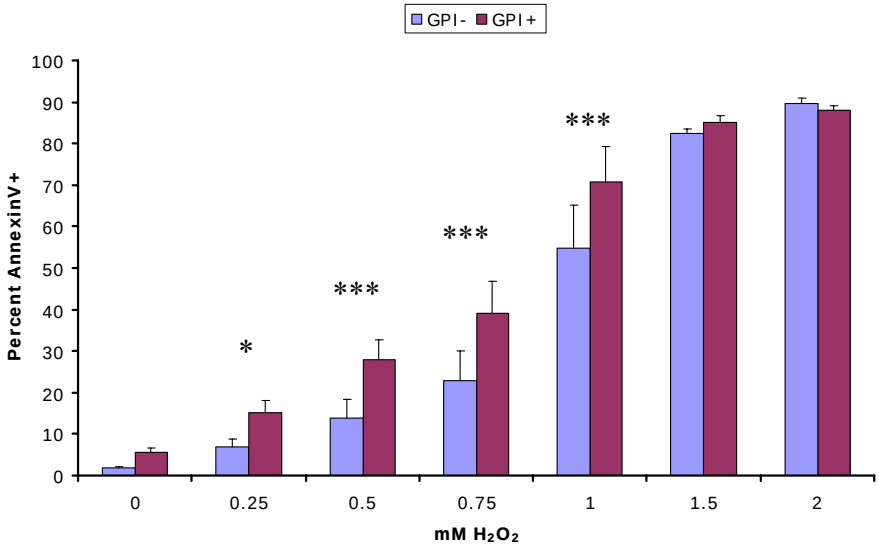

0.25, 0.5, and 0.75 mM H_2O_2. The only significant GPI-dependent difference in the percentage of early apoptotic cells was observed when a concentration of 1 mM H_2O_2 was used. At this concentration there was a significantly higher percentage of apoptotic cells in H_2O_2-treated GPI-deficient cells (Figure 4.20a). However, the total percentage of nonviable cells at this concentration (Figure 4.20b) was higher in GPI-positive cells, and this difference likely reflects an increased contribution of necrosis to the total cell death observed in GPI-expressing cells at this dose. In agreement with these observations, a single preliminary experiment found that PARP cleavage was detectable at concentrations of 0.5, 0.75, and 1 mM in GPI-deficient cells, and at concentrations of 0.5 to 0.75 mM in GPI-positive cells (data not shown), which is consistent with activation of caspases during apoptosis. The percentage of total annexin V-positive cells is difficult to interpret in this experimental context, as it includes cells that are in the early phases of apoptosis, as well as late apoptotic and necrotic cells. It is likely that necrosis is the predominant mode of cell death in Ramos517 cells treated with 1.5 mM and 2 mM H_2O_2, as almost no annexin V-positive/PI-negative cells are detected at these concentrations, even though more than 80% of cells are annexin V-positive. Based on the percentage of annexin V-positive/PI-negative cells compared to total annexin V-positive cells, as well as the PARP cleavage evidence, it is likely that apoptosis is the primary mode of cell death at lower concentrations of H_2O_2, with necrosis beginning to become significant at concentrations above 0.75 mM H_2O_2. At concentrations of 1 mM H_2O_2 and below, it is tempting to speculate that the significant differences observed in the percentage of nonviable cells in GPI-expressing versus GPI-deficient cells (Figure 4.20b) are due to an increased susceptibility of GPI-positive cells to necrosis at lower concentrations of H_2O_2.

However, it is clear that at concentrations of H_2O_2 less than 1 mM, where apoptosis is likely to be more predominant than necrosis based on these results and other reports (Tohyama et al., 2004), the amount of cell death that can clearly be attributed to apoptosis (namely the annexin V-positive, PI-negative cells) is similar in both wildtype and GPI-deficient Ramos517 cells. This finding suggests that the GPI-deficient Ramos517 cells do not possess a broadly generalized resistance to apoptosis that is independent of the apoptosis-inducing stimuli used, further supporting the idea that differences in the extent of apoptosis induced by both CD20 and the B cell receptor in GPI-deficient and wildtype B cells are due to specific and GPI-dependent differences in the receptor-mediated signals produced.

4.2.4 Total and raft cholesterol levels are unchanged in GPI-deficient cells

Previous work has shown that a GPI-deficient T lymphoma cell line, as well as erythrocytes from PNH patients exhibit increased total membrane and raft cholesterol levels (Abrami et al., 2001; Samuel et al., 2001). Membrane cholesterol can bind noncovalently to transmembrane signalling receptors and affect their function (Fahrenholz et al., 1995; Gimpl et al., 2000; Gimpl et al., 2002; Jones and McNamee, 1988; Klein et al., 1995; Narayanaswami and McNamee, 1993), and incorporation of excess exogenous cholesterol in mast cell rafts causes aberrant signalling (Baumruker et al., 2003). Therefore, I compared the total and raft-associated cholesterol levels in GPI-deficient and wildtype Ramos517 cell lines, to determine whether cholesterol-mediated mechanisms might be important in the altered signalling observed in GPI-deficient Ramos517 cells. Surprisingly, the levels of total and raft cholesterol in GPI-negative and GPI-positive Ramos517 cells were similar (Figure 4.21). In addition, comparison of

Figure 4.21. Total and raft cholesterol levels are similar in GPI-deficient and wildtype cells.

(A) Total cholesterol levels in whole cell lysates prepared from various GPI-deficient (IVEE, Raji26/vector, Ramos517/vector) and wildtype (K562, IVEE/GPI8, Raji26/pigL, and Ramos517/pigM) cell lines. Cells incubated briefly in medium containing 10 mM MβCD to deplete cholesterol, or 10 mM MβCD + 1.4 mM cholesterol to enrich cholesterol prior to lysis served as controls to show that the assay could effectively detect changes in cellular cholesterol levels. (B) Cholesterol levels in raft fractions isolated GPI-deficent Ramos517/vector and wildtype Ramos517/pigM cells were compared. Results are expressed as the means of three independent experiments, with error bars representing the standard error of the mean.

A. Total cholesterol

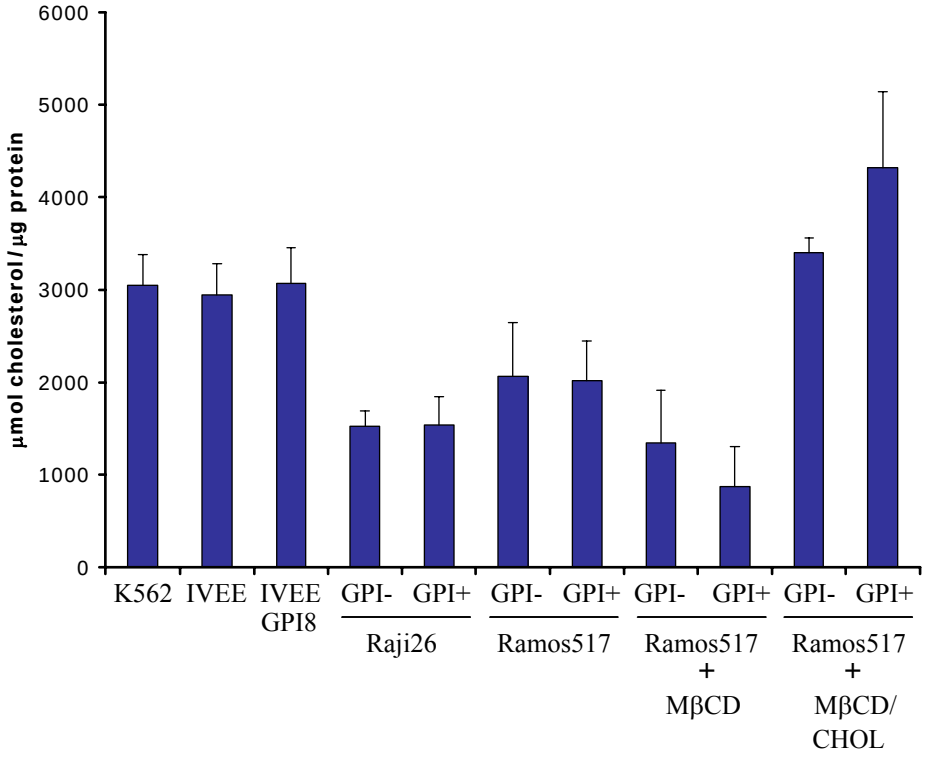

B. Raft Cholesterol

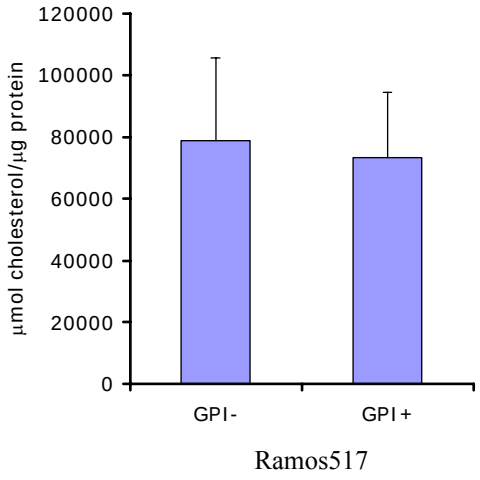

GPI-negative IVEE and Raji26/vector cells to GPI-positive K562 and IVEE/GPI8, or Raji26/pigL cells respectively, also showed no GPI-dependent differences in total cholesterol levels (Figure 4.21). The assay was capable of detecting differences in cholesterol levels between different cell types, and in cells depleted of cholesterol with MβCD, or loaded with exogenous cholesterol (Figure 4.21a). Overall these results demonstrate that cholesterol levels in Ramos517 cells are not affected by absence of GPI-anchored protein expression.

4.3 Discussion

GPI-anchored proteins are highly enriched in plasma membrane rafts, where they are involved in a wide variety of functions at the cell surface. Many GPI-anchored proteins are involved in the initiation or regulation of signal transduction through both direct and indirect mechanisms. The raft localization of GPI-anchored proteins is thought to be important in propagating many GPI-dependent signals because it facilitates the interaction of GPI-anchored proteins with both transmembrane coreceptors and with acylated cytoplasmic signalling effectors such as the Src family kinases. It seems reasonable to expect that removing GPI-anchored proteins from the raft environment could disrupt many of these interactions and have multiple effects on the composition, organization, and, ultimately, the function of these microdomains. In support of this idea, this work (Chapter 3 and Figure 4.17) and other reports (Abrami et al., 2001; Lillico et al., 2003; Samuel et al., 2001) indicate that raft protein and lipid composition is altered in GPI-deficient cells. Furthermore, a number of studies have demonstrated that signalling in GPI-deficient monocytes and T cells is substantially altered (Hazenbos et al., 2004a; Hazenbos et al., 2004b; Romagnoli and Bron, 1997; Romagnoli and Bron, 1999;

Ruggiero et al., 2004; Terrazzano et al., 2005). In this chapter, the effect of GPI deficiency on raft-mediated signalling in B cells was investigated in order to test the hypothesis that alterations in lipid raft composition or organization caused directly or indirectly by the loss of GPI-anchored proteins would affect lipid raft function in signal transduction. These studies demonstrated that the extent of apoptosis and growth inhibition induced by crosslinking either of two different raft-compartmentalized receptors, the BCR and CD20, is significantly decreased in GPI-deficient Ramos517 B lymphoma cells (Figures 43, 4.4, 4.5, 4.10, 4.11, and 4.12). These observations are consistent with the hypothesis stated above, as the decrease in apoptosis is likely due to a change in the nature or strength of the signal generated downstream of CD20 or the BCR. In the case of BCR-mediated signalling, the observation of a significant decrease in basal and stimulated raft phosphotyrosine signalling (Figure 4.8) provides direct evidence that this is indeed the case. Likewise, the differences in raft-mediated calcium signalling observed following engagement of CD20 also indicate that lipid raft signalling is altered in GPI-deficient cells.

Engagement of the BCR by multivalent antigen or by antibody crosslinking rapidly activates a number of different tyrosine kinases. The BCR complex is composed of an antigen-binding subunit, the membrane immunoglobulin molecule, associated with a signal transducing unit, the Igα/Igβ heterodimer. Upon crosslinking of the BCR, Src family kinases, particularly Lyn, phosphorylate ITAM motifs on the Igα/Igβ subunits. ITAM phosphorylation leads to the recruitment and activation of the protein tyrosine kinases Syk and Btk, and eventually tyrosine phosphorylation of multiple effector proteins and coreceptors (see (Dal Porto et al., 2004; Niiro and Clark, 2002) for review).

Several lines of evidence suggest that initiation of the phosphotyrosine signalling cascade following BCR engagement occurs within lipid rafts. Kinetic analyses have shown that clustered BCRs are recruited to lipid rafts within seconds (Petrie et al., 2000; Weintraub et al., 2000), and that this translocation precedes BCR-induced tyrosine phosphorylation (Weintraub et al., 2000). In addition, BCR accumulation in lipid rafts does not require Src kinase activation (Weintraub et al., 2000), or phosphorylation of the ITAMs on the Igα/Igβ subunits (Sproul et al., 2000). The observation of a general reduction of BCR-induced protein tyrosine phosphorylation in raft fractions from GPI-deficient cells in the absence of any GPI-dependent alterations in surface BCR expression (Figure 4.6) or in the ability of the BCR to translocate to rafts (Figure 4.7) is in agreement with the reports described above. Interestingly, although raft phosphotyrosine levels were reduced both before and after BCR crosslinking, the banding pattern observed following BCR stimulation was similar in GPI-deficient and wildtype cells, suggesting that, while signal strength is affected, association of the majority of tyrosine kinase substrates with rafts is not altered in GPI-deficient cells. The fact that BCR-induced growth inhibition and apoptosis was reduced but not eliminated in GPI-deficient cells is consistent with this observation, and together this data suggests that BCR signalling is generally intact in GPI-deficient cells, but that specific modulation of the signal strength of raft-localized phosphotyrosine signalling caused by the loss of GPI-anchored proteins alters the biological consequences of BCR stimulation. Interestingly, growth inhibition at 24 hours was similar in both GPI-deficient and wildtype B cells, with differences in the growth of the two cell lines only apparent at later timepoints. Since the amount of apoptosis measured by annexin V staining was decreased in GPI-deficient

cells compared to GPI-expressing cells at both 6 hour and 24 hour time points, it is probable that the alteration in the raft-dependent BCR signal shifts the balance towards growth inhibition and away from apoptosis in GPI-deficient cells compared to GPI-expressing cells at 24 hours. After 24 hours, the growth curve data indicates that GPI-deficient Ramos517 B cells begin to grow at a faster rate than the GPI-expressing cells, although the relative levels of apoptosis in each cell type remain consistent at these later timepoints. These data suggest that BCR-induced growth inhibition is less sustained in GPI-deficient cells compared to GPI-expressing cells, and further demonstrate that the nature of the signal generated downstream of the BCR is significantly altered in the GPI-deficient cells. The fact that the difference in the level of raft protein tyrosine phosphorylation is observed as early as 1 minute following BCR stimulation (Figure 4.8) argues that GPI deficiency specifically affects early receptor proximal activation events that involve the BCR at the plasma membrane. This further argues for a specific alteration of raft structure and function in the context of GPI deficiency, since other biochemical and immunofluorescence evidence indicates that initiation of early tyrosine phosphorylation events by BCR engagement in mature B cells occurs in lipid rafts (Gupta and DeFranco, 2003; Petrie and Deans, 2002; Petrie et al., 2000; Sproul et al., 2000; Weintraub et al., 2000). There are a number of possible mechanisms that might explain how the loss of GPI-anchored proteins leads to the observed change in raft phosphotyrosine signalling. Alteration of the basal and constitutive levels of expression and/or activity of key downstream kinases or phosphatases is one obvious mechanism. In this regard, a prime candidate kinase whose activity might be differentially regulated is the Src family kinase Lyn.

Lyn is constitutively raft-localized in B cells (Awasthi-Kalia et al., 2001; Suzuki et al., 2001). The results reported here confirm that this is the case in Ramos517 cells as well, and also demonstrate that expression levels of Lyn are similar in GPI-deficient and wildtype Ramos cells (Figure 4.17**).** In addition, raft association of Lyn is also unaffected by the loss of GPI-anchored proteins (Figure 4.17). The fact that basal raft phosphotyrosine levels were also reduced in GPI-deficient cells is fully consistent with a model in which Lyn kinase activity is altered in GPI-deficient cells. Since Lyn has important functions in the initiation and early amplification of BCR signals (Gauld and Cambier, 2004), altered Lyn kinase activity in the absence of GPI-anchored protein expression could explain the overall reduction in raft phosphotyrosine levels that is observed. The observation that Lyn directly associates with GPI-anchored proteins in diverse cellular contexts and is able to transmit signals downstream of specific GPI-anchored proteins(Kasahara et al., 2002; Suzuki et al., 2001) further supports a model in which Lyn kinase activity is either directly or indirectly affected by the loss of GPI-anchored proteins.

In addition to its positive regulatory roles however, Lyn has significant negative regulatory roles in BCR signalling. Whether Lyn promotes or inhibits BCR-dependent cell responses depends on numerous factors including the developmental stage of the cell, the nature of the antigenic stimulus, the surrounding microenvironment, and coreceptor function (Gauld and Cambier, 2004; Xu et al., 2005). It is possible that the loss of GPI-anchored proteins causes alterations in the structure or organization of the raft microenvironment in which Lyn resides that differentially affect Lyn's ability to interact with raft-localized coreceptors or downstream substrates. Although this possibility

cannot be ruled out, it seems unlikely based on the observation that the profile of tyrosine phosphorylated proteins observed in isolated raft fractions from stimulated GPI-negative and GPI-positive Ramos517 cells is similar (Figure 4.8). The alternative possibility, which is more consistent with the data presented here, is that alterations to raft structure or organization caused by the loss of expression of GPI-anchored proteins leads to disruption of one or more of the regulatory mechanisms that normally control the kinase activity of Lyn. Supporting this idea are two previous reports that describe a downregulation of the kinase activity of two other Src family kinases, Fyn and Lck in GPI-deficient T lymphoma cell lines, and in clonal T cell lines generated from PNH patient samples (Romagnoli and Bron, 1997; Romagnoli and Bron, 1999). In the PNH-derived T cell clones, the decrease in Lck kinase activity following TCR stimulation was accompanied by a reduction in levels of total protein tyrosine phosphorylation, reduced phosphorylation of the TCR ζ chain, delayed TCR capping and internalization, and reduced cellular proliferation (Romagnoli and Bron, 1999).

The regulation of Lyn kinase activity is closely linked to its raft localization, and so might easily be affected by the absence of GPI-anchored proteins. In mast cells, lipid raft association is thought to enhance Lyn kinase activity by protecting the active site tyrosine from dephosphorylation by excluding negative regulatory phosphatases (Young et al., 2003). In resting B cells, Lyn kinase activity is maintained in a continuously changing balance between "active" and "partially active" states due to the opposing effects of the tyrosine kinase Csk, and the transmembrane phosphatase CD45 (Gauld and Cambier, 2004). Csk negatively regulates the activity of Src family kinases by phosphorylating their inhibitory C-terminal tyrosine residue. The SH2 domain of Csk

binds to phosphorylated tyrosine residues in the cytoplasmic domain of the transmembrane adaptor protein Cbp (Horejsi, 2004). Cbp is constitutively localized to lipid rafts, providing a mechanism to allow recruitment of cytoplasmic Csk to lipid rafts, where its kinase substrates are localized. Hence, increased activity of Csk, or higher levels of Csk localized to rafts containing Lyn might explain the reduced basal raft phosphotyrosine levels observed in GPI-deficient Ramos517 cells. Alternatively, dephosphorylation of the C-terminal inhibitory tyrosine residue is required for full activation of the Src family kinases, and the protein tyrosine phosphatase CD45 is thought to be one of the phosphatases that accomplishes this (Ashwell and D'Oro, 1999). Initially CD45 is thought to prime Src family kinases for activation, by maintaining a proportion of the kinases in a "de-repressed" state that is responsive to BCR activation (Gauld and Cambier, 2004). Given the general reduction in basal raft phosphotyrosine levels (Figure 4.8), it is possible that a decrease in CD45-mediated dephosphorylation of Lyn could result in a decrease in Lyn kinase activity in resting GPI-deficient Ramos517 cells. This model is supported by the observation that Lyn is hyper-phosphorylated on the C-terminal inhibitory tyrosine residue in CD45-deficient B cells, resulting in a decrease in its kinase activity (Gauld and Cambier, 2004; Pao et al., 1997). There have been conflicting reports of CD45 raft association, but this may be due in part to the experimental approaches that were used. Cheng *et al.* were unable to detect CD45 in detergent-insoluble raft fractions following BCR stimulation, and proposed a model in which CD45 was excluded from rafts to permit amplification of raft-localized phosphotyrosine signalling (Cheng et al., 1999). In contrast, live cell imaging of stimulated B cells demonstrated colocalization of CD45 and raft markers providing some

evidence (though it is not definitive due to the limited resolution of light microscopy) that CD45 is associated with at least some subsets of rafts (Gupta and DeFranco, 2003). Whether CD45 is localized to, or excluded from, rafts at various times after BCR stimulation is still an open question. Nevertheless, the studies described above suggest that rafts are important in the regulation of the subcellular localization of both Csk and CD45, and therefore, in their access to and regulation of Lyn. To the best of my knowledge, there have been no reports of altered Csk or CD45 function in GPI-deficient cells, although it is tempting to speculate that alterations in raft structure or composition in GPI-deficient cells might change the localization or activity of either Csk or CD45 and alter the balance of Src family kinase activation in resting or stimulated B cells. If this were the case, it might provide an explanation for the reduced protein tyrosine phosphorylation in GPI-deficient rafts proximal to BCR activation.

A number of positive and negative coreceptors can modulate the strength and quality of the BCR signal depending on the context of activation, and some of these receptors have been found in rafts. An important positive regulatory coreceptor in B cell responses is the transmembrane protein CD19. BCR crosslinking induces Lyn-dependent tyrosine phosphorylation of residues on the cytoplasmic tail of CD19, which results in the recruitment and activation of downstream signalling effectors, including PI3K, Btk, and Vav, leading to increased BCR signalling (Dal Porto et al., 2004; Niiro and Clark, 2002). CD19 and Lyn are thought to be involved in a "progressive amplification loop" that enhances BCR-induced signals. In this model, Lyn is essential for CD19 phosphorylation, and phosphorylated CD19 is then able to further recruit and activate Lyn (Gauld and Cambier, 2004). Studies in CD19 knockout cells have shown that lack

of CD19 leads to a reduction in tyrosine phosphorylation of multiple effector molecules after BCR stimulation, including Lyn (Buhl et al., 1997). CD19 has been shown to translocate into lipid rafts after BCR engagement, where it appears to prolong BCR signalling, and delay BCR internalization from rafts (Cherukuri et al., 2001; Cherukuri et al., 2004; Zipfel et al., 2000). It is possible that the loss of GPI-anchored proteins indirectly affects the Igα/Igβ signal by decreasing CD19 signalling. This might occur through downregulation of Lyn's association with CD19, a decrease in the kinase activity of the specific subset of Lyn molecules that associate with CD19, or other Lyn-independent alterations in the assembly or activity of the CD19 signalling complex. All of the previous mechanisms could plausibly take place in lipid rafts, explaining the decrease in raft protein tyrosine phosphorylation that occurs due to the loss of GPI-anchored proteins in Ramos517 cells.

Alternatively, hyperactivation of signalling via the negative regulatory coreceptor CD22 might be responsible for the decrease in raft phosphotyrosine signalling in GPI-deficient Ramos517 cells. CD22 contains three ITIMs in its cytoplasmic domain that are phosphorylated by Lyn after BCR ligation. CD22's inhibitory effects are mediated in part by recruitment of the tyrosine phosphatase SHP-1, whose possible substrates include Igα, Igβ, Vav, Syk, and CD22 itself (Dal Porto et al., 2004). It is thought that CD19 and CD22 oppose each other in regulating BCR signal strength (Gauld and Cambier, 2004), and as such, it is also possible that increased signalling downstream of CD22 might be responsible for decreased phosphotyrosine signalling in the GPI-deficient cells. CD22 is a member of the Siglec (sialic-acid-binding immunoglobulin-like lectin) family, which binds to α2,6-linked sialic acid residues via its extracellular amino-terminal Ig-like

domain (Nitschke, 2005). This sugar structure is commonly found on N-linked glycans on the surface of many cell types, and various B cell membrane glycoproteins, including IgM and CD45, are modified with N-glycan structures containing α2,6-sialic acid moieties. Corresponding with this observation, CD22 is known to interact constitutively with IgM and CD45 molecules on the surface of the same cell (Nitschke, 2005). Many GPI-anchored proteins are extensively N-glycosylated, and might be potential CD22 binding partners, though there have been no reports to date of endogenous GPI-anchored proteins interacting with CD22. However, one study has shown that the peptide portion of a soluble chimeric version of the GPI-anchored protein Ly-6A/E binds to CD22 on B cells, though this interaction seems to be independent of CD22's sialolectin activity (Pflugh et al., 2002). Since CD22 and Ly-6A/E are coexpressed on the surface of mature B cells, these authors proposed a speculative model in which Ly-6A/E binding acted to recruit and concentrate CD22 in lipid rafts, where it could exert its inhibitory effect on BCR signalling. However, if this were true, one might predict that there would be enhanced BCR signalling in GPI-deficient cells, as CD22 would presumably be lost from these domains, and less able to inhibit raft-localized BCR signals. Instead, I have observed either a reduction (with respect to phosphotyrosine; Figure 4.8) or no change (with respect to calcium flux; Figure 4.9) in BCR-mediated signalling in GPI-deficient cells. Instead, I would propose an alternative model that is more consistent with the results described in this chapter, in which GPI-anchored protein interactions with CD22 negatively regulate CD22 signalling by decreasing the degree to which CD22 can cluster with IgM. In GPI-deficient cells, the loss of GPI-anchored proteins might then enable increased access of CD22 to the BCR signalling complex

leading to increased activation of one or more of the inhibitory signals downstream of CD22. Support for this model comes from studies in T cells, in which a glycoprotein lattice increases the threshold for TCR activation by sterically restricting TCR recruitment and clustering at the site of antigen presentation (Demetriou et al., 2001). The glycoprotein lattice is formed by the binding of soluble galectin-3 to plasma membrane glycoproteins carrying the galectin-3-specific ligand, N-acetyllactosamine, on their N-glycan sugar chains. Disruption of the glycoprotein lattice with soluble sugars (to compete off galectins), or by genetic knockout of N-aceytllactosamine synthesis, caused enhanced TCR clustering leading to increased signalling and autoimmunity (Demetriou et al., 2001). One could envision a similar scenario in B cells, where extensively glycosylated GPI-anchored proteins interacting with galectins could control the clustering of entire rafts, or of subsets of raft components, and thereby affect signalling by regulating the spatial organization of the multicomponent signalling complexes that assemble in response to BCR stimulation. It is of interest in this regard that galectins have been identified in raft fractions isolated from myeloid and erythroid cells in proteomics experiments described in this work and performed by others in our laboratory (Table 3.6; Table 3.7; M.Resek, M. Ridyard, and S. Robbins, unpublished data).

Splenic B cells isolated from Cbl knockout mice display a general reduction of tyrosine phosphorylation in whole cell lysates isolated from resting and BCR-stimulated cells (Shao et al., 2004) that is reminiscent of the reduction in BCR-induced tyrosine phosphorylation observed here in GPI-deficient Ramos517 cells. In the Cbl-/- cells, the authors also specifically observed decreased phosphorylation of Syk and Btk following BCR crosslinking (Shao et al., 2004). Splenic B cells are induced to proliferate upon

BCR ligation, and this response is also inhibited (Shao et al., 2004). This observation is consistent with the reduction of the BCR-induced response in GPI-deficient Ramos517 cells downstream of the attenuated phosphotyrosine signalling cascade. However, in contrast to the results in GPI-deficient cells, the Cbl-/- B cells also had decreased calcium mobilization. Cbl functions as an adaptor protein, but also has E3 ubiquitin ligase activity mediated by its RING finger domain (Thien and Langdon, 2005). Cbl binds to specific signalling proteins and receptors via its multiple protein-protein interaction domains, initiating their ubiquitination and subsequent proteasome-mediated degradation. In the Cbl-/- B cells, Lyn activity was upregulated due to the absence of Cbl-mediated ubiquitination and degradation of Lyn. Increased recruitment of Lyn to CD19 enhanced CD19 signalling. Though the phenotype of the Cbl-/- B cells is not entirely consistent with that in GPI-deficient cells, it does provide an example of a context in which a similar change in anti-IgM-mediated phosphotyrosine signalling is correlated with reduced B cell responses, supporting the idea that the decrease in raft protein tyrosine phosphorylation in GPI-deficient cells is directly linked to the reduction in growth inhibition and apoptosis that is observed. This in turn supports the stated hypothesis that the loss of GPI-anchored proteins alters raft-dependent signalling in Ramos517 cells (as illustrated by the reduced protein tyrosine phosphorylation in rafts) in a manner which significantly impacts the biological response to antigen receptor engagement.

Once tyrosine kinases such as Lyn, Syk, Btk and PI3K are activated, the elevation of intracellular calcium is an important next step in BCR signal transduction. The BCR-mediated calcium flux is initially dependent on the recruitment and activation of PLCγ2, which hydrolyzes PIP_2 to form diacylglycerol (DAG) and IP_3 (DeFranco, 1997). The

former second messenger activates most isoforms of PKC, while the latter is responsible for inducing the release of calcium from intracellular stores. Sustained elevation of intracellular free calcium involves the entry of extracellular calcium through plasma membrane calcium channels (DeFranco, 1997; Li et al., 2003a). There are several lines of evidence implicating a role for rafts in the initiation or regulation of BCR calcium signals. PIP_2 is enriched in rafts in several cell types (Hope and Pike, 1996; Petrie et al., 2000; Xavier et al., 1998), and IP_3 has been reported to accumulate in raft fractions after BCR stimulation (Petrie et al., 2000). It is thought that CD20 is a component of a store-operated calcium channel that regulates the BCR-induced calcium flux (Li et al., 2003a). CD20 has been shown to transiently colocalize with the BCR upon antigen receptor engagement (Petrie and Deans, 2002), and both cholesterol depletion and downregulation of CD20 using siRNA inhibit BCR-induced calcium influx (Li et al., 2003a). Consistent with the idea that at least some PLCγ2 activation occurs within rafts, Guo *et al.* showed that proteins necessary for activation of PLCγ2, including Lyn, Syk, Btk, the adaptor protein BLNK, and PI3K, copurified with a subset of PLCγ2 in detergent-insoluble raft fractions isolated in pre-B cells, and that pre-treatment of cells with MβCD or nystatin inhibited the pre-BCR-induced calcium flux (Guo et al., 2000). In mature B cells, PLCγ2 appears to translocate to raft fractions after BCR stimulation (Aman and Ravichandran, 2000). Pretreatment of cells with different cholesterol-depleting drugs has had contradictory effects on the BCR-induced calcium flux, which is likely due to the different mechanisms of action of each drug resulting in different effects on raft structure. MβCD, which extracts cholesterol from the plasma membrane, has

been observed to either enhance (Awasthi-Kalia et al., 2001), or leave unchanged (Unruh et al., 2005) the calcium flux observed after anti-IgM crosslinking of Ramos and tonsillar B cells. In contrast, filipin, which inserts into the membrane where it binds and sequesters cholesterol, has been found to inhibit the BCR-induced calcium flux (Aman and Ravichandran, 2000; Awasthi-Kalia et al., 2001). Though the exact role of rafts in the calcium response initiated downstream of the BCR still needs to be clarified, it seems likely based on the above observations that raft-dependent signalling does play a role in the regulation of BCR-induced calcium signalling. Taken together, these observations suggest that there are several (not necessarily mutally exclusive) explanations for the observation that calcium signalling is unaffected in GPI-deficient Ramos517 cells, in spite of the changes apparent in raft phosphotyrosine signalling following BCR stimulation. First, it is possible that calcium signalling in these cells is initiated in distinct subsets of rafts that are not affected by the loss of GPI-anchored proteins, whereas the tyrosine kinase-mediated signalling is concentrated in rafts that are affected by GPI-deficiency. The data presented here are consistent with the idea that some raft-mediated signals are unaffected by the loss of GPI-anchored proteins from B cell rafts. Specifically, the observation that CD20 expression levels and raft association are not changed in GPI-deficient cells (Figures 4.13, 4.14, 4.15, 4.16 and 4.17), combined with the observation that the BCR-induced calcium flux is similarly unaffected (Figure 4.9) provides direct evidence that at least one raft-localized signal downstream of the BCR (*i.e.* CD20's calcium channel-dependent regulation of BCR-induced calcium signalling) is not affected by the lack of expression of GPI-anchored proteins. In addition, the lack of an effect of GPI deficiency on the BCR-induced calcium response also implies that the

tyrosine kinase signalling cascade upstream of PLCγ2 activation and calcium mobilization is unaffected by alterations to the structure of rafts in GPI-deficient cells. This data may imply that distinct subsets of rafts exist in GPI-deficient cells—some of which are structurally and functionally affected by the loss of GPI-anchored proteins, and other raft subsets that are not. It is also possible that any changes in the structure of CD20-containing rafts introduced by GPI deficiency do not affect CD20's function as a store-operated calcium channel (though they may affect signalling initiated by CD20 hypercrosslinking, as discussed below). Similarly, PLCγ2 activation may be unaffected by GPI-dependent changes in raft structure, even though many other signalling events dependent on protein tyrosine phosphorylation are affected in rafts in GPI-deficient cells. Alternatively, it is possible that lipid rafts may be dispensable for BCR-stimulated PLCγ2 activation and phosphoinositide hydrolysis in Ramos cells.

Cholesterol is essential in the maintenance of the integrity of lipid raft domains, and relative cholesterol levels might also affect the function of raft-associated proteins. Recently, developmentally regulated differences in membrane cholesterol content have been linked to raft function in B cells (Karnell et al., 2005). This study demonstrated that transitional immature B cells maintained significantly lower membrane cholesterol content than mature splenic B cells and relative cholesterol content affected the ability of the BCR to translocate to lipid rafts. In immature B cells, the BCR fails to enter into rafts after BCR stimulation, whereas it is able to do so in mature cells (Sproul et al., 2000). The authors found that culturing immature B cells in medium enriched in a MβCD/cholesterol mixture increased their membrane cholesterol and increased the

amount and types of proteins in isolated raft fractions in a manner that resembled mature B cells (Karnell et al., 2005). Cholesterol enrichment of immature cells also enabled the BCR translocation to raft fractions following BCR crosslinking and altered their signalling phenotype to resemble that of mature cells (specifically, increased activation of PLCγ2 and sustained expression of c-myc) (Karnell et al., 2005). Since previous evidence suggested that membrane and raft cholesterol levels were altered in a GPI-deficient T lymphoma cell line and in erythrocytes isolated from PNH patients (Abrami et al., 2001; Samuel et al., 2001), the cholesterol content of GPI-deficient and wildtype Ramos517 cells was compared, to see if there was evidence for a cholesterol-dependent effect on lipid raft structure that might explain the differences in signalling and growth observed in these cell lines. In contrast to the previous reports in the literature, both total and raft cholesterol levels were found to be similar in GPI-deficient and wildtype B cell and erythroid cell lines (Figure 4.21). It is possible that some of these differences might be explained by cell type dependent differences. Another possibility is that the difference between the current results and those in the literature are due to the different isolation procedures and/or cholesterol assays used. Both the T cell paper (Abrami et al., 2001), and the erythrocyte paper (Samuel et al., 2001) analyzed total membrane cholesterol following chloroform/methanol extraction of cell extracts, whereas in this study, cholesterol was measured in whole cell detergent lysates that were not subjected to any further extraction or fractionation procedures. It is possible that the presence or absence of GPI-anchored proteins differentially affected the efficiency of the chloroform/methanol extraction. On the other hand, in the analysis of PNH erythrocytes, the increase in membrane cholesterol in GPI-deficient cells was confirmed independently

by flow cytometry with the cholesterol-binding drug filipin. In a single experiment comparing GPI-positive and GPI-negative Raji26 B cells, I could detect no differences in the level of filipin staining by flow cytometry (data not shown), which is consistent with the results obtained by quantitating cholesterol in Raji26 cell lysates. This suggests that the increased cholesterol content observed in some other GPI-deficient cells is probably real, but that increased membrane cholesterol is not a universal feature of PNH cells. It is possible that this discrepancy reflects tissue-specific differences in the regulation of cholesterol homeostasis. In any case, there is no evidence to suggest that alterations in cholesterol levels that would affect lipid raft structure or the activity of raft-associated molecules are present in GPI-deficient Ramos517 cells, and therefore, cholesterol-dependent effects do not explain the changes in raft-mediated signalling that are observed in these cells.

The data presented here also demonstrate that the loss of GPI-anchored protein expression caused a decrease in the levels of growth inhibition and apoptosis observed in Ramos517 cells following hypercrosslinking of CD20 (Figures 4.10, 4.11, and 4.12). The calcium flux generated by CD20 hypercrosslinking in Ramos cells has previously been shown to be raft-dependent on the basis of both biochemical and functional data (Janas et al., 2005; Unruh et al., 2005). The fact that a delay in the calcium flux induced by CD20 hypercrosslinking (Figure 4.18) was directly correlated with the resistance to growth inhibition and apoptosis in GPI-deficient cells supports the hypothesis that the loss of GPI-anchored proteins affects the structure or organization of lipid rafts, altering their function in signal transduction and changing the extent of the biological response. In support of this, there is evidence that rituximab-induced CD20 translocation to lipid

rafts alters the membrane organization and function of lipid rafts in the Raji B lymphoma cell line (Semac et al., 2003) and that CD20 associates with GPI-anchored proteins (Li et al., 2004a; Semac et al., 2003). In Raji cells, CD20 translocation did not appear to alter the gross protein and lipid composition of Triton-insoluble raft fractions, but it did cause both sphingolipids and Cbp to become more resistant to extraction by n-octyl-β-pyranoside, which is a detergent that dissociates sphingolipid clusters (Semac et al., 2003). In Raji cells that express high levels of Cbp, Lyn kinase activity was downregulated by CD20 translocation, but in another cell line expressing lower levels of Cbp, Lyn kinase activity was unaffected (Semac et al., 2003). Interestingly, in the same report, redistribution of CD20 in rafts was shown to significantly increase the susceptibility of the GPI-anchored protein CD55 to cleavage by PI-PLC and PI-PLD (Semac et al., 2003). Overall, these observations support the hypothesis that changes in raft structure caused by the loss of GPI-anchored proteins could directly affect the signalling complex assembled following hypercrosslinking of CD20, and explain the alterations in calcium signalling and apoptosis observed in GPI-deficient Ramos517 cells. Interestingly, the anti-CD20 antibody B1, unlike rituximab, fails to induce translocation of CD20 into Triton-insoluble raft fractions, and is reported to induce apoptosis via a raft-independent pathway (Chan et al., 2003). In the future, it would be interesting to compare the extent of B1-induced apoptosis in GPI-deficient and wildtype Ramos517 cells. If crosslinking of CD20 using B1 induced similar levels of apoptosis in GPI-negative and GPI-positive cells, this would provide additional evidence that GPI deficiency results in raft-specific alterations in signalling.

It is important to note that the GPI-dependent differences in calcium signalling induced by CD20 hypercrosslinking do not contradict the observation that the anti-IgM-induced calcium flux is unaffected by GPI deficiency, as there is clear evidence that the signal initiated by CD20 hypercrosslinking occurs independently of CD20's postulated function as a calcium channel (Unruh et al., 2005). Rather, crosslinking of CD20 by rituximab is thought to induce apoptosis by the serendipitous clustering of lipid rafts enriched in Src family kinases, which CD20 becomes stably associated with upon antibody binding (Deans et al., 2002; Unruh et al., 2005). Transactivation of the clustered Src family kinases is then thought to lead to activation of PLCγ and mobilization of intracellular calcium (Figure 4.2, (Deans et al., 2002; Unruh et al., 2005)). Since both Src family kinases and PLCγ are implicated upstream of calcium signalling in response to crosslinking of the BCR as well, it is important to consider why anti-IgM-mediated calcium signalling would be unaffected by GPI deficiency, even though the calcium response to CD20 hypercrosslinking is altered. Dysregulation of Src family kinase activity in the GPI-deficient Ramos517 B cells could explain both the reduced raft phosphotyrosine signalling observed before and after BCR stimulation, and the delayed calcium response after hypercrosslinking of CD20. These results also indicate that PLCγ activation must be inhibited in response to CD20 crosslinking, but not BCR crosslinking in GPI-deficient cells. This might be explained by activation of distinct subcellular pools of PLCγ in response to the two different stimuli or by differences in the specific Src family kinases or other upstream signalling events that lead to PLCγ activation in response to the two different stimuli.

Since GPI-deficient Ramos517 cells were resistant to growth inhibition and apoptosis downstream of both BCR and CD20 crosslinking, it was of interest to determine whether or not these cells were also resistant to other apoptosis-inducing stimuli. Some reports have suggested that PNH cells are resistant to apoptosis induced by multiple stimuli, and that this is one of the reasons that the PNH clone is able to expand in comparison to normal cells (Brodsky et al., 1997; Horikawa et al., 1997; Ismail et al., 2003). In addition, if the GPI-deficient cells were generally resistant to apoptosis due to GPI-dependent but raft-independent changes, this would present a confounding factor in the analysis of raft-dependent changes in apoptotic signalling. For these reasons, the response of GPI-positive and GPI-negative Ramos517 cells to two additional apoptosis-inducing stimuli, UV radiation and H_2O_2 was compared. The observation that the GPI-deficient cells appear to have a similar level of susceptibility to H_2O_2-mediated apoptosis (Figure 4.20) suggests that resistance to apoptosis in these cells is specific to certain stimuli, and that a generalized constitutive resistance to apoptosis is not present within these cells. In contrast, GPI-deficient Ramos517 cells are strikingly resistant to apoptosis induced by UV irradiation (Figure 4.19). At present the raft-dependence or independence of UV-induced apoptosis in Ramos517 cells is unknown. Although DNA is a primary target of UV damage, UV irradiation has also been shown to directly affect multiple cell membrane and cytoplasmic targets, including membrane receptors, kinases, phosphatases, and transcription factors (Bender et al., 1997; Schwarz, 1998). It is conceivable that some of the targets of UV irradiation in Ramos517 cells are raft-associated, and that their UV-induced activation might be involved in signalling apoptosis. In this regard, UV irradiation of Ramos cells has previously been observed to

induce rapid tyrosine phosphorylation of a number of cellular proteins (Schieven et al., 1993). In the future, it would be interesting to see if cholesterol depletion of wildtype Ramos517 B cells inhibited UV-induced apoptosis to determine if there was a possible raft-dependent effect. If so, it might be of interest to further investigate the molecular basis of the resistance to UV-induced apoptosis in GPI-deficient cells.

In conclusion, GPI-deficient Ramos517 cells have been shown to be resistant to growth inhibition and apoptosis induced by BCR stimulation, UV irradiation, and CD20 hypercrosslinking, but not to apoptosis induced by treatment with H_2O_2. With respect to BCR signalling, although BCR expression levels and ability to translocate to lipid rafts are not affected by the absence of GPI-anchored protein expression, there is a significant reduction in the level of protein tyrosine phosphorylation observed in raft fractions. Although calcium signalling in response to BCR stimulation is not affected by the loss of GPI-anchored proteins, a delay in the calcium flux induced by rituximab-mediated hypercrosslinking of CD20 was observed. Taken together, these observations support a model in which alterations in raft structure and/or organization caused by the absence of GPI-anchored proteins change the quality of the raft-mediated signal, leading to differences in the cell's response to these stimuli. Further investigation of the specific molecular mechanisms involved should improve our understanding of the pathogenesis of PNH, and provide insight into the regulation of B cell signalling by GPI-anchored proteins and lipid rafts.

Chapter Five: Final Conclusions

Lipid rafts are liquid-ordered membrane microdomains enriched in specific proteins, cholesterol, and glycosphingolipids, which participate in the regulation of many cellular functions including signal transduction (Simons and Toomre, 2000; Smart et al., 1999; Zajchowski and Robbins, 2002). The highly organized, yet highly dynamic nature of lipid rafts is a distinctive feature of these membrane microdomains that enables them to function effectively in the organization of signalling complexes. Only a subset of membrane proteins appears to be enriched in rafts. Although relatively little is known about how this targeting is achieved in many instances, transmembrane sequences, lipid modifications and protein-protein interactions with resident raft proteins appear to be involved in the sorting of specific proteins into lipid rafts (Kimura et al., 2001; Morrow and Parton, 2005; Robbins et al., 1995; Scheiffele et al., 1997; Yamabhai and Anderson, 2002). It is also apparent that raft proteins and lipids can move in or out of rafts, and that smaller rafts can be induced to cluster into large assemblies, in response to specific cellular signals. The high degree of organization and specificity that characterizes rafts is also illustrated by the heterogeneous nature of these microdomains. The protein and lipid composition of rafts varies in different cell types. Distinct subpopulations of lipid rafts, with different protein and lipid compositions, are also present in the membranes of a single cell. Combined, all of these lipid raft properties enable the cell to employ multiple mechanisms to facilitate and regulate specific compartmentalized signal transduction pathways.

The overall hypothesis of this thesis is that the specific properties of a given lipid raft, including its protein and lipid composition, size, structure, abundance, and

localization, define its function in signal transduction. In simpler terms, raft structure translates into raft function. This hypothesis predicts that changes in the properties of lipid rafts caused by physiological or pathological events can alter raft-mediated signalling and its consequent biological effects.

As a means of investigating a major component of raft structure that could provide potential insight into raft function, I chose to use a novel and relatively unbiased proteomic approach to analyze the protein composition of lipid raft fractions isolated from hematopoietic cells. These experiments successfully identified a large number of novel and previously characterized raft proteins. A surprisingly large number of the novel raft proteins were observed to localize primarily to the ER and the mitochondria, although rafts were not previously known to exist in these subcellular locations. These observations have been corroborated by other reports in the literature and reflect the likely presence of lipid rafts in mitochondrial and ER membranes. The identification of raft-associated ER and mitochondrial proteins also illustrates the value of the unbiased nature of global proteomic approaches, as earlier studies examining raft protein composition using more classical targeted approaches failed to identify these raft constituents. Further characterization of the structure, organization, and functional significance of rafts in ER and mitochondrial membranes would be an interesting avenue to pursue in the future that is likely to provide additional novel insights into lipid raft biology. In particular, these studies could be directed towards analyzing a potentially novel role of lipid rafts in facilitating inter-organelle communication. The regulation of inter-organelle cross-talk between the plasma membrane, the ER, and the mitochondria is vitally important in the delivery and integration of pro-apoptotic signals generated as a

result of ER stress or downstream of receptor-mediated signals (d'Azzo et al., 2006; Le Bras et al., 2006). Gangliosides, which are enriched in rafts, are believed to have an important role in the coordination of ER and mitochondrial calcium signalling in this context (d'Azzo et al., 2006). An open question in lipid raft biology is whether or not lipid raft signalling function is coordinately regulated with other raft functions in membrane transport processes or cholesterol homeostasis. Future characterization of the potential contribution of raft-dependent vesicular trafficking and/or raft-dependent organization of inter-membrane contact sites in the modulation of cross-talk between these different organelles during apoptosis could begin to provide answers to these questions.

The Robbins' laboratory was interested in further characterizing the structure and function of non-caveolar lipid rafts in cells of hematopoietic origin because we thought that these rafts might have unique properties or be governed by unique regulatory mechanisms. However, the results of the proteomics experiments described herein have generally not supported this idea. In contrast, many of the proteins identified in the myeloid and erythroid cell lines examined here are also identified in the proteomes of an exceptionally diverse array of non-hematopoietic cells, most of which express caveolins and have identifiable caveolae on their cell surface. The commonly identified proteins include cytoskeletal, mitochondrial, and ER proteins, members of the prohibitin family, proteins involved in vesicular trafficking, and heterotrimeric G proteins. The existence of a common lipid raft proteome implies that rafts share similar structural and functional roles in many different cell types. This idea is supported by evidence that lipid rafts are found not only in the membranes of mammalian cells, but also in many other eukaryotes,

including yeast (Insenser et al., 2006; Wachtler et al., 2006), plants (Borner et al., 2005; Peskan et al., 2000), Dictyostelium (Morrow and Parton, 2005), fruit flies (Eroglu et al., 2003; Zhai et al., 2004), and worms (Sedensky et al., 2004). Taken together, these observations suggest that the structure and function of these domains has been conserved as a fundamental mechanism responsible for the lateral organization of membrane proteins and lipids. Components of the common lipid raft proteome may be involved in conserved regulatory interactions between the cytoskeleton and rafts, in conserved raft-based mechanisms of vesicular trafficking, or in the organization of "housekeeping" metabolic processes or conserved signalling pathways.

This work has also demonstrated the challenges associated with lipid raft proteomics with respect to the identification and analysis of signalling proteins and the development of techniques to efficiently perform differential raft proteomics studies. Since the identification of numerous signalling molecules within lipid rafts had prompted the initial proposal of the lipid raft signalling hypothesis, it was surprising that relatively few signalling molecules were identified in hematopoietic cell raft fractions. However, this is likely due to the relatively low abundance of these molecules, combined with technical limitations during initial implementation of the proteomics experiments. In the future, further fractionation of raft membranes prior to proteomic analysis and continued improvement of the resolution and sensitivity of both gel-based and gel-free proteomics approaches will be necessary to obtain a more comprehensive picture of the signalling and other proteins that are present in relatively low abundance in rafts.

Comparison of the lipid raft proteomes from different cell types in this work, and in other reports in the literature demonstrate that, in addition to a conserved lipid raft

proteome, there are also specific differences in raft protein composition in different cell types that may be related to changes in physiological or pathological factors (*i.e.* to differentiation status, or GPI deficiency, respectively). In the future, the application of increasingly sensitive quantitative gel-based and gel-free MS screens will be of great utility in efficiently screening for and identifying proteins differentially associated with rafts in response to specific signalling events, differentiation events, or disease states.

Since the proteomic experiments described in Chapter 3 were unsuccessful in identifying specific raft proteins whose differential association with rafts in either a physiological or pathological context impacted either known or novel raft-dependent signalling pathways, an alternative approach was enlisted to test the hypothesis that lipid raft structure is intimately linked to its function in signal transduction. The experiments detailed in Chapter 4 were designed to examine the effects of an experimentally defined change in lipid raft structure on signalling pathways that had previously been established to be compartmentalized in rafts. Specifically, the effect of GPI deficiency on raft-mediated signalling in B cells was investigated in order to test the hypothesis that alterations in lipid raft composition or organization caused directly or indirectly by the loss of GPI-anchored proteins would affect lipid raft function in signal transduction. In support of this hypothesis, GPI deficiency caused Ramos517 B cells to become resistant to growth inhibition and apoptosis induced by two separate raft-dependent signalling pathways initiated downstream of BCR or CD20 crosslinking. Consistent with the change in the biological response to engagement of the BCR, the basal and BCR-stimulated levels of raft phosphotyrosine signalling in Ramos517 cells were significantly reduced in the absence of GPI-anchored protein expression, although BCR-induced

calcium flux was unaltered. Also correlating with the decrease in apoptosis induced by CD20 hypercrosslinking, the calcium flux observed after rituximab-mediated hypercrosslinking of CD20 was delayed in the absence of GPI-anchored proteins. Dysregulation of the kinase activity of raft-localized Src family kinases, particularly Lyn, in GPI-deficient cells is a plausible mechanism that could explain both of the observed alterations in raft signalling in GPI-deficient B cells. It would be interesting in the future to examine the regulation of Src family kinase activity associated with the BCR signalling complex, as well as other Src family kinase-dependent B cell coreceptors. Unfortunately, it may be impossible to replicate the initially observed correlation between the resistance to CD20-mediated apoptosis and the delay in calcium signalling observed in GPI-deficient Ramos517 cells, since these cell lines may have altered their responses due to unknown cell-specific or environmental factors. In this instance, it may be beneficial instead to obtain fresh GPI+/- Ramos cell lines in which GPI-anchored protein expression has been stably knocked down by siRNA, or to investigate the possible use of the GPI+/- Raji26 cell lines as alternative model systems in which to further examine the effect of GPI deficiency on raft-mediated CD20 signalling.

The specific nature of the alterations to lipid raft structure or organization that affect the raft-dependent signals downstream of CD20 and BCR crosslinking is currently unknown. The loss of the GPI-anchored proteins themselves may directly disrupt protein-protein, protein-lipid, or lipid-lipid interactions, resulting in changes to the raft microenvironment that affect the activity or spatial organization of specific rafts or of individual raft-localized proteins. Perturbation of the raft microenvironment by any of these mechanisms could ultimately be responsible for the observed differences in

signalling. It is also possible that the levels of other non-GPI raft proteins or lipids are altered in GPI-deficient cells through direct or indirect mechanisms. In support of this possible mechanism, comparison of the silver stains of Triton X100-insoluble and Brij58-insoluble raft fractions isolated from Ramos517 cells demonstrated that raft levels of a small subset of proteins were altered by GPI deficiency, including proteins that are not GPI-anchored since they are enriched in raft fractions isolated from GPI-negative cells. However, the identity of these proteins and whether any of them are functionally important in the signalling pathways examined remains to be determined in the future. In contrast, alterations in total membrane and raft cholesterol are not observed in GPI-deficient Ramos517 cells, and therefore cholesterol-dependent effects on lipid raft structure and organization do not explain the altered signalling in GPI-deficient cells. Taken together, these results support the hypothesis that GPI deficiency in B cells leads to alterations in lipid raft structure or organization that affect lipid raft function in signal transduction and lead to specific changes in biological responses to extracellular stimuli. Further investigation and characterization of the precise molecular mechanisms involved should enhance our understanding of the role of GPI-anchored proteins in the regulation of lipid raft structure and function in signalling in hematopoietic cells. In the future, analysis of the effects of GPI deficiency on these and other raft-mediated signalling pathways in B cells as well as other types of hematopoietic cells could provide insight into the molecular pathogenesis of the human disease PNH. It is tempting to speculate that alterations in the structure and organization of rafts caused by the absence of GPI-anchored proteins in mature cells could lead to aberrant signalling and biological responses in mature hematopoietic cells that could help explain peripheral symptoms of

PNH such as the increased propensity for thrombosis. Similarly, since bone marrow disorders are commonly found in PNH patients, and abnormal hematopoietic stem cell development in the bone marrow is thought to be an important contributing factor to the expansion of the PNH clone (Boccuni et al., 2000; Hall et al., 2002), it is also possible that aberrant raft structure and function in signalling is involved in the abnormal growth and expansion of the GPI-negative stem cells. In the future, it would therefore be of interest to examine raft structure and function in other *in vitro* cell models of GPI deficiency, as well as in primary cells isolated from PNH patients or from the different mouse models of GPI deficiency that are currently available (Abrami et al., 2001; Bastisch et al., 2000; Hazenbos et al., 2004a; Hazenbos et al., 2004b; Jasinski et al., 2001; Keller et al., 2001; Mohney et al., 1994; Murakami et al., 1999).

References

Abrami, L., Fivaz, M., Kobayashi, T., Kinoshita, T., Parton, R. G., and van der Goot, F. G. (2001). Cross-talk between caveolae and glycosylphosphatidylinositol-rich domains. J Biol Chem *276*, 30729-30736.

Abulrob, A., Giuseppin, S., Andrade, M. F., McDermid, A., Moreno, M., and Stanimirovic, D. (2004). Interactions of EGFR and caveolin-1 in human glioblastoma cells: evidence that tyrosine phosphorylation regulates EGFR association with caveolae. Oncogene *23*, 6967-6979.

Achleitner, G., Gaigg, B., Krasser, A., Kainersdorfer, E., Kohlwein, S. D., Perktold, A., Zellnig, G., and Daum, G. (1999). Association between the endoplasmic reticulum and mitochondria of yeast facilitates interorganelle transport of phospholipids through membrane contact. Eur J Biochem *264*, 545-553.

Adachi, H., Kubota, I., Okamura, N., Iwata, H., Tsujimoto, M., Nakazato, H., Nishihara, T., and Noguchi, T. (1989). Purification and characterization of human microsomal dipeptidase. J Biochem (Tokyo) *105*, 957-961.

Ahmed, S. N., Brown, D. A., and London, E. (1997). On the origin of sphingolipid/cholesterol-rich detergent-insoluble cell membranes: physiological concentrations of cholesterol and sphingolipid induce formation of a detergent-insoluble, liquid-ordered lipid phase in model membranes. Biochemistry *36*, 10944-10953.

Alaiya, A. A., Franzen, B., Auer, G., and Linder, S. (2000). Cancer proteomics: from identification of novel markers to creation of artifical learning models for tumor classification. Electrophoresis *21*, 1210-1217.

Alitalo, R. (1990). Induced differentiation of K562 leukemia cells: a model for studies of gene expression in early megakaryoblasts. Leuk Res *14*, 501-514.

Allport, J. R., Donnelly, L. E., Kefalas, P., Lo, G., Nunn, A., Yadollahi-Farsani, M., Rendell, N. B., Murray, S., Taylor, G. W., and MacDermot, J. (1996). A possible role for mono (ADP-ribosyl) transferase in the signalling pathway mediating neutrophil chemotaxis. British Journal of Clinical Pharmacology *42*, 99-106.

Aman, M. J., and Ravichandran, K. S. (2000). A requirement for lipid rafts in B cell receptor induced Ca^{2+} flux. Current Biology *10*, 393-396.

An, S., Park, I. C., Rhee, C. H., Hong, S. I., and Knox, K. (2003a). Temporal ordering of caspase activation and substrate cleavage during antigen receptor-triggered apoptosis in Ramos-Burkitt lymphoma B cells. Int J Oncol *23*, 257-268.

An, S., Park, M. J., Park, I. C., Hong, S. I., and Knox, K. (2003b). Procaspase-3 and its active large subunit localized in both cytoplasm and nucleus are activated following

application of apoptotic stimulus in Ramos-Burkitt lymphoma B cells. Int J Mol Med *12*, 311-317.

Anderson, H. A., Hiltbold, E. M., and Roche, P. A. (2000). Concentration of MHC class II molecules in lipid rafts facilitates antigen presentation. Nat Immunol *1*, 156-162.

Anderson, R. G. (1998). The caveolae membrane system. Annual Reviews in Biochemistry *67*, 199-225.

Anderson, R. G. W. (1993). Plasmalemmal caveolae and GPI-anchored membrane proteins. Current Opinion in Cell Biology *5*, 647-652.

Anderson, R. G. W., Kamen, B. A., Rothberg, K. G., and Lacey, S. W. (1992). Potocytosis: sequestration and transport of small molecules by caveolae. Science *255*, 410-411.

Ardail, D., Gasnier, F., Lerme, F., Simonot, C., Louisot, P., and Gateau-Roesch, O. (1993). Involvement of mitochondrial contact sites in the subcellular compartmentalization of phospholipid biosynthetic enzymes. J Biol Chem *268*, 25985-25992.

Arni, S., Keilbaugh, S. A., Ostermeyer, A. G., and Brown, D. A. (1998). Association of GAP-43 with detergent-resistant membranes requires two palmitoylated cysteine residues. Journal of Biological Chemistry *273*, 28478-28485.

Ashwell, J. D., and D'Oro, U. (1999). CD45 and Src-family kinases: and now for something completely different. Immunol Today *20*, 412-416.

Awasthi-Kalia, M., Schnetkamp, P. P. M., and Deans, J. P. (2001). Differential effects of filipin and methyl-β-cyclodextrin on B cell receptor signaling. Biochemical and Biophysical Research Communications *287*, 77-82.

Babiychuk, E. B., and Draeger, A. (2006). Regulation of ecto-5'-nucleotidase activity via Ca2+-dependent, annexin 2-mediated membrane rearrangement? Biochem Soc Trans *34*, 374-376.

Babiychuk, E. B., Palstra, R. J., Schaller, J., Kampfer, U., and Draeger, A. (1999). Annexin VI participates in the formation of a reversible, membrane-cytoskeleton complex in smooth muscle cells. J Biol Chem *274*, 35191-35195.

Babiychuk, V. S., Draeger, A., and Babiychuk, E. B. (2000). Smooth muscle actomyosin promotes Ca2+-dependent interactions between annexin VI and detergent-insoluble glycosphingolipid-enriched membrane domains. Acta Biochim Pol *47*, 579-589.

Bae, T. J., Kim, M. S., Kim, J. W., Kim, B. W., Choo, H. J., Lee, J. W., Kim, K. B., Lee, C. S., Kim, J. H., Chang, S. Y.*, et al.* (2004). Lipid raft proteome reveals ATP synthase complex in the cell surface. Proteomics *4*, 3536-3548.

Baggerman, G., Vierstraete, E., De Loof, A., and Schoofs, L. (2005). Gel-based versus gel-free proteomics: a review. Comb Chem High Throughput Screen *8*, 669-677.

Bagshaw, R. D., Mahuran, D. J., and Callahan, J. W. (2005). A proteomic analysis of lysosomal integral membrane proteins reveals the diverse composition of the organelle. Mol Cell Proteomics *4*, 133-143.

Balamuth, F., Brogdon, J. L., and Bottomly, K. (2004). CD4 raft association and signaling regulate molecular clustering at the immunological synapse site. J Immunol *172*, 5887-5892.

Banfi, C., Brioschi, M., Wait, R., Begum, S., Gianazza, E., Fratto, P., Polvani, G., Vitali, E., Parolari, A., Mussoni, L., and Tremoli, E. (2006). Proteomic analysis of membrane microdomains derived from both failing and non-failing human hearts. Proteomics *6*, 1976-1988.

Basile, M., Lin, R., Kabbani, N., Karpa, K., Kilimann, M., Simpson, I., and Kester, M. (2006). Paralemmin interacts with D3 dopamine receptors: implications for membrane localization and cAMP signaling. Arch Biochem Biophys *446*, 60-68.

Bastisch, I., Tiede, A., Deckert, M., Ziolek, A., Schmidt, R. E., and Schubert, J. (2000). Glycosylphosphatidylinositol (GPI)-deficient Jurkat T cells as a model to study functions of GPI-anchored proteins. Clin Exp Immunol *122*, 49-54.

Baumruker, T., Csonga, R., Pursch, E., Pfeffer, A., Urtz, N., Sutton, S., Bofill-Cardona, E., Cooke, M., and Prieschl, E. (2003). Activation of mast cells by incorporation of cholesterol into rafts. Int Immunol *15*, 1207-1218.

Becher, A., and McIlhinney, R. A. (2005). Consequences of lipid raft association on G-protein-coupled receptor function. Biochem Soc Symp, 151-164.

Bender, K., Blattner, C., Knebel, A., Iordanov, M., Herrlich, P., and Rahmsdorf, H. J. (1997). UV-induced signal transduction. J Photochem Photobiol B *37*, 1-17.

Berger, M. L., Wilson, H. M., and Liss, C. L. (1996). A comparison of the tolerability and efficacy of lovastatin 20 mg and fluvastatin 20 mg in the treatment of primary hypercholesterolemia. Journal of Cardiovascular Pharmacological Therapy *1*, 101-106.

Berkelman, T., and Stenstedt, T. (2001). 2-D Electrophoresis: Principles and Methods (Uppsala, Sweden, Amersham Biosciences).

Bezombes, C., Grazide, S., Garret, C., Fabre, C., Quillet-Mary, A., Muller, S., Jaffrezou, J. P., and Laurent, G. (2004). Rituximab antiproliferative effect in B-lymphoma cells is

associated with acid-sphingomyelinase activation in raft microdomains. Blood *104*, 1166-1173.

Bi, K., and Altman, A. (2001). Membrane lipid microdomains and the role of PKCθ in T cell activation. Seminars in Immunology *13*, 139-146.

Bi, K., Tanaka, Y., Coudronniere, N., Sugie, K., Hong, S., van Stipdonk, M. J. B., and Altman, A. (2001). Antigen-induced translocation of PKC-theta to membrane rafts is required for T cell activation. Nature Immunology *2*, 556-563.

Bickel, P. E., Scherer, P. E., Schnitzer, J. E., Oh, P., Lisanti, M. P., and Lodish, H. F. (1997). Flotillin and epidermal surface antigen define a new family of caveolae-associated integral membrane proteins. *272*, 13793-13802.

Bini, L., Pacini, S., Liberatori, S., Valensin, S., Pellegrini, M., Raggiaschi, R., Pallini, V., and Baldari, C. T. (2003). Extensive temporally regulated reorganization of the lipid raft proteome following T-cell antigen receptor triggering. Biochem J *369*, 301-309.

Blonder, J., Hale, M. L., Chan, K. C., Yu, L. R., Lucas, D. A., Conrads, T. P., Zhou, M., Popoff, M. R., Issaq, H. J., Stiles, B. G., and Veenstra, T. D. (2005). Quantitative profiling of the detergent-resistant membrane proteome of iota-b toxin induced vero cells. J Proteome Res *4*, 523-531.

Blonder, J., Hale, M. L., Lucas, D. A., Schaefer, C. F., Yu, L. R., Conrads, T. P., Issaq, H. J., Stiles, B. G., and Veenstra, T. D. (2004a). Proteomic analysis of detergent-resistant membrane rafts. Electrophoresis *25*, 1307-1318.

Blonder, J., Terunuma, A., Conrads, T. P., Chan, K. C., Yee, C., Lucas, D. A., Schaefer, C. F., Yu, L. R., Issaq, H. J., Veenstra, T. D., and Vogel, J. C. (2004b). A proteomic characterization of the plasma membrane of human epidermis by high-throughput mass spectrometry. J Invest Dermatol *123*, 691-699.

Blum, H., Beier, H., and Gross, H. J. (1987). Improved silver staining of plant proteins, RNA and DNA in polyacrylamide gels. Electrophoresis *8*, 93-99.

Boccuni, P., Del Vecchio, L., Di Noto, R., and Rotoli, B. (2000). Glycosyl phosphatidylinositol (GPI)-anchored molecules and the pathogenesis of paroxysmal nocturnal hemoglobinuria. Crit Rev Oncol Hematol *33*, 25-43.

Bonnin, S., El Kirat, K., Becchi, M., Dubois, M., Grangeasse, C., Giraud, C., Prigent, A. F., Lagarde, M., Roux, B., and Besson, F. (2003). Protein and lipid analysis of detergent-resistant membranes isolated from bovine kidney. Biochimie *85*, 1237-1244.

Borner, G. H., Sherrier, D. J., Weimar, T., Michaelson, L. V., Hawkins, N. D., Macaskill, A., Napier, J. A., Beale, M. H., Lilley, K. S., and Dupree, P. (2005). Analysis of

detergent-resistant membranes in Arabidopsis. Evidence for plasma membrane lipid rafts. Plant Physiol *137*, 104-116.

Bos, J. L. (1989). Ras oncogenes in human cancer: a review. Cancer Research *49*, 4682-4689.

Braccia, A., Villani, M., Immerdal, L., Niels-Christiansen, L. L., Nystrom, B. T., Hansen, G. H., and Danielsen, E. M. (2003). Microvillar membrane microdomains exist at physiological temperature. Role of galectin-4 as lipid raft stabilizer revealed by "superrafts". J Biol Chem *278*, 15679-15684.

Brdicka, T., Cerny, J., and Horejsi, V. (1998). T cell receptor signalling results in rapid tyrosine phosphorylation of the linker protein LAT present in detergent-resistant microdomains. Biochemical and Biophysical Research Communications *248*, 356-360.

Brdicka, T., Pavlistova, D., Leo, A., Bruyns, E., Korinek, V., Angelisova, P., Scherer, J., Shevchenko, A., Shevchenko, A., Hilgert, I., *et al.* (2000). Phosphoprotein associated with glycosphingolipid-enriched microdomains (PAG), a novel ubiquitously expressed transmembrane adaptor protein, binds the tyrosine kinase Csk and is involved in regulation of T cell activation. Journal of Experimental Medicine *191*, 1591-1604.

Brodsky, R. A., Vala, M. S., Barber, J. P., Medof, M. E., and Jones, R. J. (1997). Resistance to apoptosis caused by PIG-A gene mutations in paroxysmal nocturnal hemoglobinuria. Proceedings of the National Academy of Sciences USA *94*, 8756-8760.

Bromley, S. K., Burack, W. R., Johnson, K. G., Somersalo, K., Sims, T. N., Sumen, C., Davis, M. M., Shaw, A. S., Allen, P. M., and Dustin, M. L. (2001). The immunological synapse. Annual Reviews in Immunology *19*, 375-396.

Browman, D. T., Resek, M. E., Zajchowski, L. D., and Robbins, S. M. (2006). Erlin-1 and erlin-2 are novel members of the prohibitin family of proteins that define lipid-raft-like domains of the ER. J Cell Sci *119*, 3149-3160.

Brown, D. A., and London, E. (1997). Structure of detergent-resistant membrane domains: does phase separation occur in biological membranes? Biochemical and Biophysical Research Communications *240*, 1-7.

Brown, D. A., and Rose, J. K. (1992). Sorting of GPI-anchored proteins to glycolipid-enriched membrane subdomains during transport to the apical cell surface. Cell *68*, 533-544.

Buhl, A. M., Pleiman, C. M., Rickert, R. C., and Cambier, J. C. (1997). Qualitative regulation of B cell antigen receptor signaling by CD19: selective requirement for PI3-kinase activation, inositol-1,4,5-trisphosphate production and Ca2+ mobilization. J Exp Med *186*, 1897-1910.

Cashman, N. R., Loertscher, R., Nalbantoglu, J., Shaw, I., Kascsak, R. J., Bolton, D. C., and Bendheim, P. E. (1990). Cellular isoform of the scrapie agent protein participates in lymphocyte activation. Cell *61*.

Champagne, E., Martinez, L. O., Collet, X., and Barbaras, R. (2006). Ecto-F1Fo ATP synthase/F1 ATPase: metabolic and immunological functions. Curr Opin Lipidol *17*, 279-284.

Chan, B. L., Chao, M. V., and Saltiel, A. R. (1989). Nerve growth factor stimulates the hydrolysis of glycosyl-phosphatidylinositol in PC-12 cells: a mechanism of protein kinase C regulation. Proceedings of the National Academy of Sciences USA *86*, 1756-1760.

Chan, H. T., Hughes, D., French, R. R., Tutt, A. L., Walshe, C. A., Teeling, J. L., Glennie, M. J., and Cragg, M. S. (2003). CD20-induced lymphoma cell death is independent of both caspases and its redistribution into triton X-100 insoluble membrane rafts. Cancer Res *63*, 5480-5489.

Chang, W.-J., Ying, Y.-S., Rothberg, K. G., Hooper, N. M., Turner, A. J., Gambliel, H. A., De Gunzberg, J., Mumby, S. M., Gilman, A. G., and Anderson, R. G. W. (1994a). Purification and characterization of smooth muscle cell caveolae. Journal of Cell Biology *126*, 127-138.

Chang, W. J., Ying, Y. S., Rothberg, K. G., Hooper, N. M., Turner, A. J., Gambliel, H. A., De Gunzburg, J., Mumby, S. M., Gilman, A. G., and Anderson, R. G. (1994b). Purification and characterization of smooth muscle cell caveolae. J Cell Biol *126*, 127-138.

Chapman, H. A. (1997). Plasminogen activators, integrins, and the coordinated regulation of cell adhesion and migration. Current Opinion in Cell Biology *9*, 714-724.

Chasserot-Golaz, S., Vitale, N., Umbrecht-Jenck, E., Knight, D., Gerke, V., and Bader, M. F. (2005). Annexin 2 promotes the formation of lipid microdomains required for calcium-regulated exocytosis of dense-core vesicles. Mol Biol Cell *16*, 1108-1119.

Cheng, E. H., Sheiko, T. V., Fisher, J. K., Craigen, W. J., and Korsmeyer, S. J. (2003). VDAC2 inhibits BAK activation and mitochondrial apoptosis. Science *301*, 513-517.

Cheng, P. C., Cherukuri, A., Dykstra, M., Malapati, S., Sproul, T., Chen, M. R., and Pierce, S. K. (2001). Floating the raft hypothesis: the roles of lipid rafts in B cell antigen receptor function. Semin Immunol *13*, 107-114.

Cheng, P. C., Dykstra, M. L., Mitchell, R. N., and Pierce, S. K. (1999). A role for lipid rafts in B cell antigen receptor signaling and antigen targeting. Journal of Experimental Medicine *190*, 1549-1560.

Cherukuri, A., Cheng, P. C., Sohn, H. W., and Pierce, S. K. (2001). The CD19/CD21 complex functions to prolong B cell antigen receptor signaling from lipid rafts. Immunity *14*, 169-179.

Cherukuri, A., Shoham, T., Sohn, H. W., Levy, S., Brooks, S., Carter, R., and Pierce, S. K. (2004). The tetraspanin CD81 is necessary for partitioning of coligated CD19/CD21-B cell antigen receptor complexes into signaling-active lipid rafts. J Immunol *172*, 370-380.

Chigorno, V., Palestini, P., Sciannamblo, M., Dolo, V., Pavan, A., Tettamanti, G., and Sonnino, S. (2000). Evidence that ganglioside enriched domains are distinct from caveolae in MDCK II and human fibroblast cells in culture. European Journal of Biochemistry *267*, 4187-4197.

Corley Mastick, C., Brady, M. J., and Saltiel, A. R. (1995). Insulin stimulates the tyrosine phosphorylation of caveolin. Journal of Cell Biology *129*, 1523-1531.

Cragg, M. S., Morgan, S. M., Chan, H. T., Morgan, B. P., Filatov, A. V., Johnson, P. W., French, R. R., and Glennie, M. J. (2003). Complement-mediated lysis by anti-CD20 mAb correlates with segregation into lipid rafts. Blood *101*, 1045-1052.

Cragg, M. S., Walshe, C. A., Ivanov, A. O., and Glennie, M. J. (2005). The biology of CD20 and its potential as a target for mAb therapy. Curr Dir Autoimmun *8*, 140-174.

d'Azzo, A., Tessitore, A., and Sano, R. (2006). Gangliosides as apoptotic signals in ER stress response. Cell Death Differ *13*, 404-414.

Dal Porto, J. M., Gauld, S. B., Merrell, K. T., Mills, D., Pugh-Bernard, A. E., and Cambier, J. (2004). B cell antigen receptor signaling 101. Mol Immunol *41*, 599-613.

Davis, S., Aldrich, T. H., Ip, N. Y., Stahl, N., Scherer, S., Farruggella, T., DiStefano, P. S., Curtis, R., Panayotatos, N., Gascan, H., and al, e. (1993). Released form of CNTF receptor alpha component as a soluble mediator of CNTF responses. Science *259*, 1736-1739.

Davy, A., Feuerstein, C., and Robbins, S. M. (2000). Signaling within a caveolae-like membrane microdomain in human neuroblastoma cells in response to fibroblast growth factor. Journal of Neurochemistry *74*, 676-683.

Davy, A., Gale, N. W., Murray, E. W., Klinghoffer, R. A., Soriano, P., Feuerstein, C., and Robbins, S. M. (1999). Compartmentalized signaling by GPI-anchored ephrin-A5 requires the fyn tyrosine kinase to regulate cellular adhesion. Genes and Development *13*, 3125-3135.

Davy, A., and Robbins, S. M. (2000). Ephrin-A5 modulates cell adhesion and morphology in an integrin-dependent manner. EMBO Journal *19*, 5396-5405.

Deans, J. P., Li, H., and Polyak, M. J. (2002). CD20-mediated apoptosis: signalling through lipid rafts. Immunology *107*, 176-182.

Deans, J. P., Robbins, S. M., Polyak, M. J., and Savage, J. A. (1998). Rapid redistribution of CD20 to a low density detergent-insoluble membrane compartment. Journal of Biological Chemistry *273*, 344-348.

DeFranco, A. L. (1997). The complexity of signaling pathways activated by the BCR. Curr Opin Immunol *9*, 296-308.

Demetriou, M., Granovsky, M., Quaggin, S., and Dennis, J. W. (2001). Negative regulation of T-cell activation and autoimmunity by Mgat5 N-glycosylation. Nature *409*, 733-739.

Dermine, J. F., Duclos, S., Garin, J., St-Louis, F., Rea, S., Parton, R. G., and Desjardins, M. (2001). Flotillin-1-enriched lipid raft domains accumulate on maturing phagosomes. J Biol Chem *276*, 18507-18512.

Dickson, G., Peck, D., Moore, S. E., Barton, C. H., and Walsh, F. S. (1990). Enhanced myogenesis in NCAM-transfected mouse myoblasts. Nature *344*, 348-351.

Dietrich, C., Bagatolli, L. A., Volovyk, Z. N., Thompson, N. L., Levi, M., Jacobson, K., and Gratton, E. (2001). Lipid rafts reconstituted in model membranes. Biophys J *80*, 1417-1428.

Domon, B., and Aebersold, R. (2006). Mass spectrometry and protein analysis. Science *312*, 212-217.

Draberova, L., Amoui, M., and Draber, P. (1996). Thy-1 mediated activation of rat mast cells: the role of Thy-1 membrane microdomains. Immunology *87*, 141-148.

Draeger, A., Wray, S., and Babiychuk, E. B. (2005). Domain architecture of the smooth-muscle plasma membrane: regulation by annexins. Biochem J *387*, 309-314.

Drescher, U., Bonhoeffer, F., and Muller, B. K. (1997). The Eph family in retinal axon guidance. Current Opinion in Neurobiology *7*, 75-80.

Drevot, P., Langlet, C., Guo, X. J., Bernard, A. M., Colard, O., Chauvin, J. P., Lasserre, R., and He, H. T. (2002). TCR signal initiation machinery is pre-assembled and activated in a subset of membrane rafts. Embo J *21*, 1899-1908.

Dunphy, J. T., Greentree, W. K., and Linder, M. E. (2001). Enrichment of G-protein palmitoyltransferase activity in low density membranes: in vitro reconstitution of Galphai to these domains requires palmitoyltransferase activity. J Biol Chem *276*, 43300-43304.

Dykstra, M. L., Longnecker, R., and Pierce, S. K. (2001). Epstein-Barr virus coopts lipid rafts to block the signaling and antigen transport functions of the BCR. Immunity *14*, 57-67.

Edidin, M. (2003a). Lipids on the frontier: a century of cell-membrane bilayers. Nat Rev Mol Cell Biol *4*, 414-418.

Edidin, M. (2003b). The state of lipid rafts: from model membranes to cells. Annu Rev Biophys Biomol Struct *32*, 257-283.

Eidelman, F. J., Fuks, A., DeMarte, L., Taheri, M., and Stanners, C. P. (1993). Human carcinoembryonic antigen, an intercellular adhesion molecule, blocks fusion and differentiation of rat myoblasts. Journal of Cell Biology *123*, 467-475.

Eldering, E., and VanLier, R. A. (2005). B-cell antigen receptor-induced apoptosis: looking for clues. Immunol Lett *96*, 187-194.

Engelman, J. A., Wykoff, C. C., Yasuhara, S., Song, K. S., Okamoto, T., and Lisanti, M. P. (1997). Recombinant expression of caveolin-1 in oncogenically transformed cells abrogates anchorage-independent growth. Journal of Biological Chemistry *272*, 16374-16381.

Englbrecht, C. C., and Facius, A. (2005). Bioinformatics challenges in proteomics. Comb Chem High Throughput Screen *8*, 705-715.

Eroglu, C., Brugger, B., Wieland, F., and Sinning, I. (2003). Glutamate-binding affinity of Drosophila metabotropic glutamate receptor is modulated by association with lipid rafts. Proc Natl Acad Sci U S A *100*, 10219-10224.

Fahrenholz, F., Klein, U., and Gimpl, G. (1995). Conversion of the myometrial oxytocin receptor from low to high affinity state by cholesterol. Adv Exp Med Biol *395*, 311-319.

Fenn, J. B., Mann, M., Meng, C. K., Wong, S. F., and Whitehouse, C. M. (1989). Electrospray ionization for mass spectrometry of large biomolecules. Science *246*, 64-71.

Field, K. A., Holowka, D., and Baird, B. (1997). Compartmentalized activation of the high affinity immunoglobulin E receptor within membrane domains. Journal of Biological Chemistry *272*, 4276-4280.

Field, K. A., Holowka, D., and Baird, B. (1999). Structural aspects of the association of FcεRI with detergent-resistant membranes. Journal of Biological Chemistry *274*, 1753-1758.

Fielding, C. J., and Fielding, P. E. (2000). Cholesterol and caveolae: structural and functional relationships. Biochimica et Biophysica Acta *1529*, 210-222.

Fielding, P. E., Chau, P., Liu, D., Spencer, T. A., and Fielding, C. J. (2004). Mechanism of platelet-derived growth factor-dependent caveolin-1 phosphorylation: relationship to sterol binding and the role of serine-80. Biochemistry *43*, 2578-2586.

Fielding, P. E., Russel, J. S., Spencer, T. A., Hakamata, H., Nagao, K., and Fielding, C. J. (2002). Sterol efflux to apolipoprotein A-I originates from caveolin-rich microdomains and potentiates PDGF-dependent protein kinase activity. Biochemistry *41*, 4929-4937.

Fivaz, M., Abrami, L., and van der Goot, F. G. (1999). Landing on lipid rafts. Trends in Cell Biology *9*, 212-213.

Fivaz, M., Vilbois, F., Pasquali, C., and van der Goot, F. G. (2000). Analysis of glycosyl phosphatidylinositol-anchored proteins by two-dimensional gel electrophoresis. Electrophoresis *21*, 3351-3356.

Flieger, D., Renoth, S., Beier, I., Sauerbruch, T., and Schmidt-Wolf, I. (2000). Mechanism of cytotoxicity induced by chimeric mouse human monoclonal antibody IDEC-C2B8 in CD20-expressing lymphoma cell lines. Cell Immunol *204*, 55-63.

Foster, L. J., De Hoog, C. L., and Mann, M. (2003). Unbiased quantitative proteomics of lipid rafts reveals high specificity for signaling factors. Proc Natl Acad Sci U S A *100*, 5813-5818.

Fournier, A. E., GrandPre, T., and Strittmatter, S. M. (2001). Identification of a receptor mediating Nogo-66 inhibition of axonal regeneration. Nature *409*, 341-346.

Fra, A., Williamson, E., Simons, K., and Parton, R. G. (1994). Detergent-insoluble glycolipid microdomains in lymphocytes in the absence of caveolae. Journal of Biological Chemistry *269*, 30745-30748.

Fra, A. M., Williamson, E., Simons, K., and Parton, R. G. (1995). De novo formation of caveolae in lymphocytes by expression of VIP21-caveolin. Proceedings of the National Academy of Sciences USA *92*, 8655-8659.

Fragoso, R., Ren, D., Zhang, X., Su, M. W., Burakoff, S. J., and Jin, Y. J. (2003). Lipid raft distribution of CD4 depends on its palmitoylation and association with Lck, and evidence for CD4-induced lipid raft aggregation as an additional mechanism to enhance CD3 signaling. J Immunol *170*, 913-921.

Freiberg, B. A., Kupfer, H., Maslanik, W., Delli, J., Kappler, J., Zaller, D. M., and Kupfer, A. (2002). Staging and resetting T cell activation in SMACs. Nat Immunol *3*, 911-917.

Fridriksson, E. K., Shipkova, P. A., Sheets, E. D., Holowka, D., Baird, B., and McLafferty, F. W. (1999). Quantitative analysis of phospholipids in functionally

important membrane domains from RBL-2H3 mast cells using tandem high-resolution mass spectrometry. Biochemistry *38*, 8056-8063.

Friedrichson, T., and Kurzchalia, T. V. (1998). Microdomains of GPI-anchored proteins in living cells revealed by crosslinking. Nature *394*, 802-805.

Fujimoto, T. (1996). GPI-anchored proteins, glycosphingolipids, and sphingomyelin are sequestered to caveolae only after cross-linking. Journal of Histochemistry and Cytochemistry *44*, 929-941.

Fukushima, K., Ikehara, Y., and Yamashita, K. (2005). Functional role played by the glycosylphosphatidylinositol anchor glycan of CD48 in interleukin-18-induced interferon-gamma production. J Biol Chem *280*, 18056-18062.

Fukushima, K., Ishiyama, C., and Yamashita, K. (2004). Recognition by TNF-alpha of the GPI-anchor glycan induces apoptosis of U937 cells. Arch Biochem Biophys *426*, 298-305.

Furuchi, T., and Anderson, R. G. W. (1998). Cholesterol depletion of caveolae causes hyperactivation of extracellular signal-related kinase (ERK). Journal of Biological Chemistry *273*, 21099-21104.

Fusaro, G., Dasgupta, P., Rastogi, S., Joshi, B., and Chellappan, S. (2003). Prohibitin induces the transcriptional activity of p53 and is exported from the nucleus upon apoptotic signaling. J Biol Chem *278*, 47853-47861.

Gabison, E. E., Hoang-Xuan, T., Mauviel, A., and Menashi, S. (2005). EMMPRIN/CD147, an MMP modulator in cancer, development and tissue repair. Biochimie *87*, 361-368.

Gafencu, A., Stanescu, M., Toderici, A. M., Heltianu, C., and Simionescu, M. (1998). Protein and fatty acid composition of caveolae from apical plasmalemma of aortic endothelial cells. Cell Tissue Res *293*, 101-110.

Gagnon, E., Duclos, S., Rondeau, C., Chevet, E., Cameron, P. H., Steele-Mortimer, O., Paiement, J., Bergeron, J. J., and Desjardins, M. (2002). Endoplasmic reticulum-mediated phagocytosis is a mechanism of entry into macrophages. Cell *110*, 119-131.

Gahmberg, C. G., and Andersson, L. C. (1981). K562--a human leukemia cell line with erythroid features. Semin Hematol *18*, 72-77.

Gajate, C., and Mollinedo, F. (2005). Cytoskeleton-mediated death receptor and ligand concentration in lipid rafts forms apoptosis-promoting clusters in cancer chemotherapy. J Biol Chem *280*, 11641-11647.

Galbiati, F., Razani, B., and Lisanti, M. P. (2001). Emerging themes in lipid rafts and caveolae. Cell *106*, 403-411.

Galbiati, F., Volonte, D., Engelman, J. A., Watanabe, G., Burk, R., Pestell, R. G., and Lisanti, M. P. (1998). Targeted downregulation of caveolin-1 is sufficient to drive cell transformation and hyperactivate the p42/p44 MAP kinase cascade. EMBO Journal *17*, 6633-6648.

Galeva, N., and Altermann, M. (2002). Comparison of one-dimensional and two-dimensional gel electrophoresis as a separation tool for proteomic analysis of rat liver microsomes: cytochromes P450 and other membrane proteins. Proteomics *2*, 713-722.

Garcia-Ruiz, C., Colell, A., Morales, A., Calvo, M., Enrich, C., and Fernandez-Checa, J. C. (2002). Trafficking of ganglioside GD3 to mitochondria by tumor necrosis factor-alpha. J Biol Chem *277*, 36443-36448.

Gardai, S. J., McPhillips, K. A., Frasch, S. C., Janssen, W. J., Starefeldt, A., Murphy-Ullrich, J. E., Bratton, D. L., Oldenborg, P. A., Michalak, M., and Henson, P. M. (2005). Cell-surface calreticulin initiates clearance of viable or apoptotic cells through trans-activation of LRP on the phagocyte. Cell *123*, 321-334.

Garin, J., Diez, R., Kieffer, S., Dermine, J. F., Duclos, S., Gagnon, E., Sadoul, R., Rondeau, C., and Desjardins, M. (2001). The phagosome proteome: insight into phagosome functions. J Cell Biol *152*, 165-180.

Garnett, D., Barclay, A. N., Carmo, A. M., and Beyers, A. D. (1993). The association of the protein tyrosine kinases p56lck and p60fyn with the glycosyl phosphatidylinositol-anchored proteins Thy-1 and CD48 in rat thymocytes is dependent on the state of cellular activation. European Journal of Immunology *23*, 2540-2544.

Garofalo, T., Giammarioli, A. M., Misasi, R., Tinari, A., Manganelli, V., Gambardella, L., Pavan, A., Malorni, W., and Sorice, M. (2005). Lipid microdomains contribute to apoptosis-associated modifications of mitochondria in T cells. Cell Death Differ *12*, 1378-1389.

Gasteiger, E., Hoogland, C., Gattiker, A., Duvaud, S., Wilkins, M., Appel, R., and Bairoch, A. (2005). Protein identification and analysis tools on the ExPASy server. In The Proteomics Protocols Handbook, J. M. Walker, ed. (Totowa, Humana Press), pp. 571-607.

Gauld, S. B., and Cambier, J. C. (2004). Src-family kinases in B-cell development and signaling. Oncogene *23*, 8001-8006.

Gaus, K., Chklovskaia, E., Fazekas de St Groth, B., Jessup, W., and Harder, T. (2005). Condensation of the plasma membrane at the site of T lymphocyte activation. J Cell Biol *171*, 121-131.

George, J., Penner, S. J., Weber, J., Berry, J., and Claflin, J. L. (1993). Influence of membrane Ig receptor density and affinity on B cell signaling by antigen. Implications for affinity maturation. J Immunol *151*, 5955-5965.

Gevaert, K., and Vandekerckhove, J. (2000). Protein identification methods in proteomics. Electrophoresis *21*, 1145-1154.

Ghiran, I., Klickstein, L. B., and Nicholson-Weller, A. (2003). Calreticulin is at the surface of circulating neutrophils and uses CD59 as an adaptor molecule. J Biol Chem *278*, 21024-21031.

Gimpl, G., Burger, K., Politowska, E., Ciarkowski, J., and Fahrenholz, F. (2000). Oxytocin receptors and cholesterol: interaction and regulation. Exp Physiol *85 Spec No*, 41S-49S.

Gimpl, G., Wiegand, V., Burger, K., and Fahrenholz, F. (2002). Cholesterol and steroid hormones: modulators of oxytocin receptor function. Prog Brain Res *139*, 43-55.

Gkantiragas, I., Brugger, B., Stuven, E., Kaloyanova, D., Li, X. Y., Lohr, K., Lottspeich, F., Wieland, F. T., and Helms, J. B. (2001). Sphingomyelin-enriched microdomains at the Golgi complex. Mol Biol Cell *12*, 1819-1833.

Gleizes, P. E., Noaillac-Depeyre, J., Dupont, M.-A., and Gas, N. (1996). Basic fibroblast growth factor (FGF-2) is addressed to caveolae after binding to the plasma membrane of BHK cells. European Journal of Cell Biology *71*, 144-153.

Glenney, J. R., and Soppet, D. (1992). Sequence and expression of caveolin, a protein component of caveolae plasma membrane domains phosphorylated on tyrosine in RSV-transformed fibroblasts. Proceedings of the National Academy of Sciences USA *89*, 10517-10521.

Glenney Jr., J. R. (1992). The sequence of human caveolin reveals identity with VIP21, a component of transport vesicles. FEBS Letters *314*, 45-48.

Goetz, J. G., and Nabi, I. R. (2006). Interaction of the smooth endoplasmic reticulum and mitochondria. Biochem Soc Trans *34*, 370-373.

Golub, T., and Caroni, P. (2005). PI(4,5)P2-dependent microdomain assemblies capture microtubules to promote and control leading edge motility. J Cell Biol *169*, 151-165.

Gomez-Mouton, C., Abad, J. L., Mira, E., Lacalle, R. A., Gallardo, E., Jimenez-Baranda, S., Illa, I., Bernad, A., Manes, S., and Martinez-A., C. (2001). Segregation of leading-edge and uropod components into specific lipid rafts during T cell polarization. Proceedings of the National Academy of Sciences USA *98*, 9642-9647.

Gorg, A., Obermaier, C., Boguth, G., Harder, A., Scheibe, B., Wildgruber, R., and Weiss, W. (2000). The current state of two-dimensional electrophoresis with immobilized pH gradients. Electrophoresis *21*, 1037-1053.

Grakoui, A., Bromley, S. K., Sumen, C., Davis, M. M., Shaw, A. S., Allen, P. M., and Dustin, M. L. (1999). The immunological synapse: a molecular machine controlling T cell activation. Science *285*, 221-227.

Gumley, T. P., McKenzie, I. F., and Sandrin, M. S. (1995). Tissue expression, structure and function of the murine Ly-6 family of molecules. Immunol Cell Biol *73*, 277-296.

Guo, B., Kato, R. M., Garcia-Lloret, M., Wahl, M. I., and Rawlings, D. J. (2000). Engagement of the human pre-B cell receptor generates a lipid raft-dependent calcium signaling complex. Immunity *13*, 243-253.

Gupta, N., and DeFranco, A. L. (2003). Visualizing lipid raft dynamics and early signaling events during antigen receptor-mediated B-lymphocyte activation. Mol Biol Cell *14*, 432-444.

Gupta, N., Wollscheid, B., Watts, J. D., Scheer, B., Aebersold, R., and DeFranco, A. L. (2006). Quantitative proteomic analysis of B cell lipid rafts reveals that ezrin regulates antigen receptor-mediated lipid raft dynamics. Nat Immunol *7*, 625-633.

Gustavsson, J., Parpal, S., Karlsson, M., Ramsing, C., Thorn, H., Borg, M., Lindroth, M., Holmgren, P. K., Magnusson, K.-E., and Stralfors, P. (1999). Localization of the insulin receptor in caveolae of adipocyte plasma membrane. FASEB Journal *13*, 1961-1971.

Gustavsson, J., Parpal, S., and Stralfors, P. (1996). Insulin-stimulated glucose uptake involves the transition of glucose transporters to a caveolae-rich fraction within the plasma membrane: implications for type II diabetes. Molecular Medicine *2*, 367-372.

Haasemann, M., Cartaud, J., Muller-Esterl, W., and Dunia, I. (1998). Agonist-induced redistribution of bradykinin B_2 receptor in caveolae. Journal of Cell Science *111*, 917-928.

Hailstones, D., Sleer, L. S., Parton, R. G., and Stanley, K. K. (1998). Regulation of caveolin and caveolae by cholesterol in MDCK cells. Journal of Lipid Research *39*, 369-379.

Hakomori, S. (1998). Cancer-associated glycosphingolipid antigens: their structure, organization, function. Acta Anatomica *161*, 79-90.

Hakomori, S., Yamamura, S., and Handa, K. (1998). Signal transduction through glyco(sphingo)lipids. Introduction and recent studies on glyco(sphingo)lipid-enriched microdomains. Annals of the New York Academy of Sciences *845*, 1-10.

Hall, C., Richards, S. J., and Hillmen, P. (2002). The glycosylphosphatidylinositol anchor and paroxysmal nocturnal haemoglobinuria/aplasia model. Acta Haematol *108*, 219-230.

Hanash, S. M. (2000). Biomedical applications of two-dimensional electrophoresis using immobilized pH gradients: current status. Electrophoresis *21*, 1202-1209.

Hancock, J. F. (2006). Lipid rafts: contentious only from simplistic standpoints. Nat Rev Mol Cell Biol *7*, 456-462.

Hancock, J. F., Paterson, H., and Marshall, C. J. (1990). A polybasic domain or palmitoylation is required in addition to the CAAX motif to localize p21ras to the plasma membrane. Cell *63*, 133-139.

Hansen, G. H., Immerdal, L., Thorsen, E., Niels-Christiansen, L. L., Nystrom, B. T., Demant, E. J., and Danielsen, E. M. (2001). Lipid rafts exist as stable cholesterol-independent microdomains in the brush border membrane of enterocytes. J Biol Chem *276*, 32338-32344.

Hao, J. J., Carey, G. B., and Zhan, X. (2004). Syk-mediated tyrosine phosphorylation is required for the association of hematopoietic lineage cell-specific protein 1 with lipid rafts and B cell antigen receptor signalosome complex. J Biol Chem *279*, 33413-33420.

Hao, S., and August, A. (2005). Actin depolymerization transduces the strength of B-cell receptor stimulation. Mol Biol Cell *16*, 2275-2284.

Harder, T., Scheiffele, P., Verkade, P., and Simons, K. (1998). Lipid domain structure of the plasma membrane revealed by patching of membrane components. Journal of Cell Biology *141*, 929-942.

Harder, T., and Simons, K. (1999). Clusters of glycolipid and glycosylphosphatidylinositol-anchored proteins in lymphoid cells: accumulation of actin regulated by local tyrosine phosphorylation. Eur J Immunol *29*, 556-562.

Harris, C. L., and Morgan, B. P. (1995). Characterization of a glycosyl-phosphatidylinositol anchor-deficient subline of Raji cells. An analysis of the functional importance of complement inhibitors on the Raji cell line. Immunology *86*, 311-318.

Harris, P., and Ralph, P. (1985). Human leukemic models of myelomonocytic development: a review of the HL-60 and U937 cell lines. J Leukoc Biol *37*, 407-422.

Hatanaka, M., Maeda, T., Ikemoto, T., Mori, H., Seya, T., and Shimizu, A. (1998). Expression of caveolin-1 in human T cell leukemia cell lines. Biochemical and Biophysical Research Communications *253*, 382-387.

Hayes, M. J., Rescher, U., Gerke, V., and Moss, S. E. (2004). Annexin-actin interactions. Traffic *5*, 571-576.

Hazenbos, W. L., Clausen, B. E., Takeda, J., and Kinoshita, T. (2004a). GPI-anchor deficiency in myeloid cells causes impaired FcgammaR effector functions. Blood *104*, 2825-2831.

Hazenbos, W. L., Murakami, Y., Nishimura, J., Takeda, J., and Kinoshita, T. (2004b). Enhanced responses of glycosylphosphatidylinositol anchor-deficient T lymphocytes. J Immunol *173*, 3810-3815.

Head, B. P., Patel, H. H., Roth, D. M., Murray, F., Swaney, J. S., Niesman, I. R., Farquhar, M. G., and Insel, P. A. (2006). Microtubules and actin microfilaments regulate lipid raft/caveolae localization of adenylyl cyclase signaling components. J Biol Chem *281*, 26391-26399.

Helms, J. B., and Zurzolo, C. (2004). Lipids as targeting signals: lipid rafts and intracellular trafficking. Traffic *5*, 247-254.

Hofmeister, J. K., Cooney, D., and Coggeshall, K. M. (2000). Clustered CD20 induced apoptosis: src-family kinase, the proximal regulator of tyrosine phosphorylation, calcium influx, and caspase 3-dependent apoptosis. Blood Cells Mol Dis *26*, 133-143.

Holowka, D., Gosse, J. A., Hammond, A. T., Han, X., Sengupta, P., Smith, N. L., Wagenknecht-Wiesner, A., Wu, M., Young, R. M., and Baird, B. (2005). Lipid segregation and IgE receptor signaling: a decade of progress. Biochim Biophys Acta *1746*, 252-259.

Holowka, D., Sheets, E. D., and Baird, B. (2000). Interactions between FcεRI and lipid raft components are regulated by the actin cytoskeleton. Journal of Cell Science *113*, 1009-1019.

Hooper, N. M. (1999). Detergent-insoluble glycosphingolipid/cholesterol-rich membrane domains, lipid rafts and caveolae (review). Mol Membr Biol *16*, 145-156.

Hope, H. R., and Pike, L. J. (1996). Phosphoinositides and phosphoinositide-utilizing enzymes in detergent-insoluble lipid domains. Molecular Biology of the Cell *7*, 843-851.

Horejsi, V. (2004). Transmembrane adaptor proteins in membrane microdomains: important regulators of immunoreceptor signaling. Immunol Lett *92*, 43-49.

Horikawa, K., Nakakuma, H., Kawaguchi, T., Iwamoto, N., Nagakura, S., Kagimoto, T., and Takatsuki, K. (1997). Apoptosis resistance of blood cells from patients with paroxysmal nocturnal hemoglobinuria, aplastic anemia, and myelodysplastic syndrome. Blood *90*, 2716-2722.

Howlett, C. J., and Robbins, S. M. (2002). Membrane-anchored Cbl suppresses Hck protein-tyrosine kinase mediated cellular transformation. Oncogene *21*, 1707-1716.

Hua, H., Munk, S., and Whiteside, C. I. (2003). Endothelin-1 activates mesangial cell ERK1/2 via EGF-receptor transactivation and caveolin-1 interaction. Am J Physiol Renal Physiol *284*, F303-312.

Huang, F., Kirkpatrick, D., Jiang, X., Gygi, S., and Sorkin, A. (2006). Differential regulation of EGF receptor internalization and degradation by multiubiquitination within the kinase domain. Mol Cell *21*, 737-748.

Huber, L. A. (2003). Is proteomics heading in the wrong direction? Nat Rev Mol Cell Biol *4*, 74-80.

Hur, E. M., Park, Y. S., Lee, B. D., Jang, I. H., Kim, H. S., Kim, T. D., Suh, P. G., Ryu, S. H., and Kim, K. T. (2004). Sensitization of epidermal growth factor-induced signaling by bradykinin is mediated by c-Src. Implications for a role of lipid microdomains. J Biol Chem *279*, 5852-5860.

Hurlstone, A. F. L., Reid, G., Reeves, J. R., Fraser, J., Strathdee, G., Rahilly, M., Parkinson, E. K., and Black, D. M. (1999). Analysis of the CAVEOLIN-1 gene at human chromosome 7q31.1 in primary tumours and tumour-derived cell lines. Oncogene *18*, 1881-1890.

Ikezu, T., Trapp, B. D., Song, K. S., Schlegel, A., Lisanti, M. P., and Okamoto, T. (1998). Caveolae, plasma membrane microdomains for alpha-secretase-mediated processing of the amyloid precursor protein. Journal of Biological Chemistry *273*, 10485-10495.

Ikonen, E. (2001). Roles of lipid rafts in membrane transport. Curr Opin Cell Biol *13*, 470-477.

Ikonen, E., Fiedler, K., Parton, R. G., and Simons, K. (1995). Prohibitin, an antiproliferative protein, is localized to mitochondria. FEBS Lett *358*, 273-277.

Ilangumaran, S., Briol, A., and Hoessli, D. (1997). Distinct interactions among GPI-anchored, transmembrane and membrane associated intracellular proteins, and sphingolipids in lymphocyte and endothelial cell plasma membranes.

Inokuchi, J. (2006). Insulin resistance as a membrane microdomain disorder. Biol Pharm Bull *29*, 1532-1537.

Inoue, H., Miyaji, M., Kosugi, A., Nagafuku, M., Okazaki, T., Mimori, T., Amakawa, R., Fukuhara, S., Domae, N., Bloom, E. T., and Umehara, H. (2002). Lipid rafts as the signaling scaffold for NK cell activation: tyrosine phosphorylation and association of LAT with phosphatidylinositol 3-kinase and phospholipase C-gamma following CD2 stimulation. Eur J Immunol *32*, 2188-2198.

Insenser, M., Nombela, C., Molero, G., and Gil, C. (2006). Proteomic analysis of detergent-resistant membranes from Candida albicans. Proteomics *6 Suppl 1*, S74-81.

Ismail, M. M., Tooze, J. A., Flynn, J. A., Gordon-Smith, E. C., Gibson, F. M., Rutherford, T. R., and Elebute, M. O. (2003). Differential apoptosis and Fas expression on GPI-negative and GPI-positive stem cells: a mechanism for the evolution of paroxysmal nocturnal haemoglobinuria. Br J Haematol *123*, 545-551.

Isshiki, M., and Anderson, R. G. W. (1999). Calcium signal transduction from caveolae. Cell Calcium *26*, 201-208.

Itoh, M., Ishihara, K., Hiroi, T., Lee, B. O., Maeda, H., Iijima, H., Yanagita, M., Kiyono, H., and Hirano, T. (1998). Deletion of bone marrow stromal cell antigen-1 (CD157) gene impaired systemic thymus independent-2 antigen-induced IgG3 and mucosal TD antigen-elicited IgA responses. Journal of Immunology *161*, 3974-3983.

Iwabuchi, K., Handa, K., and Hakomori, S. (1998). Separation of "glycosphingolipid signaling domain" from caveolin-containing membrane fraction in mouse melanoma B16 cells and its role in cell adhesion coupled with signalling. Journal of Biological Chemistry *273*, 33766-33773.

Jacob, R., Heine, M., Eikemeyer, J., Frerker, N., Zimmer, K. P., Rescher, U., Gerke, V., and Naim, H. Y. (2004). Annexin II is required for apical transport in polarized epithelial cells. J Biol Chem *279*, 3680-3684.

Janas, E., Priest, R., Wilde, J. I., White, J. H., and Malhotra, R. (2005). Rituxan (anti-CD20 antibody)-induced translocation of CD20 into lipid rafts is crucial for calcium influx and apoptosis. Clin Exp Immunol *139*, 439-446.

Janes, P. W., Ley, S. C., and Magee, A. I. (1999). Aggregation of lipid rafts accompanies signaling via the T cell antigen receptor. Journal of Cell Biology *147*, 447-461.

Janes, P. W., Ley, S. C., Magee, A. L., and Kabouridis, P. S. (2000). The role of lipid rafts in T cell antigen receptor (TCR) signalling. Seminars in Immunology *12*, 23-34.

Janssen, E., Zhu, M., Zhang, W., Koonpaew, S., and Zhang, W. (2003). LAB: a new membrane-associated adaptor molecule in B cell activation. Nat Immunol *4*, 117-123.

Jasinski, M., Keller, P., Fujiwara, Y., Orkin, S. H., and Bessler, M. (2001). GATA1-Cre mediates Piga gene inactivation in the erythroid/megakaryocytic lineage and leads to circulating red cells with a partial deficiency in glycosyl phosphatidylinositol-linked proteins (paroxysmal nocturnal hemoglobinuria type II cells). Blood *98*, 2248-2255.

Jazirehi, A. R., and Bonavida, B. (2005). Cellular and molecular signal transduction pathways modulated by rituximab (rituxan, anti-CD20 mAb) in non-Hodgkin's

lymphoma: implications in chemosensitization and therapeutic intervention. Oncogene *24*, 2121-2143.

Jiang, X. Z., Toyota, H., Yoshimoto, T., Takada, E., Asakura, H., and Mizuguchi, J. (2003). Anti-IgM-induced down-regulation of nuclear Thy28 protein expression in Ramos B lymphoma cells. Apoptosis *8*, 509-519.

John, G. B., Shang, Y., Li, L., Renken, C., Mannella, C. A., Selker, J. M., Rangell, L., Bennett, M. J., and Zha, J. (2005). The mitochondrial inner membrane protein mitofilin controls cristae morphology. Mol Biol Cell *16*, 1543-1554.

Jones, O. T., and McNamee, M. G. (1988). Annular and nonannular binding sites for cholesterol associated with the nicotinic acetylcholine receptor. Biochemistry *27*, 2364-2374.

Kabouridis, P. S. (2006). Lipid rafts in T cell receptor signalling. Mol Membr Biol *23*, 49-57.

Kabouridis, P. S., Magee, A. I., and Ley, S. C. (1997). S-acylation of LCK protein tyrosine kinase is essential for its signalling function in T lymphocytes. EMBO Journal, 4983-4998.

Kakhniashvili, D. G., Griko, N. B., Bulla, L. A., Jr., and Goodman, S. R. (2005). The proteomics of sickle cell disease: profiling of erythrocyte membrane proteins by 2D-DIGE and tandem mass spectrometry. Exp Biol Med (Maywood) *230*, 787-792.

Kamiguchi, H. (2006). The region-specific activities of lipid rafts during axon growth and guidance. J Neurochem *98*, 330-335.

Kaneko, K., Vey, M., Scott, M., Pilkuhn, S., Cohen, F. E., and Prusiner, S. B. (1997). COOH-terminal sequence of the cellular prion protein directs subcellular trafficking and controls conversion into the scrapie isoform. Proceedings of the National Academy of Sciences USA *94*, 2333-2338.

Karas, M., and Hillenkamp, F. (1988). Laser desorption ionization of proteins with molecular masses exceeding 10,000 daltons. Anal Chem *60*, 2299-2301.

Karnell, F. G., Brezski, R. J., King, L. B., Silverman, M. A., and Monroe, J. G. (2005). Membrane cholesterol content accounts for developmental differences in surface B cell receptor compartmentalization and signaling. J Biol Chem *280*, 25621-25628.

Karsan, A., Blonder, J., Law, J., Yaquian, E., Lucas, D. A., Conrads, T. P., and Veenstra, T. (2005). Proteomic analysis of lipid microdomains from lipopolysaccharide-activated human endothelial cells. J Proteome Res *4*, 349-357.

Kasahara, K., Watanabe, K., Kozutsumi, Y., Oohira, A., Yamamoto, T., and Sanai, Y. (2002). Association of GPI-anchored protein TAG-1 with src-family kinase Lyn in lipid rafts of cerebellar granule cells. Neurochem Res *27*, 823-829.

Kasahara, K., Watanabe, K., Takeuchi, K., Kaneko, H., Oohira, A., Yamamoto, T., and Sanai, Y. (2000). Involvement of gangliosides in glycosylphosphatidylinositol-anchored neuronal cell adhesion molecule TAG-1 signalin in lipid rafts. Journal of Biological Chemistry *275*, 34701-34709.

Kawabuchi, M., Satomi, Y., Takao, T., Shimonishi, Y., Nada, S., Nagai, K., Tarakhovsky, A., and Okada, M. (2000). Transmembrane phosphoprotein Cbp regulates the activities of Src-family tyrosine kinases. Nature *404*, 999-1003.

Keller, P., Payne, J. L., Tremml, G., Greer, P. A., Gaboli, M., Pandolfi, P. P., and Bessler, M. (2001). FES-Cre targets phosphatidylinositol glycan class A (PIGA) inactivation to hematopoietic stem cells in the bone marrow. J Exp Med *194*, 581-589.

Kim, B. W., Choo, H. J., Lee, J. W., Kim, J. H., and Ko, Y. G. (2004a). Extracellular ATP is generated by ATP synthase complex in adipocyte lipid rafts. Exp Mol Med *36*, 476-485.

Kim, K. B., Kim, S. I., Choo, H. J., Kim, J. H., and Ko, Y. G. (2004b). Two-dimensional electrophoretic analysis reveals that lipid rafts are intact at physiological temperature. Proteomics *4*, 3527-3535.

Kim, K. B., Lee, J. W., Lee, C. S., Kim, B. W., Choo, H. J., Jung, S. Y., Chi, S. G., Yoon, Y. S., Yoon, G., and Ko, Y. G. (2006). Oxidation-reduction respiratory chains and ATP synthase complex are localized in detergent-resistant lipid rafts. Proteomics *6*, 2444-2453.

Kim, Y.-N., Wiepz, G. J., Guadarrama, A. G., and Bertics, P. J. (2000). Epidermal growth factor-stimulated tyrosine phosphorylation of caveolin-1. Journal of Biological Chemistry *275*, 7481-7491.

Kimura, A., Baumann, C. A., Chiang, S. H., and Saltiel, A. R. (2001). The sorbin homology domain: a motif for the targeting of proteins to lipid rafts. Proc Natl Acad Sci U S A *98*, 9098-9103.

Kjersti Rodal, S., Skretting, G., Garred, O., Vilhardt, F., van Deurs, B., and Sandvig, K. (1999). Extraction of cholesterol with methyl-β-cyclodextrin perturbs formation of clathrin-coated vesicles. Molecular Biology of the Cell *10*, 961-974.

Klein, U., Gimpl, G., and Fahrenholz, F. (1995). Alteration of the myometrial plasma membrane cholesterol content with beta-cyclodextrin modulates the binding affinity of the oxytocin receptor. Biochemistry *34*, 13784-13793.

Knippschild, U., Gocht, A., Wolff, S., Huber, N., Lohler, J., and Stoter, M. (2005). The casein kinase 1 family: participation in multiple cellular processes in eukaryotes. Cell Signal *17*, 675-689.

Koleske, A. J., Baltimore, D., and Lisanti, M. P. (1995). Reduction of caveolin and caveolae in oncogenically transformed cells. Proceedings of the National Academy of Sciences USA *92*, 1381-1385.

Krishna, R. G., and Wold, F. (1993). Post-translational modification of proteins. Adv Enzymol Relat Areas Mol Biol *67*, 265-298.

Kurzchalia, T. V., Dupree, P., Parton, R. G., Kellner, R., Virta, H., Lehnert, M., and Simons, K. (1992). VIP21, a 21-kD membrane protein is an integral component of trans-Golgi-network-derived transport vesicles. J Cell Biol *118*, 1003-1014.

Kusumi, A., Koyama-Honda, I., and Suzuki, K. (2004). Molecular dynamics and interactions for creation of stimulation-induced stabilized rafts from small unstable steady-state rafts. Traffic *5*, 213-230.

Kutzleb, C., Petrasch-Parwez, E., and Kilimann, M. W. (2006). Cellular and subcellular localization of paralemmin-1, a protein involved in cell shape control, in the rat brain, adrenal gland and kidney. Histochem Cell Biol.

Kutzleb, C., Sanders, G., Yamamoto, R., Wang, X., Lichte, B., Petrasch-Parwez, E., and Kilimann, M. W. (1998). Paralemmin, a prenyl-palmitoyl-anchored phosphoprotein abundant in neurons and implicated in plasma membrane dynamics and cell process formation. J Cell Biol *143*, 795-813.

Kwiatkowska, K., and Sobota, A. (2001). The clustered Fcgamma receptor II is recruited to Lyn-containing membrane domains and undergoes phosphorylation in a cholesterol-dependent manner. Eur J Immunol *31*, 989-998.

Lafont, F., Verkade, P., Galli, T., Wimmer, C., Louvard, D., and Simons, K. (1999). Raft association of SNAP receptors acting in apical trafficking in Madin-Darby canine kidney cells. Proc Natl Acad Sci U S A *96*, 3734-3738.

Lallemand-Breitenbach, V., Quesnoit, M., Braun, V., El Marjou, A., Pous, C., Goud, B., and Perez, F. (2004). CLIPR-59 is a lipid raft-associated protein containing a cytoskeleton-associated protein glycine-rich domain (CAP-Gly) that perturbs microtubule dynamics. J Biol Chem *279*, 41168-41178.

Langlet, C., Bernard, A. M., Drevot, P., and He, H. T. (2000). Membrane rafts and signaling by the multichain immune recognition receptors. Curr Opin Immunol *12*, 250-255.

Larsen, M. R., Trelle, M. B., Thingholm, T. E., and Jensen, O. N. (2006). Analysis of posttranslational modifications of proteins by tandem mass spectrometry. Biotechniques *40*, 790-798.

Lavie, Y., Fiucci, G., Czarny, M., and Liscovitch, M. (1999). Changes in membrane microdomains and caveolae constituents in multidrug-resistant cancer cells. Lipids *34 (Supplement)*, S57-S63.

Lazar, D. F., Knez, J. J., Medof, M. E., Cuatrecasas, P., and Saltiel, A. R. (1994). Stimulation of glycogen synthesis by insulin in human erythroleukemia cells requires the synthesis of glycosyl-phosphatidylinositol. Proc Natl Acad Sci U S A *91*, 9665-9669.

Le Bras, M., Rouy, I., and Brenner, C. (2006). The modulation of inter-organelle cross-talk to control apoptosis. Med Chem *2*, 1-12.

Lebedeva, T., Anikeeva, N., Kalams, S. A., Walker, B. D., Gaidarov, I., Keen, J. H., and Sykulev, Y. (2004). Major histocompatibility complex class I-intercellular adhesion molecule-1 association on the surface of target cells: implications for antigen presentation to cytotoxic T lymphocytes. Immunology *113*, 460-471.

Ledesma, M. D., Da Silva, J. S., Schevchenko, A., Wilm, M., and Dotti, C. G. (2003). Proteomic characterisation of neuronal sphingolipid-cholesterol microdomains: role in plasminogen activation. Brain Res *987*, 107-116.

Lee, S. W., Reimer, C. L., Oh, P., Campbell, D. B., and Schnitzer, J. E. (1998). Tumor cell growth inhibition by caveolin re-expression in human breast cancer cells. Oncogene *16*, 1391-1397.

Leitenberg, D., Balamuth, F., and Bottomly, K. (2001). Changes in the T cell receptor macromolecular signaling complex and membrane microdomains during T cell development and activation. Seminars in Immunology *13*, 129-138.

Leitinger, B., and Hogg, N. (2002). The involvement of lipid rafts in the regulation of integrin function. J Cell Sci *115*, 963-972.

Li, H., Ayer, L. M., Lytton, J., and Deans, J. P. (2003a). Store-operated cation entry mediated by CD20 in membrane rafts. J Biol Chem *278*, 42427-42434.

Li, H., Ayer, L. M., Polyak, M. J., Mutch, C. M., Petrie, R. J., Gauthier, L., Shariat, N., Hendzel, M. J., Shaw, A. R., Patel, K. D., and Deans, J. P. (2004a). The CD20 calcium channel is localized to microvilli and constitutively associated with membrane rafts: antibody binding increases the affinity of the association through an epitope-dependent cross-linking-independent mechanism. J Biol Chem *279*, 19893-19901.

Li, N., Mak, A., Richards, D. P., Naber, C., Keller, B. O., Li, L., and Shaw, A. R. (2003b). Monocyte lipid rafts contain proteins implicated in vesicular trafficking and phagosome formation. Proteomics *3*, 536-548.

Li, N., Shaw, A. R., Zhang, N., Mak, A., and Li, L. (2004b). Lipid raft proteomics: analysis of in-solution digest of sodium dodecyl sulfate-solubilized lipid raft proteins by liquid chromatography-matrix-assisted laser desorption/ionization tandem mass spectrometry. Proteomics *4*, 3156-3166.

Lichtenberg, D., Goni, F. M., and Heerklotz, H. (2005). Detergent-resistant membranes should not be identified with membrane rafts. Trends Biochem Sci *30*, 430-436.

Lillico, S., Field, M. C., Blundell, P., Coombs, G. H., and Mottram, J. C. (2003). Essential roles for GPI-anchored proteins in African trypanosomes revealed using mutants deficient in GPI8. Mol Biol Cell *14*, 1182-1194.

Lisanti, M. P., Scherer, P. E., Tang, Z., and Sargiacomo, M. (1994a). Caveolae, caveolin and caveolin-rich membrane domains: a signalling hypothesis. Trends Cell Biol *4*, 231-235.

Lisanti, M. P., Scherer, P. E., Vidugiriene, J., Tang, Z., Hermanowski-Vosatka, A., Tu, Y.-H., Cook, R. F., and Sargiacomo, M. (1994b). Characterization of caveolin-rich membrane domains isolated from an endothelial-rich source: implications for human disease. Journal of Cell Biology *126*, 111-126.

Liu, C., DeNardo, G., Tobin, E., and DeNardo, S. (2004). Antilymphoma effects of anti-HLA-DR and CD20 monoclonal antibodies (Lym-1 and Rituximab) on human lymphoma cells. Cancer Biother Radiopharm *19*, 545-561.

Liu, J., Oh, P., Horner, T., Rogers, R. A., and Schnitzer, J. E. (1997a). Organized endothelial cell surface signal transduction in caveolae distinct from glycosylphosphatidylinositol-anchored protein microdomains. Journal of Biological Chemistry *272*, 7211-7222.

Liu, P., and Anderson, R. G. W. (1995). Compartmentalized production of ceramide at the cell surface. Journal of Biological Chemistry *270*, 27179-27185.

Liu, P., and Anderson, R. G. W. (1999). Spatial organization of EGF receptor transmodulation by PDGF. Biochemical and Biophysical Research Communications *261*, 695-700.

Liu, P., Ying, Y., and Anderson, R. G. W. (1997b). Platelet-derived growth factor activates mitogen-activated protein kinase in isolated caveolae. Proceedings of the National Academy of Sciences USA *94*, 13666-13670.

Liu, P., Ying, Y., Ko, Y.-G., and Anderson, R. G. W. (1996). Localization of platelet-derived growth factor-stimulated phosphorylation cascade to caveolae. Journal of Biological Chemistry *271*, 10299-10303.

Lohn, M., Furstenau, M., Sagach, V., Elger, M., Schulze, W., Luft, F. C., Haller, H., and Gollasch, M. (2000). Ignition of calcium sparks in arterial and cardiac muscle through caveolae. Circ Res *87*, 1034-1039.

Lou, Z., Jevremovic, D., Billadeau, D. D., and Leibson, P. J. (2000). A balance between positive and negative signals in cytotoxic lymphocytes regulates the polarization of lipid rafts during the development of cell-mediated killing. Journal of Experimental Medicine *191*, 347-354.

Lucero, H. A., and Robbins, P. W. (2004). Lipid rafts-protein association and the regulation of protein activity. Arch Biochem Biophys *426*, 208-224.

Luciano, F., Herrant, M., Jacquel, A., Ricci, J. E., and Auberger, P. (2003). The p54 cleaved form of the tyrosine kinase Lyn generated by caspases during BCR-induced cell death in B lymphoma acts as a negative regulator of apoptosis. Faseb J *17*, 711-713.

Lund-Johansen, F., Olweus, J., Symington, F. W., Arli, A., Thompson, J. S., Vilella, R., Skubitz, K., and Horejsi, V. (1993). Activation of human monocytes and granulocytes by monoclonal antibodies to glycosylphosphatidylinositol-anchored antigens. European Journal of Immunology *23*, 2782-2791.

MacLellan, D. L., Steen, H., Adam, R. M., Garlick, M., Zurakowski, D., Gygi, S. P., Freeman, M. R., and Solomon, K. R. (2005). A quantitative proteomic analysis of growth factor-induced compositional changes in lipid rafts of human smooth muscle cells. Proteomics *5*, 4733-4742.

Madore, N., Smith, K. L., Graham, C. H., Jen, A., Brady, K., Hall, S., and Morris, R. (1999). Functionally different GPI proteins are organized in different domains on the neuronal surface. Embo J *18*, 6917-6926.

Maeda, Y., Watanabe, R., Harris, C. L., Hong, Y., Ohishi, K., Kinoshita, K., and Kinoshita, T. (2001). PIG-M transfers the first mannose to glycosylphosphatidylinositol on the lumenal side of the ER. Embo J *20*, 250-261.

Maekawa, S., Morii, H., Kumanogoh, H., Sano, M., Naruse, Y., Sokawa, Y., and Mori, N. (2001). Localization of neuronal growth-associated, microtubule-destabilizing factor SCG10 in brain-derived raft membrane microdomains. J Biochem (Tokyo) *129*, 691-697.

Man, P., Novak, P., Cebecauer, M., Horvath, O., Fiserova, A., Havlicek, V., and Bezouska, K. (2005). Mass spectrometric analysis of the glycosphingolipid-enriched microdomains of rat natural killer cells. Proteomics *5*, 113-122.

Manes, S., del Real, G., and Martinez, A. C. (2003). Pathogens: raft hijackers. Nat Rev Immunol *3*, 557-568.

Manes, S., and Viola, A. (2006). Lipid rafts in lymphocyte activation and migration. Mol Membr Biol *23*, 59-69.

Mann, M., and Jensen, O. N. (2003). Proteomic analysis of post-translational modifications. Nat Biotechnol *21*, 255-261.

Marmor, M. D., and Julius, M. (2001). Role for lipid rafts in regulating interleukin-2 receptor signaling. Blood *98*, 1489-1497.

Marquez, L., Trapote, M. A., Luque, M. A., Valverde, I., and Villanueva-Penacarrillo, M. L. (1998). Inositolphosphoglycans possibly mediate the effects of glucagon-like peptide-1(7-36)amide on rat liver and adipose tissue. Cell Biochem Funct *16*, 51-56.

Martens, J. R., Navarro-Polanco, R., Coppock, E. A., Nishiyama, A., Parshley, L., Grobaski, T. D., and Tamkun, M. M. (2000). Differential targeting of shaker-like potassium channels to lipid rafts. Journal of Biological Chemistry *275*, 7443-7446.

Martin, A. C., and Cooper, D. M. (2006). Layers of organization of cAMP microdomains in a simple cell. Biochem Soc Trans *34*, 480-483.

Matko, J., Bodnar, A., Vereb, G., Bene, L., Vamosi, G., Szentesi, G., Szollosi, J., Gaspar, R., Horejsi, V., Waldmann, T. A., and Damjanovich, S. (2002). GPI-microdomains (membrane rafts) and signaling of the multi-chain interleukin-2 receptor in human lymphoma/leukemia T cell lines. Eur J Biochem *269*, 1199-1208.

Matousek, P., Hodny, Z., Svandova, I., and Svoboda, P. (2003). Different methods of membrane domains isolation result in similar 2-D distribution patterns of membrane domain proteins. Biochem Cell Biol *81*, 365-372.

Matsuuchi, L., and Gold, M. R. (2001). New views of BCR structure and organization. Curr Opin Immunol *13*, 270-277.

Matveev, S. V., and Smart, E. J. (2002). Heterologous desensitization of EGF receptors and PDGF receptors by sequestration in caveolae. Am J Physiol Cell Physiol *282*, C935-946.

Mayor, S., and Maxfield, F. R. (1995). Insolubility and redistribution of GPI-anchored proteins at the cell surface after detergent treatment. Molecular Biology of the Cell *6*, 929-944.

Mayor, S., Rothberg, K. G., and Maxfield, F. R. (1994). Sequestration of GPI-anchored proteins in caveolae triggered by cross-linking. Science *264*, 1948-1951.

McMahon, K. A., Zhu, M., Kwon, S. W., Liu, P., Zhao, Y., and Anderson, R. G. (2006). Detergent-free caveolae proteome suggests an interaction with ER and mitochondria. Proteomics *6*, 143-152.

Michalak, M., Robert Parker, J. M., and Opas, M. (2002). Ca2+ signaling and calcium binding chaperones of the endoplasmic reticulum. Cell Calcium *32*, 269-278.

Mielenz, D., Vettermann, C., Hampel, M., Lang, C., Avramidou, A., Karas, M., and Jack, H. M. (2005). Lipid rafts associate with intracellular B cell receptors and exhibit a B cell stage-specific protein composition. J Immunol *174*, 3508-3517.

Mineo, C., Gill, G. N., and Anderson, R. G. W. (1999). Regulated migration of epidermal growth factor receptor from caveolae. Journal of Biological Chemistry *274*, 30636-30643.

Minetti, C., Sotgia, F., Bruno, C., Scartezzini, P., Broda, P., Bado, M., Masetti, E., Mazzocco, M., Egeo, A., Donati, M. A., and al., e. (1998). Mutations in the caveolin-3 gene cause autosomal dominant limb-girdle muscular dystrophy. Nature Genetics *18*, 365-368.

Mirre, C., Monlauzeur, L., Garcia, M., Delgrossi, M.-H., and Le Bivic, A. (1996). Detergent-resistant membrane microdomains from Caco-2 cells do not contain caveolin. American Journal of Physiology *271*, C887-C894.

Miyata, T., Takeda, J., Iida, Y., Yamada, N., Inoue, N., Takahashi, M., Maeda, K., Kitani, T., and Kinoshita, T. (1993). The cloning of PIG-A, a component in the early step of GPI-anchor biosynthesis. Science *259*, 1318-1320.

Mohney, R. P., Knez, J. J., Ravi, L., Sevlever, D., Rosenberry, T. L., Hirose, S., and Medof, M. E. (1994). Glycoinositol phospholipid anchor-defective K562 mutants with biochemical lesions distinct from those in Thy-1- murine lymphoma mutants. J Biol Chem *269*, 6536-6542.

Molloy, M. P. (2000). Two-dimensional electrophoresis of membrane proteins using immobilized pH gradients. Anal Biochem *280*, 1-10.

Monks, C. R., Freiberg, B. A., Kupfer, H., Sciaky, N., and Kupfer, A. (1998). Three-dimensional segregation of supramolecular activation clusters in T cells. Nature *395*, 82-86.

Monks, C. R. F., Kupfer, H., Tamir, I., Barlow, A., and Kupfer, A. (1997). Selective modulation of protein kinase C-theta during T-cell activation. Nature *395*, 82-86.

Montixi, C., Langlet, C., Bernard, A. M., Thimonier, J., Dubois, C., Wurbel, M. A., Chauvin, J. P., Pierres, M., and He, H. T. (1998). Engagement of T cell receptor triggers

its recruitment to low-density detergent-insoluble membrane domains. EMBO Journal *17*, 5334-5348.

Moran, M., and Miceli, M. C. (1998). Engagement of GPI-linked CD48 contributes to TCR signals and cytoskeletal reorganization: a role for lipid rafts in T cell activation. Immunity *9*, 787-796.

Morris, A. J., and Malbon, C. C. (1999). Physiological regulation of G protein-linked signaling. Physiol Rev *79*, 1373-1430.

Morrow, I. C., and Parton, R. G. (2005). Flotillins and the PHB domain protein family: rafts, worms and anaesthetics. Traffic *6*, 725-740.

Morrow, I. C., Rea, S., Martin, S., Prior, I. A., Prohaska, R., Hancock, J. F., James, D. E., and Parton, R. G. (2002). Flotillin-1/reggie-2 traffics to surface raft domains via a novel golgi-independent pathway. Identification of a novel membrane targeting domain and a role for palmitoylation. J Biol Chem *277*, 48834-48841.

Movahedi, S., and Hooper, N. M. (1997). Insulin stimulates the release of glycosyl phosphatidylinositol-anchored membrane dipeptidase from 3T3-L1 adiopocytes through the action of a phospholipase C. Biochemical Journal *326*, 531-537.

Munro, S. (2003). Lipid rafts: elusive or illusive? Cell *115*, 377-388.

Murakami, Y., Kinoshita, T., Maeda, Y., Nakano, T., Kosaka, H., and Takeda, J. (1999). Different roles of glycosylphosphatidylinositol in various hematopoietic cells as revealed by a mouse model of paroxysmal nocturnal hemoglobinuria. Blood *94*, 2963-2970.

Muramatsu, T., and Miyauchi, T. (2003). Basigin (CD147): a multifunctional transmembrane protein involved in reproduction, neural function, inflammation and tumor invasion. Histol Histopathol *18*, 981-987.

Murray, E. W., and Robbins, S. M. (1998). Antibody cross-linking of the glycosylphosphatidyl-linked protein CD59 on hematopoietic cells induces signaling pathways resembling activation by complement. Journal of Biological Chemistry *273*, 25279-25284.

Narayanaswami, V., and McNamee, M. G. (1993). Protein-lipid interactions and Torpedo californica nicotinic acetylcholine receptor function. 2. Membrane fluidity and ligand-mediated alteration in the accessibility of gamma subunit cysteine residues to cholesterol. Biochemistry *32*, 12420-12427.

Nebl, T., Pestonjamasp, K. N., Leszyk, J. D., Crowley, J. L., Oh, S. W., and Luna, E. J. (2002). Proteomic analysis of a detergent-resistant membrane skeleton from neutrophil plasma membranes. J Biol Chem *277*, 43399-43409.

Neufeld, E. B., Cooney, A. M., Pitha, J., Dawidowicz, E. A., Dwyer, N. K., Pentchev, P. G., and Blanchette-Mackie, E. J. (1996). Intracellular trafficking of cholesterol monitored with a cyclodextrin. J Biol Chem *271*, 21604-21613.

Newman, A. (1998). RNA splicing. Curr Biol *8*, R903-905.

Nguyen, H. T., Amine, A. B., Lafitte, D., Waheed, A. A., Nicoletti, C., Villard, C., Letisse, M., Deyris, V., Roziere, M., Tchiakpe, L.*, et al.* (2006). Proteomic characterization of lipid rafts markers from the rat intestinal brush border. Biochem Biophys Res Commun *342*, 236-244.

Nichols, B. (2005). Cell biology: without a raft. Nature *436*, 638-639.

Nichols, B. J., Kenworthy, A. K., Polishchuk, R. S., Lodge, R., Roberts, T. H., Hirschberg, K., Phair, R. D., and Lippincott-Schwartz, J. (2001). Rapid cycling of lipid raft markers between the cell surface and Golgi complex. J Cell Biol *153*, 529-541.

Niiro, H., and Clark, E. A. (2002). Regulation of B-cell fate by antigen-receptor signals. Nat Rev Immunol *2*, 945-956.

Nijtmans, L. G., Artal, S. M., Grivell, L. A., and Coates, P. J. (2002). The mitochondrial PHB complex: roles in mitochondrial respiratory complex assembly, ageing and degenerative disease. Cell Mol Life Sci *59*, 143-155.

Nijtmans, L. G., de Jong, L., Artal Sanz, M., Coates, P. J., Berden, J. A., Back, J. W., Muijsers, A. O., van der Spek, H., and Grivell, L. A. (2000). Prohibitins act as a membrane-bound chaperone for the stabilization of mitochondrial proteins. Embo J *19*, 2444-2451.

Nitschke, L. (2005). The role of CD22 and other inhibitory co-receptors in B-cell activation. Curr Opin Immunol *17*, 290-297.

Novak, E. J., and Rabinovitch, P. S. (1994). Improved sensitivity in flow cytometric intracellular ionized calcium measurement using fluo-3/Fura Red fluorescence ratios. Cytometry *17*, 135-141.

Noyama, K., and Maekawa, S. (2003). Localization of cyclic nucleotide phosphodiesterase 2 in the brain-derived Triton-insoluble low-density fraction (raft). Neurosci Res *45*, 141-148.

Nuhse, T. S., Stensballe, A., Jensen, O. N., and Peck, S. C. (2003). Large-scale analysis of in vivo phosphorylated membrane proteins by immobilized metal ion affinity chromatography and mass spectrometry. Mol Cell Proteomics *2*, 1234-1243.

Nyasae, L. K., Hubbard, A. L., and Tuma, P. L. (2003). Transcytotic efflux from early endosomes is dependent on cholesterol and glycosphingolipids in polarized hepatic cells. Mol Biol Cell *14*, 2689-2705.

O'Farrell, P. H. (1975). High resolution two-dimensional electrophoresis of proteins. J Biol Chem *250*, 4007-4021.

Oh, P., and Schnitzer, J. E. (1999). Immunoisolation of caveolae with high affinity antibody binding to the oligomeric caveolin cage. Journal of Biological Chemistry *274*, 23144-23154.

Oh, P., and Schnitzer, J. E. (2001). Segregation of heterotrimeric G proteins in cell surface microdomains. G(q) binds caveolin to concentrate in caveolae, whereas G(i) and G(s) target lipid rafts by default. Mol Biol Cell *12*, 685-698.

Ohishi, K., Inoue, N., Maeda, Y., Takeda, J., Riezman, H., and Kinoshita, T. (2000). Gaa1p and gpi8p are components of a glycosylphosphatidylinositol (GPI) transamidase that mediates attachment of GPI to proteins. Mol Biol Cell *11*, 1523-1533.

Okamoto, T., Schlegel, A., Scherer, P. E., and Lisanti, M. P. (1998). Caveolins, a family of scaffolding proteins for organizing "preassembled signaling complexes" at the plasma membrane. Journal of Biological Chemistry *273*, 5419-5422.

Okazaki, Y., Ohno, H., Takase, K., Ochiai, T., and Saito, T. (2000). Cell surface expression of calnexin, a molecular chaperone in the endoplasmic reticulum. J Biol Chem *275*, 35751-35758.

Okuyama, Y., Ishihara, K., Kimura, N., Hirata, Y., Sato, K., Itoh, M., Ok, L. B., and Hirano, T. (1996). Human BST-1 expressed on myeloid cells functions as a receptor molecule. Biochemical and Biophysical Research Communications *228*, 838-845.

Oliferenko, S., Paiha, K., Harder, T., Gerke, V., Schwarzler, C., Schwarz, H., Beug, H., Gunthert, U., and Huber, L. A. (1999). Analysis of CD44-containing lipid rafts: Recruitment of annexin II and stabilization by the actin cytoskeleton. J Cell Biol *146*, 843-854.

Ollila, J., and Vihinen, M. (2003). Stimulation-induced gene expression in Ramos B-cells. Genes Immun *4*, 343-350.

Ong, S. E., Mittler, G., and Mann, M. (2004). Identifying and quantifying in vivo methylation sites by heavy methyl SILAC. Nat Methods *1*, 119-126.

Oram, J. F., and Yokoyama, S. (1996). Apolipoprotein-mediated removal of cellular cholesterol and phospholipids. Journal of Lipid Research *37*, 2473-2491.

Ossowski, L., and Aguirre-Ghiso, J. A. (2000). Urokinase receptor and integrin partnership: coordination of signaling for cell adhesion, migration and growth. Current Opinion in Cell Biology *12*, 613-620.

Ostermeyer, A. G., Beckrich, B. T., Ivarson, K. A., Grove, K. E., and Brown, D. A. (1999). Glycosphingolipids are not essential for formation of detergent-resistant membrane rafts in melanoma cells. Journal of Biological Chemistry *274*, 34459-34466`.

Otabor, I., Tyagi, S., Beurskens, F. J., Ghiran, I., Schwab, P., Nicholson-Weller, A., and Klickstein, L. B. (2004). A role for lipid rafts in C1q-triggered O2- generation by human neutrophils. Mol Immunol *41*, 185-190.

Palade, G. E. (1953). Fine structure of blood capillaries. Journal of Applied Physics *24*, 1424.

Paladino, S., Sarnataro, D., Pillich, R., Tivodar, S., Nitsch, L., and Zurzolo, C. (2004). Protein oligomerization modulates raft partitioning and apical sorting of GPI-anchored proteins. J Cell Biol *167*, 699-709.

Palazzo, A. F., Eng, C. H., Schlaepfer, D. D., Marcantonio, E. E., and Gundersen, G. G. (2004). Localized stabilization of microtubules by integrin- and FAK-facilitated Rho signaling. Science *303*, 836-839.

Palestini, P., Pitto, M., Tedeschi, G., Ferraretto, A., Parenti, M., Brunner, J., and Masserini, M. (2000). Tubulin anchoring to glycolipid-enriched, detergent-resistant domains of the neuronal plasma membrane. J Biol Chem *275*, 9978-9985.

Pandey, A., and Mann, M. (2000). Proteomics to study genes and genomes. Nature *405*, 837-846.

Pao, L. I., Bedzyk, W. D., Persin, C., and Cambier, J. C. (1997). Molecular targets of CD45 in B cell antigen receptor signal transduction. J Immunol *158*, 1116-1124.

Pappin, D. J., Hojrup, P., and Bleasby, A. J. (1993). Rapid identification of proteins by peptide-mass fingerprinting. Curr Biol *3*, 327-332.

Paramio, J. M., and Jorcano, J. L. (2002). Beyond structure: do intermediate filaments modulate cell signalling? Bioessays *24*, 836-844.

Paratcha, G., Ledda, F., Baars, L., Coulpier, M., Besset, V., Anders, J., Scott, R., and Ibanez, C. F. (2001). Released GFRalpha1 potentiates downstream signaling, neuronal survival, and differentiation via a novel mechanism of recruitment of c-ret to lipid rafts. Neuron *29*, 171-184.

Parkin, E. T., Turner, A. J., and Hooper, N. M. (1996). Isolation and characterization of two distinct low-density, Triton-insoluble, complexes from porcine lung membranes. Biochem J *319 (Pt 3)*, 887-896.

Parkin, E. T., Turner, A. J., and Hooper, N. M. (2001). Differential effects of glycosphingolipids on the detergent-insolubility of the glycosylphosphatidylinositol-anchored membrane dipeptidase. Biochem J *358*, 209-216.

Parolini, I., Sargiacomo, M., Lisanti, M. P., and Peschle, C. (1996). Signal transduction and glycophosphatidylinositol-linked proteins (lyn, lck, CD4, CD45, G proteins, and CD55) selectively localize in triton-insoluble plasma membrane domains of human leukemic cell lines and normal granulocytes. Blood *87*, 3783-3794.

Parton, R. G. (2003). Caveolae--from ultrastructure to molecular mechanisms. Nat Rev Mol Cell Biol *4*, 162-167.

Parton, R. G., Joggerst, B., and Simons, K. (1994). Regulated internalization of caveolae. Journal of Cell Biology *127*, 1199-1215.

Parton, R. G., and Richards, A. A. (2003). Lipid rafts and caveolae as portals for endocytosis: new insights and common mechanisms. Traffic *4*, 724-738.

Pasquali, C., Fialka, I., and Huber, L. A. (1997). Preparative two-dimensional gel electrophoresis of membrane proteins. Electrophoresis *18*, 2573-2581.

Patton, W. F. (2000). A thousand points of light: the application of fluorescence detection technologies to two-dimensional gel electrophoresis and proteomics. Electrophoresis *21*, 1123-1144.

Penninger, J. M., and Crabtree, G. R. (1999). The actin cytoskeleton and lymphocyte activation. Cell *96*, 9-12.

Peskan, T., Westermann, M., and Oelmuller, R. (2000). Identification of low-density Triton X-100-insoluble plasma membrane microdomains in higher plants. Eur J Biochem *267*, 6989-6995.

Petrie, R. J., and Deans, J. P. (2002). Colocalization of the B cell receptor and CD20 followed by activation-dependent dissociation in distinct lipid rafts. J Immunol *169*, 2886-2891.

Petrie, R. J., Schnetkamp, P. P. M., Patel, K. D., Awasthi-Kalia, M., and Deans, J. P. (2000). Transient translocation of the B Cell Receptor and Src Homology 2 domain-containing inositol phosphatase to lipid rafts: evidence toward a role in calcium regulation. Journal of Immunology *165*, 1220-1227.

Pflugh, D. L., Maher, S. E., and Bothwell, A. L. (2002). Ly-6 superfamily members Ly-6A/E, Ly-6C, and Ly-6I recognize two potential ligands expressed by B lymphocytes. J Immunol *169*, 5130-5136.

Pichler, H., Gaigg, B., Hrastnik, C., Achleitner, G., Kohlwein, S. D., Zellnig, G., Perktold, A., and Daum, G. (2001). A subfraction of the yeast endoplasmic reticulum associates with the plasma membrane and has a high capacity to synthesize lipids. Eur J Biochem *268*, 2351-2361.

Pielsticker, L. K., Mann, K. J., Lin, W. L., and Sevlever, D. (2005). Raft-like membrane domains contain enzymatic activities involved in the synthesis of mammalian glycosylphosphatidylinositol anchor intermediates. Biochem Biophys Res Commun *330*, 163-171.

Pike, L. J., and Casey, L. (2002). Cholesterol levels modulate EGF receptor-mediated signaling by altering receptor function and trafficking. Biochemistry *41*, 10315-10322.

Polyak, M. J., and Deans, J. P. (2002). Alanine-170 and proline-172 are critical determinants for extracellular CD20 epitopes; heterogeneity in the fine specificity of CD20 monoclonal antibodies is defined by additional requirements imposed by both amino acid sequence and quaternary structure. Blood *99*, 3256-3262.

Polyak, M. J., Tailor, S. H., and Deans, J. P. (1998). Identification of a cytoplasmic region of CD20 required for its redistribution to a detergent-insoluble membrane compartment. Journal of Immunology *161*, 3242-3248.

Poteryaev, D., Titievsky, A. D., Sun, Y. F., Thomas-Crusells, J., Lindahl, M., Billaud, M., Arumae, U., and Saarma, M. (1999). GDNF triggers a novel Ret-independent Src-kinase family-coupled signaling via a GPI-linked GDNF receptor α1. FEBS Letters *463*, 63-66.

Pralle, A., Keller, P., Florin, E.-L., Simons, K., and Horber, J. K. H. (2000). Sphingolipid-cholesterol rafts diffuse as small entities in the plasma membrane of mammalian cells. Journal of Cell Biology *148*, 997-1007.

Pratt, W. B., and Toft, D. O. (2003). Regulation of signaling protein function and trafficking by the hsp90/hsp70-based chaperone machinery. Exp Biol Med (Maywood) *228*, 111-133.

Prinz, W. (2002). Cholesterol trafficking in the secretory and endocytic systems. Semin Cell Dev Biol *13*, 197-203.

Puri, C., Tosoni, D., Comai, R., Rabellino, A., Segat, D., Caneva, F., Luzzi, P., Di Fiore, P. P., and Tacchetti, C. (2005). Relationships between EGFR signaling-competent and endocytosis-competent membrane microdomains. Mol Biol Cell *16*, 2704-2718.

Quadroni, M., and James, P. (1999). Proteomics and automation. Electrophoresis *20*, 664-677.

Quarto, N., and Amalric, F. (1994). Heparan sulfate proteoglycans as transducers of FGF-2 signalling. Journal of Cell Science *107*, 3201-3212.

Quinton, T. M., Kim, S., Jin, J., and Kunapuli, S. P. (2005). Lipid rafts are required in Galpha(i) signaling downstream of the P2Y12 receptor during ADP-mediated platelet activation. J Thromb Haemost *3*, 1036-1041.

Quintrell, N., Lebo, R., Varmus, H., Bishop, J. M., Pettenati, M. J., Le Beau, M. M., Diaz, M. O., and Rowley, J. D. (1987). Identification of a human gene (HCK) that encodes a protein-tyrosine kinase and is expressed in hemopoietic cells. Mol Cell Biol *7*, 2267-2275.

Rabilloud, T., Carpentier, G., and Tarroux, P. (1988). Improvement and simplification of low-background silver staining of proteins by using sodium ditihionite. Electrophoresis *9*, 288-291.

Racine, C., Belanger, M., Hirabayashi, H., Boucher, M., Chakir, J., and Couet, J. (1999). Reduction of caveolin-1 gene expression in lung carcinoma cell lines. Biochemical and Biophysical Research Communications *255*, 580-586.

Rademacher, T. W., Caro, H., Kunjara, S., Wang, D. Y., Greenbaum, A. L., and McLean, P. (1994). Inositolphosphoglycan second messengers. Braz J Med Biol Res *27*, 327-341.

Rao, M., and Mayor, S. (2005). Use of Forster's resonance energy transfer microscopy to study lipid rafts. Biochim Biophys Acta *1746*, 221-233.

Resta, R., and Thompson, L. F. (1997). T cell signalling through CD73. Cell Signal *9*, 131-139.

Ridyard, M. S., and Robbins, S. M. (2003). Fibroblast growth factor-2-induced signaling through lipid raft-associated fibroblast growth factor receptor substrate 2 (FRS2). J Biol Chem *278*, 13803-13809.

Ringerike, T., Blystad, F. D., Levy, F. O., Madshus, I. H., and Stang, E. (2002). Cholesterol is important in control of EGF receptor kinase activity but EGF receptors are not concentrated in caveolae. J Cell Sci *115*, 1331-1340.

Robbins, S. M., Quintrell, N. A., and Bishop, J. M. (1995). Myristoylation and differential palmitoylation of the HCK protein-tyrosine kinases govern their attachment to membranes and association with caveolae. Molecular and Cellular Biology *15*, 3507-3515.

Rodgers, W., and Zavzavadjian, J. (2001). Glycolipid-enriched membrane domains are assembled into membrane patches by associating with the actin cytoskeleton. Exp Cell Res *267*, 173-183.

Roepstorff, K., Thomsen, P., Sandvig, K., and van Deurs, B. (2002). Sequestration of epidermal growth factor receptors in non-caveolar lipid rafts inhibits ligand binding. J Biol Chem *277*, 18954-18960.

Romagnoli, P., and Bron, C. (1997). Phosphatidylinositol-based glycolipid-anchored proteins enhance proximal TCR signaling events. J Immunol *158*, 5757-5764.

Romagnoli, P., and Bron, C. (1999). Defective TCR signaling events in glycosylphosphatidylinositol-deficient T cells derived from paroxysmal nocturnal hemoglobinuria patients. Int Immunol *11*, 1411-1422.

Roper, K., Corbeil, D., and Huttner, W. B. (2000). Retention of prominin in microvilli reveals distinct cholesterol-based lipid microdomains in the apical plasma membrane. Nature Cell Biology *2*, 582-592.

Rothberg, K. G., Heuser, J. E., Donzell, W. C., Ying, Y.-S., Glenney, J. R., and Anderson, R. G. W. (1992). Caveolin, a protein component of caveolae membrane coats. Cell *68*, 673-682.

Roy, S., Luetterforst, R., Harding, A., Apolloni, A., Etheridge, M., Stang, E., Rolls, B., Hancock, J. F., and Parton, R. G. (1999). Dominant-negative caveolin inhibits H-Ras function by disrupting cholesterol-rich plasma membrane domains. Nature Cell Biology *1*, 98-105.

Ruaro, M. E., Stebel, M., Vatta, P., Marzinotto, S., and Schneider, C. (2000). Analysis of the domain requirement in Gas1 growth suppressing activity. FEBS Letters *481*, 159-163.

Ruggiero, G., Terrazzano, G., Becchimanzi, C., Sica, M., Andretta, C., Masci, A. M., Racioppi, L., Rotoli, B., Zappacosta, S., and Alfinito, F. (2004). GPI-defective monocytes from paroxysmal nocturnal hemoglobinuria patients show impaired in vitro dendritic cell differentiation. J Leukoc Biol *76*, 634-640.

Runembert, I., Queffeulou, G., Federici, P., Vrtovsnik, F., Colucci-Guyon, E., Babinet, C., Briand, P., Trugnan, G., Friedlander, G., and Terzi, F. (2002). Vimentin affects localization and activity of sodium-glucose cotransporter SGLT1 in membrane rafts. J Cell Sci *115*, 713-724.

Rutter, G. A. (2006). Moving Ca2+ from the endoplasmic reticulum to mitochondria: is spatial intimacy enough? Biochem Soc Trans *34*, 351-355.

Saarma, M. (2000). GDNF--a stranger in the TGF-β superfamily? European Journal of Biochemistry *267*, 6968-6971.

Saeki, K., Miura, Y., Aki, D., Kurosaki, T., and Yoshimura, A. (2003). The B cell-specific major raft protein, Raftlin, is necessary for the integrity of lipid raft and BCR signal transduction. Embo J *22*, 3015-3026.

Salzer, U., and Prohaska, R. (2001). Stomatin, flotillin-1, and flotillin-2 are major integral proteins of erythrocyte lipid rafts. Blood *97*, 1141-1143.

Sammar, M., Gulbins, E., Hilbert, K., Lang, F., and Altevogt, P. (1997). Mouse CD24 as a signalling molecule for integrin-mediated cell binding: functional and physical

association with src-kinases. Biochemical and Biophysical Research Communications *234*, 330-334.

Samuel, B. U., Mohandas, N., Harrison, T., McManus, H., Rosse, W., Reid, M., and Haldar, K. (2001). The role of cholesterol and glycosylphosphatidylinositol-anchored proteins of erythrocyte rafts in regulating raft protein content and malarial infection. J Biol Chem *276*, 29319-29329.

Santoni, V., Molloy, M., and Rabilloud, T. (2000). Membrane proteins and proteomics: un amour impossible? Electrophoresis *21*, 1054-1070.

Sargiacomo, M., Sudol, M., Tang, Z., and Lisanti, M. P. (1993). Signal transducing molecules and glycosyl-phosphatidylinositol-linked proteins form a caveolin-rich insoluble complex in MDCK cells. Journal of Cell Biology *122*, 789-807.

Sariola, H., and Saarma, M. (2003). Novel functions and signalling pathways for GDNF. J Cell Sci *116*, 3855-3862.

Sarnataro, D., Campana, V., Paladino, S., Stornaiuolo, M., Nitsch, L., and Zurzolo, C. (2004). PrP(C) association with lipid rafts in the early secretory pathway stabilizes its cellular conformation. Mol Biol Cell *15*, 4031-4042.

Scheiffele, P., Roth, M. G., and Simons, K. (1997). Interaction of influenza virus haemagglutinin with sphingolipid-cholesterol membrane domains via its transmembrane domain. Embo J *16*, 5501-5508.

Scheiffele, P., Verkade, P., Fra, A. M., Virta, H., Simons, K., and Ikonen, E. (1998). Caveolin-1 and -2 in the exocytic pathway of MDCK cells. Journal of Cell Biology *140*, 795-806.

Scherer, P. E., Lewis, R. Y., Volonte, D., Engelman, J. A., Galbiati, F., Couet, J., Kohtz, D. S., van Donselaar, E., Peters, P., and Lisanti, M. P. (1997). Cell-type and tissue-specific expression of caveolin-2. Caveolins 1 and 2 co-localize and form a stable hetero-oligomeric complex in vivo. Journal of Biological Chemistry *272*, 29337-29346.

Scherer, P. E., Okamoto, T., Chum, M., Nishimoto, I., Lodish, H. F., and Lisanti, M. P. (1996). Identification, sequence, and expression of caveolin-2 defines a caveolin gene family. *93*, 131-135.

Scherer, P. E., Tang, Z., Chun, M., Sargiacomo, M., Lodish, H. F., and Lisanti, M. P. (1995). Caveolin isoforms differ in their N-terminal protein sequence and subcellular distribution. Identification and epitope mapping of an isoform-specific monoclonal antibody probe. Journal of Biological Chemistry *270*, 16395-16401.

Schieven, G. L., Kirihara, J. M., Gilliland, L. K., Uckun, F. M., and Ledbetter, J. A. (1993). Ultraviolet radiation rapidly induces tyrosine phosphorylation and calcium signaling in lymphocytes. Mol Biol Cell *4*, 523-530.

Schmitt, E., Gehrmann, M., Brunet, M., Multhoff, G., and Garrido, C. (2007). Intracellular and extracellular functions of heat shock proteins: repercussions in cancer therapy. J Leukoc Biol *81*, 1-13.

Schmitz, G., and Orso, E. (2002). CD14 signalling in lipid rafts: new ligands and co-receptors. Curr Opin Lipidol *13*, 513-521.

Schnitzer, J. E., Liu, J., and Oh, P. (1995). Endothelial caveolae have the molecular transport machinery for vesicle budding, docking, and fusion including VAMP, NSF, SNAP, annexins, and GTPases. J Biol Chem *270*, 14399-14404.

Schroeder, R. J., Ahmed, S. N., Zhu, Y., London, E., and Brown, D. A. (1998). Cholesterol and sphingolipid enhance the Triton X-100 insolubility of glycosylphosphatidylinositol-anchored proteins by promoting the formation of detergent-insoluble ordered membrane domains. Journal of Biological Chemistry *273*, 1150-1157.

Schuck, S., Honsho, M., Ekroos, K., Shevchenko, A., and Simons, K. (2003). Resistance of cell membranes to different detergents. Proc Natl Acad Sci U S A *100*, 5795-5800.

Schutz, G. J., Kada, G., Pastushenko, V., and Schindler, H. (2000). Properties of lipid microdomains in a muscle cell membrane visualized by single molecule microscopy. EMBO Journal *19*, 892-901.

Schwarz, T. (1998). UV light affects cell membrane and cytoplasmic targets. J Photochem Photobiol B *44*, 91-96.

Schwencke, C., Okumura, S., Yamamoto, M., Geng, Y. J., and Ishikawa, Y. (1999). Colocalization of beta-adenergic receptors and caveolin within the plasma membrane. Journal of Cellular Biochemistry *75*, 64-72.

Schwiebert, E. M., and Zsembery, A. (2003). Extracellular ATP as a signaling molecule for epithelial cells. Biochim Biophys Acta *1615*, 7-32.

Scorrano, L., Petronilli, V., Di Lisa, F., and Bernardi, P. (1999). Commitment to apoptosis by GD3 ganglioside depends on opening of the mitochondrial permeability transition pore. J Biol Chem *274*, 22581-22585.

Screaton, R. A., DeMarte, L., Draber, P., and Stanners, C. P. (2000). The specificity for the differentiation blocking activity of carcinoembryonic antigen resides in its glycophosphatidyl-inositol anchor. Journal of Cell Biology *150*, 613-625.

Sedensky, M. M., Siefker, J. M., Koh, J. Y., Miller, D. M., 3rd, and Morgan, P. G. (2004). A stomatin and a degenerin interact in lipid rafts of the nervous system of Caenorhabditis elegans. Am J Physiol Cell Physiol *287*, C468-474.

Seibenhener, M. L., Babu, J. R., Geetha, T., Wong, H. C., Krishna, N. R., and Wooten, M. W. (2004). Sequestosome 1/p62 is a polyubiquitin chain binding protein involved in ubiquitin proteasome degradation. Mol Cell Biol *24*, 8055-8068.

Semac, I., Palomba, C., Kulangara, K., Klages, N., van Echten-Deckert, G., Borisch, B., and Hoessli, D. C. (2003). Anti-CD20 therapeutic antibody rituximab modifies the functional organization of rafts/microdomains of B lymphoma cells. Cancer Res *63*, 534-540.

Setterblad, N., Becart, S., Charron, D., and Mooney, N. (2004). B cell lipid rafts regulate both peptide-dependent and peptide-independent APC-T cell interaction. J Immunol *173*, 1876-1886.

Sevlever, D., Pickett, S., Mann, K. J., Sambamurti, K., Medof, M. E., and Rosenberry, T. L. (1999). Glycosylphosphatidylinositol-anchor intermediates associate with triton-insoluble membranes in subcellular compartments that include the endoplasmic reticulum. Biochem J *343 Pt 3*, 627-635.

Shakarjian, M. P., Eiseman, E., Penhallow, R. C., and Bolen, J. B. (1993). 3-Hydroxy-3-methylglutaryl-coenzyme A reductase inhibition in a rat mast cell line. Journal of Biological Chemistry *268*, 15252-15259.

Shan, D., Ledbetter, J. A., and Press, O. W. (2000). Signaling events involved in anti-CD20-induced apoptosis of malignant human B cells. Cancer Immunol Immunother *48*, 673-683.

Shao, Y., Yang, C., Elly, C., and Liu, Y. C. (2004). Differential regulation of the B cell receptor-mediated signaling by the E3 ubiquitin ligase Cbl. J Biol Chem *279*, 43646-43653.

Sharma, A., and Qadri, A. (2004). Vi polysaccharide of Salmonella typhi targets the prohibitin family of molecules in intestinal epithelial cells and suppresses early inflammatory responses. Proc Natl Acad Sci U S A *101*, 17492-17497.

Sharma, D. K., Choudhury, A., Singh, R. D., Wheatley, C. L., Marks, D. L., and Pagano, R. E. (2003). Glycosphingolipids internalized via caveolar-related endocytosis rapidly merge with the clathrin pathway in early endosomes and form microdomains for recycling. J Biol Chem *278*, 7564-7572.

Sharma, P., Varma, R., Sarasij, R. C., Ira, Gousset, K., Krishnamoorthy, G., Rao, M., and Mayor, S. (2004). Nanoscale organization of multiple GPI-anchored proteins in living cell membranes. Cell *116*, 577-589.

Sharom, F. J., and Lehto, M. T. (2002). Glycosylphosphatidylinositol-anchored proteins: structure, function, and cleavage by phosphatidylinositol-specific phospholipase C. Biochem Cell Biol *80*, 535-549.

Shaw, A. R., and Li, L. (2003). Exploration of the functional proteome: lessons from lipid rafts. Curr Opin Mol Ther *5*, 294-301.

Sheets, E. D., Holowka, D., and Baird, B. (1999). Critical role for cholesterol in Lyn-mediated tyrosine phosphorylation of FcεRI and their association with detergent-resistant membranes. Journal of Cell Biology *145*, 877-887.

Shenoy-Scaria, A. M., Gauen, L. K., Kwong, J., Shaw, A. S., and Lublin, D. M. (1993). Palmitylation of an amino-terminal cysteine motif of protein tyrosine kinases p56lck and p59fyn mediates interaction with glycosyl-phosphatidylinositol-anchored proteins. Molecular and Cellular Biology *13*, 6385-6392.

Shin, J.-S., Gao, Z., and Abraham, S. N. (2000). Involvement of cellular caveolae in bacterial entry into mast cells. Science *289*, 785-788.

Shogomori, H., and Brown, D. A. (2003). Use of detergents to study membrane rafts: the good, the bad, and the ugly. Biol Chem *384*, 1259-1263.

Shu, L., Lee, L., Chang, Y., Holzman, L. B., Edwards, C. A., Shelden, E., and Shayman, J. A. (2000). Caveolar structure and protein sorting are maintained in NIH 3T3 cells independent of glycosphingolipid depletion. Archives of Biochemistry and Biophysics *373*, 83-90.

Sim, A. T., and Scott, J. D. (1999). Targeting of PKA, PKC and protein phosphatases to cellular microdomains. Cell Calcium *26*, 209-217.

Simionescu, N. (1983). Cellular aspects of transcapillary exchange. Physiology Reviews *63*, 1536-1560.

Simons, K., and Ikonen, E. (1997). Functional rafts in cell membranes. Nature *387*, 569-572.

Simons, K., and Toomre, D. (2000). Lipid rafts and signal transduction. Nature Reviews *1*, 31-39.

Simons, M., Friedrichson, T., Schulz, J. B., Pitto, M., Masserini, M., and Kurchalia, T. V. (1999). Exogenous Administration of gangliosides displaces GPI-anchored proteins from lipid microdomains in living cells. Molecular Biology of the Cell *10*, 3187-3196.

Simpson-Holley, M., Ellis, D., Fisher, D., Elton, D., McCauley, J., and Digard, P. (2002). A functional link between the actin cytoskeleton and lipid rafts during budding of filamentous influenza virions. Virology *301*, 212-225.

Simpson, R. J., Connolly, L. M., Eddes, J. S., Pereira, J. J., Moritz, R. L., and Reid, G. E. (2000). Proteomic analysis of the human colon carcinoma cell line (LIM 1215): development of a membrane protein database. Electrophoresis *21*, 1707-1732.

Sleight, S. B., Miranda, P. V., Plaskett, N. W., Maier, B., Lysiak, J., Scrable, H., Herr, J. C., and Visconti, P. E. (2005). Isolation and proteomic analysis of mouse sperm detergent-resistant membrane fractions: evidence for dissociation of lipid rafts during capacitation. Biol Reprod *73*, 721-729.

Smart, E. J., Graf, G. A., McNiven, M. A., Sessa, W. C., Engelman, J. A., Scherer, P. E., Okamoto, T., and Lisanti, M. P. (1999). Caveolins, liquid-ordered domains, and signal transduction. Molecular and Cellular Biology *19*, 7289-7304.

Smart, E. J., Ying, Y., Mineo, C., and Anderson, R. G. W. (1995). A detergent-free method for purifying caveolae membrane from tissue culture cells. Proceedings of the National Academy of Sciences USA *92*, 10104-10108.

Smart, E. J., Ying, Y. S., Donzell, W. C., and Anderson, R. G. W. (1996). A role for caveolin in transport of cholesterol from endoplasmic reticulum to plasma membrane. Journal of Biological Chemistry *271*, 29427-29435.

Smith, F. D., and Scott, J. D. (2006). Anchored cAMP signaling: onward and upward - a short history of compartmentalized cAMP signal transduction. Eur J Cell Biol *85*, 585-592.

Smith, M. R. (2003). Rituximab (monoclonal anti-CD20 antibody): mechanisms of action and resistance. Oncogene *22*, 7359-7368.

Sprenger, R. R., Fontijn, R. D., van Marle, J., Pannekoek, H., and Horrevoets, A. J. (2006). Spatial segregation of transport and signalling functions between human endothelial caveolae and lipid raft proteomes. Biochem J.

Sprenger, R. R., Speijer, D., Back, J. W., De Koster, C. G., Pannekoek, H., and Horrevoets, A. J. (2004). Comparative proteomics of human endothelial cell caveolae and rafts using two-dimensional gel electrophoresis and mass spectrometry. Electrophoresis *25*, 156-172.

Sproul, T. W., Malapati, S., Kim, J., and Pierce, S. K. (2000). Cutting edge: B cell antigen receptor signaling occurs outside lipid rafts in immature B cells. Journal of Immunology *165*, 6020-6023.

Staffler, G., Szekeres, A., Schutz, G. J., Saemann, M. D., Prager, E., Zeyda, M., Drbal, K., Zlabinger, G. J., Stulnig, T. M., and Stockinger, H. (2003). Selective inhibition of T cell activation via CD147 through novel modulation of lipid rafts. J Immunol *171*, 1707-1714.

Stahl, A., and Mueller, B. M. (1995). The urokinase-type plasminogen activator receptor, a GPI-linked protein, is localized in caveolae. Journal of Cell Biology *129*, 335-344.

Stan, R.-V., Roberts, W. G., Predescu, D., Ihida, K., Saucan, L., Ghitescu, L., and Palade, G. E. (1997). Immunoisolation and partial characterization of endothelial plasmalemmal vesicles (caveolae). Molecular Biology of the Cell *8*, 595-605.

Stefanova, I., Corcoran, M. L., Horak, E. M., Wahl, L. M., Bolen, J. B., and Horak, I. D. (1993). Lipopolysaccharide induces activation of CD14-associated protein tyrosine kinase p53/p56lyn. Journal of Biological Chemistry *268*, 20725-20728.

Steglich, G., Neupert, W., and Langer, T. (1999). Prohibitins regulate membrane protein degradation by the m-AAA protease in mitochondria. Mol Cell Biol *19*, 3435-3442.

Stehr, M., Adam, R. M., Khoury, J., Zhuang, L., Solomon, K. R., Peters, C. A., and Freeman, M. R. (2003). Platelet derived growth factor-BB is a potent mitogen for rat ureteral and human bladder smooth muscle cells: dependence on lipid rafts for cell signaling. J Urol *169*, 1165-1170.

Stralfors, P. (1997). Insulin second messengers. BioEssays *19*, 327-335.

Stuart, G. R., Lynch, N. J., Day, A. J., Schwaeble, W. J., and Sim, R. B. (1997). The C1q and collectin binding site within C1q receptor (cell surface calreticulin). Immunopharmacology *38*, 73-80.

Stulnig, T. M., Berger, M., Sigmund, T., Raederstorff, D., Stockinger, H., and Waldhausl, W. (1998). Polyunsaturated fatty acids inhibit T cell signal transduction by modification of detergent-insoluble membrane domains. Journal of Cell Biology *143*, 637-644.

Suzuki, T., Kiyokawa, N., Taguchi, T., Sekino, T., Katagiri, Y. U., and Fujimoto, J. (2001). CD24 induces apoptosis in human B cells via the glycolipid-enriched membrane domains/rafts-mediated signaling system. J Immunol *166*, 5567-5577.

Takeda, J., and Kinoshita, T. (1995). GPI-anchor biosynthesis. Trends Biochem Sci *20*, 367-371.

Takeda, J., Miyata, T., Kawagoe, K., Iida, Y., Endo, Y., Fujita, T., Takahashi, M., Kitani, T., and Kinoshita, T. (1993). Deficiency of the GPI anchor caused by a somatic mutation of the PIG-A gene in paroxysmal nocturnal hemoglobinuria. Cell *73*, 703-711.

Takeuchi, S., Takayama, Y., Ogawa, A., Tamura, K., and Okada, M. (2000). Transmembrane phosphoprotein Cbp positively regulates the activity of the Carboxyl-terminal Src kinase, Csk. Journal of Biological Chemistry *275*, 29183-29186.

Tang, W., and Hemler, M. E. (2004). Caveolin-1 regulates matrix metalloproteinases-1 induction and CD147/EMMPRIN cell surface clustering. J Biol Chem *279*, 11112-11118.

Tang, Z., Scherer, P. E., Okamoto, T., Song, K., Chu, C., Kohtz, S., Nishimoto, I., Lodish, H. F., and Lisanti, M. P. (1996). Molecular cloning of caveolin-3, a novel member of the caveolin gene family expressed predominantly in muscle. Journal of Biological Chemistry *271*, 2255-2261.

Tansey, M. G., Baloh, R. H., Milbrandt, J., and Johnson, E. M. J. (2000). GFRα-mediated localization of RET to lipid rafts is required for effective downstream signaling, differentiation and neuronal survival. Neuron *25*, 611-623.

Tasken, K., and Stokka, A. J. (2006). The molecular machinery for cAMP-dependent immunomodulation in T-cells. Biochem Soc Trans *34*, 476-479.

Taute, A., Watzig, K., Simons, B., Lohaus, C., Meyer, H., and Hasilik, A. (2002). Presence of detergent-resistant microdomains in lysosomal membranes. Biochem Biophys Res Commun *298*, 5-9.

Tavernarakis, N., Driscoll, M., and Kyrpides, N. C. (1999). The SPFH domain: implicated in regulating targeted protein turnover in stomatins and other membrane-associated proteins. Trends Biochem Sci *24*, 425-427.

Teixeira, A., Chaverot, N., Schroder, C., Strosberg, A. D., Couraud, P. O., and Cazaubon, S. (1999). Requirement of caveolae microdomains in extracellular signal-regulated kinase and focal adhesion kinase activation induced by endothelin-1 in primary astrocytes. Journal of Neurochemistry *72*, 120-128.

Terashima, M., Kim, K. M., Adachi, T., Nielsen, P. J., Reth, M., Kohler, G., and Lamers, M. C. (1994). The IgM antigen receptor of B lymphocytes is associated with prohibitin and a prohibitin-related protein. Embo J *13*, 3782-3792.

Terrazzano, G., Sica, M., Becchimanzi, C., Costantini, S., Rotoli, B., Zappacosta, S., Alfinito, F., and Ruggiero, G. (2005). T cells from paroxysmal nocturnal haemoglobinuria (PNH) patients show an altered CD40-dependent pathway. J Leukoc Biol *78*, 27-36.

Thien, C. B., and Langdon, W. Y. (2005). c-Cbl and Cbl-b ubiquitin ligases: substrate diversity and the negative regulation of signalling responses. Biochem J *391*, 153-166.

Thomas, J. L., Holowka, D., Baird, B., and Webb, W. W. (1994). Large-scale co-aggregation of fluorescent lipid probes with cell surface proteins. Journal of Cell Biology *125*, 795-802.

Thomas, P. M., and Samelson, L. E. (1992). The glycophosphatidylinositol-anchored Thy-1 molecule interacts with the p60 fyn protein tyrosine kinase in T cells. Journal of Biological Chemistry *267*, 12317-12322.

Tirumalai, R. S., Chan, K. C., Prieto, D. A., Issaq, H. J., Conrads, T. P., and Veenstra, T. D. (2003). Characterization of the low molecular weight human serum proteome. Mol Cell Proteomics *2*, 1096-1103.

Tohyama, Y., Takano, T., and Yamamura, H. (2004). B cell responses to oxidative stress. Curr Pharm Des *10*, 835-839.

Torgersen, K. M., Vang, T., Abrahamsen, H., Yaqub, S., Horejsi, V., Schraven, B., Rolstad, B., Mustelin, T., and Tasken, K. (2001). Release from tonic inhibition of T cell activation through transient displacement of c-terminal Src kinase (Csk) from lipid rafts. Journal of Biological Chemistry *276*, 29313-29318.

Triantafilou, M., and Triantafilou, K. (2004). Heat-shock protein 70 and heat-shock protein 90 associate with Toll-like receptor 4 in response to bacterial lipopolysaccharide. Biochem Soc Trans *32*, 636-639.

Trujillo, M. A., and Eberhardt, N. L. (2003). Kinetics of the apoptotic response induced by anti-IgM engagement of the B cell receptor is dependent on the density of cell surface immunoglobulin M expression. DNA Cell Biol *22*, 525-531.

Trupp, M., Scott, R., Whittemore, S. R., and Ibanez, C. F. (1999). Ret-dependent and -independent mechanisms of glial cell line-derived neurotrophic factor signaling in neuronal cells. Journal of Biological Chemistry *274*, 20885-20894.

Tsiftsoglou, A. S., Pappas, I. S., and Vizirianakis, I. S. (2003). Mechanisms involved in the induced differentiation of leukemia cells. Pharmacol Ther *100*, 257-290.

Tu, X., Huang, A., Bae, D., Slaughter, N., Whitelegge, J., Crother, T., Bickel, P. E., and Nel, A. (2004). Proteome analysis of lipid rafts in Jurkat cells characterizes a raft subset that is involved in NF-kappaB activation. J Proteome Res *3*, 445-454.

Unruh, T. L., Li, H., Mutch, C. M., Shariat, N., Grigoriou, L., Sanyal, R., Brown, C. B., and Deans, J. P. (2005). Cholesterol depletion inhibits src family kinase-dependent calcium mobilization and apoptosis induced by rituximab crosslinking. Immunology *116*, 223-232.

Valensin, S., Paccani, S. R., Ulivieri, C., Mercati, D., Pacini, S., Patrussi, L., Hirst, T., Lupetti, P., and Baldari, C. T. (2002). F-actin dynamics control segregation of the TCR signaling cascade to clustered lipid rafts. Eur J Immunol *32*, 435-446.

Vamosi, G., Bodnar, A., Vereb, G., Jenei, A., Goldman, C. K., Langowski, J., Toth, K., Matyus, L., Szollosi, J., Waldmann, T. A., and Damjanovich, S. (2004). IL-2 and IL-15 receptor alpha-subunits are coexpressed in a supramolecular receptor cluster in lipid rafts of T cells. Proc Natl Acad Sci U S A *101*, 11082-11087.

van't Hof, W., and Resh, M. D. (1999). Dual fatty acylation of p59(Fyn) is required for association with the T cell receptor zeta chain through phosphotyrosine-Src homology domain-2 interactions. Journal of Cell Biology *145*, 377-389.

van der Merwe, P. A., Davis, S. J., Shaw, A. S., and Dustin, M. L. (2000). Cytoskeletal polarization and redistribution of cell-surface molecules during T cell antigen recognition. Seminars in Immunology *12*, 5-21.

van Deurs, B., Roepstorff, K., Hommelgaard, A. M., and Sandvig, K. (2003). Caveolae: anchored, multifunctional platforms in the lipid ocean. Trends Cell Biol *13*, 92-100.

van Meer, G., and Lisman, Q. (2002). Sphingolipid transport: rafts and translocators. J Biol Chem *277*, 25855-25858.

Vang, T., Torgersen, K. M., Sundvold, V., Saxena, M., Levy, F. O., Skalhegg, B. S., Hansson, V., Mustelin, T., and Tasken, K. (2001). Activation of the COOH-terminal Src kinase (Csk) by cAMP-dependent protein kinase inhibits signaling through the T cell receptor. J Exp Med *193*, 497-507.

Varki, A., Cummings, R., Esko, J., Freeze, H., Hart, G., and Marth, J. (1999). Essentials of Glycobiology (Cold Spring Harbor, Cold Spring Harbor Laboratory Press).

Varma, R., and Mayor, S. (1998). GPI-anchored proteins are organized in submicron domains at the cell surface. Nature *394*, 798-801.

Vetrivel, K. S., Cheng, H., Lin, W., Sakurai, T., Li, T., Nukina, N., Wong, P. C., Xu, H., and Thinakaran, G. (2004). Association of gamma-secretase with lipid rafts in post-Golgi and endosome membranes. J Biol Chem *279*, 44945-44954.

Vial, C., Fung, C. Y., Goodall, A. H., Mahaut-Smith, M. P., and Evans, R. J. (2006). Differential sensitivity of human platelet P2X1 and P2Y1 receptors to disruption of lipid rafts. Biochem Biophys Res Commun *343*, 415-419.

Vieira, A. V., Lamaze, C., and Schmid, S. L. (1996). Control of EGF receptor signalling by clathrin-mediated endocytosis. Science *274*, 2086-2089.

Villalba, M., Bi, K., Rodriguez, F., Tanaka, Y., Schoenberger, S., and Altman, A. (2001). Vav1/Rac-dependent actin cytoskeleton reorganization is required for lipid raft clustering in T cells. J Cell Biol *155*, 331-338.

Villalba, M., Coudronniere, N., Deckert, M., Teixeiro, E., Mas, P., and Altman, A. (2000). A novel functional interaction between Vav and PKCθ is required for TCR-induced T cell activation. Immunity *12*, 151-160.

Viola, A. (2001). The amplification of TCR signaling by dynamic membrane microdomains. Trends in Immunology *22*, 322-327.

Viola, A., Schroeder, S., Sakakibara, Y., and Lanzavecchia, A. (1999). T lymphocyte costimulation mediated by reorganization of membrane microdomains. Science *283*, 680-682.

Vogel, U., Sandvig, K., and van Deurs, B. (1998). Expression of caveolin-1 and polarized formation of invaginated caveolae in Caco-2 and MDCK II cells. Journal of Cell Science *111*, 825-832.

Volonte, D., Galbiati, F., Li, S., Nishiyama, K., Okamoto, T., and Lisanti, M. P. (1999). Flotillins/cavatellins are differentially expressed in cells and tissues and form a hetero-oligomeric complex with caveolins *in vivo*. Characterization and epitope-mapping of a novel flotillin-1 monoclonal antibody probe. Journal of Biological Chemistry *274*, 12702-12709.

von Haller, P. D., Donohoe, S., Goodlett, D. R., Aebersold, R., and Watts, J. D. (2001). Mass spectrometric characterization of proteins extracted from Jurkat T cell detergent-resistant membrane domains. Proteomics *1*, 1010-1021.

Wachtler, V., Huang, Y., Karagiannis, J., and Balasubramanian, M. K. (2006). Cell cycle-dependent roles for the FCH-domain protein Cdc15p in formation of the actomyosin ring in Schizosaccharomyces pombe. Mol Biol Cell *17*, 3254-3266.

Wang, S., Nath, N., Adlam, M., and Chellappan, S. (1999). Prohibitin, a potential tumor suppressor, interacts with RB and regulates E2F function. Oncogene *18*, 3501-3510.

Wary, K. K., Mariotti, A., Zurzolo, C., and Giancotti, F. G. (1998). A requirement for caveolin-1 and associated kinase fyn in integrin signaling and anchorage-dependent cell growth. Cell *94*, 625-634.

Watzl, C., and Long, E. O. (2003). Natural killer cell inhibitory receptors block actin cytoskeleton-dependent recruitment of 2B4 (CD244) to lipid rafts. J Exp Med *197*, 77-85.

Waugh, M. G., Lawson, D., and Hsuan, J. J. (1999). Epidermal growth factor receptor activation is localized within low buoyant density, non-caveolar membrane domains. Biochemical Journal *337*, 591-597.

Waugh, M. G., Lawson, D., Tan, S. K., and Hsuan, J. J. (1998). Phosphatidylinositol 4-phosphate synthesis in immunoisolated caveolae-like vesicles and low buoyant density non-caveolar membranes. Journal of Biological Chemistry *273*, 17115-17121.

Webb, Y., Hermida-Matsumoto, L., and Resh, M. D. (2000). Inhibition of protein palmitoylation, raft localization, and T cell signaling by 2-bromopalmitate and polyunsaturated fatty acids. Journal of Biological Chemistry *275*, 261-270.

Wei, Y., Yang, X., Liu, Q., Wilkins, J. A., and Chapman, H. A. (1999). A role for caveolin and the urokinase receptor in integrin-mediated adhesion and signaling. Journal of Cell Biology *144*, 1285-1294.

Weintraub, B. C., Jun, J. E., Bishop, A. C., Shokat, K. M., Thomas, M. L., and Goodnow, C. C. (2000). Entry of B cell receptor into signaling domains is inhibited in tolerant B cells. J Exp Med *191*, 1443-1448.

Westermann, M., Leutbecher, H., and Meyer, H. W. (1999). Membrane structure of caveolae and isolated caveolin-rich vesicles. Histochem Cell Biol *111*, 71-81.

Wheaton, K., Sampsel, K., Boisvert, F.-M., Davy, A., Robbins, S., and Riabowol, K. (2001). Loss of functional caveolae during senescence of human fibroblasts. Journal of Cellular Physiology *187*, 226-235.

Williams, T. M., and Lisanti, M. P. (2005). Caveolin-1 in oncogenic transformation, cancer, and metastasis. Am J Physiol Cell Physiol *288*, C494-506.

Wilm, M., and Mann, M. (1996). Analytical properties of the nanoelectrospray ion source. Anal Chem *68*, 1-8.

Wilson, B. S., Pfeiffer, J. R., and Oliver, J. M. (2000). Observing FcεRI signaling from the inside of the mast cell membrane. Journal of Cell Biology *149*, 1131-1142.

Wilson, B. S., Pfeiffer, J. R., Surviladze, Z., Gaudet, E. A., and Oliver, J. M. (2001). High resolution mapping of mast cell membranes reveals primary and secondary domains of FcεRI and LAT. Journal of Cell Biology *154*, 645-658.

Woodage, T., and Broder, S. (2003). The human genome and comparative genomics: understanding human evolution, biology, and medicine. J Gastroenterol *38 Suppl 15*, 68-77.

Wu, C., Butz, S., Ying, Y., and Anderson, R. G. W. (1997). Tyrosine kinase receptors concentrated in caveolae-like domains from neuronal plasma membrane. Journal of Biological Chemistry *272*, 3554-3559.

Wu, C. C., and Yates, J. R., 3rd (2003). The application of mass spectrometry to membrane proteomics. Nat Biotechnol *21*, 262-267.

Xavier, R., Brennan, T., Li, Q., McCormack, C., and Seed, B. (1998). Membrane compartmentation is required for efficient T cell activation. Immunity *8*, 723-732.

Xu, Y., Harder, K. W., Huntington, N. D., Hibbs, M. L., and Tarlinton, D. M. (2005). Lyn tyrosine kinase: accentuating the positive and the negative. Immunity *22*, 9-18.

Yamabhai, M., and Anderson, R. G. (2002). Second cysteine-rich region of epidermal growth factor receptor contains targeting information for caveolae/rafts. J Biol Chem *277*, 24843-24846.

Yamada, E. (1955). The fine structure of the gall bladder epithelium of the mouse. Journal of Biophysical and Biochemical Cytology *1*, 445-458.

Yamamoto, M., Toya, Y., Jensen, R. A., and Ishikawa, Y. (1999). Caveolin is an inhibitor of platelet-derived growth factor receptor signaling. Exp Cell Res *247*, 380-388.

Yan, J., Roy, S., Apolloni, A., Lane, A., and Hancock, J. F. (1998). Ras isoforms vary in their ability to activate Raf-1 and phosphoinositide 3-kinase. Journal of Biological Chemistry *273*, 24052-24056.

Yancopoulos, G. D., Klagsbrun, M., and Folkman, J. (1998). Vasculogenesis, angiogenesis, and growth factors: ephrins enter the fray at the border. Cell *93*, 661-664.

Yang, G., Truong, L. D., Timme, T. L., Ren, C., Wheeler, T. M., Park, S. H., Nasu, Y., Bangma, C. H., Kattan, M. W., Scardino, P. T., and Thompson, T. C. (1998). Elevated expression of caveolin is associated with prostate and breast cancer. Clinical Cancer Research *4*, 1873-1880.

Yates, J. R., 3rd, Eng, J., Clauser, K. R., and Burlingame, A. L. (1996). Search of sequence databases with uninterpreted high-energy collision-induced dissociation spectra of peptides. J Am Soc Mass Spectrom *7*, 1089-1098.

Yates, J. R., 3rd, Gilchrist, A., Howell, K. E., and Bergeron, J. J. (2005). Proteomics of organelles and large cellular structures. Nat Rev Mol Cell Biol *6*, 702-714.

Yates, J. R., 3rd, Speicher, S., Griffin, P. R., and Hunkapiller, T. (1993). Peptide mass maps: a highly informative approach to protein identification. Anal Biochem *214*, 397-408.

Yebra, M., Goretzki, L., Pfeifer, M., and Mueller, B. M. (1999). Urokinase-type plasminogen activator binding to its receptor stimulates tumor cell migration by enhancing integrin-mediated signal transduction. Experimental Cell Research *250*, 231-240.

Yoon, S. S., Jung, K. I., Choi, Y. L., Choi, E. Y., Lee, I. S., Park, S. H., and Kim, T. J. (2003). Engagement of CD99 triggers the exocytic transport of ganglioside GM1 and the reorganization of actin cytoskeleton. FEBS Lett *540*, 217-222.

Young, R. M., Holowka, D., and Baird, B. (2003). A lipid raft environment enhances Lyn kinase activity by protecting the active site tyrosine from dephosphorylation. J Biol Chem *278*, 20746-20752.

Yu, C., Alterman, M., and Dobrowsky, R. T. (2005). Ceramide displaces cholesterol from lipid rafts and decreases the association of the cholesterol binding protein caveolin-1. J Lipid Res *46*, 1678-1691.

Yu, J., Nagarajan, S., Knez, J. J., Udenfriend, S., Chen, R., and Medof, M. E. (1997). The affected gene underlying the class K glycosylphosphatidylinositol (GPI) surface protein defect codes for the GPI transamidase. Proc Natl Acad Sci U S A *94*, 12580-12585.

Zacharias, D. A., Violin, J. D., Newton, A. C., and Tsien, R. Y. (2002). Partitioning of lipid-modified monomeric GFPs into membrane microdomains of live cells. Science *296*, 913-916.

Zajchowski, L. D., and Robbins, S. M. (2002). Lipid rafts and little caves. Compartmentalized signalling in membrane microdomains. Eur J Biochem *269*, 737-752.

Zhai, L., Chaturvedi, D., and Cumberledge, S. (2004). Drosophila wnt-1 undergoes a hydrophobic modification and is targeted to lipid rafts, a process that requires porcupine. J Biol Chem *279*, 33220-33227.

Zhang, W., Sloan-Lancaster, J., Kitchen, J., Trible, R. P., and Samelson, L. E. (1998a). LAT: the ZAP-70 tyrosine kinase substrate that links T cell receptor to cellular activation. Cell *92*, 83-92.

Zhang, W., Trible, R. P., and Samelson, L. E. (1998b). LAT palmitoylation: its essential role in membrane microdomain targeting and tyrosine phosphorylation during T cell activation. Immunity *9*, 239-246.

Zhao, Y., Zhang, W., Kho, Y., and Zhao, Y. (2004). Proteomic analysis of integral plasma membrane proteins. Anal Chem *76*, 1817-1823.

Zhu, M., Shen, S., Liu, Y., Granillo, O., and Zhang, W. (2005). Cutting Edge: Localization of linker for activation of T cells to lipid rafts is not essential in T cell activation and development. J Immunol *174*, 31-35.

Zipfel, P. A., Grove, M., Blackburn, K., Fujimoto, M., Tedder, T. F., and Pendergast, A. M. (2000). The c-Abl tyrosine kinase is regulated downstream of the B cell antigen receptor and interacts with CD19. J Immunol *165*, 6872-6879.